JACK MORIKKA

The Roles of Mitochondrial Protein Synthesis and of the Transcriptional Coactivator Spargel in *Drosophila* Growth and Development

JACK MORIKKA

The Roles of Mitochondrial Protein Synthesis and of the Transcriptional Coactivator Spargel in *Drosophila* Growth and Development

ACADEMIC DISSERTATION
To be presented, with the permission of
the Faculty of Medicine and Health Technology
of Tampere University,
for public discussion at Tampere University
on 24 September 2020, at 12 o'clock.

ACADEMIC DISSERTATION
Tampere University, Faculty of Medicine and Health Technology
Finland

Responsible supervisor and Custos	Professor Howard T. Jacobs Tampere University Finland	
Pre-examiners	Professor Carl Thummel University of Utah USA	Associate Professor Jorge Ruas Karolinska Institutet Sweden
Opponent	Professor Jared Rutter University of Utah USA	

The originality of this thesis has been checked using the Turnitin OriginalityCheck service.

Cover design: Roihu Inc.

To complexity and acceptance

ABSTRACT

When the capacity of mitochondrial ribosomes (mitoribosomes) to translate genes encoded in the mitochondrial genome (mtDNA) is impaired, severe effects on mitochondrial activity and, subsequently, on total cellular metabolism, result. The impacts can be observed throughout the entire organism and present as a metabolic disease. In humans, such disease is often seen when mutations arise in nuclearly or mitochondrially encoded components of the mitoribosome or its associated molecular machinery. Understanding the mechanistic pathways of these diseases and exploring methods to alleviate their symptoms requires an intricate understanding of the metabolic changes that underpin these pathologies.

The work presented within this thesis aimed at adding to this understanding by using genetic and chemical alterations to scrutinise the complex context of metabolism during development in a *Drosophila melanogaster* mutant model of mitoribosomal disease. The *Drosophila* strain *tko²⁵ᵗ*, carrying a mis-sense mutation in mitoribosomal small subunit protein S12 (mRpS12), has phenotypes including bang sensitivity, impaired hearing and developmental delay, closely phenocopying elements of human mitochondrial disease. The same is true at the cellular and molecular level where a decreased capacity for mitochondrial protein synthesis causes *tko²⁵ᵗ* to exhibit decreased electron transport chain (ETC) complex activity, a marker of mitochondrial disease in humans.

Using a combination of transcriptomic and metabolomic assays, along with genetic perturbations, dietary manipulations and developmental analyses, a sensitivity to alterations in pyruvate metabolism was identified as a key component of the *tko²⁵ᵗ* mutant phenotype, in which pyruvate levels were found to be basally higher than in wild-type flies. Adding pyruvate to the diet of *tko²⁵ᵗ* or decreasing the expression of crucial components of pyruvate metabolism led to significant changes in growth rate and provided insight into the metabolic effects of decreased mitoribosomal activity. Altered pyruvate metabolism was closely linked to an inferred compensation mechanism in *tko²⁵ᵗ* mutant flies, whereby glucose serum levels were lowered through changes in the expression of putative Malpighian tubule- and gut-specific sugar transporters. By lowering the sugar level of the culture medium, which resulted in a decreased level of serum sugar, key features of the *tko²⁵ᵗ*

mutant phenotype were alleviated; notably the extent of developmental delay and the recovery time from mechanical shock (bang sensitivity), consistent with a suggested 'sugar-toxicity' toward the mitoribosomal mutant flies.

To further explore whether the tko^{25t} phenotype could be alleviated through alterations at the genetic rather than the metabolic level, the transcriptional coactivator *spargel* was over-expressed. *spargel* belongs to the PGC1 family of coactivators that have been proposed as master regulators of mitochondrial biogenesis. In the adult *Drosophila* fat body, *spargel* has been shown to alter mitochondrial transcript expression. Additionally, the expression of *spargel* at the RNA level is decreased in the tko^{25t} mutant. It was therefore reasoned that *spargel* overexpression might correct the decreased capacity for mitochondrial protein synthesis in tko^{25t} mutant flies, and thus alleviate its developmental delay accordingly. However, *spargel* overexpression did not have the intended outcome of increased mitochondrial gene transcription and biogenesis in the tko^{25t} mutant, nor in control flies.

Whilst carrying out these experiments, *spargel* RNA expression in adult *Drosophila* females was observed to be approximately ten-fold higher than in males. Further analysis found this to be a result of *spargel* RNA levels being high in ovaries and remaining high throughout the earliest stages of embryogenesis. To gain further insight into the biological function(s) of *spargel*, its expression was knocked down at the RNA level, specifically in the female germline. The embryonic semi-lethality that resulted confirmed the essential nature of *spargel* in the developing *Drosophila* embryo. Experiments were undertaken to determine whether *spargel*, despite its lack of interaction with tko^{25t}, was functioning to boost mitochondrial biogenesis during these early stages of development. This also failed to find any evidence linking s*pargel* activity with mitochondrial regulation. These findings confirm the importance of s*pargel* function in development, but call into question its often-assumed role in mitochondrial biogenesis.

TIIVISTELMÄ

Mitokondriaalisten ribosomien (mitoribosomi) toiminnan häiriöillä on vakavia vaikutuksia solun ja organismin aineenvaihduntaan. Mitoribosomit koostuvat proteiineista sekä RNA:sta, joiden geenit sijaitsevat sekä tuman että mitokondrioiden DNA:ssa. Mutaatiot näissä geeneissä voivat johtaa ihmisellä aineenvaihdunnallisten sairauksien puhkeamiseen. Mitoribosomeista riippuvaisten sairauksien parantavan hoidon sekä oireiden lieventämisen kannalta oleellista on ymmärtää sairauksien molekulaariset syntymekanismit.

Tässä työssä on käytetty banaanikärpäsmallia mitoribosomeista riippuvaisten tautigeenien toiminnan mallintamiseen. Banaanikärpäsen tko^{25t} mutaatio johtaa mitoribosomin pienen alayksikön proteiini S12 (mRpS12) toiminnan häiriöön. tko^{25t} Kärpäsmutanteilla on useita ihmisen mitokondrioiden toiminnan häiriöiden suhteen samankaltaisia fenotyyppejä. Näihin kuuluu esimerkiksi kuulon alenema sekä yksilönkehityksen häiriöt. Myös molekulaariset mekanismit tko^{25t} mutantin fenotyypin taustalla ovat samankaltaiset ihmisen mitokondrionaalisten sairauksien kanssa, jossa alentunut mitokondrionaalinen proteiinisynteesi johtaa elektroninsiirtoketjun aktiivisuuden alenemiseen.

Käyttämällä geeniaktiivisuuden, aineenvaihdunnan, geneettisiä sekä yksilönkehityksen analyysimenetelmiä, tässä työssä löydettiin pyruvaattiaineenvaihdunnan häiriön olevan keskeinen tko^{25t} mutantin taustalla vaikuttavista syistä. Pyruvaatin pitoisuus on tko^{25t} mutantilla korkeampi kuin kontrollieläimillä. Pyruvaatin pitoisuutta muuttamalla joko geneettisesti, tai ravinnon koostumuksella voitiin tko^{25t} mutantin ilmenemistä säädellä. Pyruvaatin pitoisuuden muutoksella on vaikutusta kompensaatiomekanismiin, jossa seerumin glukoosin määrä vaihtelee suolen ja munuaiskerästen sokeritransporttereiden geeniaktiivisuuden seurauksena. Vastaavasti, ruuan sokeripitoisuuden konsentraatio säätelee tko^{25t} mutantin fenotyypin ilmenemistä. Nämä tulokset osoittavat, että mitoribosomaalisista häiriöistä kärsivät kärpäset eivät siedä korkeaa seerumin sokeripitoisuutta.

Tässä työssä tutkittiin myös geneettisiä menetelmiä tko^{25t} mutantin fenotyypin lieventämiseksi. Spargel kuuluu PGC1 perheen geenienluennan koaktivaattoreihin, jonka toiminta on osoitettu olevan yhteydessä mitokondrion toimintaan. Esimerkiksi

kärpäsen rasvakudoksessa *spargel*-geenin säätely on todettu johtavan mitokondriaalisten geenien ilmenemiseen. Tässä työssä löydettiin *spargel*-geenin ilmenemisen olevan alentunut tko^{25t} mutantilla. *spargel*-geenin ilmentäminen tko^{25t} mutantissa ei kuitenkaan vaikuttanut mutantin fenotyyppiin, eikä sen voimistunut aktiivisuus lisännyt mitokondrioiden biogeneesiä. Tämä yllättävä tulos johti lisätutkimuksiin *spargel*-geenin toiminnan ymmärtämiseksi.

Yllättäen löysimme *spargel*-geenin ilmentyvän kymmenkertaisesti naaraskärpäsillä koiraisiin verrattuna. Ero juontaa *spargel*-geenin erittäin korkeaan ilmenemiseen kärpäsen munarauhasessa. Hiljentämällä *spargel*-geenin toiminta munarauhasessa aikaansai alkionkehityksen keskeytymiseen. Viitteitä *spargel*-geenin vaikutuksesta mitokondrion toiminnan säätelyssä munarauhasessa ei löytynyt. Tutkimukseni osoittaa että *spargel*-geenillä on oleellinen funktio alkionkehityksen aikana, mutta sen rooli mitokondrion biogeneesin säätelyssä on kyseenalainen.

CONTENTS

ABBREVIATIONS

ADP	Adenosine diphosphate
AMP	Adenosine monophosphate
ATP	Adenosine triphosphate
cAMP	cyclic adenosine monophosphate
CBP	CREB-binding protein
COX	Cytochrome oxidase
CREB	cAMP response element-binding protein
ERR	Estrogen related receptor
ETC	Electron transport chain
FAD	Flavin adenine dinucleotide
FOXO	Forkhead box transcription factor
GTP	Guanosine triphosphate
IMM	Inner mitochondrial membrane
L1-3	Drosophila larval instars 1-3
Ldh	Lactate dehydrogenase
mRNA	Messenger RNA
mRpS12	Mitoribosomal small subunit protein S12
mtDNA	Mitochondrial DNA
NAD	Nicotinamide adenine dinucleotide
NADP	Nicotinamide adenine dinucleotide phosphate
nDNA	nuclear DNA
NRF	Nuclear respiratory factor
Nrf	Nuclear factor erythroid 2-related factor 2
OMM	Outer mitochondrial membrane
OXPHOS	Oxidative phosphorylation
PGC	Peroxisome proliferator-activated receptor gamma coactivator
Rheb	Ras homolog enriched in brain
RNA	Ribonucleic acid
ROS	Reactive oxygen species

ORIGINAL PUBLICATIONS

This thesis is based on the following original communications, referred to in the text by their roman numerals I-IV.

I.   Kemppainen E, George J, Garipler G, Soga T, Dunn C, Tuomela T, Kiviranta E, Jacobs HT. Mitochondrial dysfunction plus high-sugar diet provokes a metabolic crisis that inhibits growth. *Plos One*. 2016 Jan 26; 11(3): e0151421. doi: 10.1371/journal.pone.0145836.

II.   George J, Tuomela T, Kemppainen E, Nurminen A, Braun S, Yalgin C, Jacobs HT. Mitochondrial dysfunction generates a growth-restraining signal linked to pyruvate in *Drosophila* larvae. *Fly*. 2019 Sep 17; 13(1-4): 12-28. doi: 10.1080/19336934.2019.1662266.

III.   George J, Jacobs HT. Minimal effects of *spargel* (*PGC-1*) overexpression in a *Drosophila* mitochondrial disease model. *Biology Open*. 2019 Jul 19; 8(7): bio042135. doi: 10.1242/bio.042135.

IV.   George J, Jacobs HT. Germline knockdown of *spargel* (*PGC-1*) produces embryonic lethality in *Drosophila*. *Mitochondrion*. 2019 Aug 29; 49: 189-199.

1 INTRODUCTION

Throughout the complex processes of growth and development in multicellular organisms, robust coordination between mitochondrial and nuclear gene expression is essential to obtain a fully differentiated and functioning individual. Mitochondria are double-membrane bound, filamentous organelles that are central components in cellular metabolism, with multiple catabolic and anabolic pathways converging on the TCA cycle and the electron transport chain (ETC). These metabolic processes form a chain of reactions whose most well-known function is the conservation of chemical energy in the form of ATP. ATP production is crucial for the numerous energy-requiring reactions of life, including the absorption and processing of nutrients required for the creation and maintenance of new tissue during growth and development. In addition, glycolysis and the TCA cycle are central hubs for fatty acid and amino acid synthesis, providing some of the basic components required by differentiating and growing tissues. In turn, anaplerotic reactions also use nutrients and energy to feed the TCA cycle, to perpetuate this essential metabolic activity throughout an organism's lifetime. The core protein components of the TCA cycle and the ETC must therefore be expressed accurately and in synchrony with environmental cues, such as nutrient availability and temperature, so that growth and development can progress unabated and in an optimal fashion.

Mitochondria contain a DNA genome (mtDNA) encoding a core set of proteins necessary for mitochondrial oxidative phosphorylation (OXPHOS). The genes of mtDNA encode subunits of the protein complexes of the ETC and ATP synthase, as well as transfer RNAs (tRNAs) and ribosomal RNAs which contribute to protein subunit synthesis on intramitochondrial ribosomes. These genes are few in number (37 in human mtDNA) and, whilst important, they are insufficient alone to support the many functions of mitochondria. Therefore, within the nuclear genome, over 1000 genes encode proteins required for mitochondrial function. Their expression must be regulated to ensure sufficient mitochondria are produced to maintain organismal homeostasis throughout development. 'Cross-talk' between mtDNA and nuclear DNA must also ensure that expression of the relevant nuclear genes matches that of mtDNA.

One proposed method of co-regulating nuclear and mitochondrial gene expression is through the action of transcriptional coactivators. Whilst transcription factors interact directly with genomic promoters and enhancers to regulate gene expression, transcriptional coactivators interact with the transcription factors themselves (often many different transcription factors) to enact a broader reach in the regulation of gene expression than a single type of transcription factor can perform in isolation. The PGC-1 family of proteins are a set of transcriptional coactivators previously implicated in the regulation of mitochondrial genes. They aid multiple transcription factors by recruiting chromatin remodelling proteins and altering the expression of hundreds of genes. What's more, multiple post-translational modifications of the PGC-1 transcriptional coactivators integrate nutrient status and energy demand to regulate mitochondrial gene expression in growth and development according to environmental cues. Many of the genes that the PGC-1 family regulate have a direct impact on the rate of mitochondrial transcription.

As the accurate regulation of mitochondrial activity during growth and development is so important, severe consequences can occur when things go wrong. Many mitochondrial genes, if mutated, result in lethality during very early stages of development. Mitochondrial mutations that are not lethal during embryogenesis can still result in severe pathology in later life. Mitochondrial ribosomal (mitoribosomal) proteins are no exception and their mutation may lead to early lethality or common mitochondrial pathologies. Failure to sufficiently translate the few (yet crucial) genes expressed by mtDNA leads to decreased function of the ETC and to multiple repercussions throughout the inextricably linked metabolic pathways centered on the TCA cycle and ETC. This in turn impinges on growth and development.

The work outlined in this thesis makes extensive use of a *Drosophila melanogaster* mitoribosomal mutant to elucidate some of the metabolic changes that result. Particular consideration is paid to the intriguing effect on pyruvate metabolism. The potential of the *Drosophila* transcriptional coactivator and PGC-1α homologue *spargel*, to alleviate the developmental phenotype of this mitoribosomal mutant, is analysed and the findings are followed up by scrutinising the role of *spargel* in early *Drosophila* growth and development.

2 REVIEW OF THE LITERATURE

In the 'omics' era of modern biology, large and complex datasets often lead us to think in terms of broad distinctions between the different levels at which physiology is analysed: the genome, its transcriptional readout, proteins and metabolites. In the real world of living organisms, such neat compartmentalisation of cellular dynamics is non-existent. Cascades of complex expression at the transcript level are inseparably intertwined with and regulated by genomic packaging and protein-based signalling, setting up the environment for complex enzymatic and metabolic processes which themselves then feed back to influence RNA expression profiles. This cycling specifies vast networks of pathways of proteins, nucleic acids and metabolites in constant interaction between multiple tissues and with the organism's environment. Such dynamic complexity is a product of millions of years of evolution. It is always important to keep such complexity in mind when we reduce pathways, transcriptional units and protein complexes into neatly labelled boxes in an attempt to make their study more approachable and succinct. This complexity should not deter biologists; indeed, during recent history, we have made great strides through the application of cleverly conceived experiments, in starting to elucidate precisely how these integrated pathways relate to our physiology and, indeed, pathophysiology.

This thesis tackles questions concerning growth and developmental programmes with particular emphasis on mitochondrial metabolism. The experiments within look at how differences in pyruvate metabolism can impact on whole organismal development and how this links to perturbed metabolism in the context of mitochondrial translational disease. This thesis also looks at the involvement of transcriptional regulation and transcriptional coactivators in regulating mitochondrial biogenesis, both in the context of mitochondrial translational disease and in early growth and development. To provide insights into these topics, *Drosophila melanogaster*, discussed in depth in the next sections, was used as a model for observations of cellular metabolism, transcription and of organism-wide growth and development.

2.1   *Drosophila melanogaster* as a model organism

Due to derivation from a common ancestor, fundamental biological mechanisms are shared between all known life forms. This applies to "simple" single-celled organisms, right through to more complex multicellular and multi-tissued humans. Somewhere in between these two extremes lies the fruit fly *Drosophila melanogaster*. The fruit fly contains comparable intra-cellular architecture to a single-celled eukaryote, with similar cellular machinery, and a similar metabolome, genome, transciptome and proteome. Fruit flies have multicellular complexity not too different from that of humans, with differentiated tissue types such as neurons, epithelia, fat and muscle; and with organs such as a gut, eyes and brain; all of which make these animals familiar to humans. Due to their ease of handling, short life cycle, plentiful progeny and genetic tractability, *Drosophila* have been used as model organisms in the lab for over 100 years. Such popularity has led to vast online databases of shared knowledge on *Drosophila* biology, further aiding biological research. *Drosophila* has been used to gain insights into basic biology, that are interesting for their own sake, but can also translate to humans and can have tangible consequences on how we understand and further study human biology.

Over 3 days at 25°C the *Drosophila* larva grows to 200-fold the dry mass of its embryo beginnings (Robertson, 1936; Tennessen et al., 2011; Thompson et al., 1976). This happens consistently for the majority of the hundreds of eggs that an adult female can lay, requiring the accurate regulation of transcriptional and metabolic programmes for normal development (Koyama et al., 2020; Robertson, 1936). The conservation of metabolic pathways in humans and *Drosophila* means that *Drosophila* can be used as a tool to study these pathways in varied contexts (Boulan et al., 2015; Doane, 1961; Musselman and Kühnlein, 2018; Reiter et al., 2001). For example, during the larval stages, the rapid growth mentioned above is predominantly fuelled by glycolysis, allowing exploration of how the altered metabolism of glycolytic products, such as pyruvate, impact on the programme of growth (Bricker et al., 2012). Each stage of the *Drosophila* life cycle (**Fig 1**) has a different requirement of nutrients and is defined by differential growth and metabolism. During embryogenesis maternally deposited nutrients are used, at this stage mainly for the process of cell differentiation, in coordinated programmes of metabolism (Tennessen et al., 2014). As mentioned above, larval stages are mainly a period of feeding and growth with glycolysis providing the necessary ATP (Tennessen and Thummel, 2011). Pupal stages are a period of no feeding and thus the pupae rely on stored nutrients for the well-regulated steps of metamorphosis

(Bäkker, 1959; Slaidina et al., 2009). Then the adult stages are mainly defined by eating and mating to produce the next generation of offspring with particular need for nutrient uptake in the female for the process of oogenesis

Together, the different stages of the *Drosophila* life cycle and the tractability of *Drosophila* as a model organism, provide opportunities to study the tight coupling of metabolism, growth and development. It follows that *Drosophila* are increasingly used to elucidate the mechanisms of growth and metabolism (Tennessen and Thummel, 2011). Regarding the use of *Drosophila* for this purpose, this thesis is no exception. The experiments in this thesis concern the perturbation of pyruvate metabolism, and the alteration of mitochondrial biogenesis transcriptional programmes, during *Drosophila* growth and development as well as in the context of mitochondrial translational disease. As such, knowledge of *Drosophila* and the metabolic programmes during *Drosophila* development are required. The following sections discuss, in detail, the *Drosophila* life cycle and the metabolic regulation involved at each step.

2.1.1 *Drosophila* life cycle
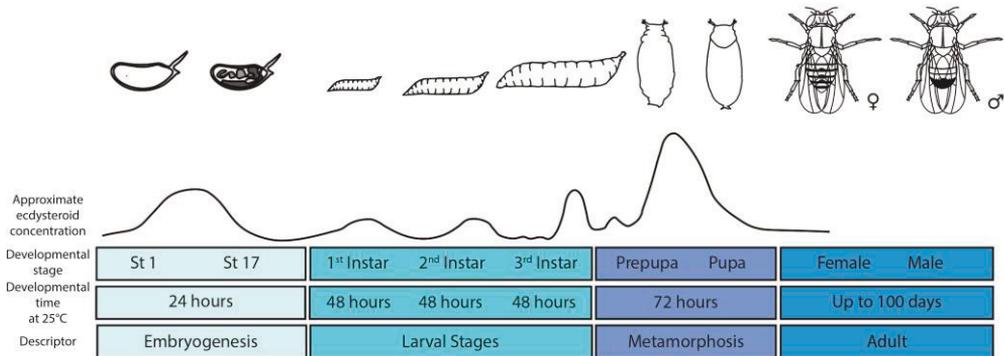
Figure 1. The life cycle of *Drosophila melanogaster*. At 25°C, fertilised *Drosophila* embryos take approximately 24 hours to transition from stage 1 (St 1) with a single nucleus, to stage 17 (St 17) where a fully differentiated embryo is formed, in a process known as embryogenesis. The embryo then hatches to become a 1st instar larva and undergoes a series of moults over 6 days at 25°C, going from 1st instar to 3rd instar larval stage before wandering to an area devoid of moisture and food to pupariate. Pupation at 25°C takes 72 hours, during which imaginal discs and tissues fully transform into adult tissues in a process called metamorphosis. Each transition stage during the *Drosophila* life cycle is associated with a peak in the steroid hormone ecdysteroid. Abitrary, relative, whole body titre levels of the ecdysteroid 20E-ecdysone are represented by the black line, adapted from (Kozlova & Thummel, 2000, Figure 1). *Own image*.

2.1.2 *Drosophila* oogenesis

Before an individual adult *Drosophila* can develop from a single fertilised egg, this egg must be formed in a process known as oogenesis (McLaughlin and Bratu, 2015; Swevers et al., 2005). Each *Drosophila* ovary, seen in (**Fig 2A**) as a pair of ovaries, contains 16-20 ovarioles. A single ovariole is depicted in (**Fig 2B**). The starting point of an ovariole, located toward the anterior end of an adult female's abdomen, is the terminal filament (**Fig 2C**). The terminal filament is a stack of 8-9 disc-shaped somatic cells, forming during late L3 instar stage and fully formed upon pupariation (Sahut-Barnola et al., 1995). The terminal filaments are adjacent to the germarium. The germarium is made up of four principle regions: 1, 2a, 2b and 3 (**Fig 2C**)(Bastock and St Johnston, 2008). At the anterior end of region 1, a niche of germline stem cells (GSCs) can be found, derived from primordial germline cells of the maternal embryonic gonad.

Approximately 48 hours after pupariation the ovaries are mature and the GSCs start to divide asymmetrically, with one progeny cell retaining stemness and the other becoming a cystoblast. Cystoblasts divide by incomplete cytokinesis 8 times, creating a cystocyte complex of 16 connected cells which then form part of region 2A of the germarium. Of these 16 interconnected cells, one is determined as the oocyte, and the others become the 'nurse cells' which grow and provide materials such as mRNA and organelles to the developing oocyte. Throughout this development in the germarium, a specialised support organelle, the fusome, helps synchronise cystoblast asymmetric mitoses, enables cell-cell communication and aids in the determination of the oocyte (Lighthouse et al., 2008). This prefollicular cystocyte is then ensheathed in a layer of follicle cells, becoming an egg chamber in region 3 of the germarium before passage into the vitellarium as a follicle. The vitellarium is a series of interconnected egg chambers, progressively developing and moving towards the oviduct through the peristaltic action of a muscular actin sheath, in a series of 14 distinct stages before being expelled into the oviduct where they are fertilised before being laid (King, 1975; Swevers et al., 2005).

In the vitellarium, the egg chambers transition from a previtellogenic to a vitellogenic state where they endocytically uptake yolk proteins from follicular cells and the fat body and the oocyte starts to grow, supported by nurse cells (Raikhel and Dhadialla, 1992; Swevers et al., 2005). This process is dependent on insulin signalling, with mutants in the *Drosophila* insulin receptor substrate *chico*, and the insulin signalling downstream effector *ribosomal protein S6 kinase* (*S6K*), showing drastically

decreased egg production and subsequent female sterility (Böhni et al., 1999; Montagne et al., 1999).

Drosophila have polytrophic meroistic ovaries, meaning that at each stage of ovarian follicle development, oocytes are connected to support or 'nurse' cells via actin ring canals, through which much of the material that will make up the fully formed embryo is passed (McLaughlin and Bratu, 2015). The polyploid nurse cells produce determinants that are distributed differentially within the oocyte and determine pattern formation in the early embryo (discussed below in **section 2.1.3**). Nurse cells also transfer organelles in a balbiani body-like compartment, a mass of golgi, endoplasmic reticulum, mitochondria, germ plasm and RNAs, into the oocyte, particularly during nurse cell dumping at stage 11 of follicular development (Cox and Spradling, 2003). After nurse cell dumping, the nurse cells undergo non-apoptotic programmed cell death and are degraded, with the remnants removed by follicular cell phagocytosis (Timmons et al., 2017). The oocyte is then coated in a vitelline membrane and a triple-layered chorion for protection and adequate gas exchange during embryogenesis (Velentzas et al., 2018)
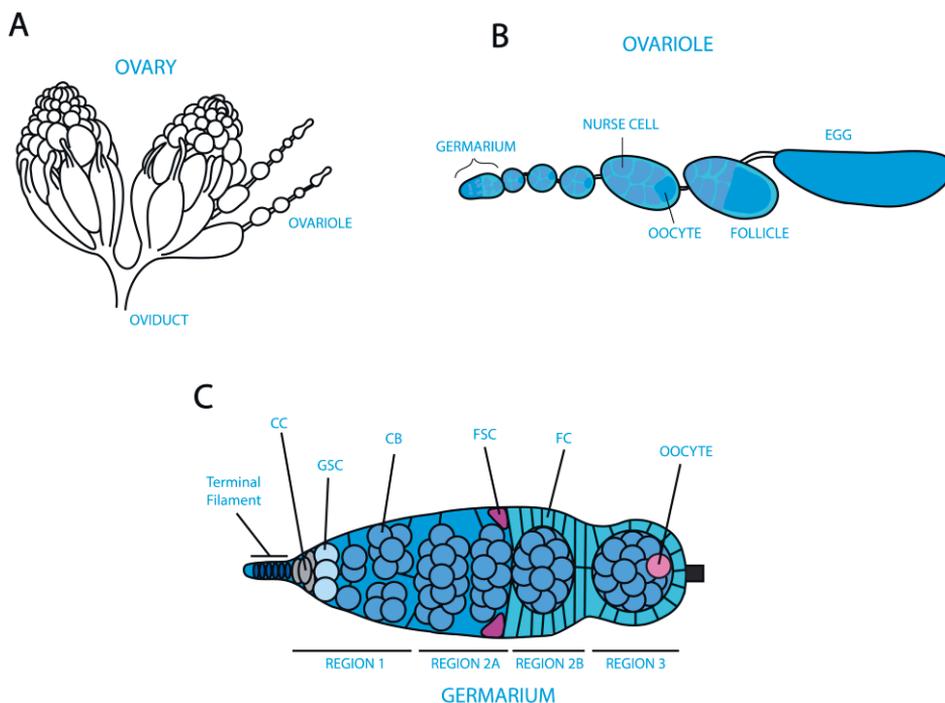
Figure 2. ***Drosophila melanogaster* ovaries. A)** A pair of *Drosophila* ovaries, with each ovary containing from 16-20 ovarioles. **B)** A single ovariole containing follicles in various stages of development, each containing an oocyte supplied with nutrients, nucleotides and organelles by the adjacent nurse cells, before forming an egg. **C)** The germarium. At the anterior most part of the germarium, the terminal filament contains a set of terminal filament cells, which sit adjacent to cap cells (CCs) and germline stem cells (GSCs) marking the start of region 1. Region 1 contains dividing cystoblasts (CBs) which undergo incomplete cytokenisis to form a cystocyte within region 2A. At the edge of region 2B sit follicle stem cells (FSCs) which divide to ensheath the developing cystocyte complex in a layer of follicle cells (FCs) as seen in region 2B, before being passed into the vitellogenic section of the ovariole as an egg chamber in region 3, by the peristaltic action of a surrounding muscular sheath. The posterior most cystoblast becomes the oocyte of that cystoblast complex, which will be fed by the other CBs which develop to become nurse cells. **A** adapted from (Pinto, 2009), **B** adapted from (Uryu et al., 2015) and **C** adapted from (Silva and Jemc, 2015).

2.1.3   *Drosophila* embryogenesis

When the *Drosophila* embryo is oviposited (laid) onto food, it contains a single nucleus surrounded by yolk within a vitelline membrane and outer chorion. During

embryonic cleavage, this nucleus divides 13 times in a common syncytial cytoplasm, giving rise to thousands of nuclei before cellularisation. Enmeshed in a network of microtubules, the nuclei then migrate to the periphery of the embryo where they form a syncytial blastoderm in a cytoskeletal rich layer (Karr and Alberts, 1986). At this point, the cells each become cellularised by enclosure in a membrane, and a series of furrows is formed based on a maternally determined pattern of proteins, which start to define the morphology of the developing embryo as cells begin to differentiate into specific tissue types. These proteins include maternal effect genes such as *hunchback, bicoid, caudal* and *nanos*, which specify cellular identity along the anterior-posterior (A-P) axis of the embryo. These and other maternal effect genes, synthesised and loaded by the nurse cells during oogenesis (see **section 2.1.2**), control the polarity and organisation of both the A-P and dorsal-ventral (D-V) embryonic axes (Nüsslein-Volhard and Wieschaus, 1980; Nüsslein-Volhard et al., 1987). Along the A-P axis, their presence determines the precise expression of a further set of gap genes. The gap genes then go on to regulate the expression of pair-rule genes. In turn, gap and pair-rule genes regulate two clusters of homeobox genes on chromosome 3, which specify body position and where appendages (halteres, antennae legs etc.) will form (McGinnis et al., 1984). Thereby, the cascade of embryo development is set in motion, with compartmentalisation effectively defined right from the single nucleus stage (Nüsslein-Volhard and Wieschaus, 1980).

Cleavage, blastoderm formation and cellularisation take only 3 hours at 25°C and encompass 1-5 of 17 well-documented embryonic stages. Briefly, stages 6-17 involve the following steps: gastrulation, with mesoderm and endoderm formation within the ectoderm, and invagination of the ventral furrow; germ band elongation and retraction; differentiation and organ development; head involution and tracheal filling; before finally the muscles start to contract and the embryo hatches as a 1st instar larva. This whole process takes only 22 hours at 25°C (Campos-Ortega and Hartenstein, 1985).

Due to the absence of feeding during embryogenesis, the embryo must rely on its stores of triacylglycerol (TAG) and glycogen, as well as stored lipids in the yolk, to undergo the developmental processes outlined above. During the first twelve hours of embryogenesis, the embryo relies on anaerobic glycolysis. Using TAG and glycogen stores gradually generates glycerol-3-phosphate, coinciding with an embryonic transition to aerobic glycolysis, seen as a significant increase in the expression of glycolytic genes, lactate dehydrogenase, β-oxidation, TCA cycle and genes for other mitochondrial enzymes after the 12-hour time-point of embryogenesis at 25°C (Tennessen et al., 2014). After steadily depleting these

maternally supplied nutrient stores the fully developed embryo contracts and hatches through the operculum of the chorion, with developed mouth hooks, ready to seek out further sources of food.

2.1.4 *Drosophila* larval stages

The 1st, 2nd and 3rd instar larval stages are primarily defined as a period of feeding and growth with massive increases in fat, protein, RNA and DNA content (Boulan et al., 2015; Church and Robertson, 1966). The two transition stages, which see the larvae moult their mouth parts and skin, are controlled by waves of 20-hydroxyecdysone (20E) steroid hormone production (Tennessen and Thummel, 2011; Warren et al., 2006; ecdysone signalling is discussed in more detail in **section 2.1.7**). The larval stages also see the maturation of 19 imaginal discs, a set of precursor structures that will become the external appendages (halteres, antennae legs etc.) of the adult 'imago' (Cohen et al., 1993). Imaginal, non-disc, histoblast nests also develop during the larval stages and will become abdominal epithelial, gut and salivary gland cells in the adult (Curtiss and Heilig, 1995; Simcox et al., 1991). The fat body is an essential larval organ controlling maturation and development of the imaginal discs. The fat body is the *Drosophila* equivalent of mammalian adipose tissue and liver, storing energy in the form of TAG and glycogen, secreting hormones and regulating metabolic processes in response to nutrient uptake (discussed in **section 2.2.2**). The mutation and decreased expression in the fat body of the genes *minidiscs* and *slimfast* causes imaginal disc growth defects, delays growth of the larva and can result in developmental arrest (Colombani et al., 2003; Martin et al., 2000), a phenotype mediated by the dTOR signalling pathway (Zhang et al., 2000).

The larval fat body is an essential component in reaching 3rd instar critical weight, the weight at which larvae become committed to wandering (the exit from the food source to find a suitable pupation site) and to pupa formation (Beadle et al., 1938; Mirth et al., 2005). Upon feeding, larval fat body growth is regulated by insulin signalling, with circulating *Drosophila* insulin-like polypeptides (dILPs) binding insulin receptors and triggering a cascade that results in cell growth, glycogenosis and lipogenesis whereupon lipids are stored in the fat body (Britton et al., 2002; insulin signalling is discussed in more detail in **section 2.2.3**). Intrinsic fat body dTOR signalling feeds back to DILP production in the insulin-producing cells, stemming DILP production in times of starvation, whilst a humoral signal, stimulating DILP production, is released by the fat body in times of nutrient abundance (Géminard et

al., 2009). Insulin signalling regulated by the fat body, in turn controls the size of the prothoracic gland, which will only release low pulses of ecdysone to signal larval cessation when it reaches a certain size (Mirth et al., 2005). Thus, the 3rd instar larva responds to its nutrient environment, only committing to wandering and pupal formation when it has reached a certain level of growth and nutrient storage (Tennessen and Thummel, 2011).

2.1.5   *Drosophila* pupal stage

Larvae wander away from food to a position devoid of moisture, in order to undergo pupation. An initial pupariation phase, the onset of which corresponds with a peak in ecdysone level, sees the larval cuticle become the pupal case as the inner epidermis retracts. The imaginal discs begin to evert, forming the external appendages, whilst head eversion begins the pupal stage (Bainbridge and Bownes, 1981; Robertson, 1936). During the pupal stage, the final cell divisions take place, the legs and wings extend, and the majority of larval tissues undergo histolysis being replaced by the developed adult tissues (Bainbridge and Bownes, 1981; Robertson, 1936). Pupation represents an extended period without feeding, with an intense energy demand for the various processes of metamorphosis. Once again, the fat body and insulin signalling play a pivotal role, providing regulated growth and development during this period of starvation. The fat body produces and secretes DILP6 under the transcriptional control of FOXO, which relays a growth signal during this period of non-feeding (Slaidina et al., 2009). The end of pupation sees the contraction of the newly formed imago and the adult *Drosophila* emerges through the operculum of the pupal case.

2.1.6   *Drosophila* adulthood

Adult *Drosophila* can live up to 100 days with a lifespan heavily determined by environmental factors, notably diet. Low-nutrient diet generally leads to decreased insulin signalling, resulting in an increase in median lifespan (Giannakou et al., 2004). Despite its relatively long lifespan, *Drosophila* reaches reproductive maturity within the first day following eclosion. Males become sexually active a mere 2 hours after eclosion and females are receptive to courtship 8 hours post eclosion. Larval-derived fat body tissue is essential for the maturation of ovaries in female adults, with programmed cell death of larval-derived adipose cells releasing nutrients for uptake

into the developing ovarioles (Aguila et al., 2013). Well-fed female *Drosophila* can lay up to 100 eggs per day with peak egg laying occurring in the first ten days and then a gradual decline until cessation toward the end of life (Partridge and Fowler, 1992)

2.1.7 Ecdysone signalling

As indicated above, ecdysone signalling is a critical regulator of the transitional phases of *Drosophila* development. Ecdysone signalling is dependent on and regulated by nutrient sensing (Mirth and Shingleton, 2012). The prothoracic gland (PG), is an endocrine gland located in the head of the fly where the 'Halloween' series of cytochrome P450 enzymes convert cholesterol into ecdysone (Boulan et al., 2015; Gilbert and Warren, 2005). From there, ecdysone is secreted into the haemolymph in regulated pulses and converted into the active form, 20-hydroxyecdysone (20E) in peripheral tissues (Warren et al., 2006). 20E then acts through a nuclear receptor, a heterodimeric complex of Ultraspiracle (USP) and Ecdysone receptor (EcR; Thomas et al., 1993). This receptor promotes the necessary gene-expression changes to facilitate each of the ecdysone-dependent transition stages throughout the *Drosophila* life cycle. As mentioned above, ecdysone production requires cholesterol. Also, PG size (and therefore function) is regulated by insulin and target of rapamycin (TOR) signalling (Mirth and Shingleton, 2012). Thus, ecdysone signalling is inherently linked to feeding and nutrient sensing. This means that *Drosophila* only progresses into the next stage of development when threshold levels of feeding criteria have been met (Edgar, 2006; Tennessen and Thummel, 2011).

2.2 *Drosophila* metabolism

The above sections dealt with the stages of growth and development in *Drosophila melanogaster*, and its reliance on energy storage metabolites such as TAG and glycogen, as well as the need for glucose and accurate insulin signalling. However, the developmental programme of *Drosophila* requires correct regulation of the full metabolic programme including many metabolic pathways which have yet to be discussed in detail. As such, the following sections will outline some of the crucial metabolic pathways involved in accurate growth and development in *Drosophila*, with particular focus on those pathways implicated in the experimental and results section of this thesis.

2.2.1 Growth and nutrient sensing

Crucial to the correct onset and regulation of ecdysone signalling is the ability of *Drosophila* to sense and adapt to the availability of nutrients in the environment, relaying such signalling through core networks of proteins, such as the insulin signalling pathway (discussed in **section 2.2.3**), which subsequently directs the activity of the TOR (target of rapamycin) pathway. The ability to sense nutrient status allows optimised utilisation of the chemical energy and building blocks that these nutrients provide, which subsequently permits accurate growth throughout all stages of development.

The highly conserved TOR pathway converges on two major complexes, TOR complex 1 (TORC1) and TOR complex 2 (TORC2). Essential subunits such as Raptor (in TORC1) and Rictor (in TORC2) enable TOR kinase activity in response to insulin, Wnt and growth factor receptor signalling (Dos et al., 2004; Gao and Pan, 2001; Kim et al., 2002). The Insulin receptor (InR) mediates a signal through Akt, which phosphorylates the TSC1/TSC2 complex, alleviating its inhibitory activity upon TORC1 (Kim et al., 2002). TOR kinase activity can then exert its regulatory activity through numerous downstream effectors, including S6K and the eukaryotic translation initiation factor 4E binding protein (4E-BP). S6K phosphorylates a series of translation initiation factors and regulators thereof, and 4E-BP also regulates translation initiation, both acting to control ribosomal activity and growth (Gingras et al., 1999; Holz et al., 2005). Other downstream effectors of the TOR pathway include CAD (carbamoyl-phosphate synthetase 2, aspartate transcarbamoylase, dihydroorotase), an enzyme required for de-novo pyrimidine synthesis (Ben-Sahra et al., 2013) and, also, sterol responsive element binding protein (SREBP1), a transcription factor regulating lipogenesis (Porstmann et al., 2008). Through these mechanisms and more, the TOR pathway can link the nutrient status of a cell to the promotion or inhibition of growth through ribosomal activity, nucleotide synthesis and lipid biosynthesis.

TOR activity is further fine-tuned by the energy and amino acid status of the cell. Through its reliance on the adenylate charge, the AMP-activated protein kinase (AMPK) complex can sense and react to a low ATP/AMP ratio by increasing TSC1/TSC2 suppression of TORC1 activity and phosphorylating Raptor to further inactivate TORC1 (Gwinn et al., 2008; Yeh et al., 1980). In this manner, AMPK permits a metabolic shift to increased catabolism and decreased biosynthesis when ATP is not being produced in sufficient quantity. When sufficient amino acids are present, they cause Rag GTPases to bind Raptor and thereby recruit TORC1 to the

lysosomal membrane. Rheb, necessary for TOR kinase activity, is only present on the lysosomal membrane and therefore, TORC1 will only be activated if sufficient amino acids are present (Kim et al., 2008). Once again, this mechanism means the cell will only expend nutrients and energy on anabolism and growth if amino acid precursors are present in sufficient amounts.

2.2.2   Sugar consumption and metabolism

An artificial mix of the disaccharide sucrose and the monosaccharides glucose and fructose are often used as dietary sugars in *Drosophila* experiments. The use of sucrose, glucose and fructose in the laboratory is, of course, an informed decision based on several historical studies showing, among other things, the ability of *Drosophila* to survive solely on these sugars (Hassett, 1948) and that these sugars support the resumption of flight ability in flight-exhausted *Drosophila* (depleted of glycogen), compared to the inability of other sugars such as arabinose and xylose (Wigglesworth, 1949). In nature, it is unsurprising then, that there is a nutritional preference for *Drosophila* to consume rotting fruit containing high levels of sucrose, glucose and fructose (Burke and Waddell, 2011).

Once consumed, complex macromolecules are broken down into constituent parts, including sugars, by a large number of region-specific digestive enzymes in the gut of *Drosophila* (Dutta et al., 2015). Such enzymes include as many as 52 carbohydrases, encompassing amylases, trehalases, glucosidases, mannosidases and others, acting in a regulated manner to break down complex polysaccharides into simples sugars (Lemaitre and Miguel-Aliaga, 2013). In its most basic form, the intestine of *Drosophila* is made up of the foregut, midgut and hindgut. The midgut is the most extensively studied region of the *Drosophila* intestine and the main site of digestion and nutrient absorption (Miguel-Aliaga et al., 2018). A microbiome of low diversity (relative to mammals) can compete for dietary sugar and alter sugar absorption and the consequent metabolism of flies (Huang and Douglas, 2015). If not taken up by the commensal microbiota, sugars are absorbed by the intestinal epithelium. Along the length of the intestinal epithelium are varying compositions of a core set of four major cell types: intestinal stem cells (ISCs), enteroblasts (EBs), hormone secretory enteroendocrine cells (EEs) and the absorptive enterocyte cells (ECs). Sugar absorption is performed by a diverse set of facilitative transporters, whose function has remained surprisingly unexplored in *Drosophila* (Miguel-Aliaga, 2012). Sugar transporters in *Drosophila* have primarily been characterised through

homology, such as with the *SLC2A1* (GLUT1) homologue, *Dmglut1* (Escher and Rasmuson-Lestander, 1999; Miguel-Aliaga et al., 2018). Recent work has shown that knocking down the GLUT6/GLUT8 homologue *CG4607* leads to starvation sensitivity in *Drosophila* (Bevers et al., 2019). However, more work on functionally characterising these sugar transporters, given the ease of diet manipulation studies in *Drosophila*, could bring greater insight into varied individual responses to similar diets and genetic predispositions to conditions that resemble metabolic syndrome, diabetes and obesity (Baker and Thummel, 2007). At the junction of the midgut and the hindgut, the *Drosophila* Malpighian tubules, considered to be the functional equivalent of the mammalian kidney, show an enriched level of sugar transporters compared to the rest of the fly, suggestive of a role in sugar uptake and excretion (Wang et al., 2004).

Different source sugars cause differing metabolic effects upon consumption, as evidenced by the mounting concern over the use of high fructose corn syrup (HFCS) and its negative health consequences in humans (Stanhope et al., 2013). In *Drosophila,* high-glucose diets were found to cause higher mortality, while high-fructose diets, although better tolerated, caused obesity through an increase in glycogen and triacylglyceride (TAG) storage (Rovenko et al., 2015a). The difference in metabolic profile after consuming either glucose or fructose could be due to several reasons. For instance, glucose and fructose enter the glycolytic pathway at different steps. Glucose enters upon conversion into glucose-6-phosphate by hexokinase. Isomerisation then converts glucose-6-phosphate to fructose-6-phosphate. Fructose-6-phosphate is then phosphorylated once more, in a rate-limiting step, by the activity of phosphofructokinase (PFK), into fructose-1,6-bisphosphate, which is then converted into glyceraldehyde-3-phosphate (GAP) and dihydroxyacetone phosphate (DHAP) by aldolase (Berg et al., 2002). Fructose, on the other hand, bypasses PFK by initially being phosphorylated into fructose-6-phosphate, which is then directly converted into GAP and DHAP by a fructose-6-phosphate specific aldolase (Berg et al., 2002). It is thought that by bypassing the PFK rate-limiting step of glycolysis, fructose is more readily converted into glycogen and TAG storage products by the liver (or fat body in the case of *Drosophila*; Havel, 2005). This could cause the differing metabolic profile of flies fed on fructose versus glucose media (Rovenko et al., 2015a). Once metabolised into GAP and DHAP, sugars are then fully processed through the glycolytic pathway (**Fig 4**) into pyruvate which is then transported into mitochondria where it is processed into acetyl-CoA for use in the TCA cycle (discussed in more detail below).

Glycolysis is, of course, not the only way ingested sugar is metabolised. It is thought that the reductive nature of monosaccharides and their ability to endogenously produce damaging advanced glycation end products (AGEs; Schalkwijk et al., 2004; Tsakiri et al., 2013) necessitates excess circulating sugar, not immediately used by tissues in glycolysis, to be converted and stored as trehalose or glycogen in insects (Yamada et al., 2018). Trehalose (**Fig 3A**) is a disaccharide of two glucose molecules and is the most abundant circulating carbohydrate in *Drosophila* with a larval third instar haemolymph concentration of ∼2000 mg/dl, compared to a glucose concentration of 5–30 mg/dl (Mattila and Hietakangas, 2017; Ugrankar et al., 2015). However, the concentration of trehalose can vary by an order of magnitude in response to environmental insults such as anoxia, cold, desiccation and starvation (Reyes-DelaTorre et al., 2012). In *Drosophila*, trehalose is synthesised by *trehalose-6-phosphate (Tre6P) synthase* (*Tps1*) in the fat body and trehalose transporter 1 (*Tret1*) subsequently excretes it into the circulating haemolymph (Kanamori et al., 2010). Trehalose, as a storage sugar, is brought into use by endocrine hormone signalling in times of need, such as for flight activity (Thorat et al., 2012; Yasugi et al., 2017). Trehalose is fully degraded into two glucose molecules by *trehalase* (*Treh*). An inability to use trehalose for energy, as seen in a null mutant of *Treh*, is not lethal in embryos or larvae but becomes lethal at pupal stage, presumably at a time when there is more reliance on stored energy due to lack of feeding (Yasugi et al., 2017). Glycogen (**Fig 3B**) is a branched-chain polymer of glucose, stored mainly in muscle and the fat body of *Drosophila*, with a crucial role in the homeostatic regulation of circulating trehalose and glucose (Yamada et al., 2018). Glycogen is synthesised from glucose monomers by the action of *glycogen synthase* (*GlyS*). Predictably, knocking down *GlyS* in *Drosophila* causes a decrease in glycogen storage. *GlyS* expression is enhanced by dietary sugar but only up to a certain threshold, beyond which increased sugar does not lead to increased *GlyS* expression (Garrido et al., 2015).

Finally, sugar is also metabolised into triacylglycerides (TAG) (**Fig 3C**), an important lipid whose metabolic functions include energy storage and serving as a building block for phospholipid membranes and signalling molecules (Heier and Kühnlein, 2018; Weiss et al., 1960). TAG are storage products made up of 3 fatty acids (FA) and a glycerol backbone, with an energy content far more concentrated than that of carbohydrates and proteins due to their heavily reduced FA component (Berg et al., 2002; Garrido et al., 2015; Weiss et al., 1960). Under normal feeding conditions, dietary lipids are broken into free fatty acids by lipases in the gut, before they are absorbed across the epithelium into the enterocytes. The enterocytes then work to convert free FA along with glycerol into diacylglycerol (DAG), which is

transported into the hemolymph and circulated by specialised apolipoproteins including the Lipophorin (Lpp) family (Palm et al., 2012). Any excess FA in the enterocytes are converted into intracellular TAG and stored in transient lipid droplets (Palm et al., 2012). In well-fed conditions, much of the circulating DAG is taken up by fat body adipocytes, converted into TAG and stored in lipid droplets (Bickel et al., 2009). When needed, these lipid droplets are mobilised as DAG which is taken up by tissues and converted into a vast array of lipid moieties (Carvalho et al., 2012), or else used to liberate energy within the mitochondria by the process of FA β-oxidation (Schulz et al., 2015). If the fly is starved of fats, then carbohydrates (mainly sugars) can also be converted into lipid products, including DAG and TAG, in the process of *de novo* lipogenesis. This process occurs within enterocytes and adipocytes, where citrate derived from the TCA-cycle (discussed below) is converted into acetyl-CoA. Acetyl-CoA is then converted into malonyl-CoA by Acetyl-CoA-carboxylase (ACC). Finally, malonyl-CoA and further acetyl-CoA are condensed together by the multienzyme FA synthase (FAS) into long-chain FA, able to then form DAG and TAG (Musselman et al., 2013). Sugars are also necessary for the synthesis of the glycerol backbone of DAG and TAG. With this and their role in *de novo* lipogenesis, sugars play a crucial role in fat metabolism.
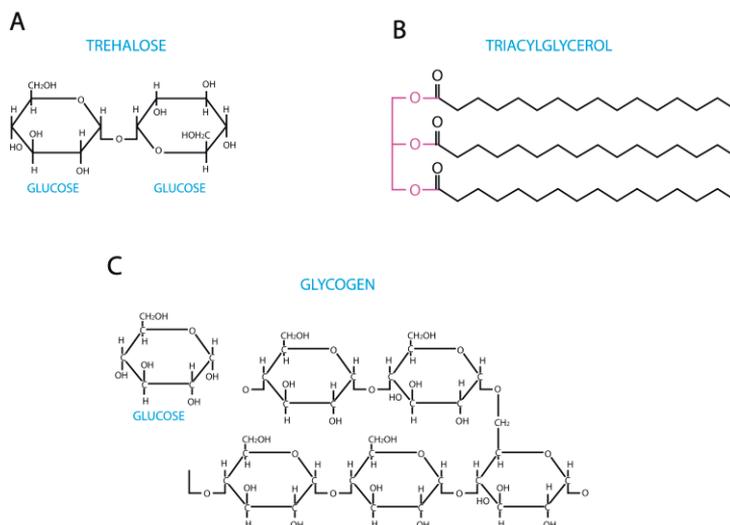
Figure 3. **Nutrient storage compounds.** The disaccharide Trehalose **A)**, made up of two covalently linked glucose moieties, is the most abundant sugar in *Drosophila melanogaster*. **B)** Glycogen is a multi-branched polymer of glucose, found in the fat body of *Drosophila*. **C)** Triacylglycerols (TAGs), consist of a glycerol backbone (shown here in purple) joined to three fatty acid moieties via ester linkages, and are major constituents of the *Drosophila* fat body. *Own image.*

2.2.3   Insulin signalling

One of the main regulatory pathways of the sugar metabolism discussed above is the insulin-glucagon signalling axis, conserved throughout evolution, including in *Drosophila* (Owusu-Ansah and Perrimon, 2014; Partridge et al., 2011). In mammals, starvation causes excretion of glucagon from alpha cells of the pancreas, which causes a subsequent breakdown of the storage products glycogen and TAG (Dean et al., 2017). In response to increased levels of circulating sugar, the mammalian system excretes insulin into the circulation from pancreatic beta cells and triggers anabolic glycogenesis and lipogenesis (Czech and Building, 2018). Mammals also have other insulin like peptides including relaxin and two insulin-like growth factors produced by the liver, which also control growth in response to a high-calorie diet and increased levels of growth hormone (GH) (Nambam and Schatz, 2017). The *Drosophila* system is similar yet has some crucial differences (Padmanabha and Baker, 2014). In *Drosophila* a set of 8 insulin like peptides (dILPs) couples with the major insulin receptor InR in response to sugar. The dILPs are produced primarily in neurosecretory insulin-producing cells (IPCs) of the brain, as well as in other organs throughout development, such as the embryonic mesoderm. Each of the dILPs has different spatiotemporal regulation, with different phenotypes observed upon interruption of their activity (Nässel and Vanden Broeck, 2016). The more recently discovered relaxin-like dILP8 is produced in imaginal tissues of the growing larvae and binds, in addition to InR, to neural Lgr3 receptors, modulating organ growth and development (Colombani et al., 2015). Despite their different regulation according to sufficient nutrition, overexpression of each of the dILPs causes an overweight phenotype in L3 larvae as they each can activate InR (Ikeya et al., 2002). Once InR has been activated by dILPs in response to circulating sugar, it triggers a signalling cascade acting primarily through phosphorylation of the insulin receptor substrates Chico and Lnk. These, in turn, activate Phosphoinositide 3-kinase (PI3K) which phosphorylates Phosphatidylinositols (PtdIns; Teleman, 2010). This subsequently regulates Akt and the TOR pathway, the main nutrient sensing pathway (discussed above in **section 2.2.1**), having direct consequences on translation and transcription of essential growth regulatory genes. One such example involves the phosphorylation of the transcription factor dFOXO, causing its translocation to the cytoplasm, in turn increasing adipogenesis and decreasing gluconeogenesis and glycogenolysis (Luong et al., 2006).

The functional homologue of glucagon in *Drosophila* is the peptide adipokinetic hormone (Akh), secreted from AKH-producing cells (APCs) in the fly corpora

cardiaca (CC) (Ahmad et al., 2019). Akh shows typical signs of glucagon-like activity, mobilising fats and trehalose in starved conditions and responding to sugar levels (Kim and Neufeld, 2015; Kim and Rulifson, 2004). However, the small (eight amino acid) Akh remains understudied, and some experiments have even cast doubt on whether Akh is, in fact, a fully canonical homologue of glucagon, as it is unnecessary for lipid homeostasis during L3 larval stage (Gáliková et al., 2015).

When insulin and glucagon signalling are perturbed from their ordinary course in humans, a cluster of conditions collectively termed 'metabolic syndrome' can present, which often leads to cardiovascular disease or diabetes mellitus. With its conserved central mechanisms of insulin signalling and its versatility as a model organism, *Drosophila* research on metabolic dysfunction has become a widespread and useful tool for studying the underpinnings of these disorders (Baker and Thummel, 2007; Padmanabha and Baker, 2014).

2.2.4   The TCA cycle

The TCA cycle **(Fig 4)** uses acetyl-CoA resulting from the breakdown of glucose, fatty acids or amino acids. Which nutrient source gets used depends on the metabolic requirements and available nutrients within each tissue, during each stage of life. The TCA cycle involves a series of 8 enzymatic steps in mitochondria which generate NADH and $FADH_2$ reducing equivalents, that will subsequently be used in the process of oxidative phosphorylation (OXPHOS), by passage along the electron transport chain (ETC) coupled to ATP generation (see **section 2.3.1**; Cappel et al., 2019; Krebs and Johnson, 1937).

While the emphasis of discussion regarding mitochondrial function and the TCA cycle is often directed at downstream ATP generation from OXPHOS via the electron transport chain (ETC), the TCA cycle also plays another critical role in growth and development. TCA cycle intermediates can be replenished anaplerotically by critical anabolic reactions, either for normal operation of the TCA cycle or for the biosynthesis of cellular components such as glucose, fatty acids and non-essential amino acids in times of need. This is balanced by the cataplerosis of TCA intermediates, which often provides the first step in diverse biosynthesis pathways. Cataplerosis and anaplerosis in differing nutritional states have to be kept in balance to ensure proper growth, development and homeostasis throughout an organism's lifetime (Owen et al., 2002). A significant example is the anaplerosis and cataplerosis of oxaloacetate (OAA). Pyruvate carboxylase converts pyruvate into

OAA in an anaplerotic reaction that can lead to fuelling of the TCA cycle or the conversion of OAA into malate and malate into cytoplasmic pyruvate, replenishing NADPH (see **section 2.2.5**; Bizeau et al., 2001). Conversely, in times of nutrient depletion, OAA can also undergo a cataplerotic reaction catalysed by phosphoenolpyruvate carboxykinase (PEPCK) which converts OAA into phosphoenolpyruvate (PEP), as the first step of gluconeogenesis in the liver (She et al., 2003). The balance of these anaplerotic/cataplerotic pivot points within the TCA cycle provides a means of finely regulating growth and development in response to nutrient excess or scarcity.
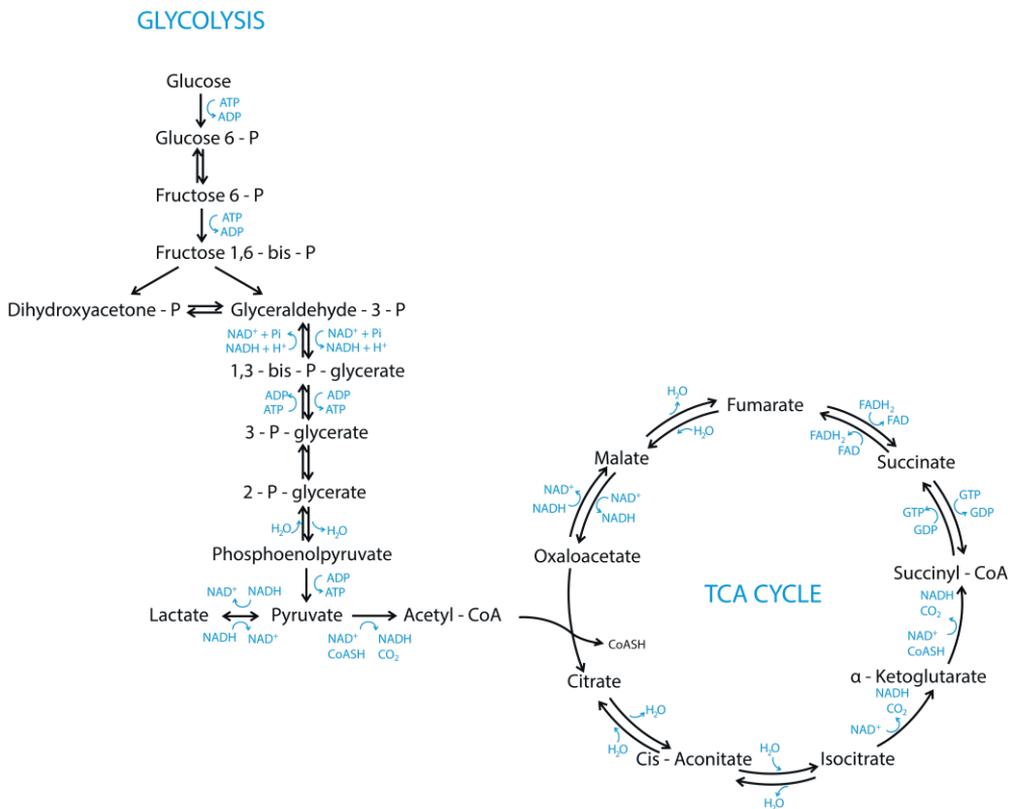
Figure 4. Glycolysis and the TCA cycle. These central metabolic pathways convert sugar into ATP, GTP, and reducing equivalents NADH and FADH$_2$. To store further energy in the form of ATP, NADH and FADH$_2$ are then used by the electron transport chain. In aerobic conditions, glycolysis converts glucose into pyruvate which is then transferred into the mitochondria and converted to acetyl-CoA, which is then used in the TCA cycle as depicted. Adapted from (Alam et al., 2016).

2.2.5   Pyruvate metabolism

A metabolite with multiple fates coupled tightly to nutrient sensing is pyruvate. The central pathways of glycolysis, the TCA cycle and the ancillary pathways that lead off them, such as the pentose phosphate pathway (PPP), amino acid and fatty acid metabolic pathways, the hexosamine biosynthetic pathway (HBP) and more, are all highly conserved throughout evolution, indicating their essential roles in organismal growth and development. These essential roles are no less critical in *Drosophila*, where the disturbance of normal glycolytic and TCA cycle activity is often lethal during development (Wong et al., 2019).

Pyruvate is a pivotal metabolite in the dynamic flux of these central metabolic pathways (**Fig 5**). Pyruvate is the endpoint of glycolysis in the cytoplasm, and its regulation determines whether the cell fully oxidises carbohydrates or relies on further glycolysis for energy; "the Warburg effect" (Olson et al., 2016). The Warburg effect was first described by Otto Warburg in the 1920s when he discovered that cancer cells were able to ferment large amounts of glucose (relative to surrounding tissues) and produce lactate, even whilst oxygen is present (Warburg, 1925). It is now known that this preference for aerobic glycolysis is also present in proliferating cells throughout development, but it is still unknown precisely what advantage this metabolic shift provides proliferating tissues (Liberti and Locasale, 2016). One hypothesis is that proliferative cells, such as cancer cells, adapt their metabolism to better uptake nutrients such as nucleotides, amino acids and lipids, and that 'Warburg-like' aerobic glycolysis is best suited to facilitate this uptake over the whole cell (Heiden et al., 2009). As noted, the Warburg effect has importance in the metabolic phenotype of cancer, where tumour pyruvate levels are consistently increased, and genes involved in pyruvate metabolism are heavily implicated in tumour development (McFate et al., 2008).

During aerobic respiration in mammals, pyruvate kinase (PK) and the pyruvate dehydrogenase complex (PDC) respectively perform the primary production and turnover of pyruvate. In *Drosophila*, as in mammals, two isoforms (M1 and M2) of pyruvate kinase (denoted PyK in *Drosophila*) convert phosphoenolpyruvate (PEP) into pyruvate, phosphorylating one molecule of ADP to ATP in the process (Hsiao et al., 2002). In humans, differential regulation of the M1 and M2 isoforms is observed in multiple tumour types and, along with other adaptations, is thought to potentiate the Warburg effect, again highlighting the importance of correct pyruvate metabolism (Desai et al., 2014). Unsurprisingly, *Drosophila* PyK expression is highly responsive to sugar levels in the diet (Ugrankar et al., 2015). Once pyruvate has been

produced in the cytoplasm, then its majority fate is to be transported into mitochondria for oxidative decarboxylation, yielding ATP and acetyl-CoA for subsequent use in the TCA cycle.

This transport of pyruvate, across the inner mitochondrial membrane (IMM) and into the mitochondrial matrix, is performed in *Drosophila* by a 150 kDa complex, termed the mitochondrial pyruvate carrier (MPC). The MPC found in yeast, *Drosophila* and humans, is made up of two proteins: Mpc1 and Mpc2 (Bricker et al., 2012; Herzig et al., 2012). A mutation in *Drosophila Mpc1* and a consequently decreased pyruvate uptake into mitochondria was shown to render flies sensitive to sugar, with rapid onset of lethality upon transfer to sucrose media (Bricker et al., 2012). This lethality was rescued by wild-type *Mpc1* expression in specific sugar-reliant tissues, including fat body, muscle and neurons. On a normal diet, the *Mpc1* mutant flies were viable but showed increased circulating carbohydrates (trehalose, glucose, glycogen), further suggestive of decreased total carbohydrate catabolism resulting from impaired pyruvate uptake into the mitochondria (Bricker et al., 2012). In a set of families with mutations in *BRP44L* (human *MPC1*), patients presented with lactic acidosis and hyperpyruvatemia (Bricker et al., 2012; Brivet et al., 2003).

In conditions of acute ATP consumption (e.g. during exercise), pyruvate is converted to lactate by *Ldh* to keep pace with energy demand, generating less ATP than full oxidation but in an expedient fashion: meaning that ATP can be quickly generated by glycolysis and provided to energy-requiring muscles. This conversion of pyruvate to lactate also replenishes the NAD+ pool, allowing glycolysis to continue unconstrained. Usually, when a resting aerobic state returns, this lactate is excreted from tissues by monocarboxylate transporters (MCTs) and carried via the blood to the liver, where it is reconverted into glucose by gluconeogenesis. This process is known as the Cori cycle (Sun et al., 2017). As with *MPC1*, when mutations in pyruvate metabolism occur, the Cori cycle is not always sufficient to manage the excess of lactate and therefore lactic acidosis along with hyperpyruvatemia can result. These phenotypes also occur in a broad spectrum of mitochondrial diseases with nuclear and mitochondrial DNA mutations at their root, such as the MELAS syndrome (Alston et al., 2017), as well as mitochondrial rRNA- and tRNA-based translation disorders (Bursle et al., 2017; Ueki et al., 2006, and **section 2.3.3.2**). As with PK, MPC activity is sensitive to glucose levels, this being of particular importance in pancreatic β-cells, in humans, where it has an important role in insulin signalling and secretion (McCommis et al., 2016).

Once in the mitochondria, the PDC converts pyruvate into acetyl-CoA. The PDC is heavily regulated by its phosphorylation status which is modified in response to

nutrient sensing by serine-specific pyruvate dehydrogenase kinases (PDK) and pyruvate dehydrogenase phosphatases (PDP) (Park et al., 2018). PDK activity causes inhibition of PDC, which subsequently decreases the rate at which pyruvate is oxidised into acetyl-CoA, thus decreasing OXPHOS metabolism. The major isoenzyme of PDK is PDK1. Expression of *PDK1* is up-regulated in cancer cells, increasing the inhibition of PDC and, in turn, increasing pyruvate levels (McFate et al., 2008). As such, PDK is another important mediator of the Warburg effect in tumours (Kaplon et al., 2013).

While the Warburg effect results in increased pyruvate and lactate levels and increased glucose consumption through glycolysis (but not the TCA cycle), Warburg posited that these underlying metabolic changes were the direct cause of cancer and not just a by-product of tumorous growth (Warburg, 1956). This is now known as "the Warburg Hypothesis". This hypothesis has since been dampened by the knowledge that mutated oncogenes and tumour suppressor genes, not directly linked to metabolism, are the primary cause of cancer. Nonetheless, the metabolic phenotype of tumours has been of increasing interest as a target for therapeutic strategies (Pavlova and Thompson, 2016), including strategies related to pyruvate. Due to the significance of pyruvate metabolism in developing cancers, altering the regulation of pyruvate has become a prominent target for cancer therapeutics. The best example is the use of dichloroacetate (DCA), an inhibitor of PDK, which thus acts to increase PDH activity and the oxidation of pyruvate, with the aim of reversing the Warburg effect in developing tumours. Although DCA has shown promise as an adjunct to chemotherapy (Olszewski et al., 2010), its therapeutic potential in clinical trials against cancer has so far been limited (Olson et al., 2016). Its crucial role in glycolysis and the TCA cycle is not the only fate of pyruvate (**Fig 5**). Pyruvate derived from glycolysis in muscle is also converted, along with glutamate derived from glutamine, into α-ketoglutarate and alanine by the enzyme alanine aminotransferase (ALT). In mammals, ALT also catalyses the reverse reaction in liver, with pyruvate being created from alanine and α-ketoglutarate, and subsequently used in gluconeogenesis to create glucose. This process is collectively termed the Cahill cycle. Two isoforms of ALT in humans perform these reactions, with the cytosolic ALT1 prevalent in the liver and plasma serum and the mitochondrial ALT2 mainly found in skeletal muscle, heart, pancreas and brain (Glinghammar et al., 2009). Less is known of the Cahill cycle in *Drosophila*.

Pyruvate and malate are interconverted in a pyruvate-malate cycle taking place on both sides of the mitochondrial double membrane (MacDonald, 1995; Pongratz et al., 2007). Malate, produced by anaplerosis in the mitochondria, is exported in

significant amounts into the cytoplasm. In mammals, malic enzyme 1 (ME1) converts cytoplasmic malate into pyruvate in an NADP+ dependent manner, replenishing NADPH levels. Two mitochondrial isoforms of malic enzyme ME2 and ME3 also perform the same reaction within the mitochondria, utilising malate derived from the TCA cycle (Pongratz et al., 2007). ME3 is particularly important for adequate insulin secretion in pancreatic β-cells (Hasan et al., 2015). In *Drosophila* two enzymes; the cytoplasmic malic enzyme (Men) and mitochondrial Men-b, have hardly been studied to date.

In developing organisms, including *Drosophila*, the ability of metabolism to respond dynamically to a wide range of environments is essential. The various modes of pyruvate regulation outlined above are necessary providers of this metabolic flexibility at a nexus point of central metabolism, throughout growth and development (Olson et al., 2016). Pyruvate is a crucial determinant of the activity of enzymatic processes found in mitochondria, double-membraned organelles described in detail in the next section.
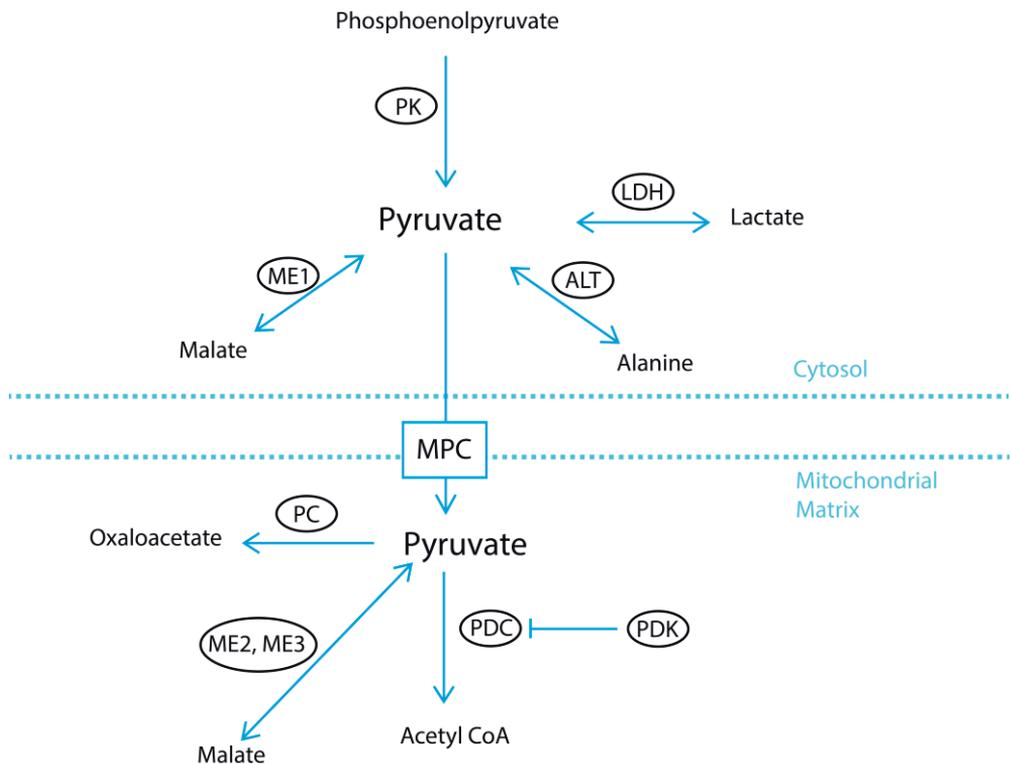
Figure 5. **The multiple fates of pyruvate.** In the last step of glycolysis phosphoenolpyruvate is converted into pyruvate by pyruvate kinase (PK). Pyruvate can then be converted into multiple different metabolites, or derived from multiple metabolites, dependent on cellular metabolic need. The mitochondrial pyruvate carrier (MPC) transfers pyruvate into mitochondria, where it is then converted into acetyl-CoA by the pyruvate dehydrogenase complex (PDC). Pyruvate dehydrogenase kinase (PDK) is able to regulate this conversion by inhibiting the action of PDC. Pyruvate can be converted in the cytoplasm to and from lactate in the Cori cycle by lactate dehydrogenase (LDH). Pyruvate can be converted in the cytoplasm to and from alanine in the Cahill cycle, by alanine transferase (ALT). Pyruvate is converted to malate by malic enzyme 1 (ME1) in the cytosol and the same reaction is performed by malic enzyme 2 and 3 (ME2, ME3) in the mitochondria. Finally, pyruvate can be converted to oxaloacetate in the mitochondria by pyruvate carboxylase (PC). *Own image*.

2.3   Mitochondria

All of the metabolic pathways discussed above rely heavily on correct functioning of mitochondria. The relationship of mitochondria and metabolism is a crucial aspect of the experiments laid out in this thesis. As such, the following sections detail the mitochondrial organelle, transcriptional regulation of mitochondrial biogenesis and

the factors involved, and what happens when mitochondrial function is disturbed, with particular emphasis on disorders of mitochondrial protein synthesis, to which many of the experiments performed and presented in the results section of this thesis are related.

2.3.1   Mitochondrial structure, function and DNA

With only a few exceptions, all known eukaryotes carry mitochondria. The prevailing hypothesis for the evolutionary origin of mitochondria is that the organelle arose out of an ancient endosymbiosis between a bacterial cell, that would go on to become the mitochondria, and a host cell to which it provided a metabolic advantage (Sagan, 1967). Although this theory is now well established, the details of this endosymbiosis are still hotly debated (Cox et al., 2008).

In present-day eukaryotes, tubular units of mitochondria consist of an outer mitochondrial membrane (OMM) enshrouding an inner mitochondrial membrane (IMM) that is organised into multiple folds termed 'cristae'. These cristae form a large surface area of IMM in which are located copies of the transmembrane electron transport chain (ETC). The ETC consists of 5 protein complexes termed, in order from I to V: NADH:ubiquinone oxidoreductase (Baradaran et al., 2013), succinate:ubiquinone oxidoredictase, commonly known as succinate dehydrogenase (Sun et al., 2005), ubiquinol:cytchrome *c* oxidoreductase, commonly known as the cytochrome bc_1 complex (Gao et al., 2003), cytochrome *c* oxidase (Zong et al., 2018) and ATP synthase (Abrahams et al., 1994). In the process known as oxidative phosphorylation (OXPHOS), complexes I-IV, along with ubiquinol and cytochrome-*c*, use the oxidation of TCA cycle-derived NADH and $FADH_2$ to transfer electrons and reduce matrix oxygen to water, while at the same time shuttling hydrogen ions into the space between the IMM and the OMM termed the inter-membrane space (IMS). This hydrogen ion shuttling creates a membrane potential, the energy from which is used by ATP synthase (complex V) to drive the phosphorylation of ADP into ATP, which is then exported throughout the cell for many energy-requiring reactions (Mitchell, 1961). While ATP production is the most well-known function of mitochondria, it is not the only crucial process taking place within these double-membrane organelles. Mitochondria are well known as the site of the essential TCA cycle, which operates within the mitochondrial matrix, creating both NADH and $FADH_2$ for OXPHOS and, equally as importantly, creating carbon precursors for critical biosynthesis of glucose, fatty acids and non-essential amino

acids (see **section 2.2.4;** Owen et al., 2002). In addition, through association with the endoplasmic reticulum (and sarcoplasmic reticulum in muscles), mitochondria provide an essential role in regulating intracellular Ca^{2+} pools which can affect rates of contraction in muscle tissue (Boncompagni et al., 2009). Mitochondrial $[Ca^{2+}]$ can also influence the activity of TCA cycle reactions and subsequent ATP production (Hajnóczky et al., 1995), as well as modulate the Bcl-2, BAX and BAK protein family, regulating mitochondrially induced apoptosis (Scorrano et al., 2003). Furthermore, mitochondria also regulate cell-fate decisions in differentiating cells (Buck et al., 2016) and contain enzymes of the urea cycle, for detoxifying ammonia; plus the heme synthesis pathway, for the assembly of hemoproteins involved in diverse biological roles such as erythropoiesis and xenobiotic detoxification (in mammals, in the liver; Medlock et al., 2015).

The diversity and importance of these roles make it difficult to understate the importance of mitochondria. None of these mitochondrial functions is possible without the accurate, regulated transcription of around 1500 genes (in humans) coding for mitochondrial proteins, most of which are located and therefore transcribed in the nucleus and translated in the cytoplasm before the products are imported to mitochondria. The specificity of mitochondrial targeting is defined, for most such proteins, by a mitochondrial targeting peptide sequence (Vögtle et al., 2009) and their import mediated by the TOM/TIM complexes of outer and inner mitochondrial membrane proteins, respectively (Tamura et al., 2009). A basic set of genes, however, is found on the small mitochondrial DNA genome (mtDNA). In the circular, human (~16500 bp) and *Drosophila* mtDNA (~20000 bp), 37 genes are found. Thirteen of these genes code for subunits of the ETC, whilst 22 encode tRNAs, and the remaining two code for mitochondrial ribosomal RNAs. The molecules of mtDNA can be found bound to membranes (Gerhold et al., 2015), compacted by the DNA-binding protein TFAM, in a network of support proteins involved in mtDNA replication and transcription, making up complexes termed nucleoids (Gerhold et al., 2015). The number of mitochondria and thus, the number of nucleoids and mtDNA molecules per cell, varies from hundreds to thousands, depending on cell type (Bonekamp and Larsson, 2018). Mitochondria are present in almost every cell, with rare exceptions, such as human erythrocytes. Therefore, as with cells, mitochondria number in the trillions in whole adult animals. This large number of adult mitochondria necessitates a substantial proliferation from the far fewer mitochondria that are maternally inherited in the embryo. The proliferation of mitochondria happens in a process known as mitochondrial biogenesis.

2.3.2 Mitochondrial biogenesis

Given the crucial roles of mitochondria (above), it is unsurprising that their propagation is well regulated during growth. While mitochondrial biogenesis is loosely defined, it usually encompasses a handful of hallmarks (**Fig 6**) including increased mtDNA copy number, increased mitochondrial mRNA expression, increased mitochondrial protein expression and stabilisation, increased mitochondrial mass as seen by immunofluorescence staining or electron microscopy and also, often, an increase in respiratory activity (Lehman et al., 2000; Scarpulla, 2011; Viscomi et al., 2011). These properties vary between proliferating and quiescent tissues and are counterbalanced by further mitochondrial quality control mechanisms such as mitophagy (Palikaras et al., 2018). A crucial feature of mitochondrial biogenesis, in accord with the endosymbiont hypothesis, is that mitochondria always arise by the growth and division of pre-existing mitochondria.

The number of mitochondria per cell can vary dramatically depending on the energy and biosynthetic demands of the cell or tissue type in question. For example, the heart, kidneys, liver and brain show distinct differences in mitochondrial density and mtDNA copy number whereas, as stated, erythrocytes contain no mitochondria at all (Veltri et al., 1990). The regulation of mitochondrial biogenesis determines this variation in mitochondrial density between cell types during development and growth.

Several transcription factors have been implicated in the regulation of mitochondrial biogenesis. The redox-responsive nuclear respiratory factors 1 and 2 (NRF1 and NRF2), for example, are positive regulators of nuclear-coded mitochondrial genes, including all ten nuclear-encoded COX subunits (Dhar et al., 2008). One study showed NRF1 occupying sites in 691 genes, many of which were involved in mitochondrial biogenesis but also cell-cycle regulation, suggesting concurrence between NRF1 induction of mitochondrial biogenesis and cell growth (Cam et al., 2004). The peroxisome proliferator-activated receptor (PPAR) family of nuclear receptors, while mainly known for their regulation of fatty acid oxidation enzymes (including those acting in mitochondrial fatty acid oxidation), may also indirectly regulate mitochondrial biogenesis. For instance, the (albeit modest) mitochondrial biogenesis observed in the hearts of insulin-resistant transgenic mice requires PPARα (Duncan et al., 2007). Of the three estrogen-related receptors isoforms, ERRα and ERRγ can work as non-obligatory heterodimers, inducing the expression of a network of genes involved in energy metabolism, including TCA-cycle enzyme subunits, constituents of the OXPHOS machinery and genes for ATP

translocation across the mitochondrial membrane (Dufour et al., 2007). The expression of ERRs is highest in mitochondria-rich tissues such as heart, brain, kidney and liver. In the liver, ERRα binds every promoter region of the genes encoding enzymes in the glycolytic, TCA-cycle and pyruvate metabolism pathways, showing it is a potent regulator of energy metabolism and mitochondrial function (Charest-Marcotte et al., 2010). Finally, Yin Yang 1 (YY1), whose function is required for accurate cell-cycle regulation and brain development, is also necessary for mitochondrial gene expression in skeletal muscle, in a manner dependent on the TOR growth-regulatory pathway (Blattler et al., 2012; Cunningham et al., 2007). These transcription factors, of course, do not act independently but instead rely on a network of chromatin remodellers and transcriptional coactivators, the latter of which are discussed in detail in the next section, using the example of the PGC-1 family.
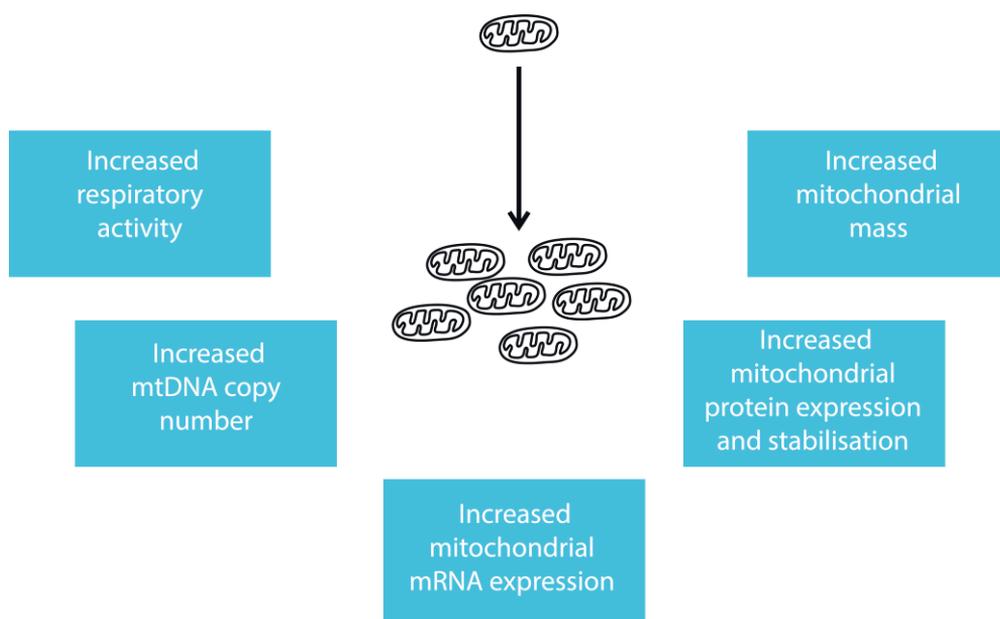
Figure 6. The hallmarks of mitochondrial biogenesis. A number of hallmarks are often observed as indicating a programme of mitochondrial biogenesis. These hallmarks are depicted in the blue boxes here. *Own image.*

2.3.2.1   PGC-1 transcriptional coactivators

The mammalian peroxisome proliferator-activated gamma coactivator (PGC-1) family of transcriptional coactivators are considered pivotal mediators of mitochondrial biogenesis and nuclear-mitochondrial crosstalk. The three mammalian homologues of the PGC-1 family are PGC-1α, PGC-1β and PRC. While they have no known DNA binding activity, the PGC-1 family of proteins instead act by binding transcription factors and recruiting chromatin remodelers to alter gene expression (Puigserver et al., 1999). Their full-length variants contain phylogenetically conserved domains at the carboxy- and amino- termini. The carboxy-terminus of the long-form PGC-1 proteins contains an RNA recognition motif (RRM), as well as an arginine-serine (RS) rich domain, both of which are known to be involved in mRNA processing. Consistent with this, mutation of these domains in PGC-1α has been shown to affect mRNA processing *in vitro*, and PGC-1α is known to bind the TRAP/Mediator complex, which interacts directly with the transcriptional machinery and RNA polymerase II (Monsalve et al., 2000; Wallberg et al., 2003).

The mRNA processing function(s) of the PGC-1 family remain to be fully investigated. However, short PGC-1α variants can promote mitochondrial biogenesis in brown adipose tissue, even without the presence of the RS and RRM motifs, suggesting that these domains are unnecessary for mitochondrial biogenesis activity (Zhang et al., 2009). The amino-terminus of all three mammalian PGC-1 homologues contains LXXLL motifs or 'NR boxes' which allow binding to nuclear receptors such as those discussed above, including ERRα and the PPARs (Kamei et al., 2003). Once bound to transcription factors, a conserved activation domain, also located within the amino terminus, binds histone acyltransferase proteins including SRC-1 and CBP/p300, which subsequently remodel chromatin and alter the expression of proximal genes (Puigserver et al., 1999).

The picture of PGC-1 activity has been complicated by the discovery (so far) of 10 alternatively spliced variants of PGC-1α (**Fig 7**), each defined by differential use of distal promoter regions and each resulting in functionally different protein sequences (Martínez-Redondo et al., 2015). These variants are expressed in varying degrees in different tissues. For example, in humans the *L-PGC-1a* transcript is only expressed in liver and lacks 127 aa from the N-terminus, meaning it is missing an LXXLL motif. This variant cannot bind SRC-1/p300 but does coactivate *HNF4a* and the PPARs, though not liver X receptor α (LXRα). It has subsequently been found to promote gluconeogenesis (Felder et al., 2011). Probing the outcomes of

differential expression of these variants in different tissues is a nascent field. As such, a consistent nomenclature for PGC-1 variants is yet to be put in place, and more isoforms are likely to be discovered in the future (Martínez-Redondo et al., 2015).

Different isoforms of PGC-1α can elicit systemic metabolic changes. One study has shown myokine (muscle-derived small peptide) secretion upon PGC-1α overexpression in skeletal muscle, causing browning of subcutaneous adipose tissue (Boström et al., 2012). Therefore, the effects of PGC-1 transcriptional coactivation are not just limited to the cells or tissues with altered transcriptional activity, further complicating investigation of these coactivators.
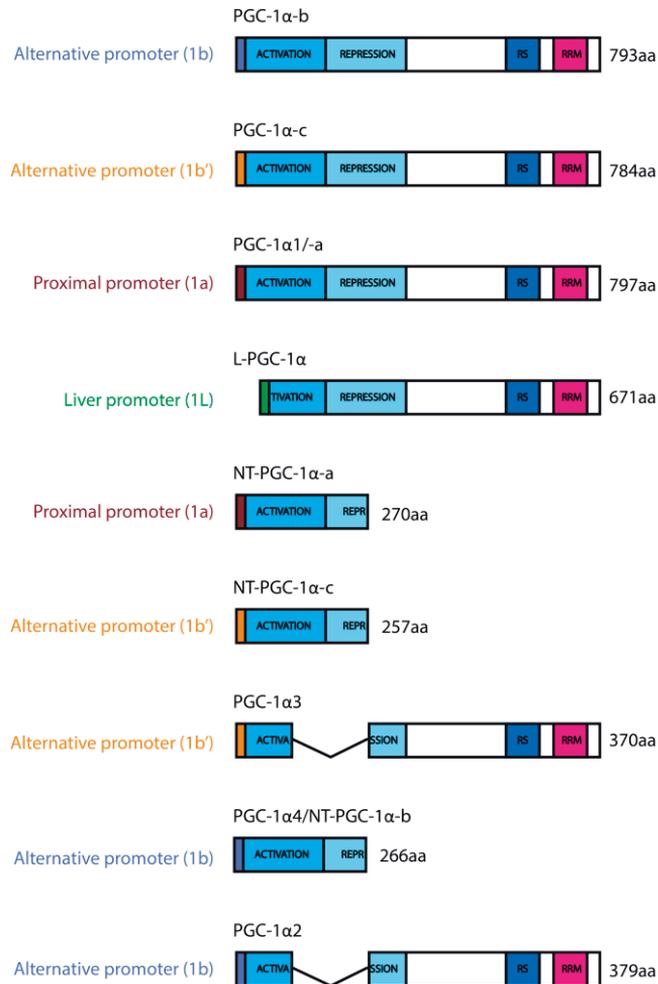
Figure 7. Isoforms of PGC-1α. The known protein isoforms derived from the mouse *Ppargc1a (PGC-1α)* gene are shown. The promoters from which they are expressed are indicated to the left of each isoform, with the differing initial exons that each promoter includes in brackets. The given names are shown above each isoform in black. The size of the isoform in amino acids (aa) is given to the right of each isoform. Each isoform contains one or more of the following domains: activation domain, repression domain, arginine/serine rich domain (RS) and an RNA recognition motif (RRM). Figure modified from (Martínez-Redondo et al., 2015, Figure 1).

2.3.2.2 Regulation of the mammalian PGC-1 family and mitochondrial biogenesis

Much of the above discussion is focussed on PGC-1α, by far the most researched member of the PGC-1 family of transcriptional coactivators. This is in part due to the large number of post-translational modifications (PTMs) known to regulate PGC-1α. The focus on the PGC-1 family as mediators of mitochondrial biogenesis relates to the ability of cellular energy status to influence their activity in coactivating sets of nuclear-coded mitochondrial genes. Depending on the AMP/ATP ratio, AMPK has been shown to phosphorylate PGC-1α and alter transcriptional activity (Jäer et al., 2007). Similarly, GCN5 heavily acetylates PGC-1α, whilst the NAD(+)-dependent deacetylase SIRT1 removes these acetyl groups, in a cycle tightly linked to the energy status of the cell. Thus, the ATP output and NADH usage of mitochondria can be linked to a transcriptional programme of mitochondrial biogenesis. The array of PTMs which modify PGC-1α is illustrated in **figure 8** and includes a wide diversity of acetylation, phosphorylation, methylation, ubiquitylation and GlcNAcylation events (Fernandez-Marcos and Auwerx, 2011).

Environmental stimuli regulate *PGC-1a* mRNA expression in a variety of ways. As a response to exercise, PGC-1α is upregulated by the activity of Ca^{2+}-dependent protein phosphatase calcineurin A (CnA) and calcium/calmodulin-dependent protein kinase IV (CaMKIV; Handschin et al., 2003). Through the binding of the cAMP response element-binding transcription factor (CREB), and the CaMKIV activation of myocyte enhancer factor 2 (MEF2), *PGC-1a* expression is up-regulated in an autoregulatory feedback loop, as MEF2 requires *PGC-1a* binding for its transcriptional activity. This exercise-induced transcriptional programme can lead to muscle fibre-type switching and mitochondrial biogenesis in skeletal muscle (Handschin et al., 2003). *PGC-1a* induced mitochondrial biogenesis may be regulated by insulin signalling. One report, again using skeletal muscle, shows how insulin signalling causes Akt-mediated phosphorylation of the nuclear transcription factor FOXO, which subsequently relocates to the cytoplasm causing a decrease in *PGC-1a* expression (Southgate et al., 2005). This regulation of PGC-1α suggests that mitochondrial biogenesis activity may be driven by decreased dietary sugar. Finally, *PGC-1a* expression is also induced upon cold exposure in subcutaneous and brown adipose tissue. This increased *PGC-1a* expression then results in the activation of transcription of uncoupling protein (UCP-1), potentially increasing mitochondrial capacity for calcium buffering and limiting mitochondrial disassembly (Kazak et al., 2017). Subsequent browning of white adipose tissue into brown adipose tissue follows (Puigserver et al., 1998).

All three of the mammalian members of the PGC-1 family have been reported to promote mitochondrial biogenesis in specific contexts. *PGC-1β* mRNA is highly expressed in heart, brown fat and skeletal muscle, similarly to *PGC-1a*. However, unlike *PGC-1a* expression, *PGC-1β* expression is not induced in adipose tissue upon exposure to cold (Lin et al., 2002). *PGC-1β* overexpression in skeletal muscle can drive the formation of oxidative muscle fibres, along with the induction of OXPHOS genes and an increase in mitochondrial mass (Arany et al., 2007). PGC-1β also plays a complementary role with PGC-1α in the induction of mitochondrial biogenesis in differentiating pre-adipocyte cells. Only when both PGC-1α and PGC-1β were both deficient was an impact on mitochondrial biogenesis observed, suggesting redundancy between their activity (Uldry et al., 2006). This effect is also seen in mice. While PGC-1α knockout mice and PGC-1β knockout mice are viable and are therefore able to proliferate mitochondria throughout development, PGC-1α/PGC-1β double knockout mice die postnatally before 14 days from cardiac arrest and show substantial decreases in mitochondrial number, size and function (Lai et al., 2008). That these double knockout mice can survive to 14 days of age still requires mitochondrial biogenesis from the single-cell stage to a formed mouse pup. Thus, PGC-1α and PGC-1β are not the only factors responsible for the programme of mitochondrial biogenesis during early development. One suggested candidate for mediating mitochondrial biogenesis during early development is the lesser-studied PGC-1α-related coactivator (PRC). Knockout PRC mice die during early embryogenesis (He et al., 2012). PRC is induced upon serum stimulation of quiescent cells and, like PGC-1α and PGC-1β, can induce the expression of nuclear genes for respiratory-chain subunits, suggesting a role in mitochondrial biogenesis in proliferating cells, although this is yet to be clarified *in vivo* (Scarpulla, 2008; Vercauteren et al., 2006). Unlike PGC-1α and PGC-1β, high expression of PRC is not observed in mitochondria-rich tissues such as the heart, brain and skeletal muscle (Andersson and Scarpulla, 2001). It is now apparent that the contribution to mitochondrial biogenesis of the PGC-1 family is complex and context-dependent.
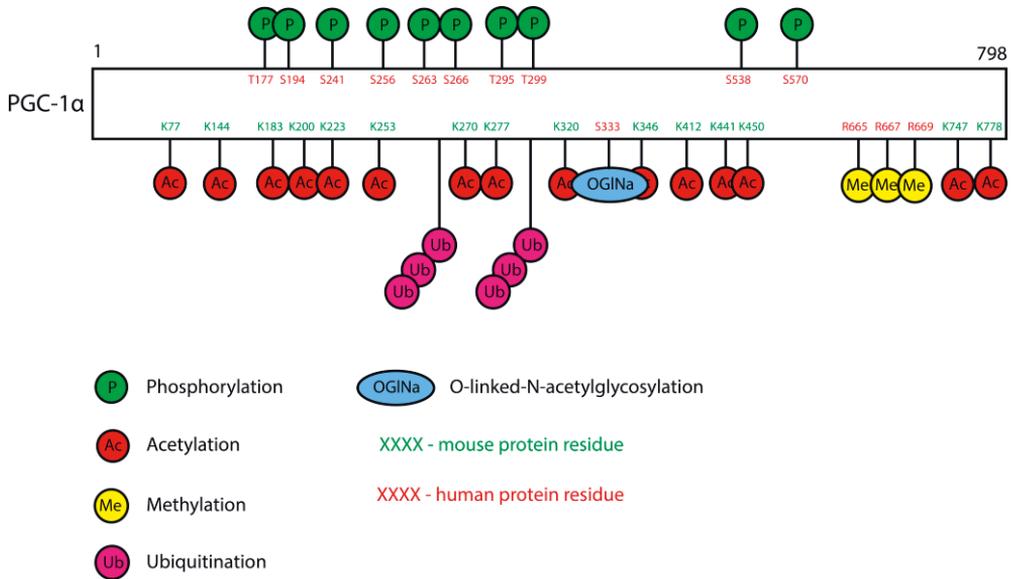
Figure 8. Post translational modifications of the PGC-1α protein. Modifications include: phosphorylation (P), methylation (Me), ubiquitination (Ub) and O-linked-N-acetylglucosylation (OGlNa). These post translational modifications can have activating or inactivating effects on the PGC-1α protein. The sites of modification indicated were discovered to be modified post-translationally in mouse (green protein residues) or in humans (red protein residues). Figure modified from (Fernandez-Marcos and Auwerx, 2011, Figure 2).

2.3.2.3   The PGC-1 family and nuclear-mitochondrial DNA cross-talk

The vast majority of mitochondrial genes are located in the nuclear genome (see **section 2.3.1**). Therefore, nuclear-mitochondrial crosstalk must be established, so as to ensure that transcriptional induction of mitochondrial biogenesis happens in concert from both the nuclear and mitochondrial genomes in times of low energy availability or during growth. An ideal mediator of nuclear-mitochondrial crosstalk should be able to regulate the activity of the nuclear transcription factors discussed above in response to energy status, biosynthetic needs and in response to environmental signals, while at the same time regulating transcription of mtDNA-encoded genes in the same fashion. The PGC-1 family of transcriptional coactivators fits these criteria.

As outlined above, the PGC-1 transcriptional coactivators can induce (or co-induce) a transcriptional programme of mitochondrial gene expression in the nucleus. Also, one of the genes that PGC-1α is known to regulate is the

mitochondrial transcription factor A (TFAM). PGC-1α coactivates NRF1 bound to the promoter of *TFAM*, which in turn induces *TFAM* expression (Wu et al., 1999). In this manner, the activity of PGC-1α can be dynamically regulated to provide a co-ordinated nuclear DNA and mtDNA transcriptional mitochondrial biogenesis response when necessary.

Most of the PGC-1α isoforms contain a nuclear localisation sequence (NLS) and are therefore localised to the nucleus where they are active. Not all such isoforms have an NLS, however. The 270 aa NT-PGC-1α isoform lacks an NLS and is found mainly in the cytoplasm. Upon cyclic adenosine monophosphate (cAMP) exposure, NT-PGC-1α is shuttled to the nucleus where its intact activation domain can elicit a transcriptional response (Zhang et al., 2009). In addition to nuclear localisation, two studies have suggested a mitochondrial localisation of PGC-1α, enabling an interaction with mitochondrial transcription factor A (TFAM) and the NAD(+)-dependent deacetylase SIRT1 (Baldelli et al., 2010; Safdar et al., 2011). This mitochondrial localisation may also be a component of regulated nuclear-mitochondrial DNA cross-talk.

2.3.2.4 Other known roles of the PGC-1 family

Based on the above, each of the PGC-1 family members is considered a mediator of mitochondrial biogenesis and a functional unit in nuclear-mitochondrial crosstalk. However, these are not the only known roles of these transcriptional coactivators.

Along with mitochondrial biogenesis, PGC-1α can induce an antioxidant response by coactivating Nuclear factor erythroid 2-related factor 2 (Nrf2), not to be confused with NRF2 (Cherry et al., 2014). In this manner, PGC-1α can ensure adequate antioxidant activity alongside increased mitochondrial activity and ROS production, through the coactivation of superoxide dismutase (*Sod2*) and enzymes involved in the production of glutathione. PGC-1α has also been shown to promote angiogenesis in a hypoxia inducible factor (HIF) -independent manner, by coactivating ERRα, which induces vascular endothelial growth factor (VEGF) (Arany et al., 2008).

In the liver, while PGC-1α and PGC-1β can both induce mitochondrial gene expression, they regulate divergent functions in response to nutrient environment. Upon starvation, increased PGC-1α activity promotes gluconeogenesis, acting together with hepatocyte nuclear factor 4alpha (HNF4α; Rhee et al., 2003). Importantly, this hepatic gluconeogenic activity can be switched off by S6K-mediated phosphorylation of the RS domain of PGC-1α, while leaving

mitochondrial gene induction intact, providing a prime example of how PGC-1α function can be differentially regulated in a tissue-specific manner by post-translational modification (Lustig et al., 2011). Instead of being regulated by starvation, increased PGC-1β activity in liver is elicited by dietary saturated fatty acids and induces a hepatic programme of *de novo* lipogenesis (Lin et al., 2005). This hepatic programme is partly achieved through the binding and coactivation of sterol responsive element binding protein-1c (SREBP1c), at a domain unique to PGC-1β and not found in PGC-1α, illustrating one means by which these coactivators perform divergent functions in the liver (Lin et al., 2005). The function of these coactivators in the regulation of lipids is further shown by the induction of genes involved in fatty acid oxidation upon both PGC-1α and PGC-1β overexpression (Lin et al., 2003).

2.3.2.5   *spargel*

The only known homologue of the PGC-1 family in *Drosophila* is *spargel* (*srl*). The first description of *srl* was in a 2007 paper outlining the homology between *srl* and mammalian *PGC-1a* and *PGC-1β* in the RRM and RS domains as well as the N-terminal 'activation domain' (Gershman et al., 2007a). The authors showed that refeeding starved flies caused an increase in *srl* mRNA and a concurrent increase in the expression of a significant proportion of nuclear-encoded mitochondrial genes. They also showed that constitutively active dFOXO caused a down-regulation of *srl* expression consistent with observations of FOXO inhibition of PGC-1α expression in mammals (see above **section 2.3.2.2**) (Gershman et al., 2007a; Southgate et al., 2005). Since then, *srl* has further been inferred to share many of the functional properties of its mammalian counterparts, including a role in mitochondrial biogenesis and dependence on insulin signalling.

   A transcriptomic analysis of the *Drosophila* fat body, in a mutant where *srl* mRNA expression was constitutively decreased by insertion of a P-element in the *srl* 5' UTR, showed dysregulated expression of many genes involved in mitochondrial processes (Tiefenböck et al., 2010). As with PGC-1α knockout mice, these *srl* mutants showed no decrease in basal mitochondrial mass but did show a decrease in fat body respiratory activity. However, when combined with a mutant of the *Drosophila* homologue of *NRF-2*, *delg*, an additional decrease in mitochondrial mass and defects in mitochondrial morphology could be seen. This implied synergy, between *srl* and *delg*, is consistent with the mammalian data showing coactivation of NRF2 by the PGC-1 homologues (Tiefenböck et al., 2010). An alteration in fatty acid oxidation

was also observed in the fat body transcriptomics analysis, which might explain results of another study showing lipid accumulation when *srl* function was downregulated (Diop et al., 2015). A link between *srl* activity and nutrition was further noted in studies linking *srl* as an effector of insulin signalling through the TOR pathway (Mukherjee and Duttaroy, 2013). Overexpression of *srl* was also able to overcome growth defects caused by inhibition of TOR and S6K in the fat body (Mukherjee and Duttaroy, 2013). Finally, *srl* overexpression was shown to increase expression of mitochondrial protein subunits, increase mtDNA copy number and, when specifically overexpressed in the gut, extend lifespan in *Drosophila* (Rera et al., 2011). Taken together, the literature suggests *that srl* has a vital role in *Drosophila* metabolism with some functions that parallel those of its mammalian counterparts, including context-specific mitochondrial biogenesis. However, *srl* is currently understudied with much less known about its functions than is known of PGC-1α in mammals. Therefore, further elucidation of its activity in varying tissues and contexts is necessary before drawing firm parallels between *srl* and the PGC-1 mammalian family members.

2.3.3   Mitochondrial disorders

Mitochondrial disorders present when a mutation perturbs one or more of the critical functions of mitochondria outlined in **section 2.3.1**. Given the presence of mitochondria in the vast majority of cells in the body, mitochondrial disorders can affect any tissue or organ but typically cause issues in those tissues with high energy demand such as skeletal muscle, heart and brain. Mitochondrial diseases are one of the most common forms of adult inherited disorders, with a prevalence rate of, for example, 1 in 4300 in the North East of England (Gorman et al., 2015). Due to the presence of genes encoding mitochondrial products in both nuclear DNA (nDNA) and mtDNA (see **section 2.3.1**), mitochondrial disorders can present with autosomal, X-linked or maternal inheritance. The latter is due to the passage of only maternal mtDNA to offspring. Furthermore, as multiple copies of mtDNA are passed to the next generation, cells and tissues of the resultant progeny can contain a mixture of wild-type and mutant mtDNA molecules, resulting in a state known as heteroplasmy (Duan et al., 2018; Monnat et al., 1985). Heteroplasmy, in some cases, is responsible for the clinical heterogeneity seen with mitochondrial disorders. For example, a mutation in the mtDNA-encoded ATPase6 subunit of complex V causes adult-onset retinopathy, ataxia and neuropathy when found at low heteroplasmy

levels but causes Leigh syndrome in infants when high doses of the mutation are present (Holt et al., 1990; Tatuch et al., 1992). Clinical heterogeneity is common amongst mitochondrial disorders, but there are often standard features which allow certain disorders to be clustered according to their symptoms. For example, Leigh syndrome (mentioned above) presents as infantile onset progressive neuropathy with hyperlacticacidemia, the accumulation of harmful reactive oxygen species (ROS) and depletion of ATP (Lake et al., 2015). Adult-onset subacute blindness is found with Leber hereditary optic neuropathy (LHON) (Meyerson et al., 2015), while the acronyms MELAS (mitochondrial encephalopathy, lactic acidosis, and stroke-like episodes) and MERRF (myoclonic epilepsy and ragged red fibres), indicate typical symptoms presented in these syndromic disorders. That being said, the primary feature of any mitochondrial disorder is a defect in OXPHOS, and many patients do not present with symptoms that can be defined within characteristic disorders, making diagnosis difficult (Lightowlers et al., 2015).

As the mitochondrial proteome contains upward of 1500 different proteins, mitochondrial disease can arise from mutations in a vast array of genes. This includes many disorders arising from mutations affecting the mitochondrial translation machinery, discussed in the next section.

2.3.3.1   Mitochondrial translation

Both cytosolic and mitochondrial ribosomes are ribonucleoprotein complexes consisting of a small and large subunit. These subunits work together to polymerise amino acids in a sequence translated from that of bound mRNA strands. Cognate aminoacyl–transfer RNA (tRNA) molecules deliver the correct amino acids to the mRNA-ribosome complex to be appended onto the growing peptide. Mitochondrial ribosomes (mitoribosomes) are found within the mitochondrial matrix and in clusters at the IMM (Englmeier et al., 2017). Mitoribosomes have a much lower RNA:protein ratio than their cytosolic counterparts but are still able to efficiently translate the 13 hydrophobic ETC polypeptides encoded in mtDNA (van der Sluis et al., 2015). In humans and *Drosophila*, mitoribosomes consist of two rRNAs (12S and 16S), both encoded in mtDNA, and a large number of mitochondrial ribosomal proteins (MRPs) encoded in the nuclear genome. There have been suggestions that a 5S rRNA is also important for mitoribosomal function (Smirnov et al., 2011). Several auxiliary proteins aid the mitoribosome in processing mRNA and translating proteins. In the well documented human mitochondrial translation process, initiation factors 2 and 3 (IF2 and IF3) enable the formation of an initiation complex

involving mRNA, ribosomal subunits and tRNA. An AUG or AUA start site is recognised and IF2 combines an initiator formyl-methionine tRNA (fMet-tRNA) with this start site, forming the initiation complex (Spencer and Spremulli, 2004). Processive elongation of the peptide then proceeds with elongation factor Tu (EF-Tu_{mt}) and elongation factor Ts (EF-Ts_{mt}) using the energy from GTP to GDP hydrolysis to join the amino acid of cognate tRNAs to the growing peptide chain. Elongation factor G1 (EF-$G1_{mt}$) then catalyzes the translocation of the mitoribosome and tRNAs and the process repeats (Christian and Spremulli, 2012). During termination, release factor mtRF1a recognises a stop codon on the mRNA and a further GTP hydrolysis causes full dissociation of the polypeptide from tRNA and the mitoribosome. Mitochondrial ribosome recycling factors 1 and 2 ($RRF1_{mt}$ and $RRF2_{mt}$) then dissociate the mitoribosomal large and small subunits which are subsequently recycled for further translation unless turned over (Christian and Spremulli, 2012; Tsuboi et al., 2009).

2.3.3.2   Mitochondrial translation disorders

Mutations in the translational apparatus of mitochondria can disrupt mitoribosome activity and result in pathology with an associated defect in OXPHOS capacity. Any of the 22 tRNAs in human mtDNA can be mutated, resulting in translational disruption, although the resulting clinical phenotypes are highly varied. For example, mutations in the mitochondrial tRNAPhe gene can lead to epilepsy and ragged red fibres (Mancuso et al., 2004), whilst mutation of mitochondrial tRNASer, such as U7445C, can cause non-syndromic deafness (Reid et al., 1994). Most commonly, point mutations in mitochondrial tRNALeu, such as A3243G or T3271C, can cause myopathy, encephalopathy, lactic acidosis, and stroke-like episodes (MELAS) in patients (Goto et al., 1991, 1990). It is estimated that over 100 proteins are required for translation of mitochondrial mRNAs, and all of them are encoded in the nuclear genome (Rötig, 2011). Mutations in many of these genes have been found to cause pathology. Defective mitochondrial Met-tRNA transformylase results in infantile-onset Leigh syndrome (Tucker et al., 2011) showing the necessity, unlike in yeast, of formylated tRNAMet in humans for mitochondrial translation initiation. Mutation in any of the three elongation factors (mentioned above) leads to encephalopathy and lethality (Smeitink et al., 2006). The most obvious nuclear mutations leading to defective mitochondrial translation are in the approximately 80 genes coding for protein subunits of the mitoribosomal small and large ribosomal subunits, the MRPs. The pathology of MRP mutations is heterogeneous and different mutations in the

same MRP gene may cause varied clinical presentations. For example, the Arg170His mutation in MRPS22 causes oedema, hypotonia and cardiomyopathy (Saada et al., 2007), whereas the Leu215Pro mutation in the same gene has been shown to cause Cornelia de Lange-like dysmorphic features (Smits et al., 2011). That said, while pathological heterogeneity of this type is frequently observed (see above **section 2.3.3**) some commonalities are evident within the broad range of mitochondrial disorders, including with MRP mutations, such as lactic acidosis, renal dysfunction, cardiomyopathy, encephalopathy, epilepsy and sensorineural deafness (Menezes et al., 2015; Rötig, 2011). Finally, whilst a substantial number of mutant variants have been observed to exist along the 12S and 16S rRNA sequences in mtDNA, an association with pathogenicity has proven difficult to confirm (Smith et al., 2014). There are some definite observations of disease with mitoribsomal RNA mutations, however. For example A1555G and C1494T 12S rRNA mutations have both been shown to cause hearing loss (Prezant et al., 1993; Zhao et al., 2004), in combination with treatment with aminoglycoside antibiotics.

The clinical manifestations of mitochondrial translation disorders are diverse and questions surrounding the metabolic shifts onset by mutations in the mitochondrial translation machinery still remain (Pearce et al., 2013). Animal models of mitochondrial translation disorders can provide insight into the phenotypes and pathogenic mechanims of mitochondrial disorders at both a cellular and systemic level. The following section describes a *Drosophila* model of mitoribosomal dysfunction, which has been used in this thesis to gain novel insights into the effects of this dysfunction on pyruvate and sugar metabolism.

2.3.3.3   *tko[25t]*, a *Drosophila* model of mitochondrial translation disease

In *Drosophila*, the mutant line *tko[25t]* was discovered to contain an X-linked missense mutation in the *technical knockout* (*tko*) gene, coding for mitoribosomal small subunit protein MRPS12 (Royden et al., 1987; Toivonen et al., 2001). The *tko[25t]* mutant flies have phenotypes resembling those seen in mitochondrial disorders in humans, including developmental delay, a mechanical-shock sensitivity arguably resembling epilepsy (bang-sensitivity) and impaired hearing/sound-responsiveness (Toivonen et al., 2001). Similarly, these overlapping phenotypes seen with *tko[25t]* and mammalian mitochondrial disorders are also found in other *Drosophila* mutants, such as *sesB[1]*, with a mutation in the adenine nucleotide translocase (Zhang et al., 1999), and *kdn[PC64]* carrying a point mutation in *knockdown*, coding for a major isoform of citrate synthase (Fergestad et al., 2006).

The phenotype of *tko²⁵ᵗ* is attributable to a single L85H substitution in a conserved residue of the tko protein (Toivonen et al., 2001). The equivalent mutation in *E. coli* causes impaired ribosome assembly but has no effect on translational accuracy (Toivonen et al., 1999). Similarly in *tko²⁵ᵗ* mutant flies, steady-state levels of 12S mitoribosomal rRNA are decreased, indicating a depletion of functional mitoribosomes (Toivonen et al., 2001). As a consequence, during the larval stages, the activity of the mitochondrial OXPHOS enzymes that depend on mitochondrial translation products (i.e. complexes I, III, IV and V) is decreased, while the activity of citrate synthase, the enzyme that catalyzes the first step in the TCA cycle, remains the same (Toivonen et al., 2001, 2003). Attempts to induce a defect in translational stringency by another mutation in the tko gene, Q116K, resulted in female sterility, an entirely different phenotype to those observed in *tko²⁵ᵗ* mutant flies (Toivonen et al., 2001). This indicates that heterogeneity in phenotypes of mitochondrial translational disorders can be caused by the precise nature of the effect of differing mutations on translation, and that structural and functional relationships exist between mitoribosomes and their component proteins.

Consistent with larval defects in OXPHOS activity, the 3-5 day developmental delay caused by the *tko²⁵ᵗ* mutation, observed as increased time to eclosion, is due to a decreased rate of developmental progression specifically during the larval stages (Toivonen et al., 2001). The bang-sensitivity and impaired response to sound (deafness) exhibited by the *tko²⁵ᵗ* adult mutant flies is potentially due to an energy insufficiency in mechanosensory neurons, with all major bang-sensitive mutants (including *tko²⁵ᵗ*) showing a failure of excitatory neuron stimulation of dorsal longitudinal muscles through the giant fiber pathway (Pavlidis and Tanouye, 1995). However, the precise mechanistic link between neuronal dysfunction and mitochondrial OXPHOS has not been explored.

A transcriptome-wide analysis of adult *tko²⁵ᵗ* mutant flies showed systematic changes in the expression of genes linked to metabolism, including those involved in protein and fat catabolism, anaplerotic pathways and central metabolic pathways (including an up-regulation of *Lactate dehydrogenase*) (Fernández-Ayala et al., 2010). Further exploration of this model can bring mechanistic insight into how mitochondrial translational defects during development in humans produce specific physiological disturbances in later life.

The *tko²⁵ᵗ* mutant flies are viable, albeit developmentally delayed, implying that the *tko²⁵ᵗ* mutation does not altogether abolish the ability of the mitoribosome to translate the mRNAs for the 13 essential OXPHOS polypeptides encoded in mtDNA. Instead, mitoribosomal translational activity appears to be required above

a certain threshold, as *tko²⁵ᵗ* heterozygotes, as well as homozygotes expressing extra copies of the mutant *tko²⁵ᵗ* locus, are phenotypically wild type even if 12S rRNA levels are not fully restored (Kemppainen et al., 2009).

Defective mitochondrial translation and the resultant decreased OXPHOS activity has ramifications on the activity of central metabolic pathways such as insulin signaling, glycolysis, pyruvate metabolism and the TCA-cycle (these pathways are discussed in detail in sections **2.2.3-2.2.5**). Using *tko²⁵ᵗ* as a model of mitochondrial translation disease allows for exploration of the metabolic effects of defective mitochondrial translation.

2.4   Questions addressed in this thesis

By reviewing the literature in the sections above, a picture has emerged of the importance of central metabolic pathways and mitochondria in the growth and development of *Drosophila melanogaster*. This picture also shows how these pathways and the activity of mitochondria are conserved in *Drosophila* and humans and why *Drosophila* can therefore be used to further our knowledge of human metabolism and pathophysiology.

In this thesis, the *Drosophila* model is therefore used to provide insight on pathological features of metabolism in the context of defective mitochondrial translation. Studying *tko²⁵ᵗ* mutant flies (see **section 2.3.3.3**) provides a means of elucidating the relevant pathological mechanisms, using the knowledge and technology available for a tractable model organism. Specifically, this model is used in the following chapters to ask questions about the metabolic shifts generated by defective mitochondrial translation, in particular those related to sugar and pyruvate, and whether dietary, genetic or pharmacological manipulation can alleviate the deleterious phenotypes of the *tko²⁵ᵗ* model. In this endeavour, I first considered some of the key enzymes of pyruvate metabolism, as discussed above. In the second, I tested the potential of the transcriptional coactivator *spargel* (**section 2.3.2.5**) to alleviate the *tko²⁵ᵗ* mutant phenotype, by activating mitochondrial biogenesis as predicted.

The unexpected nature of the results obtained led me to test the more general role of *spargel* and mitochondrial biogenesis in early development, in wild-type *Drosophila*. The literature presented above provides a foundational overview of the knowledge required to understand the premise behind the experiments that will follow and the discussion of the results that were obtained.

3   AIMS OF THE RESEARCH

The broad aim of experiments performed in this thesis was to elucidate further how sugar and pyruvate metabolism, along with the coordinated expression of nuclear and mitochondrial genes, regulate growth and development in *Drosophila melanogaster*. To this end, both wild-type flies and a mitochondrial disease-like mutant, *tko²⁵ᵗ*, were used as experimental subjects. More specifically the aims were as follows:

1) Probe the effects of dietary sugar on the development and metabolism of *tko²⁵ᵗ* mutant flies (I).

2) Analyse the outcome of manipulations to pyruvate metabolism during the development of *tko²⁵ᵗ* mutant flies (II).

3) Overexpress the transcriptional coactivator *spargel* in an attempt to alleviate the phenotypes caused by decreased mitochondrial protein synthesis in *tko²⁵ᵗ* mutant flies (III).

4) Investigate the role of *spargel* RNA expression in *Drosophila* oogenesis and embryogenesis through induction of germline-specific RNA interference for *spargel* (IV).

4   MATERIALS AND METHODS

4.1   Maintenance *Drosophila* stocks and S2 cells

Balancer, GAL4 driver, RNAi and overexpression fly lines were sourced as outlined in Table 1. Flies were maintained at 25 °C on a 12 hour light-dark cycle in plugged plastic vials containing standard medium, supplemented with 0.5% propionic acid (Sigma-Aldrich) and 0.1% (w/v) methyl 4-hydroxybenzoate (Nipagin, Sigma-Aldrich), except where otherwise stated. Full descriptions of sugar diets can be found in **(I)**, and full descriptions of pyruvate, DCA and UK5099 diets in **(II)**.

S2 cells (Invitrogen) were cultured at 25°C in Schneider's medium (Sigma) with regular passaging of cells into fresh media as described previously ((Schneider, 1972).

4.2   Developmental time and bang-sensitivity assays

Three or more replicate crosses were set up and tipped five times to fresh food vials for egg laying. The mean developmental time to eclosion (at 25 °C), as well as bang-sensitivity, were measured as described previously (Kemppainen et al., 2009). Unweighted means and standard deviations of eclosion day for each sex and inferred genotype were then computed for each cross, and used in statistical analyses, applying Student's t-test (unpaired, two-tailed) for pairwise comparisons of the mean eclosion day of flies of two classes, or one-way ANOVA where more than two genotypes or manipulations were compared. Further details can be found in **(I,II,III)**.

4.3   Drosophila embryo to adult development assay

10 virgin female flies were premated with 5 Oregon-R wild type males on standard medium for 2 days, then tipped to fresh vials and allowed to lay eggs over a 24 hour period. The adult flies were then discarded and the laid eggs were counted. The number of adult flies eclosing from each vial was also counted, from which a

percentage was derived, for the proportion of embryos reaching the adult stage. Between 10-20 such vials were assessed for each female parental genotype studied. Full details in **(IV).**

4.4   Molecular cloning

Genomic DNA was extracted from adult Drosophila. 20 adult flies were homogenized in 400µl of buffer containing: 100 mM Tris-HCl (pH 7.5), 100 mM EDTA, 100 mM NaCl, 0.5% SDS, using a plastic disposable homogenising pestle. Samples were then incubated in this buffer for 30 min at 65 °C. 800 µl of buffer containing 1 M potassium acetate and 4 M lithium chloride was added and mixed by inverting several times. Samples were incubated on ice for 2 hours, centrifuged at 12,000 g_{max}. for 15 min at room temperature, and supernatants were transferred to 2 ml Eppendorf tubes containing 600 µl of isopropanol and mixed by inverting several times. Samples were centrifuged at 12,000 g_{max} for 15 min at room temperature. The supernatant was discarded and the pellet was washed with 70% ethanol, air-dried for 5 min, and resuspended in 150µl of TE buffer (10 mM Tris-HCl, 1 mM EDTA, 20 µg/ml RNaseA (ThermoFisher Scientific), pH 7.8) and incubated for 1 hour at 37 °C. DNA from adult flies was used as a PCR template with chimeric gene-specific primers containing appropriate restriction sites for cloning into linearized DNA of the copper-inducible expression vector plasmid pMT-V5/HisB (Thermo Fisher Scientific). All plasmids were sequence-verified before use in transfections. A list of all oligonucleotides used in this thesis is shown as Table 2; full details in **(III)**.

4.5   RNA extraction and analysis

Total RNA was extracted from either: 20 pairs of ovaries (dissected and placed in PBS), batches of 100-200 embryos (dechorionated in 50% household bleach for 2 min and rinsed three times in PBS), batches of 15 3rd instar larvae, or of 10 2 day-old adult flies per sample, using a plastic disposable homogenising pestle and the trizol method as previously described (Fernández-Ayala et al., 2010). cDNA was synthesized using the High-capacity cDNA Reverse Transcription Kit (ThermoFisher Scientific) according to manufacturer's instructions. Expression levels were determined by qRTPCR in Applied Biosystems StepOnePlus™ Real-Time PCR System with Fast SYBR™ Green Master Mix kit from Applied

Biosystems, using as template 2 μl of cDNA product diluted 10-fold in a 20 μl reaction, together with 500 nM of each gene-specific primer pair (see Table 2). Mean values were normalized first against those for RpL32 and then against an arbitrary standard, namely wild-type (Oregon R) adult females. 4 biological repeats and 3 technical repeats were used. Primer pairs were validated based on standard curves showing efficiencies of at least 90% and uniform melting profiles.

4.6 Metabolite assays

Steady-state levels of ATP, lactate and pyruvate were measured by enzyme-linked luminometry (ATP) or fluorometry from extracts of batches of 20 larvae, using commercially available kits according to manufacturer's protocols (Molecular Probes, Life Technologies for ATP, Abcam for pyruvate and lactate). For global metabolite analysis, batches of 15 larvae were rinsed with PBS and snap-frozen in liquid nitrogen, and sent to Tomoyoshi Soga at the Institute for Advanced Biosciences, Keio University, Tsuruoka, Yamagata, Japan for separate anion and cation analysis by CE-TOFMS, in the presence of relevant standards. Full details of metabolite analyses can be found in supplementary information file S1 in **(I)**.

4.7 Western blot analysis

S2 cell pellets (rinsed twice in PBS), batches of 20 pairs of ovaries (dissected and placed in PBS), batches of 100-200 embryos (staged to approx. 80 or 160 min AEL, dechorionated in 50% household bleach for 2 min and rinsed three times in PBS), or of 10 2 day-old adult flies, were crushed in (per sample) 50 μl of lysis buffer (0.3% SDS in PBS, plus one EDTA-free cOmplete™ Protease Inhibitor Cocktail tablet (Roche)). The homogenate was incubated for 10 min and centrifuged at 15,000 g_{max} for 10 min, both at room temperature, after which the supernatant was isolated and protein quantified using a standard Bradford assay. Samples were electrophoresed on an AnyKD midi criterion™ gel (Bio-Rad) in ProSieve™ EX running buffer (Lonza) with Prestained Pageruler™ Plus Ladder (ThermoFisher Scientific) as a molecular weight marker. Transfer was performed using the Trans-Blot® Turbo™ Transfer System and the midi nitrocellulose-specific transfer pack (Bio-Rad). Membranes were blocked in 5% milk in PBS-0.05% Tween (Medicago) for 30 min at room temperature, with gentle shaking. Primary antibody in 5% milk in PBS-

0.05% Tween was added and incubated at 4 °C overnight with gentle shaking. Membranes were washed three times for 10 min, with gentle shaking. Secondary antibody in 5% milk in PBS-0.05% Tween was added and membranes were incubated for a further 2 hours at room temperature, with gentle shaking. Final 10 min washes were twice in PBS-0.05% Tween, followed by once in PBS. 5 ml of Luminata™ Crescendo Western HRP substrate solution (Merck) was added for 5 min before imaging with a Bio-Rad imager. Primary antibodies and dilutions were as follows: ATP5A, Abcam #14748, 1:50,000; COXIV, Abcam #16056, 1:1,000; NDUFS3, Abcam #14711, 1:2,500; GAPDH, EverestBiotech #EB06377, 1:5,000; V5, LifeTechnologies #R960-25, 1:1,000. Custom primary antibodies Srl214AA (against peptide CFDLADFITKDDFAENL) and Srl306AA (against peptide CPAKMGQTPDELRYVDNVKA)(21st Century Biochemicals) were both used at 1:5,000. Appropriate HRP-conjugated secondary antibodies (Vector Laboratories, 1:5,000) were used.

4.8   Immunohistochemistry and immunocytochemistry

Transfection and induction of S2 cells, and subsequent immunostaining were performed as described previously (González de Cózar et al., 2019). Primary antibodies V5, LifeTechnologies #R960-25, 1:500, and ATP5A, Abcam #14748, 1:5,000, were used, along with the corresponding Alexa Fluor® 488 or Alexa Fluor® 647 secondary antibodies (Abcam), diluted 1:1,000. Cells were mounted in ProLong™ Gold Antifade Mountant with DAPI (ThermoFisher Scientific).

Approx. 20 ovaries were dissected in PBS and fixed in 4% paraformaldehyde (PFA, pH 7.2) on ice for 20 min. The ovaries were then rinsed twice with PBT (PBS with 0.01% Triton X-100 (ThermoFisher Scientific) twice, washed twice for 15 min in PBT-0.5% BSA (bovine serum albumin, SigmaAldrich) and incubated with primary antibody ATP5A, Abcam #14748, diluted 1:2,000, in PBT-0.5% BSA overnight at 4 °C, rinsed twice with PBT, washed twice for 15 min in PBT-0.5% BSA, incubated with Alexa Fluor® 488 secondary antibody (Abcam) in PBT-0.5% BSA for 2 hours at room temperature, rinsed twice with PBT, washed three times for 15 min in PBT-0.5% BSA and mounted in ProLong™ Gold Antifade Mountant with DAPI (ThermoFisher Scientific).

Approximately 200 females and 100 males were placed in mating chambers with mating chamber plates containing standard media and a drop of yeast paste. Embryos laid over 4 hours at 25 °C were collected from mating-chamber plates,

dechorionated using 50% household bleach, rinsed three times in PBS and fixed in 500 μl of heptane and 500 μl of 4% PFA (pH 7.2) for 10-60 min. The aqueous bottom layer was removed, leaving the embryos in the heptane layer. 500 μl of methanol was added and the embryos were vortexed for 2 min for devittelination. Heptane, methanol and material at the interphase were removed, leaving only the devitellinised embryos, which were washed three times in methanol. They were then washed three times for 15 min in PBT, blocked in PBT-0.5% BSA for 15 min, incubated in primary antibody in PBT-0.5% BSA at 4 °C overnight, rinsed twice in PBT, washed three times for 15 min in PBT-0.5% BSA, incubated in secondary antibody in PBT-0.5% BSA for 2 hours, washed three times for 15 min in PBT-0.5% BSA in the dark and mounted in ProLong™ Gold Antifade Mountant with DAPI (Thermo Fisher Scientific).

Primary antibodies used for embryos were as follows: EVE, DevelopmentalStudiesHybridomaBank #2B8; Hunchback, Abcam #197787; Dorsal, DevelopmentalStudiesHybridomaBank #7A4; all at a dilution of 1:500. Corresponding Alexa Fluor® 488 secondary antibodies (Abcam) were used at a 1:1,000 dilution.

A Zeiss LSM800 confocal microscope was used for all confocal image acquisition. A Hamamatsu S60 nanozoomer WSI digital slide scanner C13210-01 microscope was used for large-scale, embryo image acquisition for size analysis, and to generate staining-pattern histograms.

4.9   Brightfield imaging

Embryos laid over 24 hours at 25 °C were collected from mating-chamber plates (as above in **section 4.7**), placed in PBS, rinsed twice in PBS, mounted on a slide in PBS and imaged on an OLYMPUS DP73 microscope; full details in **(IV)**.

4.10   Time-lapse imaging of embryonic development

Embryos laid over 30 min at 25 °C were collected from mating-chamber plates (as above in **section 4.7**). Embryos were placed individually in a droplet of PBS in a 6-well plate. Humidity was maintained using cotton-wool doused in water in adjacent wells. Images were taken every 2 min for up to 24 hours, using a Cell-IQ® live-cell

imaging platform (Chip-Man Technologies) at 10x magnification and a constant 25 °C. Full details and movies can be found in **(IV)**.

4.11   mtDNA copy number analysis

Batches of 10 ovary pairs, 50-200 embryos, or 10 adult flies were taken in quadruplicate for each genotype and crushed in 500 µl of DNA lysis buffer (75 mM NaCl, 50 mM EDTA and 20 mM HEPES/NaOH, pH7.8). 5 µl of 20% SDS and 20 µl of Proteinase K (ThermoFisher Scientific, 10 mg/ml) were added to each sample, which was mixed by vortexing. Samples were briefly centrifuged, then incubated at 50 °C for 4 hours. Samples were then vortexed and centrifuged at 16,000 g_{max} for 1 min to pellet debris. Supernatants were transferred to fresh tubes and 420 µl of isopropanol was added, with gentle mixing (by inverting 20 times). Samples were incubated at -20 °C overnight, and then centrifuged at 16,000 g_{max} for 30 min at 4 °C to pellet the DNA. Supernatants were removed and discarded and pellets were washed in 70% ethanol, air-dried for 10 min and resuspended in 100 µl TE buffer (10 mM Tris/HCl, 1 mM EDTA, pH 7.8) overnight at 55 °C in a heat block to dissolve the DNA. DNA concentration was measured using a NanoDrop™ spectrophotometer (ThermoFisher Scientific) and samples were diluted to 2.5 ng/µl. Relative amounts of nuclear and mitochondrial DNA were determined by qPCR using primers, respectively for RpL32 and 16S rDNA (see Table 2) in an Applied Biosystems StepOnePlus™ Real-Time PCR system, with Fast SYBR™ Green Master Mix kit (Applied Biosystems), using as template 2 µl of DNA (2.5 ng/µl) in a 20 µl reaction, together with 500 nM of each gene-specific primer as appropriate. To obtain mtDNA copy number the following calculations were performed: ΔCt = Ct(nDNA gene RpL32)−Ct(mtDNA gene 16S), mtDNA copy number = 2 × 2ΔCt. Standard deviation was calculated for each of the 4 mtDNA Ct values in a developmental stage/genotype group. Finally, mtDNA copy number values were normalised to that of OR wild-type females

Table 1. *Drosophila* strains

Name (as used throughout this thesis)	Type	Stock Centre ID	Chromosome (insertion, mutation or balancer)	Features
OR	Wild-type	n/a	n/a	Wild-type, Oregon R
tko^{25t}	Mutant	n/a	X	Mutant in small mitoribosomal subunit 12
FM7	Balancer	BL 995	X	Balancer chromosome
CyO	Balancer	BL 4959	2	Balancer chromosome
TM3Sb	Balancer	n/a	3	Balancer chromosome
UAS-*Mpc1* RNAi	RNAi	BL 67817	2	UAS-RNAi construct against Mpc1.
UAS-*Pdk* RNAi	RNAi	BL 28635	3	Contains a UAS-RNAi construct against Pdk
*srl*33914RNAi	RNAi	BL 33914	3	Contains a UAS-RNAi construct against srl (CG9808)
*srl*33915RNAi	RNAi	BL 33915	3	Contains a UAS-RNAi construct against srl (CG9808)
*srl*GL01019RNAi	RNAi	BL 57043	2	Contains a UAS-RNAi construct against srl (CG9808)
CG3285		VDRC 51060	2	Contains a UAS-RNAi construct against CG3285.
CG7882		VDRC 109918	2	Contains a UAS-RNAi construct against CG7882.

CG15406		VDRC 105077	2	Contains a UAS-RNAi construct against CG15406.
CG33282		VDRC 100325	2	Contains a UAS-RNAi construct against CG33282.
CG6484		VDRC 109481	2	Contains a UAS-RNAi construct against CG6484.
tobi		VDRC 103544	2	Contains a UAS-RNAi construct against tobi (CG11909).
CG9489		VDRC 106405	2	Contains a UAS-RNAi construct against CG9489. Now known as two genes: CG31332 and CG31352
CG30360		VDRC 104905	2	Contains a UAS-RNAi construct against CG30360.
da-GAL4	GAL4 driver	BL8614	3	Ubiquitous GAL4 driver
MTD-GAL4	GAL4 driver	BL31777	1,2,3	Germline-specific GAL4 driver
nos-GAL4	GAL4 driver	BL4442	2	Germline-specific GAL4 driver
nos-GAL4	GAL4 driver	BL32563	3	Germline-specific GAL4 driver
srlGR	Overexpression	gift from Christian Frei (ETH Zürich, Switzerland)	2	Strain containing extra genomic copy of *srl* (Tiefenböck et al., 2010)
UAS-srl	Overexpression	gift from Christian Frei (ETH Zürich, Switzerland)	2	*srl* overexpression strain (Tiefenböck et al., 2010)

Table 2. Oligonucleotide primers

Gene Name	Primer Pair sequence, 5' to 3' (or identifier)	Quantitect Qiagen Gene Globe Catalog No. (where applicable)	Primer use
spargel	TAACGGAATTCATGCTAAATGTGTTCCAAGGAGA and ATAGCGGCCGCACATCTGACTGTGGCCCTGAA		Molecular cloning of *spargel* into inducible vector.
RpL32 (CG7939)	TGTGCACCAGGAACTTCTTGAA and AGGCCCAAGATCGTGAAGAA		qPCR and qRTPCR
16S	ACCTGGCTTACACCGGTTTG and GGGTGTAGCCGTTCAAATTT		qPCR and qRTPCR
CG30360	Dm_CG30360_1_SG	QT00990507	qRTPCR
CG9468	Dm_CG9468_1_SG	QT00932778	qRTPCR
CG3285	Dm_CG3285_1_SG	QT00928907	qRTPCR
CG33282	Dm_CG33282_1_SG	QT00514717	qRTPCR
CG15406	GGCCATCCAACAGCAAAACA and GCTTTCAAGGAGCGCTTGGT		qRTPCR
CG6484	CCTGGAGGAGTCCCAGAAGC and GGAGCACAGCGATTCCAAGA		qRTPCR
CG7882	ATTGAGGGAACCCGCACCTA and TGATCATCGTCTGCGCCTTT		qRTPCR
Pdk (CG8808)	GGATTCGGAACAGATGCAAT and CGCGATAGAACTTTGAGCTTG		qRTPCR
Mpc1 (CG14290)	GCCGACACACAAAAGAGTCC and GCTGGACCTTGTAGGCAAAT		qRTPCR
ND-ACP (CG9160)	ACAAGATCGATCCCAGCAAG and ATGTCGGCAGGTTTAAGCAG		qRTPCR
ND-30 (CG12079)	AAGGCGGATAAGCCCACT and GCAATAAGCACCTCCAGCTC		qRTPCR
mt:ND5 (CG34083)	GGGTGAGATGGTTTAGGACTTG and AAGCTACATCCCCAATTCGAT		qRTPCR
SdhA (CG17246)	CATGTACGACACGGTCAAGG and CCTTGCCGAACTTCAGACTC		qRTPCR
TFAM (CG4217)	AACCGCTGACTCCCTACTTTC and CGACGGTGGTAATCTGGGG		qRTPCR
RFeSp (CG7361)	GGGCAAGTCGGTTACTTTCA and GCAGTAGTAGCCACCCCAGT		qRTPCR
UQCR-C2 (CG4169)	GAGGAACGCGCCATTGAG and ACGTAGTGCAGCAGGCTCTC		qRTPCR
Blw (CG3612)	GACTGGTAAGACCGCTCTGG and GGCCAAGTACTGCAGAGGAG		qRTPCR

COX5A (CG14724)	AGGAGTTCGACAAGCGCTAC and ATAGAGGGTGGCCTTTTGGT		qRTPCR
COX4 (CG10664)	TCTTCGTGTACGATGAGCTG and GGTTGATTTCCAGGTCGATG		qRTPCR
mt:CoII (CG34069)	AAAGTTGACGGTACACCTGGA and TGATTAGCTCCACAGATTTC		qRTPCR
mt:Cyt-b (CG34090)	GAAAATTCCGAGGGATTCAA and AACTGGTCGAGCTCCAATTC		qRTPCR
ATPsynF (CG4692)	CTACGGCAAAGCCGATGT and CGCTTTGGGAACACGTACT		qRTPCR
mt:lrRNA (CR34094)	ACCTGGCTTACACCGGTTTG and GGGTGTAGCCGTTCAAATTT		qRTPCR
SdhD (CG10219)	GTTGCAATGCCGCAAATCT and GCCACCAGGGTGGAGTAG		qRTPCR
srl (CG9809)	GGAGGAAGACGTGCCTTCTG and TACATTCGGTGCTGGTGCTT		qRTPCR
yip2 (CG4600)	GTCCTCCTCCACCGATGGTAT and CAAAGCCGGTTGATTCCAAGG		qRTPCR
Thiolase (CG4581)	GGAGTCCGCACACCCTTTC and TGCAGCAATGACAAAAGCGAG		qRTPCR
PCB (CG1516)	AATCGGTGGCGGTCTACTC and TTGCCCACTATGTACGACTCG		qRTPCR
Pepck1 (CG17725)	TGATCCCGAACGCACCATC and CTCAGGGCGAAGCACTTCTT		qRTPCR

5 RESULTS

The tko^{25t} mutation is a nuclear mis-sense mutation of the gene coding for mitochondrial ribosomal protein S12 (*MRPS12*) in *D. melanogaster*. This mutation causes a deficiency of mitochondrial protein synthesis by the mitochondrial ribosome and subsequent OXPHOS and respiratory insufficiency throughout development of the albeit viable flies (Toivonen et al., 2001). This causes phenotypes of developmental delay, expressed as increased time to eclosion, bang-sensitivity expressed as paralytic seizures in response to mechanical shock. defective response to sound and finally, impaired male courtship (Toivonen et al., 2001) (see **section 2.3.3.3**). Correct mitochondrial function is necessary to effectively receive, mediate and process the nutrient status of an organism into metabolism, development and growth. Mitochondrial function is itself regulated by the nutrient environment. Thus, it was reasoned that differing nutrient status may affect the severity of the phenotypes manifested by tko^{25t} mutant flies. A series of experiments was therefore designed to analyse the effects of different diets in the context of tko^{25t}.

5.1 Alteration of tko^{25t} mutant fly phenotype through dietary manipulation (I)

Initial experiments tested whether altering levels of core dietary components (sugar, protein, fat), whilst keeping the caloric content of the diet the same, could alter either the developmental delay phenotype, or the bang-sensitivity phenotype of tko^{25t}. Only increased sugar content was seen to exacerbate both of these tko^{25t} mutant phenotypes, with developmental delay increased by approximately 2 days and bang-sensitivity, measured as time to recover, increased (albeit with a high degree of variance) by approximately 40 seconds in both male and female mutant flies, **(Fig 9A and B).** High-fat and high-protein diets had no effect on developmental time or bang-sensitivity of either mutant or wild-type flies.

5.1.1 Increasing dietary sugar causes further developmental delay in *tko²⁵ᵗ* mutant flies

Follow-up experiments were performed to test whether altering the level of dietary sugar in a gradient fashion, this time without maintaining a constant caloric content, could alter the developmental phenotype of the *tko²⁵ᵗ* mutant flies correspondingly. Flies were grown on 3.5% (w/v) dried yeast, 1% (w/v) agar diets, with increasing sucrose content from 0-10% (w/v). Increasing levels of sucrose resulted in greater time to eclosion of *tko²⁵ᵗ* mutant flies, correlating with the incremental steps of the sucrose gradient, whilst having no effect on the eclosion time of wild-type (wt) flies **(Fig 9C)**. The exacerbation of developmental delay by sugar was seen regardless of whether sucrose, glucose or fructose were used **(Fig 9D)**. Of note, even on 0% sucrose diets, *tko²⁵ᵗ* mutant flies still showed a developmental delay of 2 days **(Fig 9C)**. It must be remembered, however, that the yeast component of this diet may well contain some sugars due to the preference of *Saccharomyces cerevisiae* for mono- and di-saccharides as a food source (Lagunas, 1993).
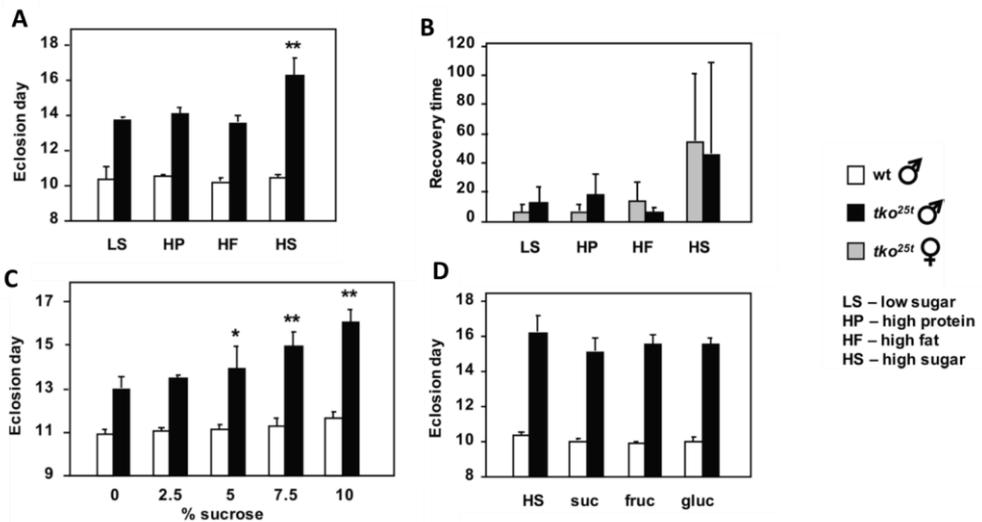
Figure 9. Dietary sugar induces delayed development in *tko²⁵ᵗ* mutant flies. **A)** Time to eclosion on isocaloric diets with increased protein, fat and sugar. **B)** Bang-sensitivity recovery time on isocaloric diets with increased protein, fat and sugar. **C)** Time to eclosion on diets with a gradient of sucrose from 0-10% (w/v). **D)** Time to eclosion on diets with differing sugar types; suc – sucrose, fruc – fructose, gluc – glucose. All statistical analysis using Student's t test, * showing $p < 0.05$, ** showing $p < 0.01$. (Wide variance in bang-sensitivity recovery time precludes a statistical analysis in **B**). Figure reproduced and modified from **(I)**.

5.1.2 *tko²⁵ᵗ* mutant flies exhibit altered expression of sugar transporter and α-glucosidase mRNAs

A set of specific Malpighian tubule sugar transporters and gut specific glucosidases were observed to have dysregulated mRNA expression in an earlier transcriptomic analysis of *tko²⁵ᵗ* (Fernández-Ayala et al., 2010). Due to the above finding that dietary sugar can alter the mutant *tko²⁵ᵗ* developmental delay phenotype, a follow up on these transcriptomic findings was instigated to test whether these transporters were critical for relaying the sugar signal to increased developmental time in the mutant flies. Increased mRNA expression of a set of Malpighian tubule specific sugar transporters in *tko²⁵ᵗ* mutant flies was confirmed using qRTPCR **(Fig 10A)**. Additionally, mRNA levels of gut enriched α-glucosidases were confirmed as decreased in *tko²⁵ᵗ* mutant flies **(Fig 10B)**. Expression of a subset of these sugar transporters was shown to be sensitive to dietary sugar level in original communication **(I)**. With the finding that increasing dietary sugar levels causes exacerbated developmental delay **(see section 5.1.1)** RNAi was used to knockdown mRNA expression of these Malpighian tubule specific sugar transporters to attempt to modify sugar uptake, and/or re-uptake/excretion. If these transporters were necessary for causing increased developmental time in the presence of greater dietary sugar levels, knocking them down would potentially modify the developmental phenotype of *tko²⁵ᵗ* mutant flies. To do this, the GAL4/UAS-RNAi system was used, with the first generation of RNAi lines available from VDRC, and knockdown driven ubiquitously using the *daughterless*-GAL4 (*da*GAL4) driver. These knockdowns, whilst effective **(Fig 10C),** gave no effect on the time to eclosion of *tko²⁵ᵗ* mutant flies **(Fig 10D)**, even though altering dietary sugar levels clearly influenced the development of *tko²⁵ᵗ* mutant flies **(see section 5.1.1)**. It must be noted however, that the efficacy of these knockdowns in altering circulating sugar levels was not measured. Knockdown of these transporters also had no effect on wild-type time to eclosion (data not shown).
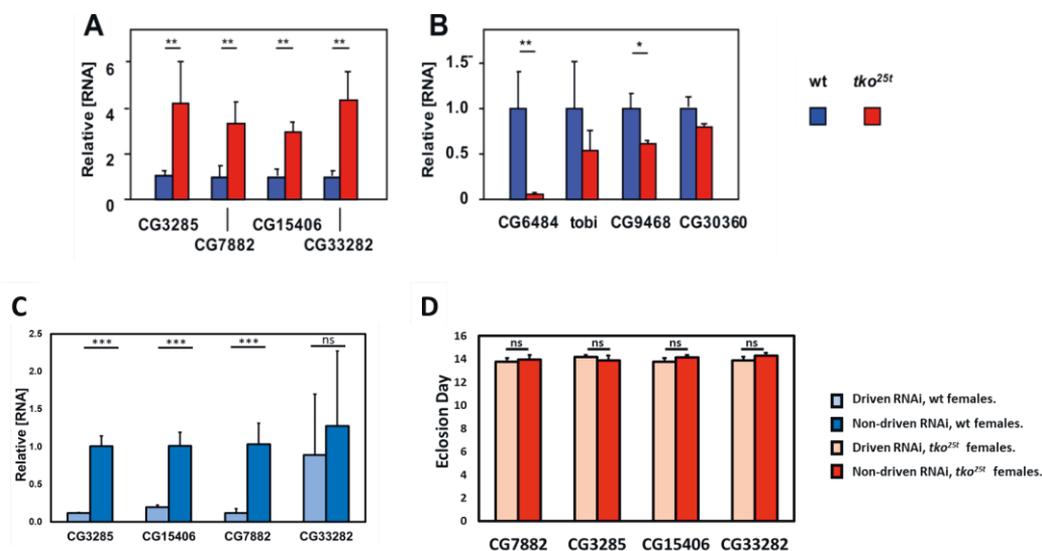
Figure 10. Sugar transporter and α-glucosidase altered mRNA expression and RNAi knockdown in *tko²⁵ᵗ* mutant flies, reared on a standard high-sugar (HS) medium, as measured by qRTPCR relative to *RpL32*. **A and B)** Relative mRNA expression levels of **(A)** Malpighian tubule specific sugar transporters and of **(B)** gut enriched α-glucosidases in wild-type (wt) and *tko²⁵ᵗ* mutant flies with the gene identifiers indicated. n ≥ 3 for each group. **C)** Relative mRNA expression in wild-type females of the Malpighian tubule specific sugar transporters shows efficacy of ubiquitous RNAi knockdown when driven by *da*GAL4 (Driven) vs controls (Non-Driven). n ≥ 3 for each group. **D)** Time to eclosion of *tko²⁵ᵗ* mutant females when Malpighian tubule specific sugar transporters were ubiquitously knocked down by *da*GAL4 (Driven) vs controls (Non-Driven). All statistical analysis using Student's t test, * showing $p < 0.05$, ** showing $p < 0.01$ and *** showing $p < 0.001$. Figure 2A and 2B reproduced and modified from **(I)**.

5.2 ATP, NADPH, lactate and pyruvate levels are altered in *tko²⁵ᵗ* mutant flies (I, II)

As mitochondria are essential organelles mediating critical catabolic and anabolic pathways, it was reasoned that the *tko²⁵ᵗ* mutation, with its decreased capacity to synthesise mtDNA-encoded proteins and its consequently decreased OXPHOS activity (Toivonen et al., 2001), may well give rise to severe metabolic alterations. As such, a mass-spectrometry metabolomics analysis was undertaken on *tko²⁵ᵗ* mutant L3 larvae to assess the metabolic landscape when this mutation is present, resulting in mitochondrial dysfunction **(I)**. Metabolomics analysis was undertaken on L3 larvae, both wild-type and mutant, reared on a standard high-sugar (HS) diet (in %w/v composed of 1 % agar, 3% treacle, 3.5% dried yeast, 1% soya flour 1.5%

maize flour 3% glucose, and 1.5% sucrose) and also on a 'zero-sugar' (ZS) diet (in %w/v composed of 1 % agar, 3.5% dried yeast, 1% soya flour, 1.5% maize flour) which whilst lacking glucose and sucrose, as noted above, likely still contains a small amount of sugar due to the presence of yeast. 35 metabolites were found to be consistently up- or down-regulated due to the tko^{25t} mutation. Regardless of tko genotype, the sugar content of the diet caused far less metabolic alteration than the tko^{25t} mutation; only 9 metabolites were significantly up- or down-regulated on HS vs. ZS diets. Full data and further description of the total metabolomics analysis can be found in original communication **(I)**. The perturbation of selected metabolites important for growth and development (pyruvate, lactate, ATP, NADH and NADPH), was verified using enzymatic assays **(Fig 11)**. The tko^{25t} mutant L3 larvae were deficient in ATP on both HS and ZS diets **(Fig 11B)**. This was not, however, reflected in the $NAD^+/NADH$ ratio **(Fig 11C)**, considered as the main indicator of redox potential, the regulation of which is crucial for ATP synthesis. NADPH levels on the other hand, were significantly decreased, indicative of defective homeostatic maintenance of the $NADPH/NADP^+$ ratio **(Fig 11C)**. Pyruvate levels were found to be far higher in tko^{25t} mutant flies, along with lactate, the conversion product of Ldh (a.k.a $Impl3$) encoded lactate dehydrogenase activity (whose mRNA expression was found to be upregulated in tko^{25t} mutant flies in a previous study (Fernández-Ayala et al., 2010)) **(Fig 11A)**. The importance of these metabolites (ATP, NADPH, lactate and pyruvate) in organismal growth and development (see **section 2.2**) justified following up on these results.

5.3 tko^{25t} mutant flies are sensitive to genetic and chemical perturbations of pyruvate metabolism (I, II)

Sugar metabolism is tightly bound to OXPHOS through pyruvate, a critical product of glycolysis. Pyruvate is transported into the mitochondria by the mitochondrial pyruvate carrier complex (MPC) and is then converted by pyruvate dehydrogenase (PDH) activity into acetyl-CoA which feeds the TCA cycle. Given that tko^{25t} mutant flies are sensitive to dietary sugar content **(section 5.)**, that sugars are the fuel for glycolysis, and that the mutant flies also exhibit elevated levels of pyruvate **(Fig 11A)**, it was hypothesised that manipulation of pyruvate metabolism may lead to alterations of the tko^{25t} mutant phenotype.
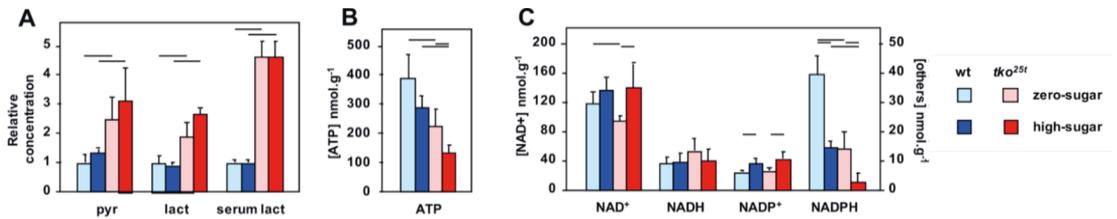
Figure 11. Metabolite levels in tko^{25t} L3 larvae on high-sugar and zero-sugar diets. **A)** Pyruvate and lactate levels relative to those in wild-type larvae on zero-sugar diet measured by fluorescence-based enzymatic assays. **B)** ATP steady-state levels measured by luminescence-based enzymatic assay. **C)** Levels of redox metabolites as determined by mass-spectrometry. Horizontal bars denote significantly different data classes (Student's t test, $p < 0.05$). Work performed by Esko Kemppainen and Tomoyoshi Soga. Figure reproduced and modified from **(I)**.

5.3.1 Dietary addition of pyruvic acid and chemical antagonists of pyruvate metabolism alters the development of tko^{25t} mutant flies

Pyruvate was added to the diets of wild-type and tko^{25t} mutant flies, on a zero-sugar (ZS) diet, to see if this would cause a difference in the time to eclosion **(Fig 12)**. As can be seen, pyruvate was able to extend the time to eclosion in a dose dependent manner in wild-type flies **(Fig 12B)**. When fed to tko^{25t} mutant flies, pyruvate had an additional effect on development, prolonging the time to eclosion beyond the delay caused by just the mutation itself **(Fig 12B)**. This was seen to be the case regardless of dietary sugar levels, as the exacerbating effect of sugar on the development of tko^{25t} mutant flies was still seen between ZS and HS diets regardless of pyruvate supplementation **(Fig 12A)**. The effect of dietary pyruvate addition on time to eclosion was additive in the tko^{25t} mutant flies **(Fig 12B)** rather than being masked by the already high levels of pyruvate attributable to the mutation. This was suggestive of 'total pyruvate level' being a direct predictor of time to eclosion and potentially being the sole mediator of developmental delay in tko^{25t} mutant flies. This hypothesis was tested further using drugs and RNAi targeted on genes of pyruvate metabolism.

Chemical antagonists of pyruvate metabolism were used in the form of the pyruvate dehydrogenase kinase (PDK) inhibitor dichloroacetate (DCA) and the mitochondrial pyruvate carrier (MPC) inhibitor UK5099. By antagonising PDK with DCA, the inhibitory action of PDK on pyruvate dehydrogenase (PDH) should theoretically be decreased, allowing PDH to convert greater levels of pyruvate into acetyl-CoA, thus decreasing the level of mitochondrial (and total) pyruvate. In light

of the above results, this pyruvate reduction would potentially decrease time to eclosion. However, as with pyruvate supplementation, the addition of DCA increased time to eclosion in a dose-dependent manner in both wild-type flies and *tko²⁵ᵗ* mutant flies **(Fig 12B),** again being additional to developmental delay caused by the mutation, and regardless of dietary sugar content **(Fig 12A)**. This result is contrary to the hypothesis that elevated pyruvate is the direct cause of developmental delay in *tko²⁵ᵗ* mutant flies, as decreasing the level of pyruvate with DCA (as confirmed in **(Fig 13)**) caused an increase in time to eclosion rather than the expected decrease. Similar reasoning would predict that treatment with UK5099 to inhibit Mpc1 activity should hinder pyruvate transport across the inner mitochondrial membrane and into the mitochondrial matrix and thus decrease the amount of pyruvate available to be converted and fed into the TCA cycle (yet possibly increasing its level in the cytosol). Although UK5099 supplementation had no effect on the time to eclosion of wild-type flies, it did cause an additional 1 day delay in *tko²⁵ᵗ* mutant flies **(Fig 12A)**. This result again suggests that increases in the level of pyruvate, particularly mitochondrial pyruvate, isn't the direct cause of increased time to eclosion in *tko²⁵ᵗ* mutant flies, because UK5099 should decrease, not increase the level of mitochondrial pyruvate. However, the finding doesn't exclude the possibility that UK5099 may more specifically cause an increase of cytoplasmic pyruvate, which could also be the cause of developmental delay in *tko²⁵ᵗ* mutant flies. A dose-response experiment was not performed with UK5099 due to lack of availability of the drug, so it must also be noted that the dosage of UK5099 used may not be optimal.

To test the effects of DCA and pyruvate supplementation on total pyruvate levels, an enzymatic assay was performed on L3 larvae (the larval stages being those when development of *tko²⁵ᵗ* mutant flies is delayed (Toivonen et al., 2001)) **(Fig 13)**. As *tko²⁵ᵗ* mutant flies showed increased lactate levels **(Fig 11A)**, the effect of dietary lactate supplementation was also tested for its ability to alter the level of pyruvate but had no effect in wild-type or *tko²⁵ᵗ* flies. None of the dietary interventions gave a significantly altered pyruvate level in wild-type larvae **(Fig 13)**, even though DCA and pyruvate supplementation gave a clear increase in time to eclosion in wild-type flies **(Fig 12)**. In *tko²⁵ᵗ* mutant flies, although high-sugar and DCA diets both caused an increase in developmental delay **(Fig 12)**, they respectively had opposing effects on the levels of pyruvate in *tko²⁵ᵗ* mutant L3 larvae, with high-sugar causing a significant increase in *tko²⁵ᵗ* mutant L3 pyruvate levels and DCA causing, as expected, a significant decrease **(Fig 13)**. This adds further weight to the inference that pyruvate is not the sole critical metabolite directly causing developmental delay in

tko²⁵ᵗ mutant flies, even if altering its metabolism does have indirect effects on time to eclosion. **(Fig 13)**. Furthermore, the addition of pyruvate to the ZS diet had no significant effect on the level of pyruvate in L3 larvae even though it did cause a significant increase in time to eclosion of both wild-type and *tko²⁵ᵗ* mutant flies **(Fig 12 and Fig 13)**. It must be noted however; this assay only represents a single time point in the life cycle of *Drosophila* and looks at the whole larva. It may therefore miss crucial information on the flux and turnover of pyruvate throughout development and within different tissues and intracellular compartments. On top of this, all dietary supplements come with potential issues of bioavailability and off target effects.
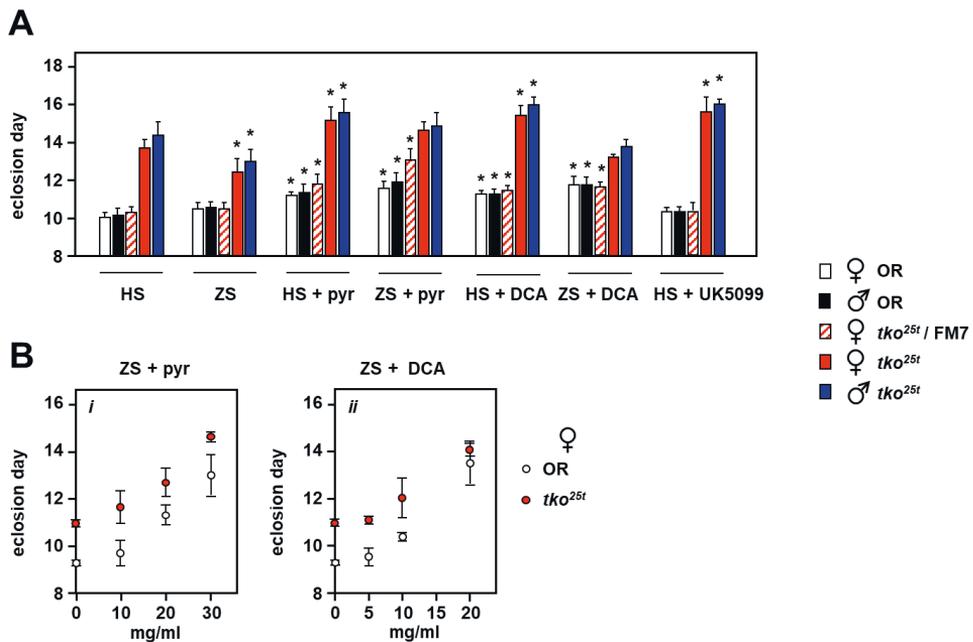
Figure 12. Pyruvate metabolism altered by chemical supplementation of diet. **A)** Supplementation of high sugar (HS) and zero sugar (ZS) diets with; pyruvate (pyr) at 25mg/ml, the pyruvate dehydrogenase kinase inhibitor dichloroacetate (DCA) at 12.5mg/ml and the mitochondrial pyruvate carrier (MPC) inhibitor UK5099 at 25µg/ml. * showing p<0.01, indicating significant differences from flies of the same sex and genotype grown on HS medium as determined from a one-way ANOVA (see appendix table 1). Significant differences between genotypes and sex have been omitted for clarity. **B)** Dose dependent response of developmental delay to pyruvate (pyr) and dichloroacetate (DCA) at the concentrations indicated. OR – Oregon R wild type. Figure reproduced and modified from **(II)**.

Pyruvate Level in L3 Larvae
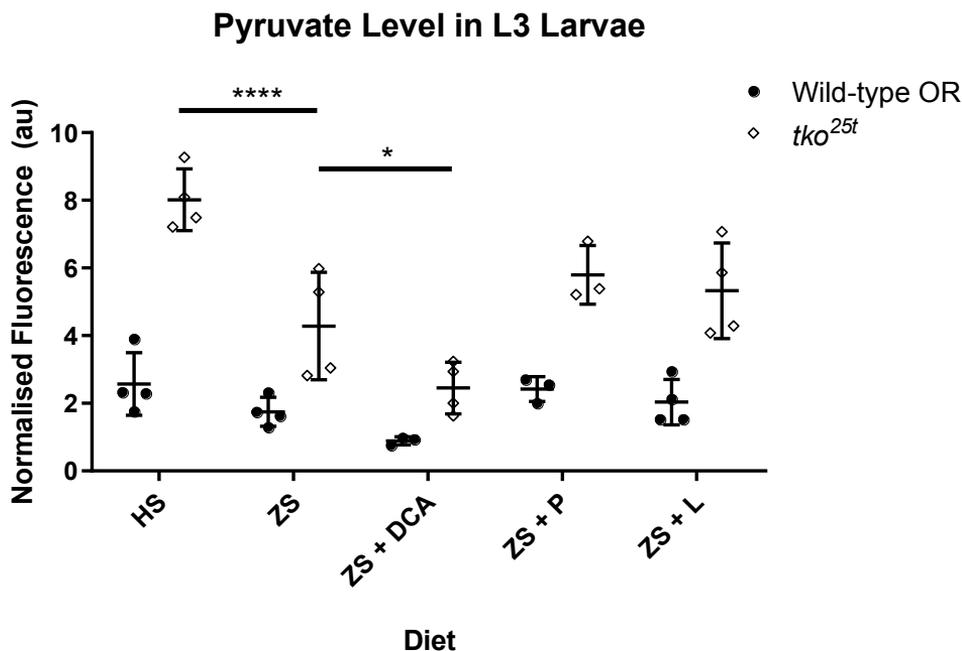
Figure 13. Levels of pyruvate in L3 larvae on supplemented diets. Type III Two-Way ANOVA with recommended Dunnett's multiple comparisons test (see appendix table 1), * showing p < 0.05, **** showing p < 0.0001. HS – high sugar, ZS – zero sugar, DCA – dichloroacetate (PDK inhibitor), P – pyruvate, L – Lactate. Figure reproduced and modified from **(II)**.

5.3.2 Knockdown of Mitochondrial Pyruvate Carrier Subunit 1 (*Mpc1*) and Pyruvate Dehydrogenase Kinase (*Pdk*) alters the development of *tko*[25t] mutant flies

As the use of chemical supplementation has the disadvantage of potential off target effects, a genetic approach was also used, knocking down mitochondrial pyruvate carrier 1 (*Mpc1*) and pyruvate dehydrogenase kinase (*Pdk*) with the GAL4/UAS-RNAi system. Ubiquitous knockdown of *Mpc1* and *Pdk* was driven by *daughterless*-GAL4 (*da*GAL4) and confirmed as effective in wild-type flies (**Fig 14A**). To understand whether *Mpc1* and *Pdk* activity is crucial during development in 'standard' metabolic conditions and/or 'pyruvate stressed' conditions, this ubiquitous knockdown of *Mpc1* and *Pdk* was driven in wild-type flies and *tko*[25t] mutant flies, cultured on a standard high-sugar (HS) diet and on an HS diet supplemented with pyruvate **(Fig 14B)**. Knockdown of *Mpc1* on standard HS medium had no effect on

the time to eclosion of wild-type or *tko²⁵ᵗ* mutant flies. It did however cause a significant increase in time to eclosion in wild-type flies cultured on pyruvate-supplemented HS medium **(Fig 14B, panel i)**. This increase in time to eclosion seen in wild-type flies was masked in the *Mpc1* knockdown *tko²⁵ᵗ* mutant flies **(Fig 14B, panel i)**. Note that this result also differed to what was found by antagonising *Mpc1* with UK5099 **(Fig 12)**. The knockdown of *Pdk* had no effect on time to eclosion of wild-type or *tko²⁵ᵗ* mutant flies cultured on HS medium **(Fig 14B, panel ii)**. *Pdk* knockdown also had no additional significant effect on eclosion time on pyruvate-supplemented medium **(Fig 14B, panel ii)**, although a slight trend towards increased time to eclosion in *tko²⁵ᵗ* flies under these conditions may be noted **(Fig 14B, panel ii)**.

Taken together, these results suggest the chemical and genetic manipulation of pyruvate metabolism was able to alter the growth and development of both wild-type and *tko²⁵ᵗ* mutant flies. These manipulations can have similar effects on wild-type and *tko²⁵ᵗ* mutant flies, as seen with pyruvate or DCA addition **(Fig 12)**; or can have opposite effects, such as with *Mpc1* knockdown on pyruvate-supplemented medium **(Fig 14B, panel i)**. Time to eclosion was not directly correlated in all cases with pyruvate concentration. It is likely that, whilst *tko²⁵ᵗ* mutant flies show elevated pyruvate levels, this alone does not give rise to developmental delay in the context of mitochondrial dysfunction. Instead, a metabolite of pyruvate, or pyruvate within a particular tissue or intracellular compartment, may be a crucial determinant of the rate of developmental progression.
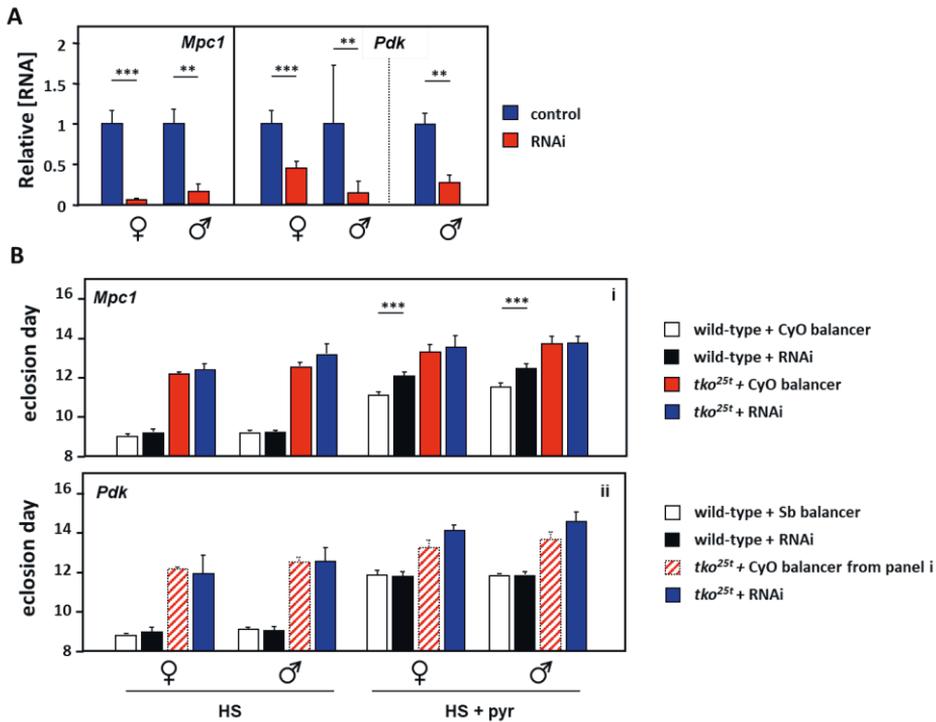
Figure 14. RNAi knockdown of *Mpc1* and *Pdk* affects time to eclosion in *tko^{25t}* mutant flies as measured by qRTPCR relative to *Rpl32*. **A)** Confirmation in wild-type flies of *Mpc1* and *Pdk* mRNA knockdown. n ≥ 4 for each group. **B)** Time to eclosion of wild-type and *tko^{25t}* mutant flies, with or without knockdown of *Mpc1* (panel **i**) or *Pdk* (panel **ii**). Student's t test, * showing p < 0.05, ** showing p < 0.01, *** showing p < 0.01. HS – High sugar, pyr – pyruvate. Figure reproduced and modified from **(II)**.

5.4 Over-expression of *spargel* (*srl*) has minimal effect on *tko^{25t}* mutant phenotype (III)

The underlying deleterious phenotype produced by the *tko^{25t}* mutation is decreased capacity for mitochondrial protein synthesis (Toivonen et al., 2001). As the PGC-1 family of transcriptional coactivators have been proposed to regulate mitochondrial biogenesis, experiments were performed to see whether *srl*, the single *Drosophila* homolog of PGC-1α, PGC-1β and PPRC1(PRC), was regulated differently in the context of the *tko^{25t}* mutation and whether overexpressing *srl* could alleviate the developmental phenotype of *tko^{25t}* mutant flies.

5.4.1 *srl* mRNA expression is decreased in *tko²⁵ᵗ* mutant flies

srl was not observed to be dysregulated in *tko²⁵ᵗ* mutant flies, in an initial transcriptome-wide, microarray-based gene-expression analysis (Fernández-Ayala et al., 2010). However, the threshold required for these analyses necessarily masks many genes that may be dysregulated to a lesser degree, which may nevertheless be phenotypically relevant. As such, an initial experiment using qRTPCR tested whether *srl* mRNA expression was altered in *tko²⁵ᵗ* mutant flies **(Fig 15A and B)**. A significant decrease in *srl* mRNA was seen in *tko²⁵ᵗ* mutant L3 larvae in both males and females and in adult flies only in the females **(Fig 15A and B)**. This result was found in repeat experiments, although with differing degrees of significance, and using flies with different combinations of the *tko²⁵ᵗ* mutation and transgenes, as reported in original communication **(III)** and in a previous article from our laboratory (Chen et al., 2012). It may also be noted **(Fig 15B)** that adult females, both wild-type and *tko²⁵ᵗ* consistently showed approximately 8-fold greater levels of *srl* mRNA expression than the corresponding males. This issue is further explored in **section 5.5**.

5.4.2 *srl* mRNA expression is not altered by dietary sugar during development

PGC-1α and the downstream OXPHOS proteins that it has been shown to regulate have been implicated in human sugar intolerance and diabetes mellitus (J. et al., 2001; Mootha et al., 2003). Due to the moderating effect of decreased dietary sugar levels on the developmental delay phenotype of *tko²⁵ᵗ* mutant flies **(see section 5.1.1)**, *srl* mRNA expression was measured in both wild-type and *tko²⁵ᵗ* mutant flies on the zero-sugar (ZS) and high-sugar (HS) diet to ascertain whether this 'sugar effect' could be acting through altered *srl* mRNA expression and *srl* signalling **(Fig 15A and B)**. A decreased level of *srl* mRNA was seen in *tko²⁵ᵗ* mutant flies on both diets, in both L3 larvae and adult flies. However, there was no differential effect of dietary sugar on the relative levels of *srl* mRNA expression **(Fig 15A and B)**, suggesting that altered *srl* mRNA expression isn't the mediator of the sugar effect on time to eclosion in *tko²⁵ᵗ* mutant flies.
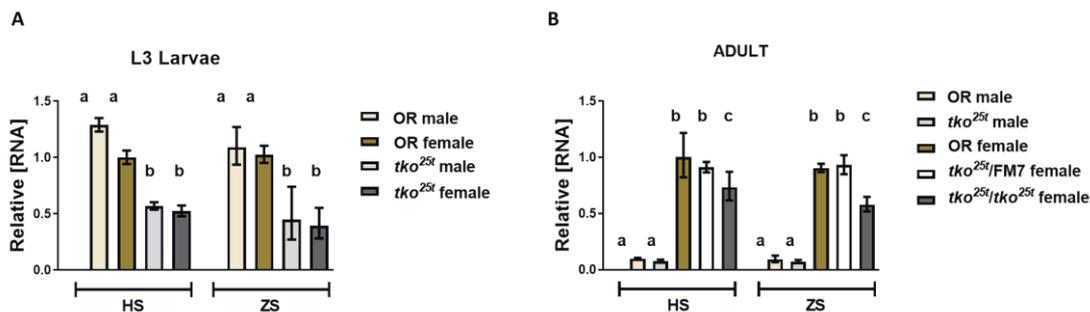
Figure 15. *spargel* mRNA expression in **A)** *tko²⁵ᵗ* mutant larvae and **B)** *tko²⁵ᵗ* mutant adult flies, reared on high sugar (HS) and zero sugar (ZS) media, as measured by qRTPCR relative to *Rpl32*. n ≥ 4 for each group. Lower case letters show statistically different classes, based on two-way ANOVA and Tukey post-hoc test on dC_T values (see appendix table 1). HS – High sugar, OR - Oregon-R wild type, FM7 – FM7 balancer chromosome (*tko²⁵ᵗ*/FM7 heterozygous females show wild-type phenotype). Figure reproduced and modified from **(III)**.

5.4.3   Over-expression of *srl* does not affect development in *tko²⁵ᵗ* mutant flies

Despite this finding, it was hypothesised that decreased *srl* expression might still be a compounding factor for the decreased capacity for mitochondrial protein synthesis in *tko²⁵ᵗ* mutant flies (Toivonen et al., 2001). Therefore, *srl* was ubiquitously overexpressed throughout development to test whether this might alter the developmental delay phenotype of *tko²⁵ᵗ* flies, by increasing mitochondrial biogenesis **(Fig 17)**. Using *daughterless*-GAL4 (*da*GAL4) to ubiquitously drive UAS-*srl* expression in *tko²⁵ᵗ* mutant flies was able to substantially increase the level of *srl* mRNA, as measured by qRTPCR **(Fig 17A)**. 2 custom antibodies were generated, denoted srlAA214 and srlAA306, respectively referring to the initial amino acid of two non-overlapping 16 and 19 amino acid peptides of the Spargel protein **(Fig 16A)**. In Western blots, both antibodies gave the same 2-band pattern, with bands at approximately 100 kDa and 120 kDa (note that the predicted molecular weight of Spargel is 118 kDa) **(Fig 16A).** The upper (~120 kDa) band was most prominent in males and only detectable in females at longer blot-exposure times **(Fig 16B)**. A V5 epitope tag was cloned in-frame into the 3' end of the *srl* coding sequence in a $CuSO_4$-inducible expression vector, both with and without the natural *srl* introns. Using the strongly specific anti-V5 antibody, two bands, at the same apparent molecular weights as detected by the srlAA214 and srlAA306 antibodies, were observed **(Fig 16E)**. The induced Spargel-V5 protein was localised to the nucleus,

as would be expected of a transcriptional coactivator, further supporting the idea that the proteins detected by these antibodies are representative of functional Spargel **(Fig 16D)**. These antibodies were then used to test if overexpression of *srl* mRNA using the *da*GAL4/UAS-*srl* expression system **(Fig17A)** is reflected at the protein level. Only a modest increase of Spargel protein was detected **(Fig 16C)**.

Even though overexpressing *srl* using this system was effective at the mRNA level, albeit less so at the protein level **(Fig 17A and 16C)**, it was unable to alter the time to eclosion in *tko^{25t}* (or control) flies **(Fig 17B)**. This is consistent with the idea that the decreased level of *srl* expression is not underlying the decreased capacity for mitochondrial protein synthesis of *tko^{25t}* mutant flies.
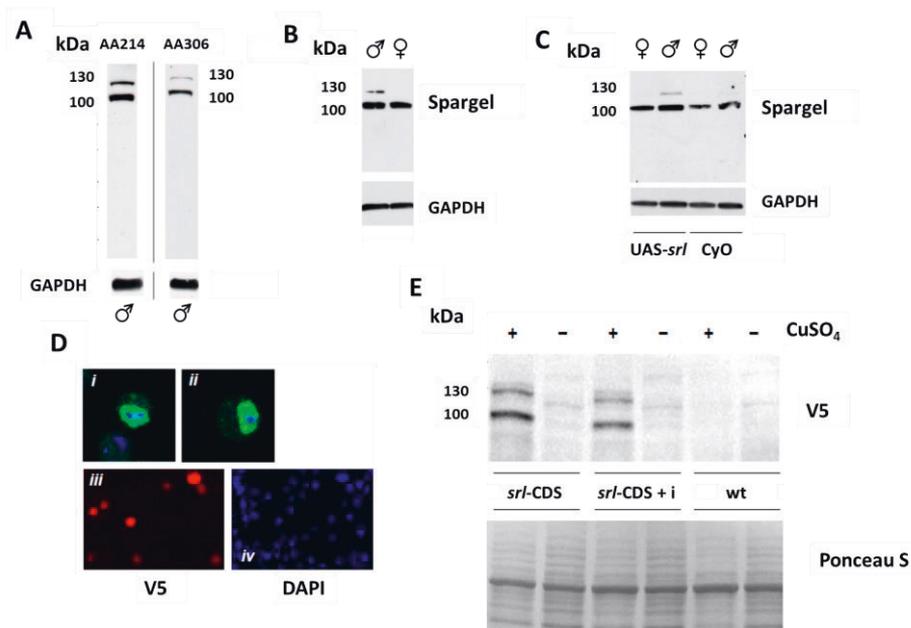
Figure 16. Custom antibodies raised against Spargel detect Spargel polypeptides. **A)** Two separate custom antibodies (srlAA214 and srlAA306) targeting two separate non-overlapping peptides of the Spargel protein both detect the same two polypeptides at approx. 105 kDa and 120 kDa. **B)** The upper (120 kDa) polypeptide is only prominent in males. **C)** Overexpression of *srl* through use of the GAL4/UAS system causes only a moderate increase in Spargel polypeptide. **D)** Transfection of S2 cells with a V5 epitope-tagged version of *srl* without introns, shows localisation of Spargel-V5 to the nucleus. Panels **i) + ii)** Spargel = Green, DAPI = blue. Panel **iii)** shows Spargel-V5 in red merges with the corresponding DAPI signal in panel **iv)**. **E)** Expression of a CuSO4 inducible vector, containing the *srl* coding sequence (*srl*-CDS) with an in frame V5 C-terminus epitope tag, expressed in S2 cells, gives 105 kDa and 120 kDa polypeptide signals when western blots are stained using anti-V5 antibody. *srl*-CDS and *srl*-CDS + i are plasmids without and with *srl* introns respectively. Figure reproduced and modified from **(III)**.
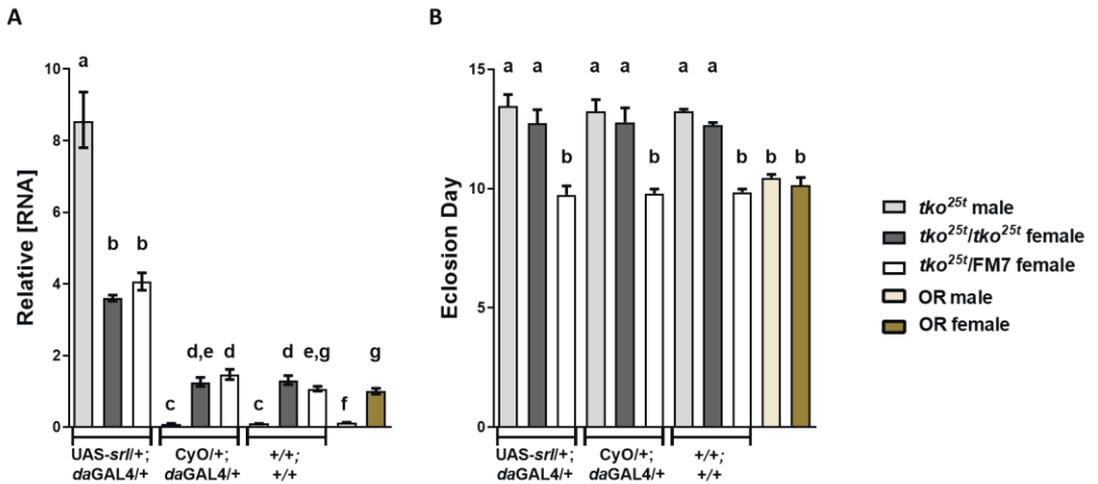
Figure 17. *srl* overexpression in *tko^{25t}* mutant flies and its effect on time to eclosion. **A)** Relative mRNA expression levels of *srl* when overexpressed through use of the GAL4/UAS system. n ≥ 4 for each group. **B)** Time to eclosion of *tko^{25t}* mutant flies, with or without overexpression of *srl* mRNA through use of the GAL4/UAS system. Lower case letters show statistically different classes, based on one-way ANOVA and Tukey post-hoc test on dC_T values (see appendix table 1). 2nd chr. contains either UAS-*srl* transgene for driven expression of *srl* or CyO – *CurlyO*-marked balancer chromosome, 3rd chr. contains *daughterless*-GAL4 (*da*GAL4) driver. OR - Oregon-R wild type, FM7 – FM7 balancer chromosome (*tko^{25t}*/FM7 heterozygous females show wild-type phenotype). Figure reproduced and modified from **(III)**.

5.4.4 Over-expression of *srl* has no effect on hallmarks of mitochondrial biogenesis

One of the hallmarks of mitochondrial biogenesis induced by the PGC-1 coactivators is increased expression at the mRNA level of subunits of the oxidative-phosphorylation (OXPHOS) complexes (Lin et al., 2003; Wu et al., 1999). To check whether overexpressing *srl* was associated with an increase in mitochondrial biogenesis, further qRTPCR measurements were performed on the *tko^{25t}* mutant flies and wild-type flies, to measure the levels of the mRNAs for 13 OXPHOS subunits, as well as 16S rRNA and TFAM mRNA. Males showed greater relative levels of all of the OXPHOS subunit mRNAs than did females, although this may well reflect a lower level of the *RpL32* normalization standard. None of the 15 mRNAs measured were altered by increased *srl* expression **(Fig 18)**. This was further corroborated by the absence of any change in mtDNA copy number in adult flies

with overexpressed *srl* **(Fig 19)**. Concluding that overexpressing *srl* mRNA was unable to enhance mitochondrial biogenesis in wild-type or *tko²⁵ᵗ* flies, and was therefore an unsuccessful strategy to alleviate the mitochondrial disease-like phenotype of the mutant.

Figure 18. *srl* overexpression in *tko²⁵ᵗ* mutant flies and its effect on the mRNA expression of mitochondrial OXPHOS and regulatory subunits. Relative mRNA expression levels of 13 OXPHOS subunits and 2 further mitochondrial genes (*16S* and TFAM) when *srl* was overexpressed using the GAL4/UAS system. Expression relative to *Rpl32*. n > 4 for each group. CyO – *CurlyO*-marked balancer chromosome, OR – Oregon-R wild type, FM7 – FM7 balancer chromosome (*tko²⁵ᵗ*/FM7 heterozygous females show wild-type phenotype). Figure reproduced and modified from (**III**).
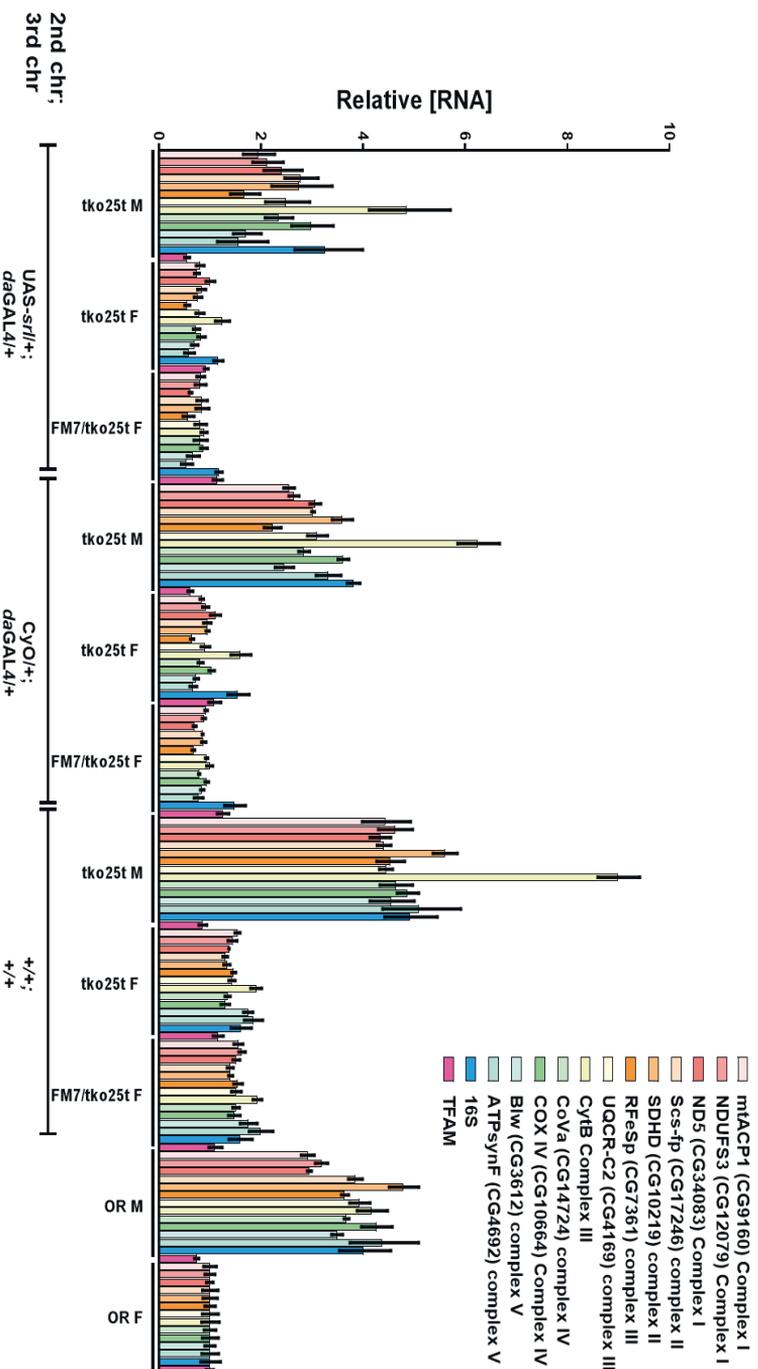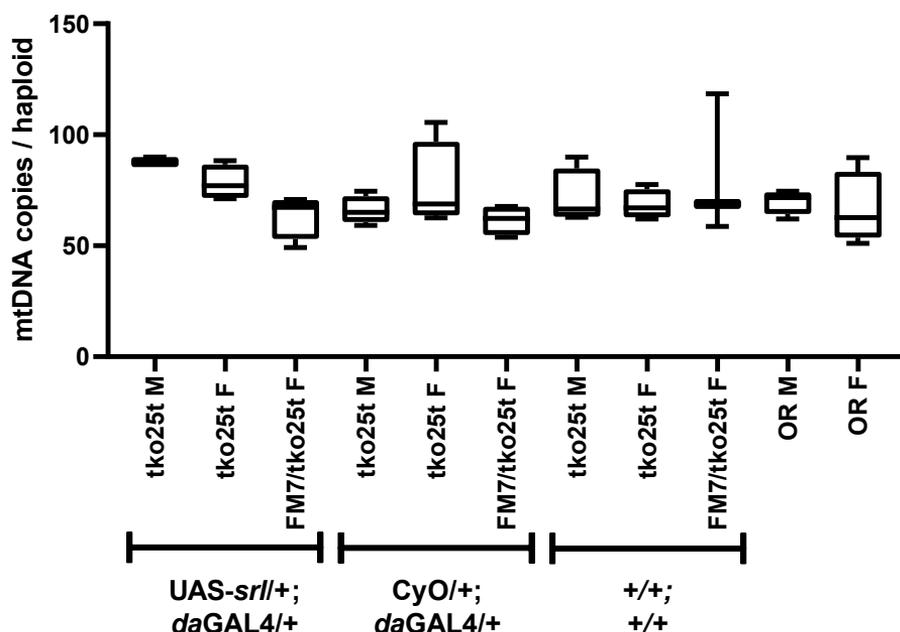
Figure 19. *srl* overexpression in *tko^{25t}* mutant flies has no effect on mtDNA copy number. Number of copies of mtDNA based on the ratio of *16S* to *Rpl32* dC$_T$ values corrected for haploidy of nuclear DNA. n $\geq$ 4 for each group. Boxes delineate first and third quartiles, bold lines the medians, and whiskers the min/max values. No significant differences between genotypes were detected using a one-way ANOVA on dC$_T$ values (see appendix table 1). CyO – *CurlyO*-marked balancer chromosome, OR - Oregon-R wild type, FM7 – FM7 balancer chromosome (*tko^{25t}*/FM7 heterozygous females show wild-type phenotype). Figure reproduced and modified from **(III)**.

5.5 Germline-specific knockdown of *spargel* (*srl*) causes semi-lethality during *Drosophila* embryogenesis (IV)

As noted above in **section 5.4.1**, a consistent observation was the approx. 8-fold higher level of *srl* mRNA in adult females than males **(Fig 15B)**. To investigate this further, the level of *srl* mRNA was measured at each stage of *Drosophila* development, separating the sexes where possible **(Fig 20A)**. *srl* mRNA was high in adult females and higher still in early embryonic development, then remained low and approximately constant at all other stages of development and in adult males **(Fig 20A)**.
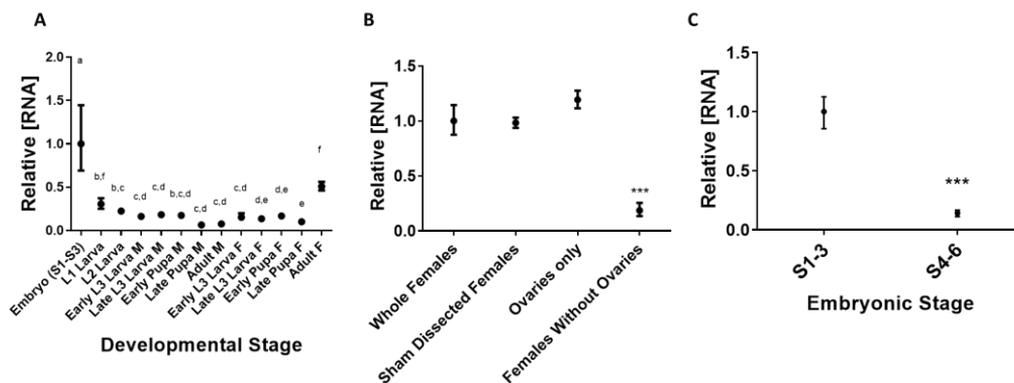
Figure 20. *srl* mRNA accumulates in ovaries and early embryos in *D. melanogaster*. Expression of *srl* mRNA relative to *Rpl32*, as measured by qRTPCR **A)** during *D. melanogaster* development, lower case letters show statistically different classes, based on one-way ANOVA and Tukey post-hoc test on dC_T values (see Appendix, Table 1), **B)** in the ovaries of *D. melanogaster* females, *** = $p < 0.001$ determined by a one-way ANOVA and Tukey post-hoc on dC_T values (see appendix table 1), **C)** in the indicated early embryonic stages, *** = $p < 0.001$ determined by Student's t-test. $n \geq 4$ for each group. S1-S3 – stages 1 to 3, S4-S6 – stages 4 to 6, L – larval instar, M – male, F – female. Figure reproduced and modified from **(IV)**.

5.5.1 *srl* mRNA accumulates during oogenesis and is maternally deposited into embryos

The high level of *srl* mRNA expression in adult females and early embryos pointed towards it being a maternal mRNA accumulating during oogenesis and and being maternally loaded into oocytes prior to subsequent embryo fertilisation and oviposition. To explore this possibility, ovaries were dissected and levels of *srl* mRNA were measured by qRTPCR. Most (approximately 80%) of the *srl* mRNA in adult females was present in ovaries, with the *srl* mRNA in the remaining female carcass (approximately 20%) being similar to levels in adult males **(Fig 20B)**. The level of *srl* mRNA increases further from adult female levels (mainly in ovaries) to early (stage 1-3) embryos **(Fig 20A)**. A sharp drop in *srl* mRNA was observed between stages 1-3 and stages 4-6 **(Fig 20C)**. These observations are consistent with those reported in online databases: FlyAtlas, measuring *srl* mRNA in different stages and tissues by micro-array transcriptomics, and showing a high level in ovaries and embryos (Chintapalli et al., 2007); and FlyExpress showing *in situ* hybridisation to *srl* mRNA and documenting a pronounced decrease between stages 1-3 and 4-6 (Konikoff et al., 2011).

5.5.2 Spargel protein does not reflect *srl* mRNA levels in ovaries and embryos

Using the customised antibody srlAA214 (see **section 5.4.3**), Western blots were performed to determine Spargel protein levels in ovaries, embryos and adult flies **(Fig 21)**. Although females have approx. 8-fold greater levels of *srl* mRNA than males **(Fig 15B, Fig 20A)**, the major ~105 kDa isoform of Spargel protein was at a similar level in females and males **(Fig 21A, lanes 1 and 5)**. Equally, although most *srl* mRNA in the adult female was found in the ovaries **(Fig 20B)**, the level of Spargel Protein did not reflect this, being far lower in ovaries than in whole females, female carcasses without ovaries and sham-dissected females **(Fig 21A)**. In early embryos, the major ~105 kDa Spargel isoform was undetectable and a 70 kDa isoform was prominent instead **(Fig 21B)**. The ~70 kDa band was also observed, though less prominently, in ovaries **(IV)**. The ~105 kDa isoform remained undetectable and the ~70 kDa isoform unchanged, during the transition from embryonic stages 1-3 to 4-6 **(Fig 21B)**, when there was a major drop in *srl* mRNA **(Fig 20C)**. The polypeptides detected by the srlAA214 antibody therefore do not follow the pattern of *srl* mRNA expression.
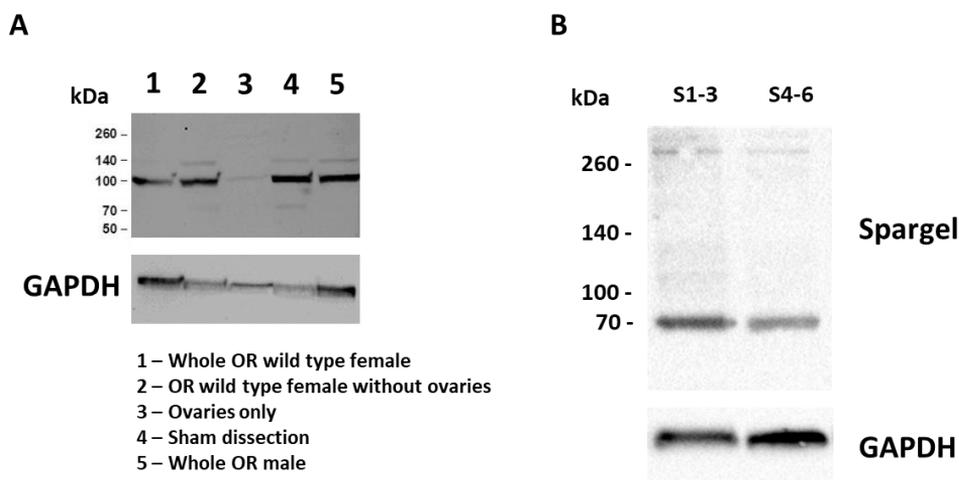
Figure 21. Spargel protein levels do not correlate with *srl* mRNA levels in ovaries and embryos. Western blots showing the levels of Spargel polypeptides detected by custom antibody srlAA214 in **A)** ovaries of *D. melanogaster* females and **B)** in the indicated early embryonic stages, with GAPDH as a loading control. S1-S3 – stages 1 to 3, S4-S6 – stages 4 to 6. Figure reproduced and modified from **(IV)**.

5.5.3   *srl* mRNA knockdown in the germline causes embryonic semi-lethality

To investigate the role of *srl* in development, its mRNA was knocked down using RNAi constructs under the control of a UAS element, driven by GAL4 under the control of a series of germline-specific promoters **(Fig 22A)**. Three RNAi constructs from the Harvard Medical School TRiP collection were used; 33914, 33915 and 57043 (see Materials and Methods for full ID). 33914 and 33915 were created using the Valium20 vector that, whilst not optimised for germline expression, can still knockdown effectively in the germline; in contrast, 57043 was created using the Valium22 vector specifically optimised for expression in the female germline (Hudson and Cooley, 2014; Ni et al., 2011). Only a single line, 33914, and only in combination with the germline specific maternal tri-driver MTD-GAL4 (Rorth, 1998), was found to drive substantial knockdown of *srl* mRNA in whole adult females **(Fig 22A)**. This knockdown was due specifically to an effect in ovaries **(Fig 22B)** and subsequently also observed in stage 1-3 and stage 4-6 embryos **(Fig 22C)**. This knockdown was associated with >90% embryonic lethality **(Fig 22D)**, defining *srl* as an essential gene during development of the early *Drosophila* embryo. The MTD-GAL4>33914 combination was therefore used in subsequent experiments attempting to elucidate the role of *srl* in early development. In combination with the MTD-GAL4 driver, the other Valium20-derived RNAi line 33915 gave weak knockdown in adults, but was unable to drive effective knockdown in ovaries and embryos; and gave no embryonic lethality **(Fig 22)**. The MTD-GAL4>33915 combination was therefore used as a background and transgene control in future experiments.
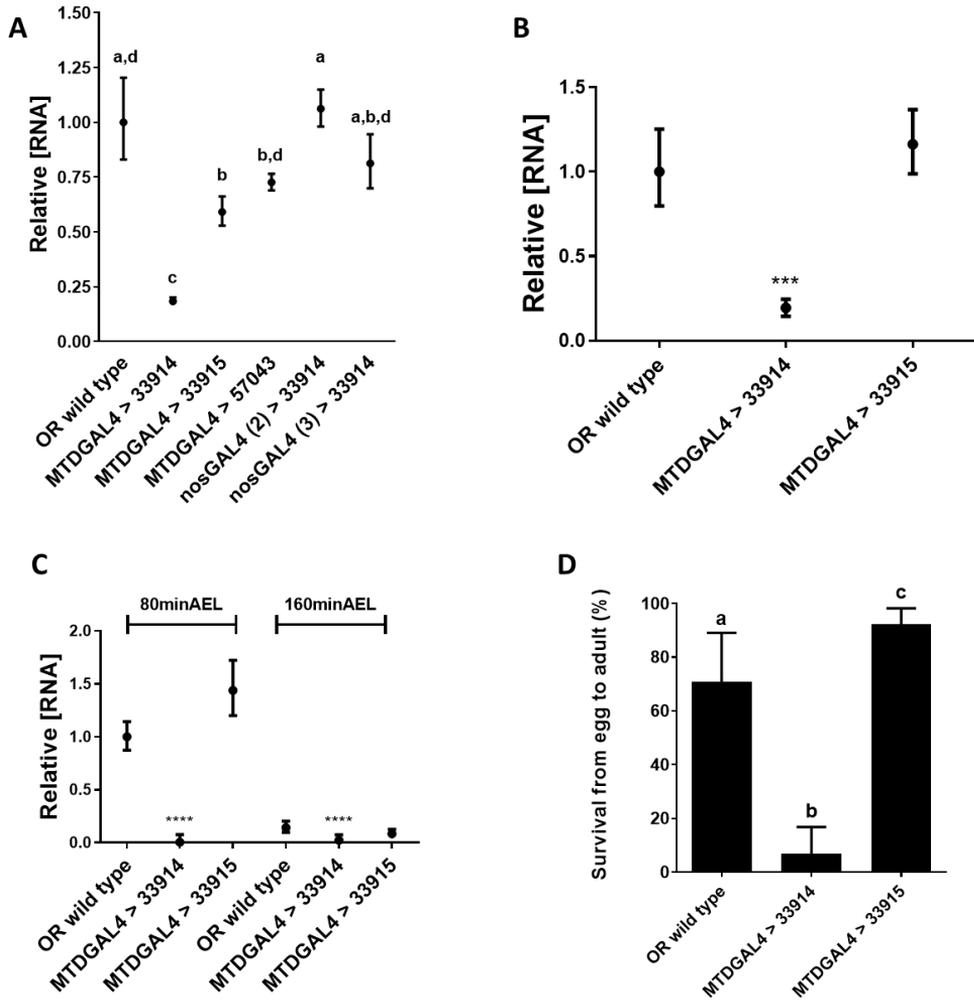
Figure 22. Germline knockdown of *srl* mRNA causes embryonic semi-lethality. Knockdown of *srl* mRNA with different combinations of driver and RNAi constructs as shown on the x-axis in the following; **A)** whole adult females, lower case letters show statistically different classes, based on one-way ANOVA with Tukey post-hoc test on dC_T values; **B)** ovaries, *** = $p < 0.001$ determined by one-way ANOVA and Tukey post-hoc on dC_T values; **C)** embryo offspring of the maternal genotype indicated on the x-axis, 80 min after egg laying (AEL) and 160minAEL, **** = $p < 0.0001$ determined by two-way ANOVA on genotype and developmental stage with Tukey post-hoc test on genotype dC_T values only. $n \geq 4$ for each group. **D)** The percentage of embryos that survive to adulthood, with maternal genotype indicated on the x-axis, lower case letters show statistically different classes, based on one-way ANOVA and Tukey post-hoc test. For full statistical tables, see appendix table 1. Figure reproduced and modified from **(IV)**.

5.5.4 *srl* mRNA knockdown in the germline causes morphological change in embryos

When the resultant embryos from the effective *srl* knockdown combination MTD-GAL4>33914 were analysed under a brightfield microscope, they showed morphological abnormalities compared to wild-type counterparts **(Fig 23)**. Compared to the normal distribution of internal constituents seen in wild-type embryos, many of the *srl* knockdown embryos exhibited unequal distribution and were unable to develop the trachea characteristic of the wild-type late-stage embryos that had developed over the same period of time **(Fig 23A)**. These *srl* knockdown embryos were smaller than either wild-type or MTD-GAL4>33915 control embryos, based on batch analysis of embryo areas in 2D projection **(Fig 23B)**. Time-lapse images of embryonic development revealed that *srl* knockdown caused catastrophic disruption of regular development already from a very early stage, with the majority of knockdown embryos unable to form a normal cellular or even syncytial blastoderm **(Fig 24)**. At 0 mins of recording (approximately 60mins after egg-laying (AEL)), when control embryos are in the midst of cleavage, both wild-type and *srl* knockdown embryos looked similar. However, at 88mins, wild-type embryos manifested a clear peripheral cellularised blastoderm, whilst *srl* knockdown embryos remain without any blastoderm **(Fig 24)**. At 100mins, when wild-type embryos began to exhibit germ band elongation, *srl* knockdown embryos still lacked blastoderm, and started to show abnormal redistribution of internal components **(Fig 24)**. At 1000mins, tracheal tissue had formed in the wild-type embryos, whilst *srl* knockdown embryos had catastrophic reorganisation of constituents, with some potentially differentiated tissues but no normal structure and no trachea **(Fig 24)**. At 1064mins, wild-type embryos had fully developed into L1 larvae that had hatched or were about to hatch, whilst *srl* knockdown embryos remained static and dead **(Fig 24)**. Over many time-lapse images, no consistent pattern of developmental disruption was identified, with each knockdown embryo that failed to develop showing a unique, abnormal organization and dynamic redistribution of internal components until the eventual cessation of any movement and embryonic death **(Fig 24 and original communication IV for full videos)**.
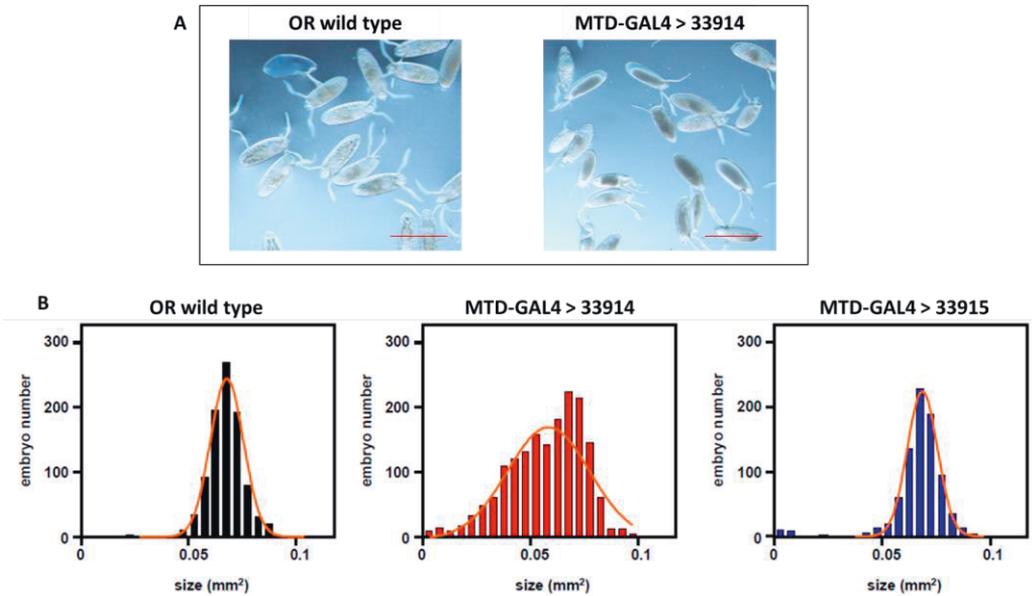
Figure 23. *srl* knockdown embryos show morphological abnormalities and a smaller overall size. **A)** Brightfield images of embryos laid and developing over 24 hours show uneven distribution of internal components and the failure to form embryonic trachea when *srl* was maternally knocked down during oogenesis and early embryogenesis (MTD-GAL4 > 33914), as compared to wild-type Oregon-R (OR) controls. Scale Bar – 500 μm. **B)** Size histograms of embryos laid over 4 hours, from mothers of the indicated genotypes. Automatically generated Gaussian curves, shown in orange, created with GraphPad prism software. Control embryos from Oregon-R (OR) wild-type mothers and MTD-GAL4 > 33915 genotypes both showed a normal distribution. Embryos from mothers with MTD-GAL4 > 33914 genotype (i.e. the effective *srl* knockdown) showed a left-skewed size distribution indicating reduced size vs. control embryos. Figure reproduced and modified from **(IV)**.
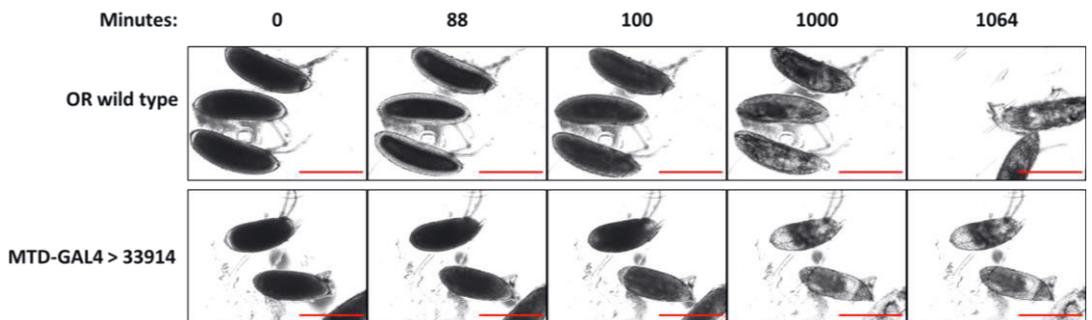
Figure 24. Timelapse images of Oregon-R (OR) wild-type and *srl* knockdown MTD-GAL4 > 33914 embryos. Scale Bar – 500 μm. 'Minutes' indicates number of minutes from the start of recording, corresponding to embryonic development approximately 60mins AEL.

5.5.5 Localisation of early developmental determinants is not disrupted in *srl* knockdown embryos

Whilst *srl* knockdown embryos were found to be smaller and morphologically abnormal, when a set of localised determinants, transcription factors important for correct early developmental progression (Even skipped, Hunchback and Dorsal), were analysed via immunohistochemistry and confocal microscopy there was no difference observed in the patterning of these determinants as compared to wild-type embryos **(Fig 25)**. This suggests that the maternal deposition and subsequent expression of axial developmental determinants into the correct embryonic territories had occurred normally in embryos of MTD-GAL4>33914 mothers. This is the case even though *srl* mRNA was knocked down from early oogenesis onwards **(Fig 22)**. This was also the case in those embryos of markedly smaller size, with a similar proportion of knockdown embryos showing the characteristic distributions of such determinants as those of of the wild-type control strain **(Fig 25)**.
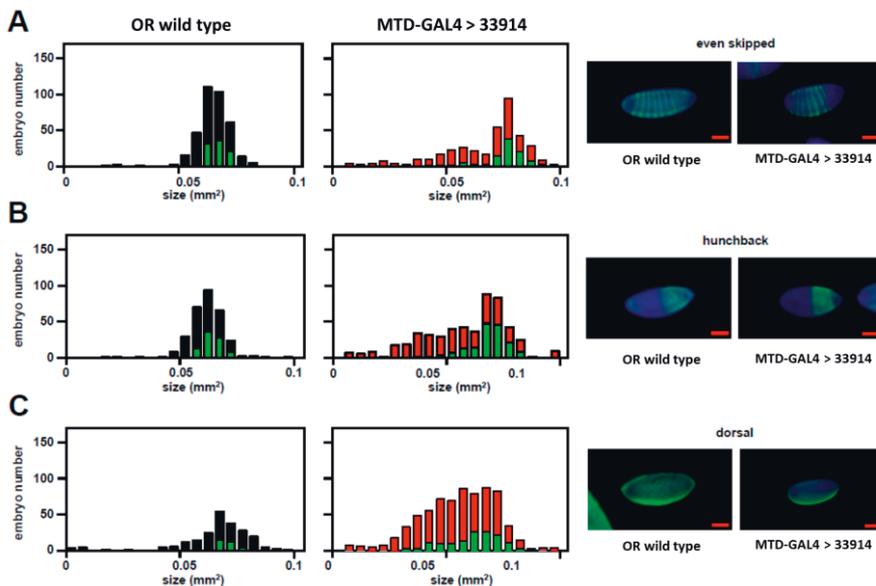
Figure 25. Embryonic knockdown of *srl* does not alter embryonic expression of canonical localized determinants of development. Size histograms of embryos laid over 4 h, from mothers of the indicated genotypes, showing the number of embryos in each size class (black and red bars) and the number of those embryos expressing the classic pattern of each localised developmental marker (in green) as follows: **A)** Even skipped, expressed in a pattern of seven stripes **B)** Hunchback, expressed in the anterior half of the embryo, often with a less visible strip of expression in the posterior territory **C)** Dorsal, expressed as a ventral stripe in the ventral furrow. Scale bars – 100 μm. Figure reproduced and modified from **(IV)**.

5.6 Mitochondrial parameters are unchanged in ovaries and embryos subject to *srl* germline knockdown (IV)

Due to the often reported role of the PGC-1 family members in mitochondrial biogenesis (Andersson and Scarpulla, 2001; Lin et al., 2003; Wu et al., 1999) and further studies that point to *srl* activity in mitochondrial biogenesis and metabolism in *Drosophila* (Mukherjee et al., 2014; Tiefenböck et al., 2010) a number of mitochondrial parameters were investigated in *srl* knockdown ovaries and embryos to establish whether altered mitochondrial regulation was associated with, and therefore a possible cause of embryonic lethality.

5.6.1 Mitochondrial localisation is unchanged in *srl* knockdown ovaries

Immunohistochemistry and confocal microscopy was used to investigate possible differences in mitochondrial localisation or morphology in the ovaries of MTD-GAL4>33914 females compared to those of Oregon R wild-type flies **(Fig 26)**. No changes were seen, suggesting that mitochondria develop, divide and are deposited correctly into oocytes, during oogenesis of ovaries with *srl* mRNA knocked down to levels that cause eventual embryonic lethality.
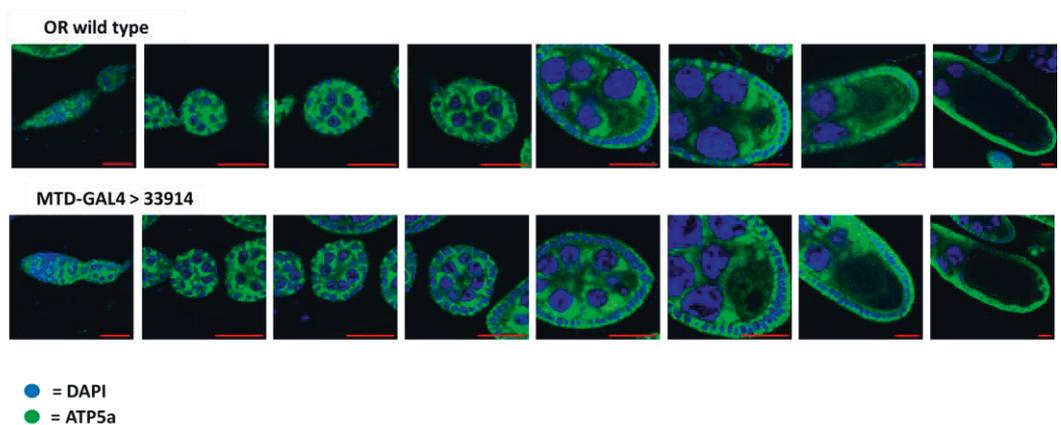
Figure 26. Confocal microscopy images of ovarian follicle stages stained for mitochondria (ATP5a) and DNA (DAPI) content in ovarian follicles from mothers of the genotypes indicated. Stages from L-R: germarium, 1-6, 10, 11 or later. Scale bar = 20 μm. Figure reproduced and modified from **(IV)**.

5.6.2 Expression of mitochondrial OXPHOS subunits in the context of germline *srl* knockdown

The PGC-1 family members (including *srl*), are transcriptional coactivators. Therefore, upon altering their activity, any change this might cause in mitochondrial biogenesis should be observed at the level of mRNA expression, particularly in the transcript levels of mitochondrial genes. As such, the mRNA level of 12 OXPHOS subunits was measured using qRTPCR in ovaries and early embryos 80 and 160 min AEL, i.e. the equivalent of embryonic stages 1-3 and 4-6 respectively. Note that the former nomenclature is more appropriate, given the lack of recognizable normal developmental stages in *srl* knockdown embryos. Ovaries with germline *srl* mRNA knockdown (i.e. from MTD-GAL4>33914 mothers) showed no differences in OXPHOS subunit mRNA levels compared with wild-type embryos **(Fig 27)**. *srl* knockdown embryos 80 mins and 160 mins AEL showed an increase in OXPHOS subunit mRNAs, although this may reflect a global effect of defective development **(Fig 28)**. The hypothesised decrease in mitochondrial biogenesis in *srl* knockdown embryos was therefore not reflected in the mRNA levels of OXPHOS subunits during these early stages of development. The levels of two further mitochondrial mRNAs (16S and *TFAM*) were measured and showed the same pattern of no significant difference in *srl* knockdown ovaries and a slight increase in early embryos. The expression of the mRNA for the glycolytic enzyme *Gapdh1* showed no difference in ovaries or at 80 min AEL. With a slight increase in 160 min AEL, in *srl* knockdown embryos **(Fig 27 and 28)**.

To investigate whether this lack of alteration in the levels of RNAs connected with mitochondrial biogenesis was also the case at the protein level in *srl* knockdown ovaries and embryos, Western blots were probed with antibodies for specific mitochondrial OXPHOS subunits. Firstly, it was observed that the major ~105 kDa Spargel isoform was not significantly downregulated in knockdown ovaries **(Fig 29A)**, consistent with data indicating that Spargel protein levels do not reflect *srl* mRNA levels **(see section 5.4.3)**. This could also explain why no change in OXPHOS mRNA levels is seen in *srl* knockdown ovaries **(Fig 27)**. Furthermore, no change was seen in OXPHOS proteins ATP5A, NDUFS3 and COXIV **(Fig 29B)**.

As before **(Fig 21)**, only the 70 kDa Spargel polypeptide band was detectable in embryos and this polypeptide was also unaffected by *srl* knockdown **(Fig 30A)**. ATP5A and NDUFS3 OXPHOS proteins were not significantly altered in *srl* knockdown embryos 80 and 160 min AEL **(Fig 30B and C)**. However, NDUFS3 showed a trend towards increased levels in MTD-GAL4>33914, but also in MTD-

GAL4>33915 derived embryos, most likely indicative of a background/strain effect **(Fig 30B and C)**.

Therefore, as with OXPHOS subunit mRNA levels, a hypothesised decrease in OXPHOS protein levels in *srl* knockdown ovaries and embryos was not observed. There was however, a consistently decreased level of GAPDH protein in *srl* knockdown ovaries **(Fig 29A)** that was not seen at the mRNA level **(Fig 27)**. This was not seen in *srl* knockdown embryos, where GAPDH levels were the same as in wild-type **(Fig 30B and C)**.
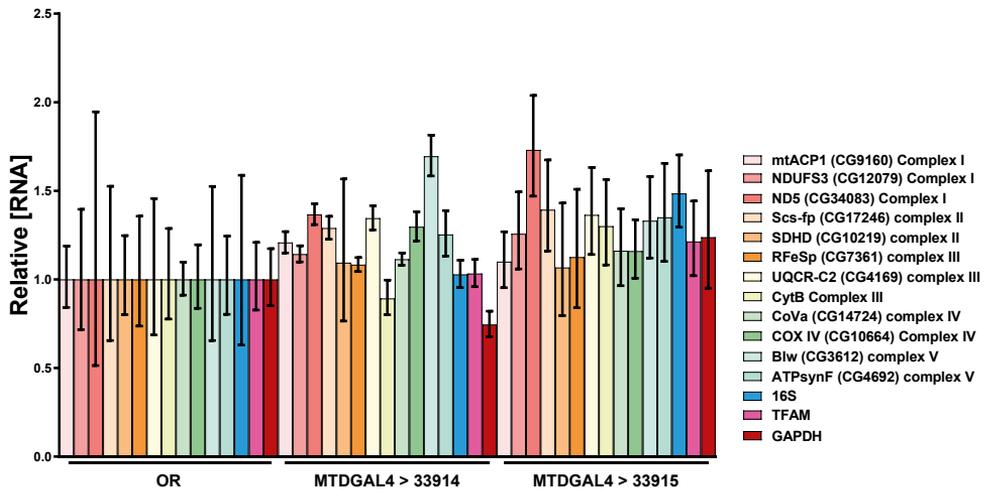
Figure 27. Relative levels of RNA for mitochondrial OXPHOS and regulatory subunits in ovaries with germline *srl* knockdown. mRNA expression levels of 13 OXPHOS subunits, 2 further mitochondrial genes (*16S* and *TFAM*) and the mRNA for one isogene of the glycolytic enzyme *GAPDH* in ovaries with germline *srl* knockdown. Expression relative to *Rpl32*. Each gene represented relative to Oregon-R wild-type (OR) expression in ovaries. $n \geq 4$ for each group. Student's t-test on dC_T values showed non-significance for all comparisons to OR. Figure reproduced and modified from **(IV)**.
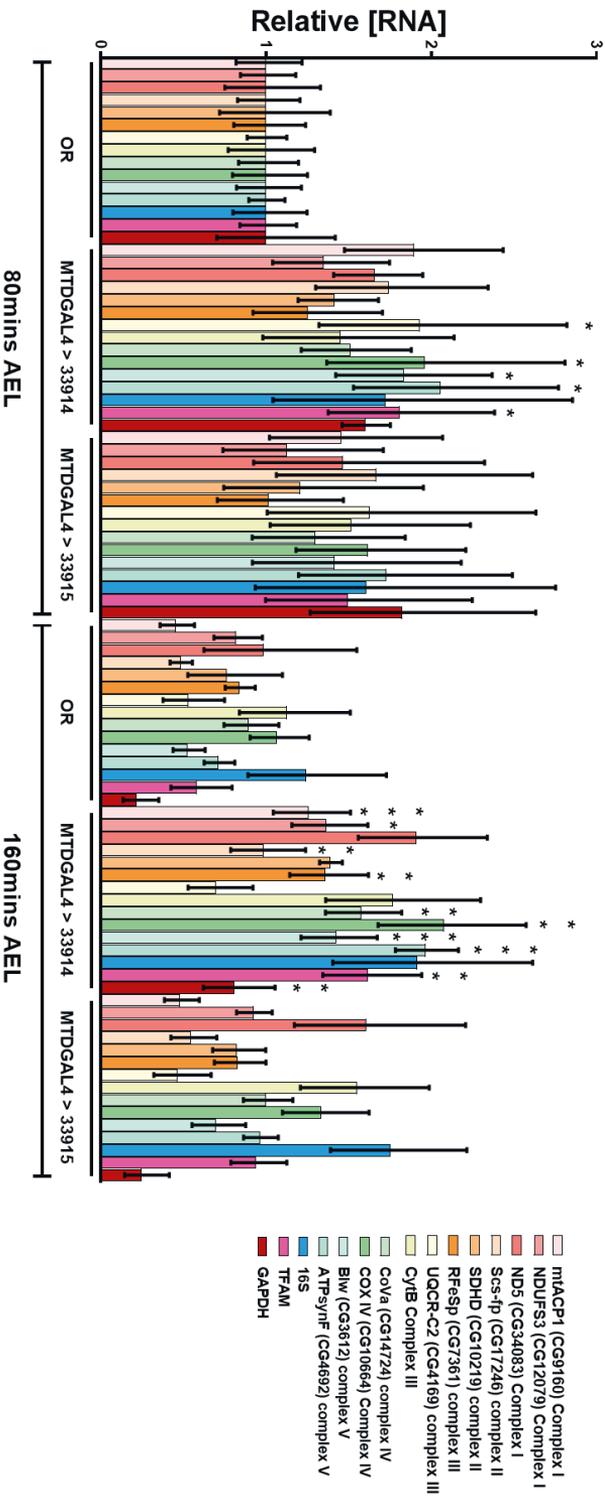
Figure 28. Relative mRNA expression of mitochondrial OXPHOS and regulatory subunits in 80 and 160mins AEL with *srl* mRNA knockdown. mRNA expression levels of 13 OXPHOS subunits, 2 further mitochondrial genes (*16S* and *TFAM*) and the mRNA for one isogene of the glycolytic enzyme *GAPDH* when *srl* is knocked down in embryos 80 and 160mins AEL. Expression relative to *Rpl32*. Each gene represented relative to Oregon-R wild-type (OR) level of expression in embryos 80mins AEL. n ≥ 4 for each group. Bonferroni corrected Student's t-test on dC$_T$ values * showing p < 0.025, ** showing p < 0.005, *** showing p < 0.0005 versus OR embryos of the same developmental stage (80 or 160mins AEL). Figure reproduced and modified from (**IV**).

98
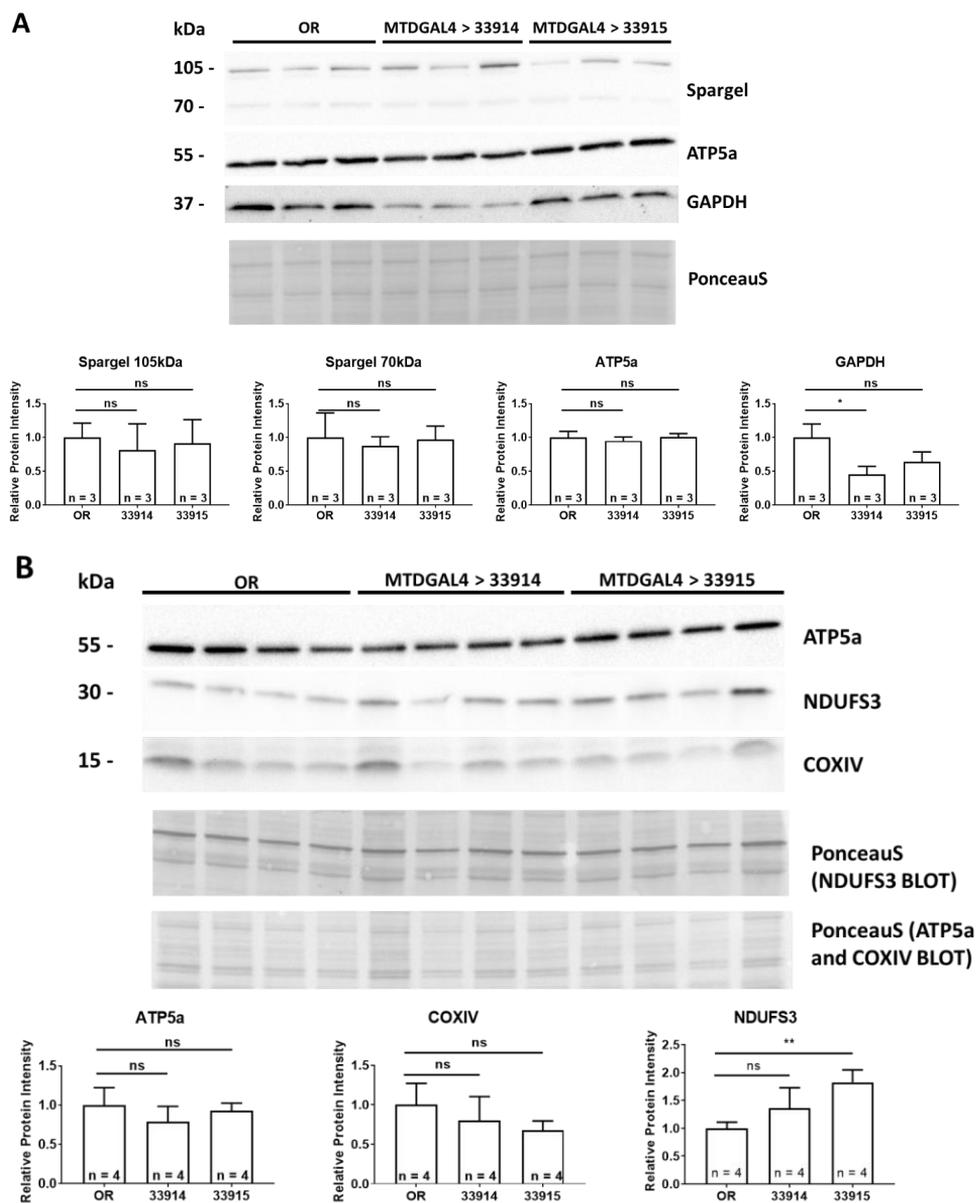
Figure 29. Western blots probing ovary protein preparations for **A)** Spargel (srlAA214), ATP5a and GAPDH, **B)** ATP5a, NDUFS3 and COXIV. Graphs inset show densitometry quantification of the western blots presented relative to PonceauS staining. Student's t-test on relative values * showing $p < 0.05$, ** showing $p < 0.01$, ns - non-significant, n - number of values.
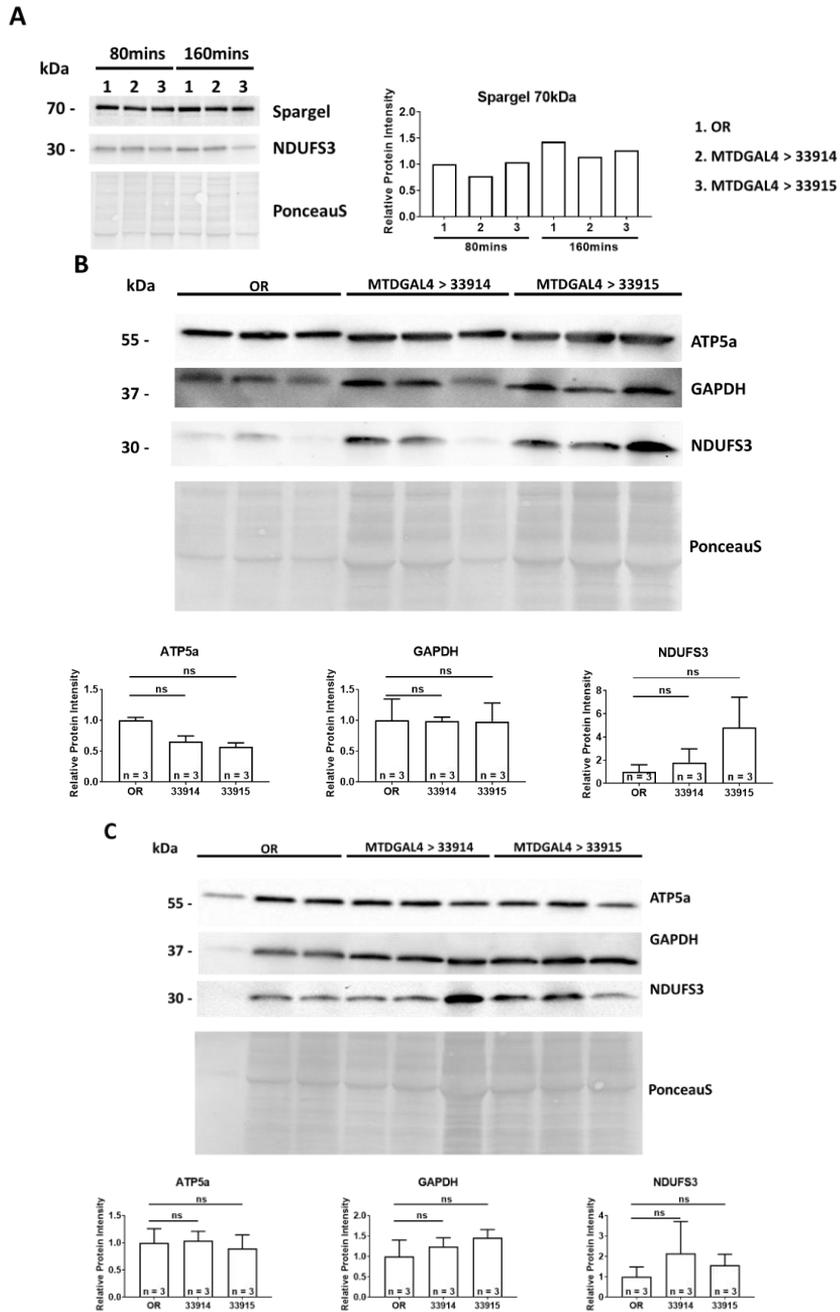
Figure 30. Western blots of embryo protein preparations, probed for **A)** Spargel (srlAA214) and NDUFS3 in embryos 80 and 160mins AEL as indicated, **B)** ATP5a, GAPDH and NDUFS3 in embryos 80mins AEL, **C)** ATP5a, GAPDH and NDUFS3 in embryos 160mins AEL. Graphs inset show densitometry quantification of the Western blots presented relative to

PonceauS staining. Student's t-test on relative values, ns - non-significant, n - number of values.

5.6.3   mtDNA copy number is unaffected by germline *srl* knockdown

As a final test of whether the embryonic lethality caused by *srl* knockdown could be due to altered mitochondrial biogenesis, mitochondrial DNA copy number was measured in ovaries and embryos 80 and 160 min AEL **(Fig 31)**. A large relative increase in mtDNA copy number was seen in embryos 80 min AEL, compared with ovary copy number, and regardless of genotype. This is indicative of the expected low levels of nuclear DNA in early cleavage-stage embryos. Copy number returned to a value similar to that in ovaries, 160 min AEL, once nuclear divisions were complete **(Fig 31)**. However, mtDNA copy number in both ovaries and embryos was not affected by *srl* knockdown **(Fig 31)**.
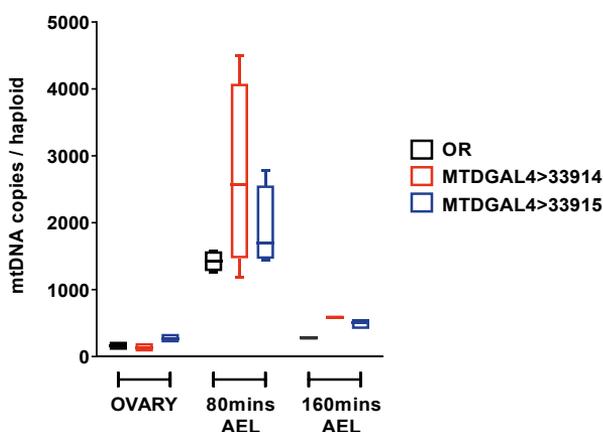
Figure 31. mtDNA copy numbers in ovaries and embryos 80 and 160mins AEL with knockdown of *srl*. Measurements based on relative dC_T values from mitochondrial gene *16S* vs nuclear gene *Rpl32*. $n \geq 4$ for each group. Boxes show first and third quartiles, centre lines show the medians, and whiskers show the min. and max. values. Two-way ANOVA showed no difference between genotypes but a $p < 0.001$ difference between the 3 developmental stages (ovary, embryos 80mins AEL, embryos 160mins AEL). Tukey multiple comparison showed this difference was $p < 0.001$ from ovary to 80mins AEL, and from 80mins AEL to 160mins AEL and no other reported differences (asterisks omitted from graph for clarity). Figure reproduced and modified from **(IV)**.

6 DISCUSSION

6.1 Dietary sugar levels can alter the degree of mitochondrial disease phenotype (I)

An initial hypothesis posited that decreased OXPHOS capacity in the tko^{25t} mutant fly (Toivonen et al., 2001) would lead to an over-reliance on glycolysis for ATP production. This hypothesis led to testing whether increasing the level of dietary sugar would feed glycolysis in an energy-starved system and potentially alleviate the phenotypes resulting from mitoribosomal dysfunction. Instead, the opposite occurred. An increasing dietary sugar content resulted in increased time to eclosion (developmental delay) and longer time to recovery after mechanical shock (bang-sensitivity) in tko^{25t} mutant flies, while having no significant effect on wild-type flies (**Fig 9**). This finding parallels recent work showing that changes in genes involved in mitoribosome biogenesis were evolutionarily important for the sugar tolerance exhibited by *Drosophila simulans* (Melvin et al., 2018), consistent with the observation that the downregulation of mitoribosomal function (such as by the tko^{25t} mutation) can lead to sugar-sensitivity, by an as yet unknown mechanism. The lack of effect of increased sugar on the development of wild-type flies showed that sugar-sensitivity is likely caused specifically by the tko^{25t} mutation. It is possible however, that a background effect is responsible for this sugar-sensitivity, and a test of this sugar sensitivity upon rescue of tko^{25t} with a ubiquitously driven UAS-*tko* transgene would essentially rule out such a possibility. Unlike a high-sugar diet, a high-fat and high-protein diet, with the same caloric content were unable to elicit a corresponding increase in time to eclosion, indicating that tko^{25t} mutant flies show sensitivity specifically to sugar and not merely to increased caloric intake. Increased TAG levels from sugar consumption and subsequent storage can also, most likely, be ruled out as the cause of the added stress to tko^{25t} mutant flies, otherwise exacerbated phenotypes would be expected on a high-fat diet too. However, it is possible that differences in nutrient absorption from food may mean that a high-sugar diet potentially causes far greater levels of TAG from *de-novo* synthesis than can be readily absorbed from a high-fat diet. Excess dietary sugar is a known driver of obesity in flies (Rovenko et al., 2015a).

Sugar-sensitivity of the mutant flies was observed regardless of whether glucose, sucrose or fructose was consumed. Each of these sugars gave the same approximately 5-day developmental delay in tko^{25t} flies (**Fig 9D**). This despite the observation that the metabolism of glucose and fructose differently affects levels of glycogen and triacylglyceride (TAG) storage in *Drosophila* (Rovenko et al., 2015a); and despite differing entry points of glucose and fructose into the glycolytic pathway (see **section 2.2.2**). The results are suggestive of a similar overall endpoint and causal effect for consumed sugar in tko^{25t} mutant flies, regardless of its source type (glucose, fructose or sucrose). In *Drosophila*, the majority of excess circulating glucose is converted to trehalose by the fat body (Mattila and Hietakangas, 2017). Most of the excess fructose and sucrose is also converted into trehalose and glucose (Miyamoto et al., 2012). Thus, a simple graduated increase in any of these sugars could be causing the same exacerbation of developmental delay by having the same effect on the final levels of circulating trehalose and glucose and on their subsequent utilisation in downstream processes.

As well as for storage purposes, it is considered that reductive glucose is converted into non-reducing trehalose to limit stress in the form of advanced glycation end-products (AGEs; Rovenko et al., 2015b). It is possible that tko^{25t} mutant flies are sensitive to AGEs caused by dietary reducing sugars and that developmental adaptation is required to accommodate this stress. AGEs are also proposed inducers of oxidative stress (Kaneto et al., 1996; Schalkwijk et al., 2004), and tko^{25t} flies could thus be showing a sensitivity to the oxidative stress induced by AGE formation upon sugar challenge. This oxidative stress sensitivity would fit with an observed induction of stress genes, including *Hsp22* and a set of glutathione-S-transferases, seen in a transcriptomic analysis of tko^{25t} flies (Fernández-Ayala et al., 2010). However, in *Drosophila*, the picture of reactive oxygen species (ROS) generation by dietary sugar is complicated by sex-specific, tissue-specific and developmental-stage specific effects (Rovenko et al., 2015b). Furthermore, the presence of an alternative oxidase, capable of decreasing the levels of mitochondrial ROS, was unable to change the developmental time or bang-sensitivity of tko^{25t} mutant flies (Kemppainen et al., 2014).

Previous studies have shown the presence of a regulatory mechanism, whereby increased sugar availability signals through TGF-β/Activin ligands and the transcription factor *sugarbabe* (*sug*) to repress the activity of carbohydrate digestion in the context of sugar abundance (Chng et al., 2014; Mattila et al., 2015). This mechanism may potentially save resources spent on the production and secretion of carbohydrases and may also be a means of regulating sugar absorption. On high-

sugar diets, repressive mechanisms such as this may become a limiting factor in the growth and development of tko^{25t} mutant flies, depleting the availability of necessary carbohydrate digestion products in an energy-starved system.

In a transcriptomic analysis of tko^{25t} mutant flies there was a significant increase of mRNAs for a set of Malpighian tubule sugar transporters and a decrease of those coding for gut-specific α-glucosidases (Fernández-Ayala et al., 2010), both of which were confirmed by qRTPCR **(Fig 10A)**. The altered regulation of these genes superficially seems to support the initial hypothesis presented above, whereby the tko^{25t} mutation may generate a signal for increased sugar uptake, and may also be an adaptive response to the sugar repression of carbohydrases. However, it is also possible that the Malpighian tubule sugar transporters may in fact be required for excreting excess sugar, and that decreased glucosidase activity in the gut may limit sugar mobilization in an adaptive 'anti-sugar' response, reflected in the effect of sugar on developmental time and bang sensitivity **(Fig 9)**. Regardless of the role of these transporters and glucosidases in the adaptation of tko^{25t} mutant flies, knocking them down did not affect developmental timing **(Fig 10C and 10D)**. Further attempts at altering sugar absorption and metabolism in this model of mitoribosomal disease would be of merit, but the potential problem of high adaptability and redundancy of genetic programmes regulating sugar absorption and use, may make complicate matters.

The idea that a decrease in dietary sugar could provide therapeutic value in cases of human mitochondrial disease is not without precedent. Very low carbohydrate or ketogenic diets, which naturally lower blood sugar levels, have been used to some positive effect in mitochondrial disease patients (Ahola et al., 2016). The discovery that increased sugar can cause exacerbation of phenotypes produced by a mitoribosomal mutation (tko^{25t}) is, however, a novel finding, though caution is appropriate when extrapolating from *Drosophila* to mammalian physiology. Particular considerations in this case are that, in *Drosophila*, sugar is metabolised by the fat body instead of the liver and the majority of circulating sugar is in the form of trehalose, a disaccharide far less prevalent in mammals (Yasugi et al., 2017). Following up these findings in a mouse model of mitoribosomal disease may bring further insight.

6.2 Pyruvate metabolism is a central component of metabolic reprogramming in *tko25t* mutant flies (II)

6.2.1 Pyruvate and its role in growth and development

Modifying pyruvate metabolism in *tko25t* mutant flies gave varying and, to some extent, contradictory results. With the importance of pyruvate in growth and development (see **section 2.2.5**) and the finding that *tko25t* mutant flies had elevated pyruvate levels, altering pyruvate levels seemed a logical strategy to attempt to elucidate metabolic mechanisms underlying the developmental delay of the *tko25t* mutant.

The addition of dietary pyruvate to both the wild-type and mutant flies increased the time to eclosion, supporting the view that pyruvate was instrumental in developmental timing and suggesting that its observed accumulation in *tko25t* mutant flies could be a direct cause of the developmental phenotype. However, the addition of DCA, a potent *Pdk* inhibitor, also increased developmental time, even though it led to the predicted decrease in pyruvate levels **(Fig 12 and Fig 13).** DCA has known off-targets, inhibiting plasma-membrane monocarboxylate transporters (MCTs)involved in lactate transport and in some instances inhibiting the pentose phosphate pathway (Carpenter and Halestrap, 1994; De Preter et al., 2016)**.** These off-target effects may be confounding those from *Pdk* perturbation and the *tko25t* mutation. Furthermore, genetic knockdown of *Pdk* had no significant effects on developmental time **(Fig 14B, panel ii)**. Inhibiting *Mpc1* activity and thus limiting pyruvate transport into the mitochondria using the inhibitor UK5099, did significantly increase the time to eclosion of *tko25t* mutant flies reared on a high-sugar diet **(Fig 12A)**. RNAi knockdown of *Mpc1* also caused an increased time to eclosion, but only in wild-type flies cultured on a high-sugar diet supplemented with pyruvate **(Fig 14B, panel i)**. These mixed results make it hard to distinguish what role mitochondrial and cytoplasmic pyruvate play in the developmental delay exhibited by *tko25t* mutant flies. However, in sum, they do suggest that pyruvate or one of the many pathways involved in the fate of pyruvate (see **section 2.2.5**) is critical to the developmental phenotype of *tko25t*.

These results also highlight the challenges of using genetic and chemical methods to alter the functions of specific proteins in a whole-organism model and show the importance of using a multifaceted strategy, avoiding the use of single, isolated approaches when studying metabolic pathways.

6.2.2   The Warburg hypothesis and *tko²⁵ᵗ*

The metabolic state of *tko²⁵ᵗ* mutant flies holds parallels to the metabolism of a developing tumour outlined by Warburg in his paper 'On the Origin of Cancer Cells' (Warburg, 1956). The Warburg effect is the observation that tumours make a switch to aerobic glycolysis and show lactic acidosis and increased pyruvate levels as a result. The Warburg hypothesis suggested underlying mitochondrial dysfunction causes cancer. With a resulting shift away from full oxidative phosphorylation and towards glycolysis, mitochondrial dysfunction might provide the causal metabolic effect in the development of a tumour. Even though the cause of cancer has since been shown primarily to be mutation of genes involved in growth regulation, cell death and cell adhesion, the Warburg effect is still a well-studied phenomenon (Senyilmaz and Teleman, 2015; Warburg, 1956). *tko²⁵ᵗ* mutant flies exhibit no evidence of tumorous growths, but the whole larva can in some ways be considered tumour-like. Under normal circumstances, a *Drosophila* larva already exhibits a massive growth rate and the same reliance on glycolysis seen in a developing tumour (Tennessen and Thummel, 2011). In addition, pyruvate and lactate are both increased approximately 3-fold in *tko²⁵ᵗ* mutant L3 larvae cultured on high-sugar medium **(Fig 11A),** akin to an 'amplified' Warburg effect**.** As in the Warburg hypothesis, this is due to an underlying mutation affecting mitochondrial functions, specifically defective mitoribosomal translation.

The strategies presented above, aimed at altering pyruvate metabolism in *tko²⁵ᵗ* mutant flies in the hope that they would restore normal development, closely resemble strategies such as DCA as a chemotherapeutic adjuvant, currently being used in clinical trials against cancer (Olszewski et al., 2010). It could prove useful therefore to further explore whether *tko²⁵ᵗ* mutants exhibit the same metabolic inflexibility as cancer cells (Olson et al., 2016) and whether this can be informative in alleviating the clinical features of human mitochondrial ribosomal diseases. It may be, that the developmental delay in *tko²⁵ᵗ* mutants is due to a delayed ability of larvae to convert to oxidative respiration, representative of wild-type adults, due to ETC deficiency. Thus, manipulating pyruvate metabolism, using the methods above, could be having their effect on time to eclosion by altering the rate of anaplerosis required to overcome the checkpoints for the transition from L3 stage to pupal stage. As opposed to the increased rate of growth and proliferation of tumours, the amplified Warburg effect in the *tko²⁵ᵗ* mutant flies instead causes a delayed growth and development of the fly, and understanding the differences between these two

systems may give insight as to how cancers can be therapeutically targeted to slow tumorous growth and development.

Knocking down *Ldh* was lethal in both wild type and *tko²⁵ᵗ* larvae **(I)**. The importance of lactate in *tko²⁵ᵗ* mutant flies is yet to be explored. However, a recent study showed intravenous infusions of ¹³C lactate into mice caused extensive labelling of TCA cycle intermediates in carbon flux analysis of multiple tissues, suggesting that lactate can be called upon as a predominant carbon source in situations of altered central metabolism (Hui et al., 2017). Disrupting this contribution in *tko²⁵ᵗ* mutants may eliminate a potential energy source in an already overburdened system. Both DCA and UK5099 have been shown to inhibit monocarboxylate transporters (MCTs) and their contradictory effects on the development of *tko²⁵ᵗ* flies may be the result of altering MCT-regulated cytoplasmic levels of lactate (Carpenter and Halestrap, 1994; Wiemer et al., 1995). Another recent study has also shown that a 'lactylation' of histones can regulate gene expression (Zhang et al., 2019), opening up the possibility that the increased lactate in *tko²⁵ᵗ* flies causes a fine-tuned regulatory effect on the transcriptome, enabling the flies to pass through development (albeit with a delay), despite their significantly perturbed energy metabolism. In this sense, it is possible that the developmental delay observed in *tko²⁵ᵗ* mutant flies is a highly optimised adaptive programme, rather than a maladaptive effect due to mitoribosomal deficiency, and that the attempts made to modify the metabolic changes underlying this developmental delay may in fact be deleterious to the mutant fly.

6.3   Over-expressing *srl* in the *tko²⁵ᵗ* mutant does not lead to the hallmark signs of mitochondrial biogenesis (III)

Due to the homology of *srl* with the mammalian PGC-1 family of transcriptional coactivators, and due to the conserved functions of *srl* in the *Drosophila* fat body (Tiefenböck et al., 2010; see **section 2.3.2.5**), it was hypothesised that the overexpression of *srl* may induce a programme of mitochondrial biogenesis in the *tko²⁵ᵗ* mutant. This mitochondrial biogenesis could potentially alleviate the underlying deficiency in OXPHOS activity rescuing the mutant phenotype. Initial experiments suggested this was the case, as overexpression of *srl* was seen to partially rescue developmental delay of the *tko²⁵ᵗ* mutants (Chen et al., 2012). The result of

this experiment was backed up in part by the discovery that *srl* mRNA expression was down-regulated in both *tko*[25t] 3rd instar larvae and adults (**Fig 15**). However, follow up of these experiments, showed that issues with *Drosophila* strains were present in the initial overexpression studies, meaning that a UAS-*srl* transgene was not present. Instead, an extra genomic copy of *srl* (*srl*[GR]) was causing the overexpression of *srl* seen previously (Chen et al., 2012). Furthermore, when these overexpression experiments were repeated, both the *srl*[GR] overexpression and a ubiquitously driven UAS-*srl* overexpression were unable to alleviate the developmental delay of *tko*[25t] mutants over several repeats (Fig 9 and **(II)**). This lack of rescue is consistent with a previous study showing an inability of *srl* overexpression to rescue the developmental delay caused by decreased OXPHOS capacity in a mutant of adenine nucleotide translocase (Vartiainen et al., 2014). While the mRNA for *srl* was overexpressed in these experiments, it is possible that an array of post-translational modifications known to be modulating the activity of PGC-1α (see **section 2.3.2.2**) are also acting on Spargel to keep protein levels constant. To test this, a customised antibody against Spargel was first verified using an expression construct in S2 cells (**Fig 16D and E**) and then used to see whether *srl* mRNA overexpression correlated with increased Spargel protein. As can be seen in **figure 16C**, only a modest increase was observed in Spargel protein levels despite an mRNA overexpression of approximately 40-fold in males and 4-fold in female flies (**Fig 17**). This suggests that *srl* mRNA levels do not necessarily reflect the level of Spargel protein. Instead, the large array of post translational modifications known to regulate PGC-1α (see **section 2.3.2.2 and Fig 8**), may well also be regulating Spargel protein in an equivalent manner, keeping it at a steady-state.

The lack of any dramatic change in Spargel protein levels might also be why measured hallmarks of mitochondrial biogenesis were unaltered in both wild-type and *tko*[25t] flies when *srl* was overexpressed. Transcriptional coactivators induce their effects at the level of gene expression, but no change was seen in the expression of both nuclear and mitochondrial subunits of the ETC upon *srl* overexpression (**Fig 18**). Nor was any change observed in mitochondrial copy number when *srl* was overexpressed (**Fig 19**).

Finally, a previous study showed that constitutively active dFOXO was able to downregulate *srl* mRNA expression (Gershman et al., 2007; **section 2.3.2.5**), linking insulin signalling to *srl* regulation. In our experiments, however, alteration of dietary sugar was unable to change the expression level of *srl* mRNA in both wild-type and *tko*[25t] mutant flies (**Fig 15**). Srl mRNA levels may be robust to fluctuations in dietary sugar and are potentially kept at a constant level in varied nutrient environments.

The unnatural constitutive activation of dFOXO may, on the other hand, alter this normal state of *srl* mRNA homeostasis, by disproportionately altering expression of transcription factors controlling the expression of *srl* through its promoter. It is therefore likely that the sugar-sensitivity observed in *tko^{25t}* mutants (see **section 6.1**) is not acting through altered *srl* mRNA expression. This does not rule out a role of post-translational regulation of Spargel in the adaptation of the *tko^{25t}* mutant to sugar, however.

6.4   *srl* and mitochondrial biogenesis during early *Drosophila* development (IV)

Embryogenesis is the critical stage during a complex organism's life cycle where either accurate development produces an organism able to thrive and pass its genes onto subsequent generations. Alternatively, if development goes awry, the organism can be left with insurmountable abnormalities and may even cease to develop at all.

When testing the effects of *srl* overexpression in *tko^{25t}* mutants (see **section 6.3**), an 8-fold higher level of *srl* mRNA in adult females as compared to males was consistently observed (**Fig 15B**). Further experiments showed that this was due to the accumulation of *srl* mRNA in ovaries and early embryos (**Fig 20**), suggesting that *srl* is a maternally deposited mRNA. This accumulation of *srl* mRNA and its subsequent decrease to very low levels at embryo stages 4-6 suggested a role of *srl* in early *Drosophila* development. To investigate this, a set of germline drivers were used in combination with a collection of *srl* RNAi constructs to see if there would be an effect on oogenesis or embryogenesis. Only a single combination, of the maternal tri-driver (MTD-GAL4) with a specific Harvard Medical School TRiP RNAi construct (33914), was able to give substantial knockdown, resulting in a lethal phenotype, specifically during embryogenesis (**Fig 22 and Fig 23**). Other driver and RNAi combinations were able to effectively knockdown *srl* mRNA to a much lesser degree. None gave a lethal phenotype, suggesting that a threshold of *srl* needs to be met for embryos to undergo a full developmental programme. Despite effectively knocking down *srl* mRNA throughout oogenesis, no noticeable effect was observed on the morphology of the germarium or vitellogenic stages (**Fig 26**). In embryos, clear morphological abnormalities were observed with an overall smaller size of the *srl* knockdown embryos (**Fig 23**). Timelapse images showed that *srl* knockdown was causing drastic corruption of the developmental programme at an early stage of embryogenesis with a failure of embryos to form a uniform blastoderm and undergo

cellularisation (**Fig 24**). Knockdown of *srl* did not affect the distribution of three maternal axis determinants in the early embryo (**Fig 25**). Considering the potential role of *srl* in mitochondrial biogenesis (see **section 2.3.2.5**), mitochondrial parameters were measured. No specific effect was observed in either ovaries or embryos, including no change in nuclearly or mitochondrially encoded genes for ETC subunits, 16S and TFAM (**Fig 27 and Fig 28**), no change in protein levels of mitochondrial OXPHOS subunits (**Fig 29 and Fig 30**), and no change in mitochondrial DNA copy number (**Fig 31**). This lack of effect on mitochondrial parameters suggests another essential role of *srl* during early *Drosophila* development, distinct from mitochondrial biogenesis, which deserves further exploration. As *srl* is a transcriptional coactivator, it acts with transcription factors to remodel chromatin. Therefore, a strategy probing chromatin availability, such as ATAC-seq (Buenrostro et al., 2013), may well bring insight into which genes are being misregulated in *srl* knockdown embryos.

That *srl* is not acting to induce mitochondrial biogenesis in early embryogenesis is consistent with previous results which show a significant increase in expression of genes for lactate dehydrogenase, glycolysis, β-oxidation, TCA cycle and OXPHOS, occurring much later than the peak of *srl* expression, namely after 12 hours of development at 25°C (Tennessen et al., 2014). This metabolic induction is also well past the stage at which development is corrupted by germline knockdown of *srl* (**Fig 24**). The same study showed a decrease in mitochondrial gene expression from hours 0-2 to 3-4 of embryo development, consistent with what is observed in the above qRTPCR measurements from stages 1-3 to 4-6 of embryogenesis (**Fig 28**). Moreover, the embryonic mitochondrial content comes largely from the delivery of the Balbiani body from nurse cells into the oocyte during oogenesis (Cox and Spradling, 2003), meaning that renewed mitochondrial biogenesis is likely only required at a later stage of embryonic or larval growth. No decrease in mitochondrial mass or abnormal morphology and localisation was seen in *srl* germline knockdown ovaries (**Fig 26**).

A parallel can be seen between the embryonic lethality caused by *srl* knockdown in the germline and embryonic lethality before embryonic day 6.5 in knockout mice of the lesser-studied member of the PGC-1 family, PGC-1-related coactivator (PRC or PPRC1; He et al., 2012). The mRNA expression of *PRC* shows accumulation in the early mouse embryo, before a decline in expression after the four-cell stage, similar to the pattern of *srl* mRNA expression during *Drosophila* embryogenesis (**Fig 20**). Furthermore, the PRC-deficient heterozygotes were indistinguishable from their wild-type littermates, suggesting embryonic lethality only occurs below a certain

threshold of PRC expression (He et al., 2012), which is also inferred to be the case with *srl* (see above). Together, this suggests *srl* may be playing a similar, as yet unknown, role as PRC in early development. As *srl* is the only homolog of PGC-1 in *Drosophila*, its function in early development might be ancestral, with the mitochondrial biogenesis programme supported by *srl* and other mammalian PGC-1 homologues, only playing a role in specific tissues later in development or in adults. That said, a simple protein BLAST of the Spargel protein sequence against human proteins gives PRC as the top hit (consistent with the parallels drawn above), albeit with only approximately 45% identity with the last 95 amino acids of the C-terminus, but PGC-1α and PGC-1β don't appear on the list at all. A previous study however, has shown a degree of conservation between the acidic amino-terminal, Arginine/Serine-Rich (RS) and RNA-recognition motif (RRM) domains of PGC-1α, PGC-1β and Spargel (see **Fig 5**, Gershman et al., 2007). This shows the importance of careful consideration when comparing Spargel to its proposed mammalian counterparts. This field would benefit from further studies showing interactions of Spargel with transcription factors before presuming directly comparable functions to PGC-1α, PGC-1β or PRC, particularly with regards to mitochondrial biogenesis (see **section 6.5**).

As with ubiquitous overexpression of *srl* mRNA showing little effect on Spargel protein levels (see **section 6.3**), germline-specific knockdown of *srl* mRNA, with a resultant lethality during embryogenesis also seemed to have little effect on Spargel protein levels (**Fig 21**). That said, only a small amount of Spargel protein could be detected in ovaries and embryos (**Fig 21**) despite the accumulation of *srl* mRNA during these early stages of development. The custom antibody created against Spargel and used in these experiments (**Fig 16**) may detect a specific isoform of Spargel more prevalent in adult tissues, and another distinct version of Spargel might instead be translated during oogenesis and embryogenesis. Mammalian PGC-1α is known to have many distinct isoforms regulated by the differential activity of a distal upstream promoter region (Martínez-Redondo et al., 2015). Additional checks of the specificity of this custom antibody would be merited, and generation of a Spargel knock-out mutant, which should be viable considering the viability of the deficiency mutant Df(3R)5046 (which also deletes the *srl* locus), would give the most confidence in these custom antibodies. If the custom antibodies used here are detecting a form of Spargel protein however, difference in *srl* isoforms might explain the contradiction seen in a recent study, where germline-specific *srl* knockdown was shown to cause a decrease in detected Spargel protein (Basar et al., 2019). These authors detected a 150 kDa band for Spargel, compared to a 105 kDa and 120 kDa

band seen in the experiments outlined above (**Fig 16 and Fig 21**). The same authors, using the germline-specific maternal tri-driver described in this thesis, but combined with two of their own custom RNAi constructs (thus controlling for off-target effects), showed that *srl* knockdown caused a drastic decrease in ovary size and a subsequent female sterility with no embryos laid (Basar et al., 2019), consistent with previous reports of female sterility and delayed oogenesis in a *srl* hypomorph (Mukherjee et al., 2014; Tiefenböck et al., 2010), but different from results in this thesis showing no effect on the number of eggs laid but a lethality during early embryogenesis instead. Finally, the same authors also show, using a different germline driver with their custom RNAi construct, that germline *srl* knockdown causes a reduction in mitochondrial mass in a single experiment staining for ATP5a (Basar et al., 2019). This mitochondrial mass reduction again contradicts the observation in this thesis of no observed change in mitochondrial intensity or localisation during oogenesis (**Fig 26**) and suggests that the differences in RNAi method might be inducing different phenotypes of oogenesis defects versus embryogenesis defects, due to as yet unknown reasons. It is possible that the different RNAi strategies target different isoforms, or that the extent of the knockdown varies between the two knockdown strategies and a full comparison using multiple primer sets against different potential isoforms, and subsequent measurement by qRTPCR might clarify the differences seen.

6.5 PGC1 transcriptional coactivators and their assumed role as 'master regulators of mitochondrial biogenesis'. (III, IV)

Much of the research done on the PGC-1 family has been performed on mitochondria-rich cell or tissue types including skeletal muscle, adipose tissue and liver (Martínez-Redondo et al., 2015; Ni et al., 2011), and the majority of these studies have provided evidence for a role of these coactivators in mitochondrial biogenesis. There are exceptions, however. For example, a previous study described the necessity of PGC-1α for the correct secretion of insulin from pancreatic β-cells but showed no influence of PGC-1α on mitochondrial parameters such as mitochondrial mass, gene expression and respiratory function (Oropeza et al., 2015). Similarly, different roles of the PGC-1 members can be decoupled, depending on their tissue and nutrient context. For example, in well-fed conditions, S6K can switch off PGC-1α mediated gluconeogenesis in the liver while PGC-1α mitochondrial gene induction is unaffected (Rhee et al., 2003). In *Drosophila* mutants of the *NRF2*

homolog *Delg*, which is coactivated by *srl*, the larval fat body shows a decreased mitochondrial mass but no change in respiratory activity, indicating that different components of mitochondrial biogenesis can also be decoupled (Baltzer et al., 2009).

Over the last two decades, it has become more apparent that the PGC-1 family also controls the regulation of transcription in important processes other than mitochondrial biogenesis (Villena, 2015 and **section 2.3.2.4**). Thus, the PGC-1 family should not merely be considered master regulators of mitochondrial biogenesis, but instead, their activity should be considered in a context-dependent manner. Different tissues have differentially expressed transcriptions factors, with their own complex array of regulatory effectors. ERRα, for instance, is regulated by acetylation and deacetylation of 4 lysines on its binding domain, and by sumoylation (Tremblay et al., 2008; Wilson et al., 2010). Depending on which transcription factors are present, and in which state of post-translational modification they are, the PGC-1 coactivators should have a varied effect on transcriptional patterns. This varied effect may or may not include regulation of genes canonically associated with mitochondrial biogenesis.

Thus, the transcriptional coactivation activity of the PGC-1 family is as complex as that of the transcription factors with which they associate. Due to their context-specific role in mitochondrial biogenesis, these coactivators, particularly PGC-1α, have evoked interest in their possible use for therapeutic purposes in metabolic diseases. However, caution should be applied in this regard. Simply increasing the activity of these coactivators non-specifically may also have deleterious effects, as might be expected from a transcriptional regulator of many essential genes. For example, heart-specific overexpression of PGC-1α, while inducing the sought after mitochondrial biogenesis, was also lethal in mice (Lehman et al., 2000).

Consistent with this complex picture of PGC-1 coactivation in varied contexts, germline-specific knockdown of *srl*, while lethal during early embryogenesis, did not alter the hallmarks of mitochondrial biogenesis (see **section 6.4**). This lack of effect on mitochondrial biogenesis suggests that *srl* is required for another function, other than mitochondrial transcriptional control, in early *Drosophila* development. Equally, when *srl* was ubiquitously overexpressed in both wild-type and *tko²⁵ᵗ* mutants, it failed to induce hallmarks of mitochondrial biogenesis (see **section 6.3**). Once again, these findings imply that *srl* may not be operating as a simple master regulator of mitochondrial biogenesis. The underlying mechanisms and effects of *srl* activity in tissue-specific and developmentally specific contexts require further study.

The experiments presented in the latter half of this thesis build upon previous work exploring Spargel transcriptional coactivator function and its often-assumed

role in mitochondrial biogenesis. Such an assumption is a convenient reduction and oversimplification, as discussed above. The results described here point in a different direction, and away from automatically assuming Spargel to act as a 'master regulator of mitochondrial biogenesis'. In doing so, this work further highlights the importance of critical evaluation when performing research on physiological processes of potential relevance to humans.

7   CONCLUSIONS

This thesis presents new insights into the dynamics of pyruvate metabolism in the context of mitochondrial translational disease, showing that simple strategies to alter pyruvate metabolism result in complex outcomes. An exacerbated Warburg-like effect can be seen in tko^{25t} mutant larvae including significantly increased levels of pyruvate. The tko^{25t} mutation results in delayed development, which can be altered by manipulation of pyruvate metabolism, but levels of pyruvate do not directly correlate with developmental time. This suggests that the complex metabolic shift seen in tko^{25t} mutant flies may involve as yet unknown mechanisms, giving rise to an adaptive developmental delay, but that pyruvate metabolism is definitely involved to some degree in this process. tko^{25t} being a mitochondrial translational mutation, it could be expected that inducing mitochondrial biogenesis might alter the phenotypes present in the mutant flies. However, attempts to alter the growth and development of these mutant flies by overexpressing *spargel*, did not result in a programme of mitochondrial biogenesis. In the light of follow-up experiments on the role of *spargel* in development, this is not surprising, as the effects of *spargel* activity were shown to be more complex than expected. Knockdown of *spargel* caused embryonic lethality but had no effect on the hallmarks of mitochondrial biogenesis. Future work will require further metabolomic analysis of the tko^{25t} mutant and a refined study of the context-specific activity of *spargel* as a transcriptional coactivator to fully elucidate where it does and does not induce a programme of mitochondrial biogenesis.

8   ACKNOWLEDGEMENTS

I have to start with Howy. Giving me the opportunity to come out here to Finland to pursue my PhD has profoundly impacted my life in many positive ways, and I will always remain grateful for that. Being a PI is a hard task as you often bear the brunt of the many frustrations PhD students, post-docs and technicians come across during their work, yet you still found patience and understanding with us all. Importantly, you hold fast to the value of the science in and amongst all the bluster that we in this field sometimes encounter, teaching me a lesson of perseverance in the face of disincentives a career in science may bring. I am infinitely grateful for the consideration and care you showed during my period of illness. You never made me feel like I was an issue or a burden, and that support played a big part in making it possible for me to reach the end of my PhD. Thank you.

Tea and Eveliina, thank you so much for all the hard work and help over the years but mainly thank you for being such lovely people and always available to talk, and not just about science, bringing some much needed calm to the workplace.

Thank you to Anna Vallius for being a genuinely kind and caring person even when you had to put up with the many foibles of us academics.

Eric, Jose, Sina, Yuliya, Maria, Grazia and Mugen. I can't even find words to describe the lunch discussions that we had. Really, I cannot. The more absurd they got, the more I knew I was working in the right place. I am entirely thankful for that level of weirdness and since moving away from it have even come to miss it, although I'm sure a psychologist would suggest this is the aftermath of some strange form of Stockholm syndrome. Thank you for all of your help and laughs over the years. From cantankerous to hyperactive, you have stomached all of my moods, and I am very thankful to you all for being great colleagues. Antti and Samuel, you are included in that mix, but I wanted to give a special thanks to you both for putting up with me as a supervisor.

Ana. Our long talks in the evenings made us delve deep into both our psychologies, and whether or not we are any better off for it, I thank you for these and the many other moments we spent over the years.

To Kira, Marten, Praveen, Charlie, Udy and the rest of the Howylab Helsinki bunch, a big thanks for making trips to Viikki and all the FinMit meetings far more memorable and friendly.

A big thank you to the rest of the crew over the years. Esko, the original gangster with whom we laughed too much sometimes. Kia, Alberto, Greg, Suvi, Priit, Marcos, Emily, Kaisa, Katharina, Guiseppe, Ashwin, Venk, Ellie, Suzy, and more to whom I'm sorry if I have forgotten to get your name in here. More big thanks to the oft-forgotten civilian servants who were the backbone of our fly lab and who always brought their unique flavour to the environment (and possibly the fly food). You know who you are.

Thank you to Nick, Mike and Tapio for being my gym partners over the years. I am yet to see my six-pack, but I am certainly much healthier for those times lifting weights (mainly chatting). A particular thanks to Tapio for our balcony discussions, which developed both of our worldly perspectives when times were tough for both of us. I can't wait to have more of these chats again in the future.

To all of my family back in the UK, although we have had our difficulties, I am thankful to you all for the love and care.

To Troy, Paul, Luke and Nick. What can I say about our friendships? I will leave it there. You are great lads who made life outside the lab a LOT of fun. Thanks for all the good times, from which we will have material to reminisce over for the rest of our lives. I hope that we will be doing this together when we're old and grey. Maybe not Nick as he will be late. Particularly thanks to Troy for being so good to me over the years.

Last but by no means least, my beautiful wife, Alina. As I write this we are in a lockdown due to a coronavirus pandemic and the fact that we haven't strangled each other yet is a testament to our love for each other. I couldn't imagine anyone better to be spending these bizarre times with. How can I even start to write what you have meant to me over these last four years that I have known you? You have been there for me through thick and thin and everything in between. Thanks to you I am less cynical (slightly at least) and have learnt what love and care mean all over again. The product of this love is our baby boy. We are under a week from his due date as I sit and type this. He could come anytime now. What exciting times we have ahead of us. I love you and thank you for standing by me. I feel like I have learnt so much from you. You are my biggest love and my greatest friend.

9 REFERENCES

Abrahams, J.P., Leslie, A.G.W., Lutter, R., and Walker, J.E. (1994). Structure at 2.8 Å resolution of F1-ATPase from bovine heart mitochondria. Nature *370*, 621–628.

Aguila, J.R., Hoshizaki, D.K., and Gibbs, A.G. (2013). Contribution of larval nutrition to adult reproduction in Drosophila melanogaster. J. Exp. Biol. *216*, 399–406.

Ahmad, M., He, L., and Perrimon, N. (2019). Regulation of insulin and adipokinetic hormone/glucagon production in flies. Wiley Interdiscip. Rev. Dev. Biol. e360.

Ahola, S., Auranen, M., Isohanni, P., Niemisalo, S., Urho, N., Buzkova, J., Velagapudi, V., Lundbom, N., Hakkarainen, A., Muurinen, T., et al. (2016). Modified Atkins diet induces subacute selective ragged-red-fiber lysis in mitochondrial myopathy patients. EMBO Mol. Med. *8*, 1234–1247.

Alam, M.M., Lal, S., FitzGerald, K.E., and Zhang, L. (2016). A holistic view of cancer bioenergetics: mitochondrial function and respiration play fundamental roles in the development and progression of diverse tumors. Clin. Transl. Med. *5*.

Alston, C.L., Rocha, M.C., Lax, N.Z., Turnbull, D.M., and Taylor, R.W. (2017). The genetics and pathology of mitochondrial disease. J. Pathol. *241*, 236–250.

Andersson, U., and Scarpulla, R.C. (2001). Pgc-1-related coactivator, a novel, serum-inducible coactivator of nuclear respiratory factor 1-dependent transcription in mammalian cells. Mol. Cell. Biol. *21*, 3738–3749.

Arany, Z., Lebrasseur, N., Morris, C., Smith, E., Yang, W., Ma, Y., Chin, S., and Spiegelman, B.M. (2007). The Transcriptional Coactivator PGC-1β Drives the Formation of Oxidative Type IIX Fibers in Skeletal Muscle. Cell Metab. *5*, 35–46.

Arany, Z., Foo, S.Y., Ma, Y., Ruas, J.L., Bommi-Reddy, A., Girnun, G., Cooper, M., Laznik, D., Chinsomboon, J., Rangwala, S.M., et al. (2008). HIF-independent regulation of VEGF and angiogenesis by the transcriptional coactivator PGC-1α. Nature *451*, 1008–1012.

Bainbridge, S.P., and Bownes, M. (1981). Staging the metamorphosis of Drosophila melanogaster. Development *66*.

Baker, K.D., and Thummel, C.S. (2007). Diabetic Larvae and Obese Flies-Emerging Studies of Metabolism in Drosophila. Cell Metab. *6*, 257–266.

Bäkker, K. (1959). Feeding period, growth, and pupation in larvae ofdrosophila melanogaster. Entomol. Exp. Appl. *2*, 171–186.

Baldelli, S., Pagliei, B., Aquilano, K., Rotilio, G., Vigilanza, P., and Ciriolo, M.R. (2010). Peroxisome Proliferator-activated Receptor γ Co-activator 1α (PGC-1α) and Sirtuin 1 (SIRT1) Reside in Mitochondria. J. Biol. Chem. *285*, 21590–21599.

Baltzer, C., Tiefenböck, S.K., Marti, M., and Frei, C. (2009). Nutrition controls mitochondrial biogenesis in the Drosophila adipose tissue through Delg and cyclin D/Cdk4. PLoS One *4*.

Baradaran, R., Berrisford, J.M., Minhas, G.S., and Sazanov, L.A. (2013). Crystal structure of the entire respiratory complex i. Nature *494*, 443–448.

Basar, M.A., Williamson, K., Roy, S.D., Finger, D.S., Ables, E.T., and Duttaroy, A. (2019). Spargel/dPGC-1 is essential for oogenesis and nutrient-mediated ovarian growth in Drosophila. Dev. Biol. *454*, 97–107.

Bastock, R., and St Johnston, D. (2008). Drosophila oogenesis. Curr. Biol. *18*.

Beadle, G.W., Tatum, E.L., and Clancy, C.W. (1938). Food level in relation to rate of development and eye pigmentation in drosophila melanogaster. Biol. Bull. *75*, 447–462.

Ben-Sahra, I., Howell, J.J., Asara, J.M., and Manning, B.D. (2013). Stimulation of de novo pyrimidine synthesis by growth signaling through mTOR and S6K1. Science (80-.). *339*, 1323–1328.

Berg, J., Tymoczko, J., and Stryer, L. (2002). Biochemistry (New York, NY: W H Freeman).

Bevers, R., Francis, D., Ghazanfar, S., Havula, E., Krycer, J.R., Senior, A., Minard, A.Y., Geddes, T., Weiss, F., and James, D.E. (2019). Genome-wide analysis of diet and gene interactions in Drosophila uncovers the glucose transporter, CG4607, as a diet-responsive gene. BioRxiv.

Bickel, P.E., Tansey, J.T., and Welte, M.A. (2009). Biochimica et Biophysica Acta PAT proteins , an ancient family of lipid droplet proteins that regulate cellular lipid stores. BBA - Mol. Cell Biol. Lipids *1791*, 419–440.

Bizeau, M.E., Short, C., Thresher, J.S., Commerford, S.R., Willis, W.T., and Pagliassotti, M.J. (2001). Increased pyruvate flux capacities account for diet-induced increases in gluconeogenesis in vitro. Am. J. Physiol. Regul. Integr. Comp. Physiol. *281*, R427-33.

Blattler, S.M., Verdeguer, F., Liesa, M., Cunningham, J.T., Vogel, R.O., Chim, H., Liu, H., Romanino, K., Shirihai, O.S., Vazquez, F., et al. (2012). Defective Mitochondrial Morphology and Bioenergetic Function in Mice Lacking the Transcription Factor Yin Yang 1 in Skeletal Muscle. Mol. Cell. Biol. *32*, 3333–3346.

Böhni, R., Riesgo-Escovar, J., Oldham, S., Brogiolo, W., Stocker, H., Andruss, B.F., Beckingham, K., and Hafen, E. (1999). Autonomous control of cell and organ size by CHICO, a Drosophila homolog of vertebrate IRS1-4. Cell *97*, 865–875.

Boncompagni, S., Rossi, A.E., Micaroni, M., Beznoussenko, G. V, Polishchuk, R.S., Dirksen, R.T., and Protasi, F. (2009). Mitochondria are linked to calcium stores in striated muscle by developmentally regulated tethering structures. Mol. Biol. Cell *20*, 1058–1067.

Bonekamp, N.A., and Larsson, N.G. (2018). SnapShot: Mitochondrial Nucleoid. Cell *172*, 388-388.e1.

Boström, P., Wu, J., Jedrychowski, M.P., Korde, A., Ye, L., Lo, J.C., Rasbach, K.A., Boström, E.A., Choi, J.H., Long, J.Z., et al. (2012). A PGC1-α-dependent myokine that drives brown-fat-like development of white fat and thermogenesis. Nature *481*, 463–468.

Boulan, L., Milán, M., and Léopold, P. (2015). The systemic control of growth. Cold Spring Harb. Perspect. Biol. *7*.

Bricker, D.K., Taylor, E.B., Schell, J.C., Orsak, T., Boutron, A., Chen, Y.C., Cox, J.E., Cardon, C.M., Van Vranken, J.G., Dephoure, N., et al. (2012). A mitochondrial pyruvate carrier required for pyruvate uptake in yeast, Drosophila, and humans. Science (80-.). *336*, 96–100.

Britton, J.S., Lockwood, W.K., Li, L., Cohen, S.M., and Edgar, B.A. (2002). Drosophila's insulin/PI3-kinase pathway coordinates cellular metabolism with nutritional conditions. Dev. Cell *2*, 239–249.

Brivet, M., Garcia-Cazorla, A., Lyonnet, S., Dumez, Y., Nassogne, M.C., Slama, A., Boutron, A., Touati, G., Legrand, A., and Saudubray, J.M. (2003). Impaired mitochondrial pyruvate importation in a patient and a fetus at risk. Mol. Genet. Metab. *78*, 186–192.

Buck, M.D.D., O'Sullivan, D., Klein Geltink, R.I.I., Curtis, J.D.D., Chang, C.H., Sanin, D.E.E., Qiu, J., Kretz, O., Braas, D., van der Windt, G.J.J.W., et al. (2016). Mitochondrial Dynamics Controls T Cell Fate through Metabolic Programming. Cell *166*, 63–76.

Buenrostro, J.D., Giresi, P.G., Zaba, L.C., Chang, H.Y., and Greenleaf, W.J. (2013). Transposition of native chromatin for fast and sensitive epigenomic profiling of open chromatin, DNA-binding proteins and nucleosome position. Nat. Methods *10*, 1213–1218.

Burke, C.J., and Waddell, S. (2011). Remembering nutrient quality of sugar in Drosophila. Curr. Biol. *21*, 746–750.

Bursle, C., Narendra, A., Chuk, R., Cardinal, J., Justo, R., Lewis, B., and Coman, D. (2017). COXPD9 an evolving multisystem disease; congenital lactic acidosis, sensorineural hearing loss, hypertrophic cardiomyopathy, cirrhosis and interstitial nephritis. In JIMD Reports, (Springer), pp. 105–109.

Cam, H., Balciunaite, E., Blais, A., Spektor, A., Scarpulla, R.C., Young, R., Kluger, Y., and Dynlacht, B.D. (2004). A common set of gene regulatory networks links metabolism and growth inhibition. Mol. Cell *16*, 399–411.

Campos-Ortega, J.A., and Hartenstein, V. (1985). The Embryonic development of Drosophila melanogaster.

Cappel, D.A., Deja, A., Duarte, J.A., Mishra, P., Browning, J.D., and Burgess Correspondence, S.C. (2019). Pyruvate-Carboxylase-Mediated Anaplerosis

Promotes Antioxidant Capacity by Sustaining TCA Cycle and Redox Metabolism in Liver.

Carpenter, L., and Halestrap, A.P. (1994). The kinetics, substrate and inhibitor specificity of the lactate transporter of Ehrlich-Lettre tumour cells studied with the intracellular pH indicator BCECF. Biochem. J. *304*, 751–760.

Carvalho, M., Sampaio, J.L., Palm, W., Brankatschk, M., Eaton, S., and Shevchenko, A. (2012). Effects of diet and development on the Drosophila lipidome. Mol. Syst. Biol. *8*, 1–17.

Charest-Marcotte, A., Dufour, C.R., Wilson, B.J., Tremblay, A.M., Eichner, L.J., Arlow, D.H., Mootha, V.K., and Giguère, V. (2010). The homeobox protein Prox1 is a negative modulator of ERRα/PGC- 1α bioenergetic functions. Genes Dev. *24*, 537–542.

Chen, S., Oliveira, M.T., Sanz, A., Kemppainen, E., and Fukuoh, A. (2012). A Cytoplasmic Suppressor of a Nuclear Mutation. *192*, 483–493.

Cherry, A.D., Suliman, H.B., Bartz, R.R., and Piantadosi, C.A. (2014). Peroxisome proliferator-activated receptor γ co-activator 1-α as a critical co-activator of the murine hepatic oxidative stress response and mitochondrial biogenesis in Staphylococcus aureus sepsis. J. Biol. Chem. *289*, 41–52.

Chintapalli, V.R., Wang, J., and Dow, J.A.T. (2007). Using FlyAtlas to identify better Drosophila melanogaster models of human disease. Nat. Genet. *39*, 715–720.

Chng, W. bin A., Sleiman, M.S.B., Schüpfer, F., and Lemaitre, B. (2014). Transforming growth factor β/activin signaling functions as a sugar-sensing feedback loop to regulate digestive enzyme expression. Cell Rep. *9*, 336–348.

Christian, B.E., and Spremulli, L.L. (2012). Mechanism of protein biosynthesis in mammalian mitochondria. Biochim. Biophys. Acta - Gene Regul. Mech. *1819*, 1035–1054.

Church, R.B., and Robertson, F.W. (1966). A biochemical study of the growth ofDrosophila melanogaster. J. Exp. Zool. *162*, 337–351.

Cohen, B., Simcox, A.A., and Cohen, S.M. (1993). Allocation of the thoracic imaginal primordia in the Drosophila embryo. Development *117*, 597–608.

Colombani, J., Raisin, S., Pantalacci, S., Radimerski, T., Montagne, J., and Léopold, P. (2003). A nutrient sensor mechanism controls Drosophila growth. Cell *114*, 739–749.

Colombani, J., Andersen, D.S., Boulan, L., Virolle, V., Texada, M., and Le, P. (2015). Drosophila Lgr3 Couples Organ Growth with Maturation and Ensures Developmental Stability Report Drosophila Lgr3 Couples Organ Growth with Maturation and Ensures Developmental Stability. 2723–2729.

Cox, R.T., and Spradling, A.C. (2003). A Balbiani body and the fusome mediate mitochondrial inheritance during Drosophila oogenesis. Development *130*, 1579–1590.

Cox, C.J., Foster, P.G., Hirt, R.P., Harris, S.R., and Embley, T.M. (2008). The archaebacterial origin of eukaryotes. Proc. Natl. Acad. Sci. U. S. A. *105*, 20356–20361.

Cunningham, J.T., Rodgers, J.T., Arlow, D.H., Vazquez, F., Mootha, V.K., and Puigserver, P. (2007). mTOR controls mitochondrial oxidative function through a YY1-PGC-1α transcriptional complex. Nature *450*, 736–740.

Curtiss, J., and Heilig, J.S. (1995). Establishment of Drosophila imaginal precursor cells is controlled by the Arrowhead gene. Development *121*.

Czech, M.P., and Building, M.M. (2018). Insulin action and resistance in obesity and type 2 diabetes. Nat. Med. *23*, 804–814.

Dean, E.D., Li, M., Prasad, N., Wisniewski, S.N., Von, A., Spaeth, J., Maddison, L., Botros, A., Sedgeman, L.R., Bozadjieva, N., et al. (2017). Interrupted Glucagon Signaling Reveals Hepatic-α-Cell Axis and Role for L-Glutamine in α-Cell Proliferation. Cell Metab. *25*, 1362–1373.

Desai, S., Ding, M., Wang, B., Lu, Z., Zhao, Q., Shaw, K., Yung, W.K.A., Weinstein, J.N., Tan, M., and Yao, J. (2014). Tissue-specific isoform switch and DNA hypomethylation of the pyruvate kinase PKM gene in human cancers. Oncotarget *5*, 8202–8210.

Dhar, S.S., Ongwijitwat, S., and Wong-Riley, M.T.T. (2008). Nuclear respiratory factor 1 regulates all ten nuclear-encoded subunits of cytochrome c oxidase in neurons. J. Biol. Chem. *283*, 3120–3129.

Diop, S.B., Bisharat-Kernizan, J., Birse, R.T., Oldham, S., Ocorr, K., and Bodmer, R. (2015). PGC-1/spargel counteracts High-fat-diet-induced obesity and cardiac lipotoxicity downstream of TOR and brummer ATGL lipase. Cell Rep. *10*, 1572–1584.

Doane, W.W. (1961). Developmental physiology of the mutantfemale sterile(2)adipose ofDrosophila melanogaster. III. Corpus allatum-complex and ovarian transplantations. J. Exp. Zool. *146*, 275–298.

Dos, D.S., Ali, S.M., Kim, D.H., Guertin, D.A., Latek, R.R., Erdjument-Bromage, H., Tempst, P., and Sabatini, D.M. (2004). Rictor, a novel binding partner of mTOR, defines a rapamycin-insensitive and raptor-independent pathway that regulates the cytoskeleton. Curr. Biol. *14*, 1296–1302.

Duan, M., Tu, J., and Lu, Z. (2018). Recent advances in detecting mitochondrial DNA heteroplasmic variations. Molecules *23*.

Dufour, C.R., Wilson, B.J., Huss, J.M., Kelly, D.P., Alaynick, W.A., Downes, M., Evans, R.M., Blanchette, M., and Giguère, V. (2007). Genome-wide Orchestration of Cardiac Functions by the Orphan Nuclear Receptors ERRα and γ. Cell Metab. *5*, 345–356.

Duncan, J.G., Fong, J.L., Medeiros, D.M., Finck, B.N., and Kelly, D.P. (2007). Insulin-resistant heart exhibits a mitochondrial biogenic response driven by the peroxisome proliferator-activated receptor-α/PGC-1α gene regulatory pathway. Circulation *115*, 909–917.

Dutta, D., Buchon, N., Xiang, J., and Edgar, B.A. (2015). Regional cell specific RNA expression profiling of FACS isolated drosophila intestinal cell populations. Curr. Protoc. Stem Cell Biol. *2015*, 2F.2.1-2F.2.14.

Edgar, B.A. (2006). How flies get their size: Genetics meets physiology. Nat. Rev. Genet. *7*, 907–916.

Englmeier, R., Pfeffer, S., and Förster, F. (2017). Structure of the Human Mitochondrial Ribosome Studied in Situ by Cryoelectron Tomography. Structure *25*, 1574-1581.e2.

Escher, S.A., and Rasmuson-Lestander, Å. (1999). The Drosophila glucose transporter gene: cDNA sequence, phylogenetic comparisons, analysis of functional sites and secondary structures. Hereditas *130*, 95–103.

Felder, T.K., Soyal, S.M., Oberkofler, H., Hahne, P., Auer, S., Weiss, R., Gadermaier, G., Miller, K., Krempler, F., Esterbauer, H., et al. (2011). Characterization of novel peroxisome proliferator-activated receptor γ coactivator-1α (PGC-1α) isoform in human liver. J. Biol. Chem. *286*, 42923–42936.

Fergestad, T., Bostwick, B., and Ganetzky, B. (2006). Metabolic disruption in drosophila bang-sensitive seizure mutants. Genetics *173*, 1357–1364.

Fernández-Ayala, D.J.M., Chen, S., Kemppainen, E., O'Dell, K.M.C., and Jacobs, H.T. (2010). Gene expression in a Drosophila model of mitochondrial disease. PLoS One *5*.

Fernandez-Marcos, P.J., and Auwerx, J. (2011). Regulation of PGC-1α, a nodal regulator of mitochondrial biogenesis. In American Journal of Clinical Nutrition, p.

Gáliková, M., Diesner, M., Klepsatel, P., Hehlert, P., Xu, Y., Bickmeyer, I., Predel, R., and Kühnlein, R.P. (2015). Energy homeostasis control in drosophila adipokinetic hormone mutants. Genetics *201*, 665–683.

Gao, X., and Pan, D. (2001). TSC1 and TSC2 tumor suppressors antagonize insulin signaling in cell growth. Genes Dev. *15*, 1383–1392.

Gao, X., Wen, X., Esser, L., Quinn, B., Yu, L., Yu, C.A., and Xia, D. (2003). Structural basis for the quinone reduction in the bc1 complex: A comparative analysis of crystal structures of mitochondrial cytochrome bc1 with bound substrate and inhibitors at the Qi site. Biochemistry *42*, 9067–9080.

Garrido, D., Rubin, T., Poidevin, M., Maroni, B., Le Rouzic, A., Parvy, J.P., and Montagne, J. (2015). Fatty Acid Synthase Cooperates with Glyoxalase 1 to Protect against Sugar Toxicity. PLoS Genet. *11*, 1–26.

Géminard, C., Rulifson, E.J., and Léopold, P. (2009). Remote Control of Insulin Secretion by Fat Cells in Drosophila. Cell Metab. *10*, 199–207.

Gerhold, J.M., Cansiz-Arda, S., Lohmus, M., Engberg, O., Reyes, A., Van Rennes, H., Sanz, A., Holt, I.J., Cooper, H.M., and Spelbrink, J.N. (2015). Human Mitochondrial DNA-Protein Complexes Attach to a Cholesterol-Rich Membrane Structure. Sci. Rep. *5*.

Gershman, B., Puig, O., Hang, L., Peitzsch, R.M., Tatar, M., and Garofalo, R.S. (2007a). High-resolution dynamics of the transcriptional response to nutrition in *Drosophila* : a key role for dFOXO. Physiol. Genomics *29*, 24–34.

Gershman, B., Puig, O., Hang, L., Peitzsch, R.M., Tatar, M., and Garofalo, R.S. (2007b). High-resolution dynamics of the transcriptional response to nutrition in Drosophila: A key role for dFOXO. Physiol. Genomics *29*, 24–34.

Giannakou, M.E., Goss, M., Jünger, M.A., Hafen, E., Leevers, S.J., and Partridge, L. (2004). Long-lived Drosophila with over-expressed dFOXO in adult fat body. Science (80-.). *305*, 361.

Gilbert, L.I., and Warren, J.T. (2005). A Molecular Genetic Approach to the Biosynthesis of the Insect Steroid Molting Hormone. Vitam. Horm. *73*, 31–57.

Gingras, A.C., Gygi, S.P., Raught, B., Polakiewicz, R.D., Abraham, R.T., Hoekstra, M.F., Aebersold, R., and Sonenberg, N. (1999). Regulation of 4E-BP1 phosphorylation: A novel two step mechanism. Genes Dev. *13*, 1422–1437.

Glinghammar, B., Rafter, I., Lindström, A.K., Hedberg, J.J., Andersson, H.B., Lindblom, P., Berg, A.L., and Cotgreave, I. (2009). Detection of the mitochondrial and catalytically active alanine aminotransferase in human tissues and plasma. Int. J. Mol. Med. *23*, 621–631.

González de Cózar, J.M., Gerards, M., Teeri, E., George, J., Dufour, E., Jacobs, H.T., and Jõers, P. (2019). RNase H1 promotes replication fork progression through oppositely transcribed regions of Drosophila mitochondrial DNA. J. Biol. Chem. *294*.

Gorman, G.S., Schaefer, A.M., Ng, Y., Gomez, N., Blakely, E.L., Alston, C.L., Feeney, C., Horvath, R., Yu-Wai-Man, P., Chinnery, P.F., et al. (2015). Prevalence of nuclear and mitochondrial DNA mutations related to adult mitochondrial disease. Ann. Neurol. *77*, 753–759.

Goto, Y. ichi, Nonaka, I., and Horai, S. (1991). A new mtDNA mutation associated with mitochondrial myopathy, encephalopathy, lactic acidosis and stroke-like episodes (MELAS). BBA - Mol. Basis Dis. *1097*, 238–240.

Goto, Y.I., Nonaka, I., and Horai, S. (1990). A mutation in the tRNALeu(UUR) gene associated with the MELAS subgroup of mitochondrial encephalomyopathies. Nature *348*, 651–653.

Gwinn, D.M., Shackelford, D.B., Egan, D.F., Mihaylova, M.M., Mery, A., Vasquez, D.S., Turk, B.E., and Shaw, R.J. (2008). AMPK Phosphorylation of Raptor Mediates a Metabolic Checkpoint. Mol. Cell *30*, 214–226.

Hajnóczky, G., Robb-Gaspers, L.D., Seitz, M.B., and Thomas, A.P. (1995). Decoding of cytosolic calcium oscillations in the mitochondria. Cell *82*, 415–424.

Handschin, C., Rhee, J., Lin, J., Tarr, P.T., and Spiegelman, B.M. (2003). An autoregulatory loop controls peroxisome proliferator-activated receptor γ coactivator 1α expression in muscle. Proc. Natl. Acad. Sci. U. S. A. *100*, 7111–7116.

Hasan, N.M., Longacre, M.J., Stoker, S.W., Kendrick, M.A., and MacDonald, M.J. (2015). Mitochondrial Malic Enzyme 3 Is Important for Insulin Secretion in Pancreatic β-Cells. Mol. Endocrinol. *29*, 396–410.

Hassett, C.C. (1948). The utilization of sugars and other substances by Drosophila. *95*, 114–123.

Havel, P.J. (2005). Dietary Fructose: Implications for Dysregulation of Energy Homeostasis and Lipid/Carbohydrate Metabolism. Nutr. Rev. *63*, 133–157.

He, X., Sun, C., Wang, F., Shan, A., Guo, T., Gu, W., Cui, B., and Ning, G. (2012). Peri-implantation lethality in mice lacking the PGC-1-related coactivator protein. Dev. Dyn. *241*, 975–983.

Heiden, M.G. Vander, Cantley, L.C., and Thompson, C.B. (2009). Understanding the warburg effect: The metabolic requirements of cell proliferation. Science (80-.). *324*, 1029–1033.

Heier, C., and Kühnlein, R.P. (2018). Triacylglycerol metabolism in drosophila melanogaster. Genetics *210*, 1163–1184.

Herzig, S., Raemy, E., Montessuit, S., Veuthey, J.L., Zamboni, N., Westermann, B., Kunji, E.R.S., and Martinou, J.C. (2012). Identification and functional expression of the mitochondrial pyruvate carrier. Science (80-.). *336*, 93–96.

Holt, I.J., Harding, A.E., Petty, R.K.H., and Morgan-Hughes, J.A. (1990). A new mitochondrial disease associated with mitochondrial DNA heteroplasmy. Am. J. Hum. Genet. *46*, 428–433.

Holz, M.K., Ballif, B.A., Gygi, S.P., and Blenis, J. (2005). mTOR and S6K1 mediate assembly of the translation preinitiation complex through dynamic protein interchange and ordered phosphorylation events. Cell *123*, 569–580.

Hsiao, P.F., Zhu, Y.-J., and Chien, Y.-C. (2002). Cloning and functional analysis of pyruvate kinase promoter region from Drosophila melanogaster. DNA Cell Biol. *21*, 1–10.

Huang, J.H., and Douglas, A.E. (2015). Consumption of dietary sugar by gut bacteria determines Drosophila lipid content. Biol. Lett. *11*, 12–15.

Hudson, A.M., and Cooley, L. (2014). Methods for studying oogenesis. Methods *68*, 207–217.

Hui, S., Ghergurovich, J.M., Morscher, R.J., Jang, C., Teng, X., Lu, W., Esparza, L.A., Reya, T., Zhan, L., Yanxiang Guo, J., et al. (2017). Glucose feeds the TCA cycle via circulating lactate. Nature *551*, 115–118.

Ikeya, T., Galic, M., Belawat, P., Nairz, K., and Hafen, E. (2002). Nutrient-dependent expression of insulin-like peptides from neuroendocrine cells in the CNS contributes to growth regulation in Drosophila. Curr. Biol. *12*, 1293–1300.

J., E., G., A., S.A., U., P.H., G., T., D., K., B.-J., and T., H. (2001). Mutation analysis of peroxisome proliferator-activated receptor-gamma coactivator-1 (PGC-1) and relationships of identified amino acid polymorphisms to Type II diabetes mellitus. Diabetologia *44*, 2220–2226.

Jäer, S., Handschin, C., St-Pierre, J., and Spiegelman, B.M. (2007). AMP-activated protein kinase (AMPK) action in skeletal muscle via direct phosphorylation of PGC-1α. Proc. Natl. Acad. Sci. U. S. A. *104*, 12017–12022.

Kamei, Y., Ohizumi, H., Fujitani, Y., Nemoto, T., Tanaka, T., Takahashi, N., Kawada, T., Miyoshi, M., Ezaki, O., and Kakizuka, A. (2003). PPARγ coactivator 1β/ERR ligand 1 is an ERR protein ligand, whose expression induces a high-energy expenditure and antagonizes obesity. Proc. Natl. Acad. Sci. U. S. A. *100*, 12378–12383.

Kanamori, Y., Saito, A., Hagiwara-Komoda, Y., Tanaka, D., Mitsumasu, K., Kikuta, S., Watanabe, M., Cornette, R., Kikawada, T., and Okuda, T. (2010). The trehalose transporter 1 gene sequence is conserved in insects and encodes proteins with different kinetic properties involved in trehalose import into

peripheral tissues. Insect Biochem. Mol. Biol.

Kaneto, H., Fujii, J., Myint, T., Miyazawa, N., Islam, K.N., Kawasaki, Y., Suzuki, K., Nakamura, M., Tatsumi, H., Yamasaki, Y., et al. (1996). Reducing sugars trigger oxidative modification and apoptosis in pancreatic β-cells by provoking oxidative stress through the glycation reaction. Biochem. J. *320*, 855–863.

Kaplon, J., Zheng, L., Meissl, K., Chaneton, B., Selivanov, V.A., MacKay, G., Van Der Burg, S.H., Verdegaal, E.M.E., Cascante, M., Shlomi, T., et al. (2013). A key role for mitochondrial gatekeeper pyruvate dehydrogenase in oncogene-induced senescence. Nature *498*, 109–112.

Karr, T.L., and Alberts, B.M. (1986). Organization of the cytoskeleton in early Drosophila embryos. J. Cell Biol. *102*, 1494–1509.

Kazak, L., Chouchani, E.T., Stavrovskaya, I.G., Lu, G.Z., Jedrychowski, M.P., Egan, D.F., Kumari, M., Kong, X., Erickson, B.K., Szpyt, J., et al. (2017). UCP1 deficiency causes brown fat respiratory chain depletion and sensitizes mitochondria to calcium overload-induced dysfunction. Proc. Natl. Acad. Sci. U. S. A. *114*, 7981–7986.

Kemppainen, E., Fernández-Ayala, D.J.M., Galbraith, L.C.A., O'Dell, K.M.C., and Jacobs, H.T. (2009). Phenotypic suppression of the Drosophila mitochondrial disease-like mutant tko25t by duplication of the mutant gene in its natural chromosomal context. Mitochondrion *9*, 353–363.

Kemppainen, E., George, J., Garipler, G., Tuomela, T., Kiviranta, E., Soga, T., Dunn, C.D., and Jacobs, H.T. (2016). Mitochondrial dysfunction plus high-sugar diet provokes a metabolic crisis that inhibits growth. PLoS One *11*, 1–28.

Kemppainen, K.K., Kemppainen, E., and Jacobs, H.T. (2014). The alternative oxidase AOX does not rescue the phenotype of tko25t mutant flies. G3 Genes, Genomes, Genet. *4*, 2013–2021.

Kim, J., and Neufeld, T.P. (2015). Dietary sugar promotes systemic TOR activation in Drosophila through AKH-dependent selective secretion of Dilp3. Nat. Commun. *6*.

Kim, S.K., and Rulifson, E.J. (2004). Conserved mechanisms of glucose sensing and regulation by Drosophila corpora cardiaca cells. Nature *431*, 316–320.

Kim, D.H., Sarbassov, D.D., Ali, S.M., King, J.E., Latek, R.R., Erdjument-Bromage, H., Tempst, P., and Sabatini, D.M. (2002). mTOR interacts with raptor to form a nutrient-sensitive complex that signals to the cell growth machinery. Cell *110*, 163–175.

Kim, E., Goraksha-Hicks, P., Li, L., Neufeld, T.P., and Guan, K.L. (2008). Regulation of TORC1 by Rag GTPases in nutrient response. Nat. Cell Biol. *10*, 935–945.

King, R.C. (1975). The Cell Cycle and Cell Differentiation in the Drosophila Ovary. pp. 85–109.

Konikoff, C.E., Karr, T.L., McCutchan, M., Newfeld, S.J., and Kumar, S. (2011). Comparison of embryonic expression within multigene families using the flyexpress discovery platform reveals more spatial than temporal divergence. Dev. Dyn. *241*, 150–160.

Koyama, T., Texada, M.J., Halberg, K.A., and Rewitz, K. (2020). Metabolism and growth adaptation to environmental conditions in Drosophila. Cell. Mol. Life Sci. *1*, 3.

Kozlova, T., and Thummel, C.S. (2000). Steroid regulation of postembryonic development and reproduction in drosophila. Trends Endocrinol. Metab. *11*, 276–280.

Krebs, H.A., and Johnson, W.A. (1937). Metabolism of ketonic acids in animal tissues. Biochem. J. *31*, 645–660.

Lagunas, R. (1993). Sugar transport in Saccharomyces cerevisiae. FEMS Microbiol. Lett. *104*, 229–242.

Lai, L., Leone, T.C., Zechner, C., Schaeffer, P.J., Kelly, S.M., Flanagan, D.P., Medeiros, D.M., Kovacs, A., and Kelly, D.P. (2008). Transcriptional coactivators PGC-lα and PGC-lβ control overlapping programs required for perinatal maturation of the heart. Genes Dev. *22*, 1948–1961.

Lake, N.J., Bird, M.J., Isohanni, P., and Paetau, A. (2015). Leigh Syndrome. J. Neuropathol. Exp. Neurol. *74*, 482–492.

Lehman, J.J., Barger, P.M., Kovacs, A., Saffitz, J.E., Medeiros, D.M., and Kelly, D.P. (2000). Peroxisome proliferator-activated receptor γ coactivator-1 promotes

cardiac mitochondrial biogenesis. J. Clin. Invest. *106*, 847–856.

Lemaitre, B., and Miguel-Aliaga, I. (2013). The Digestive Tract of Drosophila melanogaster . Annu. Rev. Genet. *47*, 377–404.

Liberti, M. V., and Locasale, J.W. (2016). The Warburg Effect: How Does it Benefit Cancer Cells? Trends Biochem. Sci. *41*, 211–218.

Lighthouse, D. V., Buszczak, M., and Spradling, A.C. (2008). New components of the Drosophila fusome suggest it plays novel roles in signaling and transport. Dev. Biol. *317*, 59–71.

Lightowlers, R.N., Taylor, R.W., and Turnbull, D.M. (2015). Mutations causing mitochondrial disease: What is new and what challenges remain? Science (80-.). *349*, 1494–1499.

Lin, J., Puigserver, P., Donovan, J., Tarr, P., and Spiegelman, B.M. (2002). Peroxisome proliferator-activated receptor γ coactivator 1β (PGC-1β), a novel PGC-1-related transcription coactivator associated with host cell factor. J. Biol. Chem. *277*, 1645–1648.

Lin, J., Tarr, P.T., Yang, R., Rhee, J., Puigserver, P., Newgard, C.B., and Spiegelman, B.M. (2003). PGC-1β in the regulation of hepatic glucose and energy metabolism. J. Biol. Chem. *278*, 30843–30848.

Lin, J., Yang, R., Tarr, P.T., Wu, P.H., Handschin, C., Li, S., Yang, W., Pei, L., Uldry, M., Tontonoz, P., et al. (2005). Hyperlipidemic effects of dietary saturated fats mediated through PGC-1β coactivation of SREBP. Cell *120*, 261–273.

Luong, N., Davies, C.R., Wessells, R.J., Graham, S.M., King, M.T., Veech, R., Bodmer, R., and Oldham, S.M. (2006). Activated FOXO-mediated insulin resistance is blocked by reduction of TOR activity. Cell Metab. *4*, 133–142.

Lustig, Y., Ruas, J.L., Estall, J.L., Lo, J.C., Devarakonda, S., Laznik, D., Choi, J.H., Ono, H., Olsen, J. V., and Spiegelman, B.M. (2011). Separation of the gluconeogenic and mitochondrial functions of pgc-1α through s6 kinase. Genes Dev. *25*, 1232–1244.

MacDonald, M.J. (1995). Feasibility of a mitochondrial pyruvate malate shuttle in pancreatic islets. Further implication of cytosolic NADPH in insulin secretion. J. Biol. Chem. *270*, 20051–20058.

Mancuso, M., Filosto, M., Mootha, V.K., Rocchi, A., Pistolesi, S., Murri, L., DiMauro, S., and Siciliano, G. (2004). A novel mitochondrial tRNAPhe mutation causes MERRF syndrome. Neurology *62*, 2119–2121.

Martin, J.F., Hersperger, E., Simcox, A., and Shearn, A. (2000). minidiscs encodes a putative amino acid transporter subunit required non-autonomously for imaginal cell proliferation. Mech. Dev. *92*, 155–167.

Martínez-Redondo, V., Pettersson, A.T., and Ruas, J.L. (2015). The hitchhiker's guide to PGC-1α isoform structure and biological functions. Diabetologia *58*, 1969–1977.

Mattila, J., and Hietakangas, V. (2017). Regulation of carbohydrate energy metabolism in Drosophila melanogaster. Genetics *207*, 1231–1253.

Mattila, J., Havula, E., Suominen, E., Teesalu, M., Surakka, I., Hynynen, R., Kilpinen, H., Väänänen, J., Hovatta, I., Käkelä, R., et al. (2015). Mondo-Mlx Mediates Organismal Sugar Sensing through the Gli-Similar Transcription Factor Sugarbabe. Cell Rep. *13*, 350–364.

McCommis, K.S., Hodges, W.T., Bricker, D.K., Wisidagama, D.R., Compan, V., Remedi, M.S., Thummel, C.S., and Finck, B.N. (2016). An ancestral role for the mitochondrial pyruvate carrier in glucose-stimulated insulin secretion. Mol. Metab. *5*, 602–614.

McFate, T., Mohyeldin, A., Lu, H., Thakar, J., Henriques, J., Halim, N.D., Wu, H., Schell, M.J., Tsz, M.T., Teahan, O., et al. (2008). Pyruvate dehydrogenase complex activity controls metabolic and malignant phenotype in cancer cells. J. Biol. Chem. *283*, 22700–22708.

McGinnis, W., Levine, M.S., Hafen, E., Kuroiwa, A., and Gehring, W.J. (1984). A conserved DNA sequence in homoeotic genes of the Drosophila Antennapedia and bithorax complexes. Nature *308*, 428–433.

McLaughlin, J.M., and Bratu, D.P. (2015). Drosophila Oogenesis (New York, NY: Springer New York).

Medlock, A.E., Shiferaw, M.T., Marcero, J.R., Vashisht, A.A., Wohlschlegel, J.A., Phillips, J.D., and Dailey, H.A. (2015). Identification of the Mitochondrial Heme Metabolism Complex. PLoS One *10*, e0135896.

Melvin, R.G., Lamichane, N., Havula, E., Kokki, K., Soeder, C., Jones, C.D., and Hietakangas, V. (2018). Natural variation in sugar tolerance associates with changes in signaling and mitochondrial ribosome biogenesis. Elife *7*, 1–29.

Menezes, M.J., Guo, Y., Zhang, J., Riley, L.G., Cooper, S.T., Thorburn, D.R., Li, J., Dong, D., Li, Z., Glessner, J., et al. (2015). Mutation in mitochondrial ribosomal protein S7 (MRPS7) causes congenital sensorineural deafness, progressive hepatic and renal failure and lactic acidemia. Hum. Mol. Genet. *24*, 2297–2307.

Meyerson, C., Van Stavern, G., and McClelland, C. (2015). Leber hereditary optic neuropathy: Current perspectives. Clin. Ophthalmol. *9*, 1165–1176.

Miguel-Aliaga, I. (2012). Nerveless and gutsy: Intestinal nutrient sensing from invertebrates to humans. Semin. Cell Dev. Biol. *23*, 614–620.

Miguel-Aliaga, I., Jasper, H., and Lemaitre, B. (2018). Anatomy and physiology of the digestive tract of drosophila melanogaster. Genetics *210*, 357–396.

Mirth, C.K., and Shingleton, A.W. (2012). Integrating body and organ size in Drosophila: Recent advances and outstanding problems. Front. Endocrinol. (Lausanne). *3*.

Mirth, C., Truman, J.W., and Riddiford, L.M. (2005). The role of the prothoracic gland in determining critical weight for metamorphosis in Drosophila melanogaster. Curr. Biol. *15*, 1796–1807.

Mitchell, P. (1961). Coupling of phosphorylation to electron and hydrogen transfer by a chemi-osmotic type of mechanism. Nature *191*, 144–148.

Miyamoto, T., Slone, J., Song, X., and Amrein, H. (2012). A Fructose Receptor Functions as a Nutrient Sensor in the Drosophila Brain. Cell *151*, 1113–1125.

Monnat, R.J., Maxwell, C.L., and Loeb, L.A. (1985). Nucleotide sequence preservation of human leukemic mitochondrial DNA. Cancer Res. *45*, 1809–1814.

Monsalve, M., Wu, Z., Adelmant, G., Puigserver, P., Fan, M., and Spiegelman, B.M. (2000). Direct coupling of transcription and mRNA processing through the thermogenic coactivator PGC-1. Mol. Cell *6*, 307–316.

Montagne, J., Stewart, M.J., Stocker, H., Hafen, E., Kozma, S.C., and Thomas, G. (1999). Drosophila S6 kinase: A regulator of cell size. Science (80-.). *285*, 2126–2129.

Mootha, V.K., Lindgren, C.M., Eriksson, K., Subramanian, A., Sihag, S., Lehar, J., Puigserver, P., Carlsson, E., Ridderstråle, M., Laurila, E., et al. (2003). PGC-1α-responsive genes involved in oxidative phosphorylation are coordinately downregulated in human diabetes. Nat. Genet. *34*, 1–7.

Mukherjee, S., and Duttaroy, A. (2013). Spargel/dPGC-1 is a new downstream effector in the insulin-TOR signaling pathway in Drosophila. Genetics *195*, 433–441.

Mukherjee, S., Basar, M.A., Davis, C., and Duttaroy, A. (2014). Emerging functional similarities and divergences between Drosophila Spargel/dPGC-1 and mammalian PGC-1 protein. Front. Genet. *5*, 1–6.

Musselman, L.P., and Kühnlein, R.P. (2018). Drosophila as a model to study obesity and metabolic disease. J. Exp. Biol. *221*, jeb163881.

Musselman, L.P., Fink, J.L., Ramachandran, P.V., Patterson, B.W., Okunade, A.L., Maier, E., Brent, M.R., Turk, J., and Baranski, T.J. (2013). Role of fat body lipogenesis in protection against the effects of caloric overload in drosophila. J. Biol. Chem. *288*, 8028–8042.

Nambam, B., and Schatz, D. (2017). Growth hormone and insulin-like growth factor-I axis in type 1 diabetes. Growth Horm. IGF Res. 0–1.

Nässel, J., and Vanden Broeck, J. (2016). Insulin / IGF signaling in Drosophila and other insects : factors that regulate production , release and post-release action of the insulin-like peptides. Cell. Mol. Life Sci. *73*, 271–290.

Ni, J.Q., Zhou, R., Czech, B., Liu, L.P., Holderbaum, L, Yang-Zhou, D., Shim, H.S., Tao, R., Handler, D., Karpowicz, P., et al. (2011). A genome-scale shRNA resource for transgenic RNAi in Drosophila. Nat. Methods *8*, 405–407.

Nüsslein-volhard, C., and Wieschaus, E. (1980). Mutations affecting segment number and polarity in drosophila. Nature *287*, 795–801.

Nüsslein-Volhard, C., Frohnhöfer, H.G., and Lehmann, R. (1987). Determination of anteroposterior polarity in Drosophila. Science (80-.). *238*,

1675–1681.

Olson, K.A., Schell, J.C., and Rutter, J. (2016). Pyruvate and Metabolic Flexibility: Illuminating a path toward selective cancer therapies. Trends Biochem Sci *41*, 219–230.

Olszewski, U., Poulsen, T.T., Ulsperger, E., Poulsen, H.S., Geissler, K., and Hamilton, G. (2010). In vitro cytotoxicity of combinations of dichloroacetate with anticancer platinum compounds. Clin. Pharmacol. Adv. Appl. *2*, 177–183.

Oropeza, D., Jouvet, N., Bouyakdan, K., Perron, G., Ringuette, L.J., Philipson, L.H., Kiss, R.S., Poitout, V., Alquier, T., and Estall, J.L. (2015). PGC-1 coactivators in β-cells regulate lipid metabolism and are essential for insulin secretion coupled to fatty acids. Mol. Metab. *4*, 811–822.

Owen, O.E., Kalhan, S.C., and Hanson, R.W. (2002). The key role of anaplerosis and cataplerosis for citric acid cycle function. J. Biol. Chem. *277*, 30409–30412.

Owusu-ansah, E., and Perrimon, N. (2014). Modeling metabolic homeostasis and nutrient sensing in Drosophila : implications for aging and metabolic diseases. 343–350.

Padmanabha, D., and Baker, K.D. (2014). Drosophila gains traction as a repurposed tool to investigate metabolism. Trends Endocrinol. Metab. *25*, 518–527.

Palikaras, K., Lionaki, E., and Tavernarakis, N. (2018). Mechanisms of mitophagy in cellular homeostasis, physiology and pathology. Nat. Cell Biol. *20*, 1013–1022.

Palm, W., Sampaio, J.L., Brankatschk, M., Carvalho, M., Mahmoud, A., Shevchenko, A., and Eaton, S. (2012). Lipoproteins in Drosophila melanogaster — Assembly , Function , and Influence on Tissue Lipid Composition. *8*.

Park, S., Jeon, J.H., Min, B.K., Ha, C.M., Thoudam, T., Park, B.Y., and Lee, I.K. (2018). Role of the pyruvate dehydrogenase complex in metabolic remodeling: Differential pyruvate dehydrogenase complex functions in metabolism. Diabetes Metab. J. *42*, 270–281.

Partridge, L., and Fowler, K. (1992). Direct and Correlated Responses to Selection on Age at Reproduction in Drosophila melanogaster. Evolution (N. Y). *46*, 76.

Partridge, L., Alic, N., Bjedov, I., and Piper, M.D.W. (2011). Ageing in Drosophila: The role of the insulin/Igf and TOR signalling network. Exp. Gerontol. *46*, 376–381.

Pavlidis, P., and Tanouye, M.A. (1995). Seizures and Failures in the Giant Fiber Pathway of Drosophila Bang-Sensitive Paralytic Mutants.

Pavlova, N.N., and Thompson, C.B. (2016). The Emerging Hallmarks of Cancer Metabolism. Cell Metab. *23*, 27–47.

Pearce, S., Nezich, C.L., and Spinazzola, A. (2013). Mitochondrial diseases: Translation matters. Mol. Cell. Neurosci. *55*, 1–12.

Pinto, B.S. (2009). Understanding the role of LEM domain proteins in Drosophila development. University of Iowa.

Pongratz, R.L., Kibbey, R.G., Shulman, G.I., and Cline, G.W. (2007). Cytosolic and mitochondrial malic enzyme isoforms differentially control insulin secretion. J. Biol. Chem. *282*, 200–207.

Porstmann, T., Santos, C.R., Griffiths, B., Cully, M., Wu, M., Leevers, S., Griffiths, J.R., Chung, Y.L., and Schulze, A. (2008). SREBP Activity Is Regulated by mTORC1 and Contributes to Akt-Dependent Cell Growth. Cell Metab. *8*, 224–236.

De Preter, G., Neveu, M.A., Danhier, P., Brisson, L., Payen, V.L., Porporato, P.E., Jordan, B.F., Sonveaux, P., and Gallez, B. (2016). Inhibition of the pentose phosphate pathway by dichloroacetate unravels a missing link between aerobic glycolysis and cancer cell proliferation. Oncotarget *7*, 2910–2920.

Prezant, T.R., Agapian, J. V., Bohlman, M.C., Bu, X., Öztas, S., Qiu, W.Q., Arnos, K.S., Cortopassi, G.A., Jaber, L., Rotter, J.I., et al. (1993). Mitochondrial ribosomal RNA mutation associated with both antibiotic-induced and non-syndromic deafness. Nat. Genet. *4*, 289–294.

Puigserver, P., Wu, Z., Park, C.W., Graves, R., Wright, M., and Spiegelman, B.M. (1998). A cold-inducible coactivator of nuclear receptors linked to adaptive thermogenesis. Cell *92*, 829–839.

Puigserver, P., Adelmant, G., Wu, Z., Fan, M., Xu, J., O'Malley, B., and Spiegelman, B.M. (1999). Activation of PPARγ coactivator-1 through

transcription factor docking. Science (80-.). *286*, 1368–1371.

Raikhel, A.S., and Dhadialla, T.S. (1992). ACCUMULATION OF YOLK PROTEINS IN INSECT OOCYTES.

Reid, F.M., Vernham, G.A., and Jacobs, H.T. (1994). A novel mitochondrial point mutation in a maternal pedigree with sensorineural deafness. Hum. Mutat. *3*, 243–247.

Reiter, L.T., Potocki, L., Chien, S., Gribskov, M., and Bier, E. (2001). A systematic analysis of human disease-associated gene sequences in Drosophila melanogaster. Genome Res. *11*, 1114–1125.

Rera, M., Bahadorani, S., Cho, J., Koehler, C.L., Ulgherait, M., Hur, J.H., Ansari, W.S., Lo, T., Jones, D.L., and Walker, D.W. (2011). Modulation of longevity and tissue homeostasis by the drosophila PGC-1 homolog. Cell Metab. *14*, 623–634.

Reyes-DelaTorre, A., Teresa, M., and Rafael, J. (2012). Carbohydrate Metabolism in Drosophila: Reliance on the Disaccharide Trehalose. Carbohydrates - Compr. Stud. Glycobiol. Glycotechnol.

Rhee, J., Inoue, Y., Yoon, J.C., Puigserver, P., Fan, M., Gonzalez, F.J., and Spiegelman, B.M. (2003). Regulation of hepatic fasting response by PPARγ coactivator-1α (PGC-1): Requirement for hepatocyte nuclear factor 4α in gluconeogenesis. Proc. Natl. Acad. Sci. U. S. A. *100*, 4012–4017.

Robertson, C.W. (1936). The metamorphosis of Drosophila melanogaster, including an accurately timed account of the principal morphological changes. J. Morphol. *59*, 351–399.

Rorth, P. (1998). Gal4 in the Drosophila female germline. Mech. Dev. *78*, 113–118.

Rötig, A. (2011). Human diseases with impaired mitochondrial protein synthesis. Biochim. Biophys. Acta - Bioenerg. *1807*, 1198–1205.

Rovenko, B.M., Perkhulyn, N. V., Gospodaryov, D. V., Sanz, A., Lushchak, O. V., and Lushchak, V.I. (2015a). High consumption of fructose rather than glucose promotes a diet-induced obese phenotype in Drosophila melanogaster. Comp. Biochem. Physiol. -Part A Mol. Integr. Physiol. *180*, 75–85.

Rovenko, B.M., Kubrak, O.I., Gospodaryov, D. V., Yurkevych, I.S., Sanz, A., Lushchak, O. V., and Lushchak, V.I. (2015b). Restriction of glucose and fructose causes mild oxidative stress independently of mitochondrial activity and reactive oxygen species in drosophila melanogaster. Comp. Biochem. Physiol. -Part A Mol. Integr. Physiol. *187*, 27–39.

Royden, C.S., Pirrotta, V., and Jan, L.Y. (1987). The tko locus, site of a behavioral mutation in D. melanogaster, codes for a protein homologous to prokaryotic ribosomal protein S12. Cell *51*, 165–173.

Saada, A., Shaag, A., Arnon, S., Dolfin, T., Miller, C., Fuchs-Telem, D., Lombes, A., and Elpeleg, O. (2007). Antenatal mitochondrial disease caused by mitochondrial ribosomal protein (MRPS22) mutation. J. Med. Genet. *44*, 784–786.

Safdar, A., Little, J.P., Stokl, A.J., Hettinga, B.P., Akhtar, M., and Tarnopolsky, M.A. (2011). Exercise increases mitochondrial PGC-1α content and promotes nuclear-mitochondrial cross-talk to coordinate mitochondrial biogenesis. J. Biol. Chem. *286*, 10605–10617.

Sagan, L. (1967). On the origin of mitosing cells. J. Theor. Biol. *14*.

Sahut-Barnola, I., Godt, D., Laski, F.A., and Couderc, J.L. (1995). Drosophila ovary morphogenesis: Analysis of terminal filament formation and identification of a gene required for this process. Dev. Biol. *170*, 127–135.

Scarpulla, R.C. (2008). Nuclear control of respiratory chain expression by nuclear respiratory factors and PGC-1-related coactivator. In Annals of the New York Academy of Sciences, (Blackwell Publishing Inc.), pp. 321–334.

Scarpulla, R.C. (2011). Metabolic control of mitochondrial biogenesis through the PGC-1 family regulatory network. Biochem Biophys Acta *1813*, 1269–1278.

Schalkwijk, C.G., Stehouwer, C.D.A., and van Hinsbergh, V.W.M. (2004). Fructose-mediated non-enzymatic glycation: Sweet coupling or bad modification. Diabetes. Metab. Res. Rev. *20*, 369–382.

Schneider, I. (1972). Cell lines derived from late embryonic stages of Drosophila melanogaster. J. Embryol. Exp. Morphol. *27*, 353–365.

Schulz, J.G., Laranjeira, A., Van Huffel, L., Gärtner, A., Vilain, S., Bastianen, J.,

Van Veldhoven, P.P., and Dotti, C.G. (2015). Glial β-Oxidation regulates drosophila energy metabolism. Sci. Rep. *5*, 1–9.

Scorrano, L., Oakes, S.A., Opferman, J.T., Cheng, E.H., Sorcinelli, M.D., Pozzan, T., and Korsmeyer, S.J. (2003). BAX and BAK regulation of endoplasmic reticulum Ca2+: A control point for apoptosis. Science (80-.). *300*, 135–139.

Senyilmaz, D., and Teleman, A.A. (2015). Chicken or the egg: Warburg effect and mitochondrial dysfunction. F1000Prime Rep. *7*, 1–13.

She, P., Burgess, S.C., Shiota, M., Flakoll, P., Donahue, E.P., Malloy, C.R., Sherry, A.D., and Magnuson, M.A. (2003). Mechanisms by which liver-specific PEPCK knockout mice preserve euglycemia during starvation. Diabetes *52*, 1649–1654.

Silva, D., and Jemc, J.C. (2015). Sorting out identities: An educational primer for use with "Novel tools for genetic manipulation of follicle stem cells in the drosophila ovary reveal an integrin-dependent transition from quiescence to proliferation." Genetics *201*, 13–22.

Simcox, A.A., Hersperger, E., Shearn, A., Whittle, J.R., and Cohen, S.M. (1991). Establishment of imaginal discs and histoblast nests in Drosophila. Mech. Dev. *34*, 11–20.

Slaidina, M., Delanoue, R., Gronke, S., Partridge, L., and Léopold, P. (2009). A Drosophila Insulin-like Peptide Promotes Growth during Nonfeeding States. Dev. Cell *17*, 874–884.

van der Sluis, E.O., Bauerschmitt, H., Becker, T., Mielke, T., Frauenfeld, J., Berninghausen, O., Neupert, W., Herrmann, J.M., and Beckmann, R. (2015). Parallel Structural Evolution of Mitochondrial Ribosomes and OXPHOS Complexes. Genome Biol. Evol. *7*, 1235–1251.

Smeitink, J.A.M., Elpeleg, O., Antonicka, H., Diepstra, H., Saada, A., Smits, P., Sasarman, F., Vriend, G., Jacob-Hirsch, J., Shaag, A., et al. (2006). Distinct clinical phenotypes associated with a mutation in the mitochondrial translation elongation factor EFTs. Am. J. Hum. Genet. *79*, 869–877.

Smirnov, A., Entelis, N., Martin, R.P., and Tarassov, I. (2011). Biological significance of 5s rRNA import into human mitochondria: Role of ribosomal protein MRP-L18. Genes Dev. *25*, 1289–1305.

Smith, P.M., Elson, J.L., Greaves, L.C., Wortmann, S.B., Rodenburg, R.J.T., Lightowlers, R.N., Chrzanowska-Lightowlers, Z.M.A., Taylor, R.W., and Vila-Sanjurjo, A. (2014). The role of the mitochondrial ribosome in human disease: Searching for mutations in 12s mitochondrial rRNA with high disruptive potential. Hum. Mol. Genet. *23*, 949–967.

Smits, P., Saada, A., Wortmann, S.B., Heister, A.J., Brink, M., Pfundt, R., Miller, C., Haas, D., Hantschmann, R., Rodenburg, R.J.T., et al. (2011). Mutation in mitochondrial ribosomal protein MRPS22 leads to Cornelia de Lange-like phenotype, brain abnormalities and hypertrophic cardiomyopathy. Eur. J. Hum. Genet. *19*, 394–399.

Southgate, R.J., Bruce, C.R., Carey, A.L., Steinberg, G.R., Walder, K., Monks, R., Watt, M.J., Hawley, J.A., Birnbaum, M.J., and Febbraio, M.A. (2005). PGC-1α gene expression is down-regulated by Akt-mediated phosphorylation and nuclear exclusion of FoxO1 in insulin-stimulated skeletal muscle. FASEB J. *19*, 2072–2074.

Spencer, A.C., and Spremulli, L.L. (2004). Interaction of mitochondrial initiation factor 2 with mitochondrial fMet-tRNA. Nucleic Acids Res. *32*, 5464–5470.

Stanhope, K.L., Schwarz, J.-M., and Havel, P.J. (2013). Adverse metabolic effects of dietary fructose: Results from recent epidemiological, clinical, and mechanistic studies. Curr. Opin. Lipidol. *24*, 198–206.

Sun, F., Huo, X., Zhai, Y., Wang, A., Xu, J., Su, D., Bartlam, M., and Rao, Z. (2005). Crystal structure of mitochondrial respiratory membrane protein Complex II. Cell *121*, 1043–1057.

Sun, S., Li, H., Chen, J., Qian, Q., Sun, * S, and Li, H. (2017). Lactic Acid: No Longer an Inert and End-Product of Glycolysis.

Swevers, L., Raikhel, A.S., Sappington, T.W., Shirk, P., and Iatrou, K. (2005). Vitellogenesis and Post-Vitellogenic Maturation of the Insect Ovarian Follicle. Compr. Mol. Insect Sci. 87–155.

Tamura, Y., Harada, Y., Shiota, T., Yamano, K., Watanabe, K., Yokota, M., Yamamoto, H., Sesaki, H., and Endo, T. (2009). Tim23 - Tim50 pair coordinates functions of translocators and motor proteins in mitochondrial protein import. J. Cell Biol. *184*, 129–141.

Tatuch, Y., Christodoulou, J., Feigenbaum, A., Clarke, J.T.R., Wherret, J., Smith, C., Rudd, N., Petrova-Benedict, R., and Robinson, B.H. (1992). Heteroplasmic mtDNA mutation (T→G) at 8993 can cause Leigh disease when the percentage of abnormal mtDNA is high. Am. J. Hum. Genet. *50*, 852–858.

Teleman, A.A. (2010). Molecular mechanisms of metabolic regulation by insulin in Drosophila. Biochem. J. *26*, 13–26.

Tennessen, J.M., and Thummel, C.S. (2011). Coordinating growth and maturation - Insights from drosophila. Curr. Biol. *21*.

Tennessen, J.M., Baker, K.D., Lam, G., Evans, J., and Thummel, C.S. (2011). The Drosophila estrogen-related receptor directs a metabolic switch that supports developmental growth. Cell Metab. *13*, 139–148.

Tennessen, J.M., Bertagnolli, N.M., Evans, J., Sieber, M.H., Cox, J., and Thummel, C.S. (2014). Coordinated metabolic transitions during Drosophila embryogenesis and the onset of aerobic glycolysis. G3 Genes, Genomes, Genet. *4*, 839–850.

Thomas, H.E., Stunnenberg, H.G., and Stewart, A.F. (1993). Heterodimerization of the Drosophila ecdysone receptor with retinoid X receptor and ultraspiracle. Nature *362*, 471–475.

Thompson, J.N., Ashburner, M., and Carson, H.L. (1976). The genetics and biology of drosophila. (Academic Press Inc.).

Thorat, L.J., Gaikwad, S.M., and Nath, B.B. (2012). Trehalose as an indicator of desiccation stress in Drosophila melanogaster larvae: A potential marker of anhydrobiosis. Biochem. Biophys. Res. Commun. *419*, 638–642.

Tiefenböck, S.K., Baltzer, C., Egli, N.A., and Frei, C. (2010). The Drosophila PGC-1 homologue Spargel coordinates mitochondrial activity to insulin signalling. EMBO J. *29*, 171–183.

Timmons, A.K., Mondragon, A.A., Meehan, T.L., and McCall, K. (2017). Control of non-apoptotic nurse cell death by engulfment genes in Drosophila. Fly (Austin). *11*, 104–111.

Toivonen, J.M., Boocock, M.R., and Jacobs, H.T. (1999). Modelling in Escherichia coli of mutations in mitoribosomal protein S12: novel mutant

phenotypes of rpsL. Mol. Microbiol. *31*, 1735–1746.

Toivonen, J.M., O'Dell, K.M.C., Petit, N., Irvine, S.C., Knight, G.K., Lehtonen, M., Longmuir, M., Luoto, K., Touraille, S., Wang, Z., et al. (2001). Technical knockout, a drosophila model of mitochondrial deafness. Genetics *159*, 241–254.

Toivonen, J.M., Manjiry, S., Touraille, S., Alziari, S., O'Dell, K.M.C., and Jacobs, H.T. (2003). Gene dosage and selective expression modify phenotype in a Drosophila model of human mitochondrial disease. Mitochondrion *3*, 83–96.

Tremblay, A.M., Wilson, B.J., Yang, X.J., and Giguère, V. (2008). Phosphorylation-dependent sumoylation regulates estrogen-related receptor-β and -γ transcriptional activity through a synergy control motif. Mol. Endocrinol. *22*, 570–584.

Tsakiri, E.N., Iliaki, K.K., Höhn, A., Grimm, S., Papassideri, I.S., Grune, T., and Trougakos, I.P. (2013). Diet-derived advanced glycation end products or lipofuscin disrupts proteostasis and reduces life span in Drosophila melanogaster. Free Radic. Biol. Med. *65*, 1155–1163.

Tsuboi, M., Morita, H., Nozaki, Y., Akama, K., Ueda, T., Ito, K., Nierhaus, K.H., and Takeuchi, N. (2009). EF-G2mt Is an Exclusive Recycling Factor in Mammalian Mitochondrial Protein Synthesis. Mol. Cell *35*, 502–510.

Tucker, E.J., Hershman, S.G., Köhrer, C., Belcher-Timme, C.A., Patel, J., Goldberger, O.A., Christodoulou, J., Silberstein, J.M., McKenzie, M., Ryan, M.T., et al. (2011). Mutations in MTFMT underlie a human disorder of formylation causing impaired mitochondrial translation. Cell Metab. *14*, 428–434.

Ueki, I., Koga, Y., Povalko, N., Akita, Y., Nishioka, J., Yatsuga, S., Fukiyama, R., and Matsuishi, T. (2006). Mitochondrial tRNA gene mutations in patients having mitochondrial disease with lactic acidosis. Mitochondrion *6*, 29–36.

Ugrankar, R., Berglund, E., Akdemir, F., Tran, C., Kim, M.S., Noh, J., Schneider, R., Ebert, B., and Graff, J.M. (2015). Drosophila glucome screening identifies Ck1alpha as a regulator of mammalian glucose metabolism. Nat. Commun. *6*, 1–10.

Uldry, M., Yang, W., St-Pierre, J., Lin, J., Seale, P., and Spiegelman, B.M. (2006). Complementary action of the PGC-1 coactivators in mitochondrial biogenesis and brown fat differentiation. Cell Metab. *3*, 333–341.

Uryu, O., Ameku, T., and Niwa, R. (2015). Recent progress in understanding the role of ecdysteroids in adult insects: Germline development and circadian clock in the fruit fly Drosophila melanogaster. Zool. Lett. *1*, 32.

Vartiainen, S., Chen, S., George, J., Tuomela, T., Luoto, K.R., O'Dell, K.M.C., and Jacobs, H.T. (2014). Phenotypic rescue of a Drosophila model of mitochondrial ANT1 disease. DMM Dis. Model. Mech. *7*.

Velentzas, A.D., Velentzas, P.D., Katarachia, S.A., Anagnostopoulos, A.K., Sagioglou, N.E., Thanou, E. V., Tsioka, M.M., Mpakou, V.E., Kollia, Z., Gavriil, V.E., et al. (2018). The indispensable contribution of s38 protein to ovarian-eggshell morphogenesis in Drosophila melanogaster. Sci. Rep. *8*.

Veltri, K.L., Espiritu, M., and Singh, G. (1990). Distinct genomic copy number in mitochondria of different mammalian organs. J. Cell. Physiol. *143*, 160–164.

Vercauteren, K., Pasko, R.A., Gleyzer, N., Marino, V.M., and Scarpulla, R.C. (2006). PGC-1-Related Coactivator: Immediate Early Expression and Characterization of a CREB/NRF-1 Binding Domain Associated with Cytochrome c Promoter Occupancy and Respiratory Growth. Mol. Cell. Biol. *26*, 7409–7419.

Villena, J.A. (2015). New insights into PGC-1 coactivators: Redefining their role in the regulation of mitochondrial function and beyond. FEBS J. *282*, 647–672.

Viscomi, C., Bottani, E., Civiletto, G., Cerutti, R., Moggio, M., Fagiolari, G., Schon, E.A., Lamperti, C., and Zeviani, M. (2011). In vivo correction of COX deficiency by activation of the AMPK/PGC-1α axis. Cell Metab. *14*, 80–90.

Vögtle, F.N., Wortelkamp, S., Zahedi, R.P., Becker, D., Leidhold, C., Gevaert, K., Kellermann, J., Voos, W., Sickmann, A., Pfanner, N., et al. (2009). Global Analysis of the Mitochondrial N-Proteome Identifies a Processing Peptidase Critical for Protein Stability. Cell *139*, 428–439.

Wallberg, A.E., Yamamura, S., Malik, S., Spiegelman, B.M., and Roeder, R.G. (2003). Coordination of p300-mediated chromatin remodeling and TRAP/mediator function through coactivator PGC-1alpha. Mol. Cell *12*, 1137–1149.

Wang, J., Kean, L., Yang, J., Allan, A.K., Davies, S.A., Herzyk, P., and Dow, J.A.T. (2004). Function-informed transcriptome analysis of Drosophila renal

tubule. Genome Biol. *5*.

Warburg, O. (1925). The metabolism of carcinoma cells. J. Cancer Res. *9*, 148–163.

Warburg, O. (1956). On the origin of cancer cells. Science (80-.). *123*, 309–314.

Warren, J.T., Yerushalmi, Y., Shimell, M.J., O'Connor, M.B., Restifo, L.L., and Gilbert, L.I. (2006). Discrete pulses of molting hormone, 20-hydroxyecdysone, during late larval development of Drosophila melanogaster: Correlations with changes in gene activity. Dev. Dyn. *235*, 315–326.

Weiss, S.B., Kennedy, E.P., and Kiyasu, J.Y. (1960). The enzymatic synthesis of triglycerides. J. Biol. Chem. *235*, 40–44.

Wiemer, E.A.C., Michels, P.A.M., and Opperdoes, F.R. (1995). The inhibition of pyruvate transport across the plasma membrane of the bloodstream form of Trypanosoma brucei and its metabolic implications. Biochem. J. *312*, 479–484.

Wigglesworth, V.B. (1949). The utilization of reserve substances in Drosophila during flight. J. Exp. Biol. *26*.

Wilson, B.J., Tremblay, A.M., Deblois, G., Sylvain-Drolet, G., and Giguère, V. (2010). An acetylation switch modulates the transcriptional activity of estrogen-related receptor α. Mol. Endocrinol. *24*, 1349–1358.

Wong, K.K.L., Liao, J.Z., and Verheyen, E.M. (2019). A positive feedback loop between Myc and aerobic glycolysis sustains tumor growth in a Drosophila tumor model. Elife *8*, 1–19.

Wu, Z., Puigserver, P., Andersson, U., Zhang, C., Adelmant, G., Mootha, V., Troy, A., Cinti, S., Lowell, B., Scarpulla, R.C., et al. (1999). Mechanisms controlling mitochondrial biogenesis and respiration through the thermogenic coactivator PGC-1. Cell *98*, 115–124.

Yamada, T., Habara, O., Kubo, H., and Nishimura, T. (2018). Correction: Fat body glycogen serves as a metabolic safeguard for the maintenance of sugar levels in Drosophila (Development, (2018) 145, 6 (dev158865), 10.1242/dev.158865). Dev. *145*.

Yasugi, T., Yamada, T., and Nishimura, T. (2017). Adaptation to dietary

conditions by trehalose metabolism in Drosophila. Sci. Rep. *7*, 2–10.

Yeh, L.A., Lee, K.H., and Kim, K.H. (1980). Regulation of rat liver acetyl-CoA carboxylase. Regulation of phosphorylation and inactivation of acetyl-CoA carboxylase by the adenylate energy charge. J. Biol. Chem. *255*, 2308–2314.

Zhang, D., Tang, Z., Huang, H., Zhou, G., Cui, C., Weng, Y., Liu, W., Kim, S., Lee, S., Perez-Neut, M., et al. (2019). Metabolic regulation of gene expression by histone lactylation. Nature *574*, 575–580.

Zhang, H., Stallock, J.P., Ng, J.C., Reinhard, C., and Neufeld, T.P. (2000). Regulation of cellular growth by the Drosophila target of rapamycin dTOR. Genes Dev. *14*, 2712–2724.

Zhang, Y., Huypens, P., Adamson, A.W., Chang, J.S., Henagan, T.M., Boudreau, A., Lenard, N.R., Burk, D., Klein, J., Perwitz, N., et al. (2009). Alternative mRNA splicing produces a novel biologically active short isoform of PGC-1α. J. Biol. Chem. *284*, 32813–32826.

Zhang, Y.Q., Roote, J., Brogna, S., Davis, A.W., Barbash, D.A., Nash, D., and Ashburner, M. (1999). stress sensitive B encodes an adenine nucleotide translocase in Drosophila melanogaster. Genetics *153*, 891–903.

Zhao, H., Li, R., Wang, Q., Yan, Q., Deng, J.H., Han, D., Bai, Y., Young, W.Y., and Guan, M.X. (2004). Maternally Inherited Aminoglycoside-Induced and Nonsyndromic Deafness Is Associated with the Novel C1494T Mutation in the Mitochondrial 12S rRNa Gene in a Large Chinese Family. Am. J. Hum. Genet. *74*, 139–152.

Zong, S., Wu, M., Gu, J., Liu, T., Guo, R., and Yang, M. (2018). Structure of the intact 14-subunit human cytochrome c oxidase. Cell Res. *28*, 1026–1034.

10 Appendix

Appendix Table 1 – Statistical analyses. All statistical analyses were performed using GraphpadPrism7 Software. The figure to which the analysis refers is indicated.

FIG 12A						
One-way analysis of variance						
Number of families	1					
Number of comparisons per family	30					
Alpha	0,05					
Sidak's multiple comparisons test	Mean Diff.	95.00% CI of diff.	Significant?	Summary	Adjusted P Value	
HS Fm7/tko vs. HS+P Fm7/tko	-1,672	-2.336 to -1.008	Yes	****	<0.0001	A-F
HS Fm7/tko vs. ZS Fm7/tko	-0,1944	-0.8582 to 0.4693	No	ns	>0.9999	A-K
HS Fm7/tko vs. ZS+P Fm7/tko	-2,85	-3.566 to -2.134	Yes	****	<0.0001	A-P
HS Fm7/tko vs. HS+DCA Fm7/tko	-1,15	-2.019 to -0.2810	Yes	**	0,0012	A-U
HS Fm7/tko vs. ZS+DCA Fm7/tko	-1,35	-2.219 to -0.4810	Yes	****	<0.0001	A-Z
HS Fm7/tko vs. HS+UK Fm7/tko	-0,125	-0.9940 to 0.7440	No	ns	>0.9999	A-AE
HS tko F vs. HS+P tko F	-1,45	-2.114 to -0.7863	Yes	****	<0.0001	B-G
HS tko F vs. ZS tko F	1,217	0.5529 to 1.880	Yes	****	<0.0001	B-L
HS tko F vs. ZS+P tko F	-0,9167	-1.633 to -0.2008	Yes	**	0,002	B-Q
HS tko F vs. HS+DCA tko F	-1,692	-2.561 to -0.8226	Yes	****	<0.0001	B-V
HS tko F vs. ZS+DCA tko F	0,4583	-0.4107 to 1.327	No	ns	0,9504	B-AA
HS tko F vs. HS+UK tko F	-1,917	-2.786 to -1.048	Yes	****	<0.0001	B-AF
HS tko M vs. HS+P tko M	-1,225	-1.889 to -0.5613	Yes	****	<0.0001	C-H
HS tko M vs. ZS tko M	1,364	0.7001 to 2.028	Yes	****	<0.0001	C-M
HS tko M vs. ZS+P tko M	-0,5631	-1.279 to 0.1528	No	ns	0,3289	C-R
HS tko M vs. HS+DCA tko M	-1,667	-2.536 to -0.7976	Yes	****	<0.0001	C-W
HS tko M vs. ZS+DCA tko M	0,5333	-0.3357 to 1.402	No	ns	0,8017	C-AB
HS tko M vs. HS+UK tko M	-1,692	-2.561 to -0.8226	Yes	****	<0.0001	C-AG
HS OR M vs. HS+P OR M	-1,214	-1.847 to -0.5807	Yes	****	<0.0001	D-I
HS OR M vs. ZS OR M	-0,3738	-1.007 to 0.2593	No	ns	0,8535	D-N
HS OR M vs. ZS+P OR M	-1,754	-2.497 to -1.011	Yes	****	<0.0001	D-S
HS OR M vs. HS+DCA OR M	-1,121	-2.085 to -0.1564	Yes	**	0,0084	D-X
HS OR M vs. ZS+DCA OR M	-1,579	-2.439 to -0.7182	Yes	****	<0.0001	D-AC
HS OR M vs. HS+UK OR M	-0,2288	-1.089 to 0.6318	No	ns	>0.9999	D-AH
HS OR F vs. HS+P OR F	-1,202	-1.835 to -0.5692	Yes	****	<0.0001	E-J
HS OR F vs. ZS OR F	-0,4423	-1.075 to 0.1908	No	ns	0,5668	E-O
HS OR F vs. ZS+P OR F	-1,576	-2.319 to -0.8327	Yes	****	<0.0001	E-T
HS OR F vs. HS+DCA OR F	-1,259	-2.223 to -0.2949	Yes	**	0,0014	E-Y
HS OR F vs. ZS+DCA OR F	-1,742	-2.603 to -0.8817	Yes	****	<0.0001	E-AD
HS OR F vs. HS+UK OR F	-0,3423	-1.203 to 0.5183	No	ns	0,9991	E-AI
Test details	Mean 1	Mean 2	Mean Diff.	SE of diff.	n1	n2	t	DF
HS Fm7/tko vs. HS+P Fm7/tko	10,25	11,92	-1,672	0,2089	12	9	8,005	212
HS Fm7/tko vs. ZS Fm7/tko	10,25	10,44	-0,1944	0,2089	12	9	0,9308	212
HS Fm7/tko vs. ZS+P Fm7/tko	10,25	13,1	-2,85	0,2253	12	7	12,65	212
HS Fm7/tko vs. HS+DCA Fm7/tko	10,25	11,4	-1,15	0,2735	12	4	4,205	212
HS Fm7/tko vs. ZS+DCA Fm7/tko	10,25	11,6	-1,35	0,2735	12	4	4,936	212
HS Fm7/tko vs. HS+UK Fm7/tko	10,25	10,38	-0,125	0,2735	12	4	0,457	212
HS tko F vs. HS+P tko F	13,68	15,13	-1,45	0,2089	12	9	6,941	212
HS tko F vs. ZS tko F	13,68	12,47	1,217	0,2089	12	9	5,824	212
HS tko F vs. ZS+P tko F	13,68	14,6	-0,9167	0,2253	12	7	4,068	212
HS tko F vs. HS+DCA tko F	13,68	15,38	-1,692	0,2735	12	4	6,185	212
HS tko F vs. ZS+DCA tko F	13,68	13,23	0,4583	0,2735	12	4	1,676	212
HS tko F vs. HS+UK tko F	13,68	15,6	-1,917	0,2735	12	4	7,008	212
HS tko M vs. HS+P tko M	14,31	15,53	-1,225	0,2089	12	9	5,864	212
HS tko M vs. ZS tko M	14,31	12,94	1,364	0,2089	12	9	6,529	212
HS tko M vs. ZS+P tko M	14,31	14,87	-0,5631	0,2253	12	7	2,499	212
HS tko M vs. HS+DCA tko M	14,31	15,98	-1,667	0,2735	12	4	6,093	212
HS tko M vs. ZS+DCA tko M	14,31	13,78	0,5333	0,2735	12	4	1,95	212

HS tko M vs. HS+UK tko M	14,31	16	-1,692	0,2735	12	4	6,185	212
HS OR M vs. HS+P OR M	10,15	11,36	-1,214	0,1993	13	10	6,092	212
HS OR M vs. ZS OR M	10,15	10,52	-0,3738	0,1993	13	10	1,876	212
HS OR M vs. ZS+P OR M	10,15	11,9	-1,754	0,2338	13	6	7,501	212
HS OR M vs. HS+DCA OR M	10,15	11,27	-1,121	0,3034	13	3	3,693	212
HS OR M vs. ZS+DCA OR M	10,15	11,73	-1,579	0,2709	13	4	5,829	212
HS OR M vs. HS+UK OR M	10,15	10,38	-0,2288	0,2709	13	4	0,8448	212
HS OR F vs. HS+P OR F	10,01	11,21	-1,202	0,1993	13	10	6,034	212
HS OR F vs. ZS OR F	10,01	10,45	-0,4423	0,1993	13	10	2,22	212
HS OR F vs. ZS+P OR F	10,01	11,58	-1,576	0,2338	13	6	6,739	212
HS OR F vs. HS+DCA OR F	10,01	11,27	-1,259	0,3034	13	3	4,149	212
HS OR F vs. ZS+DCA OR F	10,01	11,75	-1,742	0,2709	13	4	6,432	212
HS OR F vs. HS+UK OR F	10,01	10,35	-0,3423	0,2709	13	4	1,264	212

FIG 13					
Two-way ANOVA					
Alpha	0,05				
Source of Variation	% of total variation	P value	P value summary	Significant?	
Interaction	8,206	0,0075	**	Yes	
Diet	27,87	<0,0001	****	Yes	
Genotype	50,39	<0,0001	****	Yes	
ANOVA table	SS (Type III)	DF	MS	F (DFn, DFd)	P value
Interaction	1,55469E+11	4	38867168026	F (4, 27) = 4,370	P=0,0075
Diet	5,2803E+11	4	1,32007E+11	F (4, 27) = 14,84	P<0,0001
Genotype	9,54705E+11	1	9,54705E+11	F (1, 27) = 107,3	P<0,0001
Residual	2,40133E+11	27	8893832294		
Diff. between column means					
Predic. (LS) mean of Wild-type	193342				
Predic. (LS) mean of TKO Line	517407				
Diff. between predicted means	-324064				
SE of difference	31278				
95% CI of difference	-388242 to -259887				
Within each column, compare rows					
Number of families	2				
Number of comparisons per family	4				
Alpha	0,05				
Dunnett's multiple comparisons test	Predicted (LS) mean diff,	95,00% CI of diff,	Significant?	Summary	Adjusted P Value
Wild-type					
0% vs. HS	-82608	-256252 to 91035	No	ns	0,5613
0% vs. 0% + DCA	85568	-101989 to 273124	No	ns	0,5958
0% vs. 0% + P	-67368	-254925 to 120188	No	ns	0,7659
0% vs. 0%+L	-28639	-202283 to 145004	No	ns	0,9801
TKO Line					
0% vs. HS	-373320	-546649 to -199991	Yes	****	<0,0001
0% vs. 0% + DCA	183106	9777 to 356435	Yes	*	0,036
0% vs. 0% + P	-151361	-338578 to 35855	No	ns	0,1398
0% vs. 0%+L	-104333	-277661 to 68996	No	ns	0,355

Test details	Predicted (LS) mean 1	Predicted (LS) mean 2	Predicted (LS) mean diff,	SE of diff,	N1	N2	q	DF
Wild-type								
0% vs. HS	174733	257341	-82608	66685	4	4	1,239	27
0% vs. 0% + DCA	174733	89165	85568	72028	4	3	1,188	27
0% vs. 0% + P	174733	242101	-67368	72028	4	3	0,9353	27
0% vs. 0%+L	174733	203372	-28639	66685	4	4	0,4295	27
TKO Line								
0% vs. HS	428225	801545	-373320	66685	4	4	5,598	27
0% vs. 0% + DCA	428225	245119	183106	66685	4	4	2,746	27
0% vs. 0% + P	428225	579586	-151361	72028	4	3	2,101	27
0% vs. 0%+L	428225	532557	-104333	66685	4	4	1,565	27

FIG 15A								
Two-way ANOVA	Ordinary							
Alpha	0,05							
Source of Variation	% of total variation	P value	P value summary	Significant?				
Interaction	1,702	0,5592	ns	No				
Diet	3,255	0,0613	ns	No				
Genotype	84,46	<0.0001	****	Yes				
ANOVA table	SS (Type III)	DF	MS	F (DFn, DFd)	P value			
Interaction	0,1696	3	0,05654	F (3, 15) = 0.7131	P=0.5592			
Diet	0,3244	1	0,3244	F (1, 15) = 4.091	P=0.0613			
Genotype	8,417	3	2,806	F (3, 15) = 35.39	P<0.0001			
Residual	1,189	15	0,07929					
Difference between row means								
Predicted (LS) mean of HS	5,289							
Predicted (LS) mean of 0%	5,529							
Difference between predicted means	-0,2397							
SE of difference	0,1185							
95% CI of difference	-0.4922 to 0.01289							
Compare column means (main column effect)								
Number of families	1							
Number of comparisons per family	6							
Alpha	0,05							
Tukey's multiple comparisons test	Mean Diff.	95.00% CI of diff.	Significant?	Summary	Adjusted P Value			
L3 OR Male vs. L3 OR Female	-0,2282	-0.6967 to 0.2404	No	ns	0,5162			
L3 OR Male vs. L3 tko Male	-1,195	-1.687 to -0.7039	Yes	****	<0.0001			
L3 OR Male vs. L3 tko Female	-1,383	-1.852 to -0.9147	Yes	****	<0.0001			
L3 OR Female vs. L3 tko Male	-0,9672	-1.459 to -0.4757	Yes	***	0,0002			
L3 OR Female vs. L3 tko Female	-1,155	-1.624 to -0.6865	Yes	****	<0.0001			
L3 tko Male vs. L3 tko Female	-0,1879	-0.6793 to 0.3035	No	ns	0,6937			
Test details	Mean 1	Mean 2	Mean Diff.	SE of diff.	N1	N2	q	DF
L3 OR Male vs. L3 OR Female	4,698	4,927	-0,2282	0,1626	6	6	1,985	15
L3 OR Male vs. L3 tko Male	4,698	5,894	-1,195	0,1705	6	5	9,915	15
L3 OR Male vs. L3 tko Female	4,698	6,082	-1,383	0,1626	6	6	12,03	15
L3 OR Female vs. L3 tko Male	4,927	5,894	-0,9672	0,1705	6	5	8,022	15
L3 OR Female vs. L3 tko Female	4,927	6,082	-1,155	0,1626	6	6	10,05	15
L3 tko Male vs. L3 tko Female	5,894	6,082	-0,1879	0,1705	5	6	1,559	15
0% vs. 0% + DCA	174733	89165	85568	72028	4	3	1,188	27
0% vs. 0% + P	174733	242101	-67368	72028	4	3	0,9353	27
0% vs. 0%+L	174733	203372	-28639	66685	4	4	0,4295	27
TKO Line								
0% vs. HS	428225	801545	-373320	66685	4	4	5,598	27
0% vs. 0% + DCA	428225	245119	183106	66685	4	4	2,746	27
0% vs. 0% + P	428225	579586	-151361	72028	4	3	2,101	27
0% vs. 0%+L	428225	532557	-104333	66685	4	4	1,565	27

FIG 15B				
Two-way ANOVA	Ordinary			
Alpha	0,05			
Source of Variation	% of total variation	P value	P value summary	Significant?
Interaction	0,1323	0,7441	ns	No
Diet	0,1429	0,1618	ns	No
Genotype	98,37	<0.0001	****	Yes
ANOVA table	SS	DF	MS	F (DFn, DFd)	P value
Interaction	0,1087	4	0,02717	F (4, 20) = 0.4885	P=0.7441
Diet	0,1174	1	0,1174	F (1, 20) = 2.111	P=0.1618
Genotype	80,8	4	20,2	F (4, 20) = 363.2	P<0.0001
Residual	1,112	20	0,05562		
Difference between row means				
Mean of HS	4,003			
Mean of 0%	4,128			
Difference between means	-0,1251			
SE of difference	0,08612			
95% CI of difference	-0.3048 to 0.05452			
Compare column means (main column effect)				
Number of families	1			
Number of comparisons per family	10			
Alpha	0,05			
Tukey's multiple comparisons test	Mean Diff.	95.00% CI of diff.	Significant?	Summary	Adjusted P Value
OR male vs. tko25t male	-0,3706	-0.778 to 0.03688	No	ns	0,0858
OR male vs. OR female	3,331	2.923 to 3.738	Yes	****	<0.0001
OR male vs. tko25t/FM7 female	3,284	2.876 to 3.691	Yes	****	<0.0001
OR male vs. tko25t/tko25t female	2,786	2.378 to 3.193	Yes	****	<0.0001
tko25t male vs. OR female	3,701	3.294 to 4.109	Yes	****	<0.0001
tko25t male vs. tko25t/FM7 female	3,654	3.247 to 4.062	Yes	****	<0.0001
tko25t male vs. tko25t/tko25t female	3,156	2.749 to 3.564	Yes	****	<0.0001
OR female vs. tko25t/FM7 female	-0,04676	-0.4542 to 0.3607	No	ns	0,9968
OR female vs. tko25t/tko25t female	-0,5449	-0.9523 to -0.1374	Yes	**	0,0056
tko25t/FM7 female vs. tko25t/tko25t female	-0,4981	-0.9056 to -0.09068	Yes	*	0,0121
Test details	Mean 1	Mean 2	Mean Diff.	SE of diff.	N1	N2	q	DF
OR male vs. tko25t male	5,872	6,242	-0,3706	0,1362	6	6	3,849	20
OR male vs. OR female	5,872	2,541	3,331	0,1362	6	6	34,59	20
OR male vs. tko25t/FM7 female	5,872	2,588	3,284	0,1362	6	6	34,11	20
OR male vs. tko25t/tko25t female	5,872	3,086	2,786	0,1362	6	6	28,93	20
tko25t male vs. OR female	6,242	2,541	3,701	0,1362	6	6	38,44	20
tko25t male vs. tko25t/FM7 female	6,242	2,588	3,654	0,1362	6	6	37,95	20
tko25t male vs. tko25t/tko25t female	6,242	3,086	3,156	0,1362	6	6	32,78	20
OR female vs. tko25t/FM7 female	2,541	2,588	-0,04676	0,1362	6	6	0,4857	20
OR female vs. tko25t/tko25t female	2,541	3,086	-0,5449	0,1362	6	6	5,659	20
tko25t/FM7 female vs. tko25t/tko25t female	2,588	3,086	-0,4981	0,1362	6	6	5,174	20

FIG 17A					
One-way analysis of variance					
P value	< 0.0001				
P value summary	***				
Are means signif. different? (P < 0.05)	Yes				
Number of groups	11				
F	1347				
R square	0,9977				
ANOVA Table	SS	df	MS		
Treatment (between columns)	176,8	10	17,68		
Residual (within columns)	0,4067	31	0,01312		
Total	177,2	41			
Tukey's Multiple Comparison Test	Mean Diff.	q	Significant? P < 0.05?	Summary	95% CI of diff
tko25t/Y UASSrl/daGAL4 vs tko25t/tko25t UASSrl/daGAL4	-1,247	20,15	Yes	***	-1.550 to -0.9431
tko25t/Y UASSrl/daGAL4 vs FM7/tko25t UASSrl/daGAL4	-1,073	17,35	Yes	***	-1.377 to -0.7696
tko25t/Y UASSrl/daGAL4 vs tko25t/Y Cyo/daGAL4	-6,489	98,12	Yes	***	-6.813 to -6.164
tko25t/Y UASSrl/daGAL4 vs tko25t/tko25t Cyo/daGAL4	-2,766	44,71	Yes	***	-3.069 to -2.462
tko25t/Y UASSrl/daGAL4 vs FM7/tko25t Cyo/daGAL4	-2,545	41,14	Yes	***	-2.848 to -2.241
tko25t/Y UASSrl/daGAL4 vs tko25t/Y	-6,462	104,5	Yes	***	-6.766 to -6.159
tko25t/Y UASSrl/daGAL4 vs tko25t/tko25t	-2,706	43,75	Yes	***	-3.010 to -2.403
tko25t/Y UASSrl/daGAL4 vs FM7/tko25t	-2,997	48,45	Yes	***	-3.300 to -2.693
tko25t/Y UASSrl/daGAL4 vs OR Male	-6,117	98,89	Yes	***	-6.420 to -5.813
tko25t/Y UASSrl/daGAL4 vs OR Female	-3,095	50,04	Yes	***	-3.399 to -2.792
tko25t/tko25t UASSrl/daGAL4 vs FM7/tko25t UASSrl/daGAL4	0,1735	3,029	No	ns	-0.1076 to 0.4545
tko25t/tko25t UASSrl/daGAL4 vs tko25t/Y Cyo/daGAL4	-5,242	84,74	Yes	***	-5.545 to -4.938
tko25t/tko25t UASSrl/daGAL4 vs tko25t/tko25t Cyo/daGAL4	-1,519	26,53	Yes	***	-1.800 to -1.238
tko25t/tko25t UASSrl/daGAL4 vs FM7/tko25t Cyo/daGAL4	-1,298	22,67	Yes	***	-1.579 to -1.017
tko25t/tko25t UASSrl/daGAL4 vs tko25t/Y	-5,216	91,07	Yes	***	-5.497 to -4.935
tko25t/tko25t UASSrl/daGAL4 vs tko25t/tko25t	-1,46	25,49	Yes	***	-1.741 to -1.179
tko25t/tko25t UASSrl/daGAL4 vs FM7/tko25t	-1,75	30,56	Yes	***	-2.031 to -1.469
tko25t/tko25t UASSrl/daGAL4 vs OR Male	-4,87	85,04	Yes	***	-5.151 to -4.589
tko25t/tko25t UASSrl/daGAL4 vs OR Female	-1,848	32,28	Yes	***	-2.130 to -1.567
FM7/tko25t UASSrl/daGAL4 vs tko25t/Y Cyo/daGAL4	-5,415	87,55	Yes	***	-5.719 to -5.112
FM7/tko25t UASSrl/daGAL4 vs tko25t/tko25t Cyo/daGAL4	-1,693	29,56	Yes	***	-1.974 to -1.412
FM7/tko25t UASSrl/daGAL4 vs FM7/tko25t Cyo/daGAL4	-1,471	25,69	Yes	***	-1.753 to -1.190
FM7/tko25t UASSrl/daGAL4 vs tko25t/Y	-5,389	94,1	Yes	***	-5.670 to -5.108
FM7/tko25t UASSrl/daGAL4 vs tko25t/tko25t	-1,633	28,52	Yes	***	-1.914 to -1.352
FM7/tko25t UASSrl/daGAL4 vs FM7/tko25t	-1,923	33,59	Yes	***	-2.205 to -1.642
FM7/tko25t UASSrl/daGAL4 vs OR Male	-5,044	88,07	Yes	***	-5.325 to -4.763
FM7/tko25t UASSrl/daGAL4 vs OR Female	-2,022	35,31	Yes	***	-2.303 to -1.741
tko25t/Y Cyo/daGAL4 vs tko25t/tko25t Cyo/daGAL4	3,723	60,18	Yes	***	3.419 to 4.026
tko25t/Y Cyo/daGAL4 vs FM7/tko25t Cyo/daGAL4	3,944	63,76	Yes	***	3.640 to 4.247
tko25t/Y Cyo/daGAL4 vs tko25t/Y	0,02626	0,4246	No	ns	-0.2773 to 0.3298
tko25t/Y Cyo/daGAL4 vs tko25t/tko25t	3,782	61,14	Yes	***	3.479 to 4.086
tko25t/Y Cyo/daGAL4 vs FM7/tko25t	3,492	56,45	Yes	***	3.188 to 3.795
tko25t/Y Cyo/daGAL4 vs OR Male	0,3717	6,009	Yes	**	0.06810 to 0.6752
tko25t/Y Cyo/daGAL4 vs OR Female	3,393	54,86	Yes	***	3.090 to 3.697
tko25t/tko25t Cyo/daGAL4 vs FM7/tko25t Cyo/daGAL4	0,2211	3,861	No	ns	-0.05996 to 0.5021
tko25t/tko25t Cyo/daGAL4 vs tko25t/Y	-3,697	64,55	Yes	***	-3.978 to -3.415
tko25t/tko25t Cyo/daGAL4 vs tko25t/tko25t	0,05931	1,036	No	ns	-0.2217 to 0.3404
tko25t/tko25t Cyo/daGAL4 vs FM7/tko25t	-0,2309	4,032	No	ns	-0.5120 to 0.05014
tko25t/tko25t Cyo/daGAL4 vs OR Male	-3,351	58,52	Yes	***	-3.632 to -3.070
tko25t/tko25t Cyo/daGAL4 vs OR Female	-0,3294	5,751	Yes	*	-0.6104 to -0.04830
FM7/tko25t Cyo/daGAL4 vs tko25t/Y	-3,918	68,41	Yes	***	-4.199 to -3.637
FM7/tko25t Cyo/daGAL4 vs tko25t/tko25t	-0,1618	2,825	No	ns	-0.4428 to 0.1193
FM7/tko25t Cyo/daGAL4 vs FM7/tko25t	-0,452	7,893	Yes	***	-0.7331 to -0.1710
FM7/tko25t Cyo/daGAL4 vs OR Male	-3,572	62,38	Yes	***	-3.853 to -3.291
FM7/tko25t Cyo/daGAL4 vs OR Female	-0,5504	9,612	Yes	***	-0.8315 to -0.2694
tko25t/Y vs tko25t/tko25t	3,756	65,58	Yes	***	3.475 to 4.037
tko25t/Y vs FM7/tko25t	3,466	60,52	Yes	***	3.185 to 3.747
tko25t/Y vs OR Male	0,3454	6,031	Yes	**	0.06435 to 0.6265
tko25t/Y vs OR Female	3,367	58,8	Yes	***	3.086 to 3.648
tko25t/tko25t vs FM7/tko25t	-0,2902	5,068	Yes	*	-0.5713 to -0.009168
tko25t/tko25t vs OR Male	-3,41	59,55	Yes	***	-3.691 to -3.129
tko25t/tko25t vs OR Female	-0,3887	6,787	Yes	**	-0.6697 to -0.1076
FM7/tko25t vs OR Male	-3,12	54,48	Yes	***	-3.401 to -2.839
FM7/tko25t vs OR Female	-0,09844	1,719	No	ns	-0.3795 to 0.1826
OR Male vs OR Female	3,022	52,77	Yes	***	2.741 to 3.303

150

Table Analyzed	One-way ANOVA data				
Data sets analyzed	A-K				
ANOVA summary					
F	94,74				
P value	<0.0001				
P value summary	****				
Significant diff. among means (P < 0.05)?	Yes				
R square	0,9556				
Brown-Forsythe test					
F (DFn, DFd)	1.047 (10, 44)				
P value	0,4223				
P value summary	ns				
Are SDs significantly different (P < 0.05)?	No				
Bartlett's test					
Bartlett's statistic (corrected)	27,74				
P value	0,002				
P value summary	**				
Are SDs significantly different (P < 0.05)?	Yes				
ANOVA table	SS	DF	MS	F (DFn, DFd)	P value
Treatment (between columns)	129,5	10	12,95	F (10, 44) = 94.74	P< 0.0001
Residual (within columns)	6,015	44	0,1367		
Total	135,5	54			
Data summary					
Number of treatments (columns)	11				
Number of values (total)	55				
Number of families	1				
Number of comparisons per family	55				
Alpha	0,05				

Tukey's multiple comparisons test	Mean Diff.	95.00% CI of diff.	Significant?	Summary	
tko25t/Y UASSrl/daGAL4 vs. tko25t/tko25t UASSrl/daGAL4	0,7183	-0.07511 to 1.512	No	ns	A-B
tko25t/Y UASSrl/daGAL4 vs. FM7/tko25t UASSrl/daGAL4	3,715	2.922 to 4.508	Yes	****	A-C
tko25t/Y UASSrl/daGAL4 vs. tko25t/Y Cyo/daGAL4	0,2135	-0.5800 to 1.007	No	ns	A-D
tko25t/Y UASSrl/daGAL4 vs. tko25t/tko25t Cyo/daGAL4	0,6639	-0.1296 to 1.457	No	ns	A-E
tko25t/Y UASSrl/daGAL4 vs. FM7/tko25t Cyo/daGAL4	3,671	2.878 to 4.465	Yes	****	A-F
tko25t/Y UASSrl/daGAL4 vs. tko25t/Y	0,2172	-0.5763 to 1.011	No	ns	A-G
tko25t/Y UASSrl/daGAL4 vs. tko25t/tko25t	0,7939	0.0004168 to 1.587	Yes	*	A-H
tko25t/Y UASSrl/daGAL4 vs. FM7/tko25t	3,606	2.813 to 4.400	Yes	****	A-I
tko25t/Y UASSrl/daGAL4 vs. OR Male	2,996	2.203 to 3.789	Yes	****	A-J
tko25t/Y UASSrl/daGAL4 vs. OR Female	3,319	2.526 to 4.113	Yes	****	A-K
tko25t/tko25t UASSrl/daGAL4 vs. FM7/tko25t UASSrl/daGAL4	2,997	2.203 to 3.790	Yes	****	B-C
tko25t/tko25t UASSrl/daGAL4 vs. tko25t/Y Cyo/daGAL4	-0,5048	-1.298 to 0.2886	No	ns	B-D
tko25t/tko25t UASSrl/daGAL4 vs. tko25t/tko25t Cyo/daGAL4	-0,05444	-0.8479 to 0.7390	No	ns	B-E
tko25t/tko25t UASSrl/daGAL4 vs. FM7/tko25t Cyo/daGAL4	2,953	2.160 to 3.746	Yes	****	B-F
tko25t/tko25t UASSrl/daGAL4 vs. tko25t/Y	-0,5012	-1.295 to 0.2923	No	ns	B-G
tko25t/tko25t UASSrl/daGAL4 vs. tko25t/tko25t	0,07553	-0.7179 to 0.8690	No	ns	B-H
tko25t/tko25t UASSrl/daGAL4 vs. FM7/tko25t	2,888	2.094 to 3.681	Yes	****	B-I
tko25t/tko25t UASSrl/daGAL4 vs. OR Male	2,278	1.484 to 3.071	Yes	****	B-J
tko25t/tko25t UASSrl/daGAL4 vs. OR Female	2,601	1.808 to 3.395	Yes	****	B-K
FM7/tko25t UASSrl/daGAL4 vs. tko25t/Y Cyo/daGAL4	-3,502	-4.295 to -2.708	Yes	****	C-D
FM7/tko25t UASSrl/daGAL4 vs. tko25t/tko25t Cyo/daGAL4	-3,051	-3.845 to -2.258	Yes	****	C-E
FM7/tko25t UASSrl/daGAL4 vs. FM7/tko25t Cyo/daGAL4	-0,04364	-0.8371 to 0.7498	No	ns	C-F
FM7/tko25t UASSrl/daGAL4 vs. tko25t/Y	-3,498	-4.291 to -2.704	Yes	****	C-G
FM7/tko25t UASSrl/daGAL4 vs. tko25t/tko25t	-2,921	-3.715 to -2.128	Yes	****	C-H
FM7/tko25t UASSrl/daGAL4 vs. FM7/tko25t	-0,1088	-0.9022 to 0.6847	No	ns	C-I

FM7/tko25t UASSrl/daGAL4 vs. OR Male	-0,719	-1.512 to 0.07447	No	ns	C-J
FM7/tko25t UASSrl/daGAL4 vs. OR Female	-0,3956	-1.189 to 0.3979	No	ns	C-K
tko25t/Y Cyo/daGAL4 vs. tko25t/tko25t Cyo/daGAL4	0,4504	-0.3430 to 1.244	No	ns	D-E
tko25t/Y Cyo/daGAL4 vs. FM7/tko25t Cyo/daGAL4	3,458	2.664 to 4.251	Yes	****	D-F
tko25t/Y Cyo/daGAL4 vs. tko25t/Y	0,003694	-0.7897 to 0.7971	No	ns	D-G
tko25t/Y Cyo/daGAL4 vs. tko25t/tko25t	0,5804	-0.2131 to 1.374	No	ns	D-H
tko25t/Y Cyo/daGAL4 vs. FM7/tko25t	3,393	2.599 to 4.186	Yes	****	D-I
tko25t/Y Cyo/daGAL4 vs. OR Male	2,783	1.989 to 3.576	Yes	****	D-J
tko25t/Y Cyo/daGAL4 vs. OR Female	3,106	2.313 to 3.899	Yes	****	D-K
tko25t/tko25t Cyo/daGAL4 vs. FM7/tko25t Cyo/daGAL4	3,007	2.214 to 3.801	Yes	****	E-F
tko25t/tko25t Cyo/daGAL4 vs. tko25t/Y	-0,4467	-1.240 to 0.3467	No	ns	E-G
tko25t/tko25t Cyo/daGAL4 vs. tko25t/tko25t	0,13	-0.6635 to 0.9234	No	ns	E-H
tko25t/tko25t Cyo/daGAL4 vs. FM7/tko25t	2,942	2.149 to 3.736	Yes	****	E-I
tko25t/tko25t Cyo/daGAL4 vs. OR Male	2,332	1.539 to 3.126	Yes	****	E-J
tko25t/tko25t Cyo/daGAL4 vs. OR Female	2,656	1.862 to 3.449	Yes	****	E-K
FM7/tko25t Cyo/daGAL4 vs. tko25t/Y	-3,454	-4.248 to -2.661	Yes	****	F-G
FM7/tko25t Cyo/daGAL4 vs. tko25t/tko25t	-2,878	-3.671 to -2.084	Yes	****	F-H
FM7/tko25t Cyo/daGAL4 vs. FM7/tko25t	-0,06514	-0.8586 to 0.7283	No	ns	F-I
FM7/tko25t Cyo/daGAL4 vs. OR Male	-0,6753	-1.469 to 0.1181	No	ns	F-J
FM7/tko25t Cyo/daGAL4 vs. OR Female	-0,3519	-1.145 to 0.4415	No	ns	F-K
tko25t/Y vs. tko25t/tko25t	0,5767	-0.2168 to 1.370	No	ns	G-H
tko25t/Y vs. FM7/tko25t	3,389	2.596 to 4.182	Yes	****	G-I
tko25t/Y vs. OR Male	2,779	1.985 to 3.572	Yes	****	G-J
tko25t/Y vs. OR Female	3,102	2.309 to 3.896	Yes	****	G-K
tko25t/tko25t vs. FM7/tko25t	2,812	2.019 to 3.606	Yes	****	H-I
tko25t/tko25t vs. OR Male	2,202	1.409 to 2.996	Yes	****	H-J
tko25t/tko25t vs. OR Female	2,526	1.732 to 3.319	Yes	****	H-K
FM7/tko25t vs. OR Male	-0,6102	-1.404 to 0.1832	No	ns	I-J
FM7/tko25t vs. OR Female	-0,2868	-1.080 to 0.5067	No	ns	I-K
OR Male vs. OR Female	0,3234	-0.4700 to 1.117	No	ns	J-K

Test details	Mean 1	Mean 2	Mean Diff.	SE of diff.	n1	n2	q	DF
tko25t/Y UASSrl/daGAL4 vs. tko25t/tko25t UASSrl/daGAL4	13,46	12,74	0,7183	0,2338	5	5	4,344	44
tko25t/Y UASSrl/daGAL4 vs. FM7/tko25t UASSrl/daGAL4	13,46	9,74	3,715	0,2338	5	5	22,47	44
tko25t/Y UASSrl/daGAL4 vs. tko25t/Y Cyo/daGAL4	13,46	13,24	0,2135	0,2338	5	5	1,291	44
tko25t/Y UASSrl/daGAL4 vs. tko25t/tko25t Cyo/daGAL4	13,46	12,79	0,6639	0,2338	5	5	4,015	44
tko25t/Y UASSrl/daGAL4 vs. FM7/tko25t Cyo/daGAL4	13,46	9,784	3,671	0,2338	5	5	22,2	44
tko25t/Y UASSrl/daGAL4 vs. tko25t/Y	13,46	13,24	0,2172	0,2338	5	5	1,313	44
tko25t/Y UASSrl/daGAL4 vs. tko25t/tko25t	13,46	12,66	0,7939	0,2338	5	5	4,801	44
tko25t/Y UASSrl/daGAL4 vs. FM7/tko25t	13,46	9,849	3,606	0,2338	5	5	21,81	44
tko25t/Y UASSrl/daGAL4 vs. OR Male	13,46	10,46	2,996	0,2338	5	5	18,12	44
tko25t/Y UASSrl/daGAL4 vs. OR Female	13,46	10,14	3,319	0,2338	5	5	20,07	44
tko25t/tko25t UASSrl/daGAL4 vs. FM7/tko25t UASSrl/daGAL4	12,74	9,74	2,997	0,2338	5	5	18,12	44
tko25t/tko25t UASSrl/daGAL4 vs. tko25t/Y Cyo/daGAL4	12,74	13,24	-0,5048	0,2338	5	5	3,053	44
tko25t/tko25t UASSrl/daGAL4 vs. tko25t/tko25t Cyo/daGAL4	12,74	12,79	-0,05444	0,2338	5	5	0,3292	44
tko25t/tko25t UASSrl/daGAL4 vs. FM7/tko25t Cyo/daGAL4	12,74	9,784	2,953	0,2338	5	5	17,86	44
tko25t/tko25t UASSrl/daGAL4 vs. tko25t/Y	12,74	13,24	-0,5012	0,2338	5	5	3,031	44
tko25t/tko25t UASSrl/daGAL4 vs. tko25t/tko25t	12,74	12,66	0,07553	0,2338	5	5	0,4568	44
tko25t/tko25t UASSrl/daGAL4 vs. FM7/tko25t	12,74	9,849	2,888	0,2338	5	5	17,46	44
tko25t/tko25t UASSrl/daGAL4 vs. OR Male	12,74	10,46	2,278	0,2338	5	5	13,77	44
tko25t/tko25t UASSrl/daGAL4 vs. OR Female	12,74	10,14	2,601	0,2338	5	5	15,73	44
FM7/tko25t UASSrl/daGAL4 vs. tko25t/Y Cyo/daGAL4	9,74	13,24	-3,502	0,2338	5	5	21,18	44
FM7/tko25t UASSrl/daGAL4 vs. tko25t/tko25t Cyo/daGAL4	9,74	12,79	-3,051	0,2338	5	5	18,45	44
FM7/tko25t UASSrl/daGAL4 vs. FM7/tko25t Cyo/daGAL4	9,74	9,784	-0,04364	0,2338	5	5	0,2639	44
FM7/tko25t UASSrl/daGAL4 vs. tko25t/Y	9,74	13,24	-3,498	0,2338	5	5	21,15	44
FM7/tko25t UASSrl/daGAL4 vs. tko25t/tko25t	9,74	12,66	-2,921	0,2338	5	5	17,67	44
FM7/tko25t UASSrl/daGAL4 vs. FM7/tko25t	9,74	9,849	-0,1088	0,2338	5	5	0,6578	44
FM7/tko25t UASSrl/daGAL4 vs. OR Male	9,74	10,46	-0,719	0,2338	5	5	4,348	44
FM7/tko25t UASSrl/daGAL4 vs. OR Female	9,74	10,14	-0,3956	0,2338	5	5	2,392	44

tko25t/Y Cyo/daGAL4 vs. tko25t/tko25t Cyo/daGAL4	13,24	12,79	0,4504	0,2338	5	5	2,724	44
tko25t/Y Cyo/daGAL4 vs. FM7/tko25t Cyo/daGAL4	13,24	9,784	3,458	0,2338	5	5	20,91	44
tko25t/Y Cyo/daGAL4 vs. tko25t/Y	13,24	13,24	0,003694	0,2338	5	5	0,02234	44
tko25t/Y Cyo/daGAL4 vs. tko25t/tko25t	13,24	12,66	0,5804	0,2338	5	5	3,51	44
tko25t/Y Cyo/daGAL4 vs. FM7/tko25t	13,24	9,849	3,393	0,2338	5	5	20,52	44
tko25t/Y Cyo/daGAL4 vs. OR Male	13,24	10,46	2,783	0,2338	5	5	16,83	44
tko25t/Y Cyo/daGAL4 vs. OR Female	13,24	10,14	3,106	0,2338	5	5	18,78	44
tko25t/tko25t Cyo/daGAL4 vs. FM7/tko25t Cyo/daGAL4	12,79	9,784	3,007	0,2338	5	5	18,19	44
tko25t/tko25t Cyo/daGAL4 vs. tko25t/Y	12,79	13,24	-0,4467	0,2338	5	5	2,702	44
tko25t/tko25t Cyo/daGAL4 vs. tko25t/tko25t	12,79	12,66	0,13	0,2338	5	5	0,786	44
tko25t/tko25t Cyo/daGAL4 vs. FM7/tko25t	12,79	9,849	2,942	0,2338	5	5	17,79	44
tko25t/tko25t Cyo/daGAL4 vs. OR Male	12,79	10,46	2,332	0,2338	5	5	14,1	44
tko25t/tko25t Cyo/daGAL4 vs. OR Female	12,79	10,14	2,656	0,2338	5	5	16,06	44
FM7/tko25t Cyo/daGAL4 vs. tko25t/Y	9,784	13,24	-3,454	0,2338	5	5	20,89	44
FM7/tko25t Cyo/daGAL4 vs. tko25t/tko25t	9,784	12,66	-2,878	0,2338	5	5	17,4	44
FM7/tko25t Cyo/daGAL4 vs. FM7/tko25t	9,784	9,849	-0,06514	0,2338	5	5	0,3939	44
FM7/tko25t Cyo/daGAL4 vs. OR Male	9,784	10,46	-0,6753	0,2338	5	5	4,084	44
FM7/tko25t Cyo/daGAL4 vs. OR Female	9,784	10,14	-0,3519	0,2338	5	5	2,128	44
tko25t/Y vs. tko25t/tko25t	13,24	12,66	0,5767	0,2338	5	5	3,488	44
tko25t/Y vs. FM7/tko25t	13,24	9,849	3,389	0,2338	5	5	20,5	44
tko25t/Y vs. OR Male	13,24	10,46	2,779	0,2338	5	5	16,81	44
tko25t/Y vs. OR Female	13,24	10,14	3,102	0,2338	5	5	18,76	44
tko25t/tko25t vs. FM7/tko25t	12,66	9,849	2,812	0,2338	5	5	17,01	44
tko25t/tko25t vs. OR Male	12,66	10,46	2,202	0,2338	5	5	13,32	44
tko25t/tko25t vs. OR Female	12,66	10,14	2,526	0,2338	5	5	15,27	44
FM7/tko25t vs. OR Male	9,849	10,46	-0,6102	0,2338	5	5	3,69	44
FM7/tko25t vs. OR Female	9,849	10,14	-0,2868	0,2338	5	5	1,734	44
OR Male vs. OR Female	10,46	10,14	0,3234	0,2338	5	5	1,956	44

FIG 19			
Table Analyzed	One-way ANOVA data		
One-way analysis of variance			
P value	0,2554		
P value summary	ns		
Are means signif. different? (P < 0.05)	No		
Number of groups	11		
F	1,336		
R square	0,3012		
ANOVA Table	SS	df	MS
Treatment (between columns)	2362	10	236,2
Residual (within columns)	5480	31	176,8
Total	7842	41	
FIG 20A			
One-way analysis of variance			
P value	< 0.0001		
P value summary	***		
Are means signif. different? (P < 0.05)	Yes		
Number of groups	13		
F	45,30		
R square	0,9577		
ANOVA Table	SS	df	MS
Treatment (between columns)	38,11	12	3,176
Residual (within columns)	1,682	24	0,07010
Total	39,79	36	

Tukey's Multiple Comparison Test	Mean Diff.	q	Significant? P < 0.05?	Summary	95% CI of diff
Embryo (S1-3) vs L1 larva	-1,710	11,19	Yes	***	-2.502 to -0.9181
Embryo (S1-3) vs L2 Larva	-2,155	14,09	Yes	***	-2.946 to -1.363
Embryo (S1-3) vs Early L3 Larva M	-2,622	17,15	Yes	***	-3.414 to -1.831
Embryo (S1-3) vs Late L3 Larva M	-2,453	16,05	Yes	***	-3.245 to -1.662
Embryo (S1-3) vs Early Pupa M	-2,519	16,48	Yes	***	-3.311 to -1.727
Embryo (S1-3) vs Late Pupa M	-3,944	25,80	Yes	***	-4.735 to -3.152
Embryo (S1-3) vs Adult M	-3,707	24,25	Yes	***	-4.499 to -2.916
Embryo (S1-3) vs Early L3 Larva F	-2,714	17,75	Yes	***	-3.506 to -1.922
Embryo (S1-3) vs Late L3 Larva F	-2,873	18,80	Yes	***	-3.665 to -2.082
Embryo (S1-3) vs Early Pupa F	-2,577	16,86	Yes	***	-3.369 to -1.785

Embryo (S1-3) vs Late Pupa F	-3,315	19,40	Yes	***	-4.200 to -2.430
Embryo (S1-3) vs Adult F	-0,9729	5,693	Yes	*	-1.858 to -0.08781
L1 larva vs L2 Larva	-0,4447	2,909	No	ns	-1.236 to 0.3470
L1 larva vs Early L3 Larva M	-0,9125	5,969	Yes	*	-1.704 to -0.1208
L1 larva vs Late L3 Larva M	-0,7436	4,865	No	ns	-1.535 to 0.04806
L1 larva vs Early Pupa M	-0,8090	5,292	Yes	*	-1.601 to -0.01731
L1 larva vs Late Pupa M	-2,234	14,61	Yes	***	-3.026 to -1.442
L1 larva vs Adult M	-1,998	13,07	Yes	***	-2.789 to -1.206
L1 larva vs Early L3 Larva F	-1,004	6,568	Yes	**	-1.796 to -0.2124
L1 larva vs Late L3 Larva F	-1,163	7,611	Yes	***	-1.955 to -0.3718
L1 larva vs Early Pupa F	-0,8673	5,674	Yes	*	-1.659 to -0.07561
L1 larva vs Late Pupa F	-1,605	9,393	Yes	***	-2.490 to -0.7201
L1 larva vs Adult F	0,7369	4,312	No	ns	-0.1482 to 1.622
L2 Larva vs Early L3 Larva M	-0,4679	3,061	No	ns	-1.260 to 0.3238
L2 Larva vs Late L3 Larva M	-0,2990	1,956	No	ns	-1.091 to 0.4927
L2 Larva vs Early Pupa M	-0,3643	2,383	No	ns	-1.156 to 0.4274
L2 Larva vs Late Pupa M	-1,789	11,70	Yes	***	-2.581 to -0.9975
L2 Larva vs Adult M	-1,553	10,16	Yes	***	-2.345 to -0.7612
L2 Larva vs Early L3 Larva F	-0,5594	3,660	No	ns	-1.351 to 0.2323
L2 Larva vs Late L3 Larva F	-0,7188	4,702	No	ns	-1.511 to 0.07287
L2 Larva vs Early Pupa F	-0,4226	2,765	No	ns	-1.214 to 0.3691
L2 Larva vs Late Pupa F	-1,161	6,791	Yes	**	-2.046 to -0.2755
L2 Larva vs Adult F	1,182	6,913	Yes	**	0.2964 to 2.067
Early L3 Larva M vs Late L3 Larva M	0,1689	1,105	No	ns	-0.6228 to 0.9606
Early L3 Larva M vs Early Pupa M	0,1035	0,6772	No	ns	-0.6882 to 0.8952
Early L3 Larva M vs Late Pupa M	-1,321	8,644	Yes	***	-2.113 to -0.5297
Early L3 Larva M vs Adult M	-1,085	7,098	Yes	**	-1.877 to -0.2933
Early L3 Larva M vs Early L3 Larva F	-0,09156	0,5990	No	ns	-0.8833 to 0.7001
Early L3 Larva M vs Late L3 Larva F	-0,2510	1,642	No	ns	-1.043 to 0.5407
Early L3 Larva M vs Early Pupa F	0,04522	0,2958	No	ns	-0.7465 to 0.8369
Early L3 Larva M vs Late Pupa F	-0,6928	4,053	No	ns	-1.578 to 0.1924
Early L3 Larva M vs Adult F	1,649	9,651	Yes	***	0.7643 to 2.535
Late L3 Larva M vs Early Pupa M	-0,06537	0,4276	No	ns	-0.8571 to 0.7263
Late L3 Larva M vs Late Pupa M	-1,490	9,749	Yes	***	-2.282 to -0.6986
Late L3 Larva M vs Adult M	-1,254	8,203	Yes	***	-2.046 to -0.4622
Late L3 Larva M vs Early L3 Larva F	-0,2604	1,704	No	ns	-1.052 to 0.5312
Late L3 Larva M vs Late L3 Larva F	-0,4198	2,746	No	ns	-1.212 to 0.3718
Late L3 Larva M vs Early Pupa F	-0,1237	0,8090	No	ns	-0.9154 to 0.6680
Late L3 Larva M vs Late Pupa F	-0,8616	5,042	No	ns	-1.747 to 0.02349
Late L3 Larva M vs Adult F	1,481	8,663	Yes	***	0.5954 to 2.366
Early Pupa M vs Late Pupa M	-1,425	9,321	Yes	***	-2.217 to -0.6332
Early Pupa M vs Adult M	-1,189	7,775	Yes	***	-1.980 to -0.3969
Early Pupa M vs Early L3 Larva F	-0,1951	1,276	No	ns	-0.9868 to 0.5966
Early Pupa M vs Late L3 Larva F	-0,3545	2,319	No	ns	-1.146 to 0.4372
Early Pupa M vs Early Pupa F	-0,05830	0,3814	No	ns	-0.8500 to 0.7334
Early Pupa M vs Late Pupa F	-0,7963	4,659	No	ns	-1.681 to 0.08886
Early Pupa M vs Adult F	1,546	9,045	Yes	***	0.6608 to 2.431
Late Pupa M vs Adult M	0,2363	1,546	No	ns	-0.5554 to 1.028
Late Pupa M vs Early L3 Larva F	1,230	8,045	Yes	***	0.4381 to 2.022
Late Pupa M vs Late L3 Larva F	1,070	7,002	Yes	**	0.2787 to 1.862
Late Pupa M vs Early Pupa F	1,367	8,940	Yes	***	0.5749 to 2.158
Late Pupa M vs Late Pupa F	0,6286	3,678	No	ns	-0.2565 to 1.514
Late Pupa M vs Adult F	2,971	17,38	Yes	***	2.086 to 3.856
Adult M vs Early L3 Larva F	0,9935	6,499	Yes	**	0.2018 to 1.785
Adult M vs Late L3 Larva F	0,8341	5,456	Yes	*	0.04239 to 1.626
Adult M vs Early Pupa F	1,130	7,394	Yes	**	0.3386 to 1.922
Adult M vs Late Pupa F	0,3923	2,295	No	ns	-0.4929 to 1.277
Adult M vs Adult F	2,734	16,00	Yes	***	1.849 to 3.620
Early L3 Larva F vs Late L3 Larva F	-0,1594	1,043	No	ns	-0.9511 to 0.6323
Early L3 Larva F vs Early Pupa F	0,1368	0,8948	No	ns	-0.6549 to 0.9285
Early L3 Larva F vs Late Pupa F	-0,6012	3,518	No	ns	-1.486 to 0.2839
Early L3 Larva F vs Adult F	1,741	10,19	Yes	***	0.8558 to 2.626
Late L3 Larva F vs Early Pupa F	0,2962	1,937	No	ns	-0.4955 to 1.088
Late L3 Larva F vs Late Pupa F	-0,4418	2,585	No	ns	-1.327 to 0.4433
Late L3 Larva F vs Adult F	1,900	11,12	Yes	***	1.015 to 2.786
Early Pupa F vs Late Pupa F	-0,7380	4,318	No	ns	-1.623 to 0.1472
Early Pupa F vs Adult F	1,604	9,386	Yes	***	0.7191 to 2.489
Late Pupa F vs Adult F	2,342	12,51	Yes	***	1.373 to 3.312

FIG 20B			
Table Analyzed	One-way ANOVA data		
One-way analysis of variance			
P value	< 0.0001		
P value summary	***		
Are means signif. different? (P < 0.05)	Yes		
Number of groups	4		
F	97,91		
R square	0,9607		

ANOVA Table	SS	df	MS
Treatment (between columns)	19,09	3	6,364
Residual (within columns)	0,7801	12	0,06500
Total	19,87	15	

Tukey's Multiple Comparison Test	Mean Diff.	q	Significant? P < 0.05?	Summary	95% CI of diff
Whole F vs Sham F	-0,02506	0,1966	No	ns	-0.5604 to 0.5102
Whole F vs Ovaries only	0,2547	1,998	No	ns	-0.2806 to 0.7900
Whole F vs W/O ovaries	-2,434	19,09	Yes	***	-2.969 to -1.898
Sham F vs Ovaries only	0,2798	2,194	No	ns	-0.2555 to 0.8150
Sham F vs W/O ovaries	-2,408	18,89	Yes	***	-2.944 to -1.873
Ovaries only vs W/O ovaries	-2,688	21,09	Yes	***	-3.224 to -2.153

FIG 22A			
One-way analysis of variance			
P value	< 0.0001		
P value summary	***		
Are means signif. different? (P < 0.05)	Yes		
Number of groups	6		
F	85,8		
R square	0,9728		

ANOVA Table	SS	df	MS
Treatment (between columns)	13,03	5	2,607
Residual (within columns)	0,3646	12	0,03038
Total	13,4	17	

Tukey's Multiple Comparison Test	Mean Diff.	q	Significant? P < 0.05?	Summary	95% CI of diff
OR vs 33914/MTDG4	-2,441	24,26	Yes	***	-2.919 to -1.963
OR vs 33915/MTDG4	-0,7567	7,52	Yes	**	-1.235 to -0.2786
OR vs 57043/MTDG4	-0,4604	4,575	No	ns	-0.9385 to 0.01769
OR vs 33914/nosG4 (2)	0,08704	0,865	No	ns	-0.3911 to 0.5651
OR vs 33914/nosG4 (3)	-0,2982	2,963	No	ns	-0.7763 to 0.1799
33914/MTDG4 vs 33915/MTDG4	1,684	16,74	Yes	***	1.206 to 2.162
33914/MTDG4 vs 57043/MTDG4	1,981	19,68	Yes	***	1.503 to 2.459
33914/MTDG4 vs 33914/nosG4 (2)	2,528	25,12	Yes	***	2.050 to 3.006
33914/MTDG4 vs 33914/nosG4 (3)	2,143	21,29	Yes	***	1.665 to 2.621
33915/MTDG4 vs 57043/MTDG4	0,2963	2,944	No	ns	-0.1818 to 0.7744
33915/MTDG4 vs 33914/nosG4 (2)	0,8437	8,385	Yes	***	0.3657 to 1.322
33915/MTDG4 vs 33914/nosG4 (3)	0,4585	4,556	No	ns	-0.01957 to 0.9366
57043/MTDG4 vs 33914/nosG4 (2)	0,5474	5,44	Yes	*	0.06935 to 1.026
57043/MTDG4 vs 33914/nosG4 (3)	0,1622	1,612	No	ns	-0.3159 to 0.6403
33914/nosG4 (2) vs 33914/nosG4 (3)	-0,3852	3,828	No	ns	-0.8633 to 0.09287

FIG 22B					
One-way analysis of variance					
P value	< 0.0001				
P value summary	***				
Are means signif. different? (P < 0.05)	Yes				
Number of groups	3				
F	116,6				
R square	0,9709				
ANOVA Table	SS	df		MS	
Treatment (between columns)	13,04	2		6,522	
Residual (within columns)	0,3915	7		0,05593	
Total	13,44	9			
Tukey's Multiple Comparison Test	Mean Diff.	q	Significant? P < 0.05?	Summary	95% CI of diff
OR vs MTDGAL4 > Srl33914RNAi	-2,36	17,29	Yes	***	-2.929 to -1.791
OR vs MTDGAL4 > Srl33915RNAi	0,2177	1,704	No	ns	-0.3143 to 0.7496
MTDGAL4 > Srl33914RNAi vs MTDGAL4 > Srl33915RNAi	2,578	20,18	Yes	***	2.046 to 3.110

FIG 22C								
Two-way ANOVA	Ordinary							
Alpha	0,05							
Source of Variation	% of total variation	P value	P value summary	Significant?				
Interaction	20,69	<0.0001	****	Yes				
Row Factor	65,14	<0.0001	****	Yes				
Developmental Stage	11,32	<0.0001	****	Yes				
ANOVA table	SS (Type III)	DF	MS	F (DFn, DFd)	P value			
Interaction	33,68	2	16,84	F (2, 18) = 65.22	P<0.0001			
Row Factor	106	2	53,01	F (2, 18) = 205.3	P<0.0001			
Developmental Stage	18,43	1	18,43	F (1, 18) = 71.36	P<0.0001			
Residual	4,647	18	0,2582					
Difference between column means								
Predicted (LS) mean of 80minAEL	10,04							
Predicted (LS) mean of 160minAEL	11,79							
Difference between predicted means	-1,752							
SE of difference	0,2074							
95% CI of difference	-2.188 to -1.317							
Compare row means (main row effect)								
Number of families	1							
Number of comparisons per family	3							
Alpha	0,05							
Tukey's multiple comparisons test	Mean Diff.	95.00% CI of diff.	Significant?	Summary	Adjusted P Value			
OR vs. MTDGAL4 > srl33914RNAi	-4,211	-4.859 to -3.562	Yes	****	<0.0001			
OR vs. MTDGAL4 > srl33915RNAi	0,4607	-0.1878 to 1.109	No	ns	0,1936			
MTDGAL4 > srl33914RNAi vs. MTDGAL4 > srl33915RNAi	4,671	4.023 to 5.320	Yes	****	<0.0001			
Test details	Mean 1	Mean 2	Mean Diff.	SE of diff.	N1	N2	q	DF
OR vs. MTDGAL4 > srl33914RNAi	9,662	13,87	-4,211	0,2541	8	8	23,44	18
OR vs. MTDGAL4 > srl33915RNAi	9,662	9,201	0,4607	0,2541	8	8	2,564	18
MTDGAL4 > srl33914RNAi vs. MTDGAL4 > srl33915RNAi	13,87	9,201	4,671	0,2541	8	8	26	18
Compare cell means regardless of rows and columns								
Number of families	1							
Number of comparisons per family	15							
Alpha	0,05							
Tukey's multiple comparisons test	Mean Diff.	95.00% CI of diff.	Significant?	Summary	Adjusted P Value			

OR:80minAEL vs. OR:160minAEL	-2,541	-3.683 to -1.399	Yes	****	<0.0001		
OR:80minAEL vs. MTDGAL4 > srl33914RNAi:80minAEL	-6,212	-7.354 to -5.07	Yes	****	<0.0001		
OR:80minAEL vs. MTDGAL4 > srl33914RNAi:160minAEL	-4,75	-5.892 to -3.608	Yes	****	<0.0001		
OR:80minAEL vs. MTDGAL4 > srl33915RNAi:80minAEL	1,279	0.1376 to 2.421	Yes	*	0,0231		
OR:80minAEL vs. MTDGAL4 > srl33915RNAi:160minAEL	-2,899	-4.041 to -1.757	Yes	****	<0.0001		
OR:160minAEL vs. MTDGAL4 > srl33914RNAi:80minAEL	-3,671	-4.813 to -2.529	Yes	****	<0.0001		
OR:160minAEL vs. MTDGAL4 > srl33914RNAi:160minAEL	-2,209	-3.351 to -1.067	Yes	***	0,0001		
OR:160minAEL vs. MTDGAL4 > srl33915RNAi:80minAEL	3,82	2.678 to 4.962	Yes	****	<0.0001		
OR:160minAEL vs. MTDGAL4 > srl33915RNAi:160minAEL	-0,3581	-1.5 to 0.7837	No	ns	0,9131		
MTDGAL4 > srl33914RNAi:80minAEL vs. MTDGAL4 > srl33914RNAi:160minAEL	1,462	0.32 to 2.604	Yes	**	0,0080		
MTDGAL4 > srl33914RNAi:80minAEL vs. MTDGAL4 > srl33915RNAi:80minAEL	7,491	6.349 to 8.633	Yes	****	<0.0001		
MTDGAL4 > srl33914RNAi:80minAEL vs. MTDGAL4 > srl33915RNAi:160minAEL	3,313	2.171 to 4.455	Yes	****	<0.0001		
MTDGAL4 > srl33914RNAi:160minAEL vs. MTDGAL4 > srl33915RNAi:80minAEL	6,029	4.888 to 7.171	Yes	****	<0.0001		
MTDGAL4 > srl33914RNAi:160minAEL vs. MTDGAL4 > srl33915RNAi:160minAEL	1,851	0.7093 to 2.993	Yes	***	0,0008		
MTDGAL4 > srl33915RNAi:80minAEL vs. MTDGAL4 > srl33915RNAi:160minAEL	-4,178	-5.32 to -3.036	Yes	****	<0.0001		

Test details	Mean 1	Mean 2	Mean Diff.	SE of diff.	N1	N2	q	DF
OR:80minAEL vs. OR:160minAEL	8,391	10,93	-2,541	0,3593	4	4	10	18
OR:80minAEL vs. MTDGAL4 > srl33914RNAi:80minAEL	8,391	14,6	-6,212	0,3593	4	4	24,45	18
OR:80minAEL vs. MTDGAL4 > srl33914RNAi:160minAEL	8,391	13,14	-4,75	0,3593	4	4	18,7	18
OR:80minAEL vs. MTDGAL4 > srl33915RNAi:80minAEL	8,391	7,112	1,279	0,3593	4	4	5,036	18
OR:80minAEL vs. MTDGAL4 > srl33915RNAi:160minAEL	8,391	11,29	-2,899	0,3593	4	4	11,41	18
OR:160minAEL vs. MTDGAL4 > srl33914RNAi:80minAEL	10,93	14,6	-3,671	0,3593	4	4	14,45	18
OR:160minAEL vs. MTDGAL4 > srl33914RNAi:160minAEL	10,93	13,14	-2,209	0,3593	4	4	8,696	18
OR:160minAEL vs. MTDGAL4 > srl33915RNAi:80minAEL	10,93	7,112	3,82	0,3593	4	4	15,04	18
OR:160minAEL vs. MTDGAL4 > srl33915RNAi:160minAEL	10,93	11,29	-0,3581	0,3593	4	4	1,41	18
MTDGAL4 > srl33914RNAi:80minAEL vs. MTDGAL4 > srl33914RNAi:160minAEL	14,6	13,14	1,462	0,3593	4	4	5,754	18
MTDGAL4 > srl33914RNAi:80minAEL vs. MTDGAL4 > srl33915RNAi:80minAEL	14,6	7,112	7,491	0,3593	4	4	29,49	18
MTDGAL4 > srl33914RNAi:80minAEL vs. MTDGAL4 > srl33915RNAi:160minAEL	14,6	11,29	3,313	0,3593	4	4	13,04	18
MTDGAL4 > srl33914RNAi:160minAEL vs. MTDGAL4 > srl33915RNAi:80minAEL	13,14	7,112	6,029	0,3593	4	4	23,73	18
MTDGAL4 > srl33914RNAi:160minAEL vs. MTDGAL4 > srl33915RNAi:160minAEL	13,14	11,29	1,851	0,3593	4	4	7,286	18
MTDGAL4 > srl33915RNAi:80minAEL vs. MTDGAL4 > srl33915RNAi:160minAEL	7,112	11,29	-4,178	0,3593	4	4	16,45	18

FIG 22D							
ANOVA summary							
F	266,8						
P value	<0.0001						
P value summary	****						
Significant diff. among means (P < 0.05)?	Yes						
R square	0,9081						
Brown-Forsythe test							
F (DFn, DFd)	6.352 (2, 54)						
P value	0,0033						
P value summary	**						
Are SDs significantly different (P < 0.05)?	Yes						
Bartlett's test							
Bartlett's statistic (corrected)	20,96						
P value	<0.0001						
P value summary	****						
Are SDs significantly different (P < 0.05)?	Yes						
ANOVA table	SS	DF	MS	F (DFn, DFd)	P value		
Treatment (between columns)	78511	2	39255	F (2, 54) = 266.8	P<0.0001		
Residual (within columns)	7946	54	147,1				
Total	86457	56					
Data summary							
Number of treatments (columns)	3						
Number of values (total)	57						
Number of families	1						
Number of comparisons per family	3						
Alpha	0,05						
Tukey's multiple comparisons test	Mean Diff.	95.00% CI of diff.	Significant?	Summary	Adjusted P Value		
OR vs. MTDGAL4 > 33914	63,97	54.32 to 73.61	Yes	****	<0.0001	A-B	
OR vs. MTDGAL4 > 33915	-21,56	-31.20 to -11.91	Yes	****	<0.0001	A-C	
MTDGAL4 > 33914 vs. MTDGAL4 > 33915	-85,53	-94.77 to -76.28	Yes	****	<0.0001	B-C	
Test details	Mean 1	Mean 2	Mean Diff.	SE of diff.	n1	n2	q	DF
OR vs. MTDGAL4 > 33914	70,75	6,777	63,97	4,002	17	20	22,61	54
OR vs. MTDGAL4 > 33915	70,75	92,3	-21,56	4,002	17	20	7,619	54
MTDGAL4 > 33914 vs. MTDGAL4 > 33915	6,777	92,3	-85,53	3,836	20	20	31,53	54

FIG 31					
Table Analyzed	Two-way ANOVA , not RM				
Two-way ANOVA	Ordinary				
Alpha	0,05				
Source of Variation	% of total variation	P value	P value summary	Significant?	
Interaction	5,812	0,1377	ns	No	
Genotype	4,804	0,0586	ns	No	
Development time	68,84	<0.0001	****	Yes	
ANOVA table	SS	DF	MS	F (DFn, DFd)	P value
Interaction	1966251	4	491563	F (4, 27) = 1.909	P=0.1377
Genotype	1625196	2	812598	F (2, 27) = 3.156	P=0.0586
Development time	23287718	2	11643859	F (2, 27) = 45.23	P<0.0001
Residual	6950988	27	257444		
Number of missing values	0				
Compare column means (main column effect)					
Number of families	1				
Number of comparisons per family	3				
Tukey's multiple comparisons test	Mean Diff.	95.00% CI of diff.	Significant?	Summary	Adjusted P Value
Ovaries vs. Embryos 80 min	-1824	-2338 to -1311	Yes	****	<0.0001
Embryos 80 min vs. Embryos 160 min	1557	1043 to 2070	Yes	****	<0.0001

PUBLICATIONS

PUBLICATION
I

Mitochondrial dysfunction plus high-sugar diet provokes a metabolic crisis that inhibits growth

Esko Kemppainen, Jack George, Görkem Garipler, Tea Tuomela, Essi Kiviranta, Tomoyoshi Soga, Cory D. Dunn, Howard T. Jacobs

Mitochondrial Dysfunction Plus High-Sugar Diet Provokes a Metabolic Crisis That Inhibits Growth

Esko Kemppainen[1], Jack George[1], Görkem Garipler[1,2¤], Tea Tuomela[1], Essi Kiviranta[1], Tomoyoshi Soga[3], Cory D. Dunn[2], Howard T. Jacobs[1,4]*

1 BioMediTech and Tampere University Hospital, FI-33014, University of Tampere, Tampere, Finland,
2 Department of Molecular Biology and Genetics, Koç University, Sariyer, Istanbul, 34450, Turkey,
3 Institute for Advanced Biosciences, Keio University, Tsuruoka, Yamagata, 997–0035, Japan, **4** Institute of Biotechnology, FI-00014, University of Helsinki, Helsinki, Finland

¤ Current address: Department of Biology, New York University, New York, NY, 10003, United States of America
* howard.jacobs@helsinki.fi

Abstract

The *Drosophila* mutant *tko*^{25t} exhibits a deficiency of mitochondrial protein synthesis, leading to a global insufficiency of respiration and oxidative phosphorylation. This entrains an organismal phenotype of developmental delay and sensitivity to seizures induced by mechanical stress. We found that the mutant phenotype is exacerbated in a dose-dependent fashion by high dietary sugar levels. *tko*^{25t} larvae were found to exhibit severe metabolic abnormalities that were further accentuated by high-sugar diet. These include elevated pyruvate and lactate, decreased ATP and NADPH. Dietary pyruvate or lactate supplementation phenocopied the effects of high sugar. Based on tissue-specific rescue, the crucial tissue in which this metabolic crisis initiates is the gut. It is accompanied by down-regulation of the apparatus of cytosolic protein synthesis and secretion at both the RNA and post-translational levels, including a novel regulation of S6 kinase at the protein level.

Introduction

Mitochondrial DNA encodes just 13 polypeptides in most metazoans, representing a small but vital subset of the subunits of the apparatus of oxidative phosphorylation (OXPHOS). In addition it encodes the RNA components, i.e. 2 rRNAs and 22 tRNAs, that contribute to the separate machinery of protein synthesis inside mitochondria, that generates these polypeptides. Defects in mitochondrial protein synthesis are a frequent primary cause of mitochondrial disease: see reviews [1, 2]. Their genetic origin can be either nuclear or mitochondrial, and they may affect mitochondrial rRNAs, tRNAs, ribosomal proteins, translation factors, aminoacyl-tRNA synthetases, tRNA modifying enzymes or other accessory factors. They can show a wide range of tissue-specific symptoms that remains largely unexplained, varying dramatically also in severity and age of onset. Whilst the consequences of the primary molecular defect may be clear at the level of the translational machinery, the link to pathogenesis is poorly understood.

It is assumed to have metabolic, cellular, physiological and developmental dimensions, the elucidation of which requires well-controlled studies in appropriate model systems.

Our analyses have focused on a *Drosophila* model of mitochondrial disease (*tko*[25t]) [3] in which a nuclear mis-sense mutation in the gene for mitoribosomal protein S12 [4] gives rise to a quantitative defect in mitochondrial protein synthesis [5] impacting all four OXPHOS enzyme complexes dependent on mitochondrial translation products [6]. The molecular phenotype of *tko*[25t] resembles that seen in human disorders resulting from point mutations in proteins of the mitoribosomal small subunit, including MRPS16 [7] and MRPS22 [8]. At organismal level the *tko*[25t] mutation gives rise to a complex developmental and behavioral phenotype, whose main features are larval developmental delay and susceptibility to paralytic seizures induced by mechanical shock, described as bang-sensitivity [6]. *tko*[25t] adults show an altered pattern of gene expression [9] that suggests a transformation of metabolism to accommodate the OXPHOS defect engendered by the mutation. Specifically, there is up-regulation of lactate dehydrogenase and of enzymes involved in the dietary mobilization and catabolism of protein and fat that suggest a switch to glycolysis for ATP production and to other substrates for the supply of carbon skeletons for biosynthesis.

The phenotype of developmental delay and bang-sensitivity, as well as the main (bisexual) changes in gene expression in adults, are shared with the mutant strain *sesB*[1] [10], carrying a point mutation in the gene encoding the major isoform of the adenine nucleotide translocase [11]. Since the *sesB*[1] mutation limits the supply of mitochondrially supplied ATP to the cell, we infer that these common features are the signature of defective OXPHOS in *Drosophila*. Furthermore, the *tko*[25t] phenotype is not alleviated by expression of the non proton-motive alternative oxidase AOX from *Ciona intestinalis*, nor by the non proton-motive alternative NADH dehydrogenase Ndi1 from yeast [12], despite the fact that AOX and Ndi1 can partially compensate for the specific phenotypes produced by knockdown of subunits of OXPHOS complexes IV and I, respectively [9, 13, 14]. This supports the idea that the developmental phenotype of *tko*[25t] results primarily from insufficient mitochondrial ATP production, rather than disturbed redox homeostasis.

The *tko*[25t] phenotype can be partially alleviated by genetic suppressors in either nuclear or mitochondrial DNA [15, 16], which appear to increase the supply of mitochondrial translation products above a certain threshold. These findings suggested that we might also be able to manipulate the phenotype environmentally, by culturing the flies on media containing a different balance of dietary components. Specifically, we reasoned that media rich in sugars should support glycolysis and thus alleviate the mutant phenotype. If successful this could suggest a potential route to dietary management of patients with mitochondrial disease, particularly those with a global impairment of mitochondrial protein synthesis and thus of OXPHOS.

Surprisingly we found an opposite effect, namely that the *tko*[25t] phenotype was exacerbated by sugar-rich media. Analysis of metabolite levels, gene expression, drug sensitivity and the status of proteins known to be involved in growth regulation and metabolite sensing has allowed us to construct a profile of the metabolic changes produced by the combination of mitochondrial dysfunction and high sugar diet, and a mechanistic model for how this leads to severe growth impairment. This knowledge has broad implications for understanding disease processes and their relation to diet.

Results

High-sugar diet exacerbates the growth-retardation of flies with mitochondrial dysfunction

In order to test whether sugar supplementation would mitigate the developmental retardation fsof *tko*[25t] flies, we cultured flies on different media containing a standard yeast composition
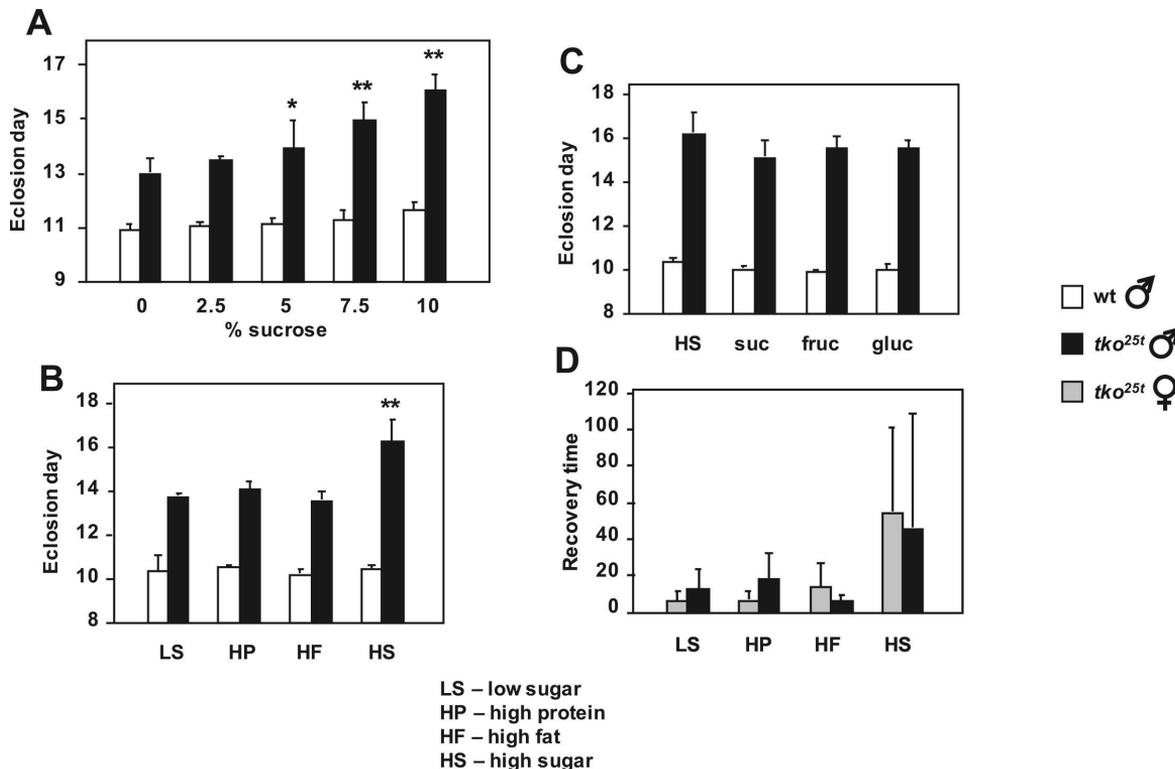
Fig 1. Modulation of *tko*[25t] phenotype by diet. (A-C) Time to eclosion and (D) recovery time from mechanical shock (bang-sensitivity) of *tko*[25t] and wild-type flies grown on media of the indicated composition (see SI for details). In (A) asterisks denote data classes significantly different from flies of the same genotype grown on 0% sucrose medium (Student's *t* test, * showing $p < 0.05$, ** showing $p < 0.01$). In (B) asterisks (**) denote significant difference from flies of the same genotype grown on all other media tested (Student's *t* test, $p < 0.01$), which were not significantly different from each other. In (C) there were no significant differences from flies of the same genotype, grown on other media (Student's *t* test, $p > 0.05$). In all experiments eclosion times for *tko*[25t] flies were also significantly different from those of wild-type flies grown on the same medium (Student's *t* test, $p < 0.01$). In (D), the wide variance inherent to the phenotype precludes a standard statistical analysis. For corresponding eclosion data of females see Panel A in S1 Fig.

doi:10.1371/journal.pone.0145836.g001

(3.5% dried yeast, w/v), but increasing amounts of sucrose. Surprisingly, whilst the wild-type control strain was only minimally affected by the amount of sugar in the food, *tko*[25t] flies developed more slowly on media with increasing sucrose concentration (Fig 1A and Panel A in S1 Fig). Males (Fig 1A) and females (Panel A in S1 Fig) were similarly affected, and the highest sucrose concentration tested (10%) doubled the developmental delay from ~2 to ~4 days at 25°C.

Because the high-sugar diets tested contain a higher caloric content than the low-sugar diets, we next tested isocaloric diets in which sugar was replaced with additional protein or fat (or a mixture). Once again, high-sugar diet exacerbated the developmental delay of *tko*[25t] flies, but the proportion of fat and protein as substitute calories made no difference, and the two sexes behaved similarly (Fig 1B and Panel C in S1 Fig). Wild-type flies developed similarly on all diets tested. The specific sugar present in the food was also immaterial: there was no significant difference in the developmental delay of *tko*[25t] flies grown on diets containing only sucrose, fructose or glucose, compared with the standard mixed-sugar diet (Fig 1C and Panel

D in S1 Fig). The bang-sensitivity of tko^{25t} adults of both sexes was also alleviated by development on diets containing lower sugar content (Fig 1D). Wild-type flies were not bang-sensitive on any diet tested.

Fly larvae with mitochondrial dysfunction exhibit a global anti-sugar response

In previous transcriptomic analyses [9] we noted that tko^{25t} adults manifested altered expression of some specific sugar transporters in the gut and Malpighian tubule (the equivalent of the mammalian kidney). Because of the unexpected observation that excess sugar is deleterious to tko^{25t} adults, we analyzed the expression of these genes, for clues to the mechanisms of sugar-responsiveness of tko^{25t}.

QRTPCR was used to profile the expression of two sets of relevant genes, in both adults and in larvae, the life-cycle stage when the growth defect manifests in tko^{25t} [6]. We first analyzed a set of Malpighian tubule transporters proposed to be involved in the excretion of excess sugar [17]. Their expression was consistently elevated in tko^{25t}, both in L3 larvae (Fig 2A) and adults (Panel A in S2 Fig), typically 3–4 fold. The most prominently expressed of these mRNAs, CG7882 and CG3285, were also tested for responsiveness to dietary sugar at larval stage. In both genotypes, their expression was elevated 2–3 fold on high-sugar compared with zero-sugar food (Fig 2C). Next we analyzed a set of α-glucosidases specific to, or highly enriched in the gut, and putatively involved in the mobilization of dietary sugars, using a similar approach. In both larvae (Fig 2B) and adults (Panel B in S2 Fig), these were down-regulated in tko^{25t}. A prominently expressed representative of the set, CG9468, was further down-regulated by high-sugar diet in both genotypes (Fig 2D).

To understand the context of these changes in gene expression, we measured the total serum sugar concentration of tko^{25t} and control larvae grown on high-sugar versus zero-sugar media. tko^{25t} larvae had significantly lower levels of total serum sugars than wild-type larvae grown on the same medium. However, larvae cultured on high-sugar food had higher serum sugar levels than those of the same genotype grown on zero-sugar food (Fig 2E). tko^{25t} larvae also exhibited a lower rate of food consumption than control flies on the corresponding diet (Fig 2F), though on zero-sugar diet, where they grew faster, they paradoxically consumed less food than on high-sugar diet. In all these aspects, the phenotype of tko^{25t} larvae is consistent with a physiological strategy to minimize the amount of glucose, despite the initially presumed reliance on glycolysis.

Metabolic derangement of fly larvae with mitochondrial dysfunction is exacerbated by high-sugar diet

The previous findings of up-regulation of lactate dehydrogenase (LDH) expression in tko^{25t} adults [9] implied the use of LDH as an alternative pathway to regenerate NAD+, under conditions where mitochondrial respiration is limiting. We hypothesized that the resulting accumulation of lactate and/or the diversion of pyruvate from mitochondria may contribute to metabolic disturbance in tko^{25t}, and underlie aspects of the mutant phenotype and its exacerbation by high-sugar diet. We therefore analyzed lactate and pyruvate levels in L3 larvae. The steady-state levels of both metabolites were found to be 2–3 fold elevated in tko^{25t} larvae compared with the wild-type control strain, when grown on either high- or zero-sugar medium (Fig 3A). When grown on high-sugar, this elevation was even more pronounced, at least for lactate, although the differences were at the border of significance. Serum lactate was also 4–5 fold elevated in tko^{25t} larvae (Fig 3A), and elevated lactate was maintained in adults (Panel A in S3 Fig).
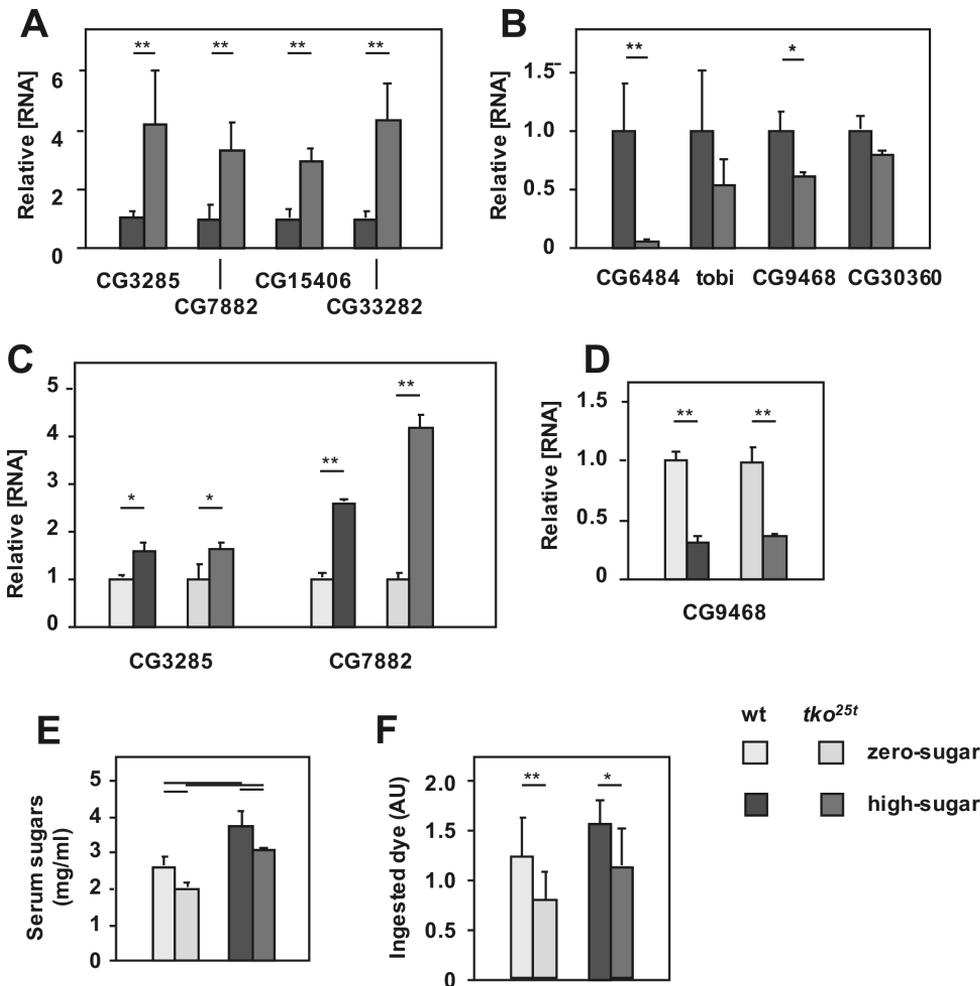
Fig 2. *tko²⁵ᵗ* flies manifest an 'anti-sugar' response. (A-D) Expression levels of various genes, based on QRTPCR, in L3 larvae of the indicated genotypes and growth conditions. (A, C) Malpighian tubule-specific sugar transporters, (B, D) gut-specific α-glucosidases; (A, B) all signals normalized to the levels in wild-type larvae, (C, D) all signals normalized to larvae of the same genotype grown on zero-sugar medium (i.e., ignoring the differences between genotypes). All values are significantly different between genotypes or diets, as plotted (Student's *t* test, *p* < 0.01). (E) Total serum sugar concentrations in larvae of the indicated genotypes and growth conditions. Horizontal bars denote significantly different data classes (Student's *t* test, *p* < 0.01). (F) Larval feeding rate, based on dye ingestion assay, in larvae of the indicated genotypes and growth conditions. Horizontal bars denote significantly different data classes (Student's *t* test, * showing *p* < 0.05, ** showing *p* < 0.01).

doi:10.1371/journal.pone.0145836.g002

Using mass-spectrometry (S1 Table) to gain a more complete insight into the metabolic abnormalities of *tko²⁵ᵗ* larvae, we observed a substantial ATP depletion (Fig 3B), as seen also in adults (Panel A in S3 Fig) [9]. ATP levels were decreased in high-sugar diet in both *tko²⁵ᵗ* and wild-type larvae, compounding the effects of genotype. NAD⁺ and NADH levels were only slightly altered by the *tko²⁵ᵗ* mutation or by diet (Fig 3C), but we observed a striking abnormality in the level of NADPH and the NADPH/NADP⁺ ratio (Fig 3C). In most physiological
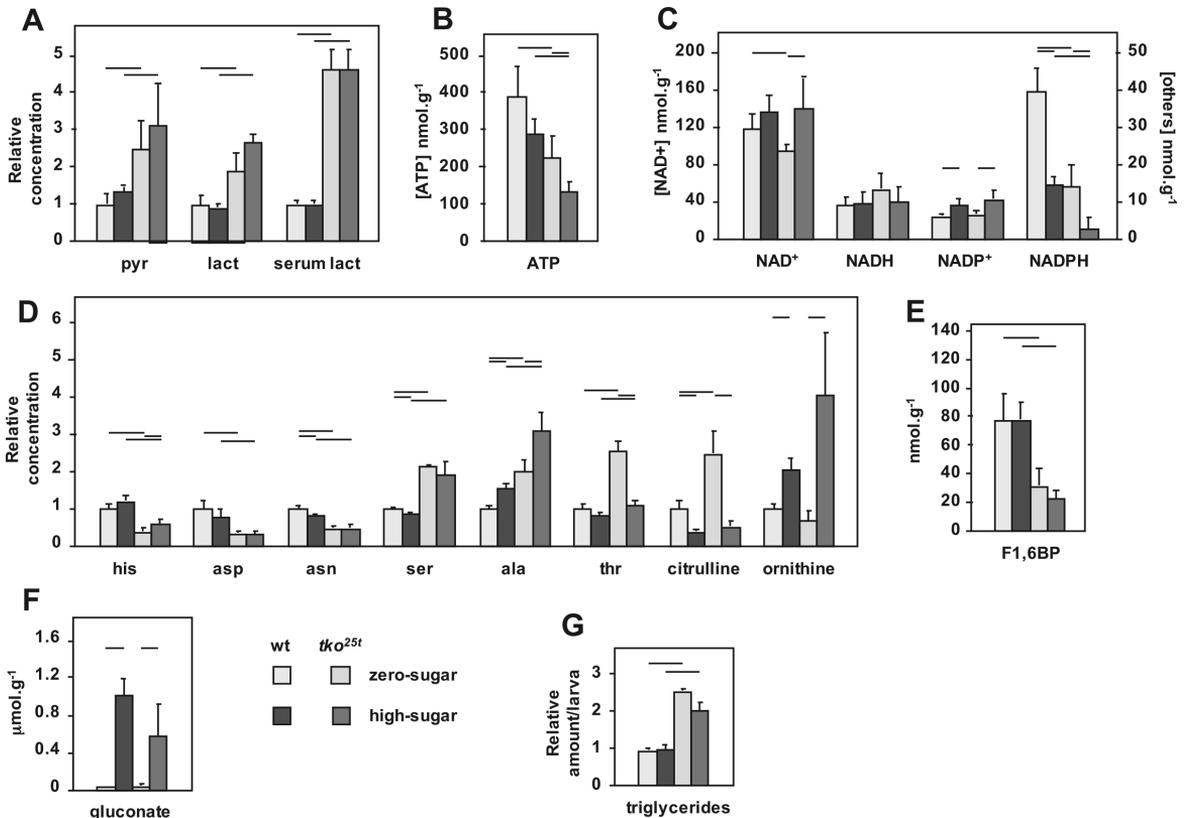
Fig 3. Metabolites showing substantial changes in *tko^{25t}* larvae. Relative levels of different metabolites in L3 larvae of the indicated genotypes and growth conditions, based on (A, B) findings from enzyme-linked assays or (C-F) mass spectrometry. Absolute values are shown for (B) ATP, (C) NAD+ and derivatives, (E) fructose 1,6-biphosphate (F1,6BP) and (F) gluconate, Values for (A) pyruvate, lactate and (D) amino acids are normalized to those for wild-type flies grown on ZS medium, enabling them to be plotted alongside for comparison. Relevant absolute values are given in S1 Table. Horizontal bars denote significantly different data classes (Student's *t* test, *p* < 0.05). See S7 Table for fuller statistical analysis of metabolite levels. (G) Triglyceride levels in L3 larvae of the indicated genotype and growth conditions, normalized to the value for wild-type larvae grown on zero-sugar medium. Horizontal bars denote significantly different data classes (Student's *t* test, *p* < 0.05). Note that we did not observe increased triglyceride levels when larvae were grown on high-sugar medium.

doi:10.1371/journal.pone.0145836.g003

contexts, there is substantially more NADPH than NADP$^+$, which was the case in control larvae grown on zero-sugar diet. The NADPH/NADP$^+$ ratio was decreased both by high-sugar diet and by the presence of the *tko^{25t}* mutation. The effects of genotype and diet were again additive, so that in *tko^{25t}* larvae grown in high-sugar the ratio was reversed. In two of the four samples analyzed, NADPH was below the detection limit in mutant larvae grown on high sugar (S1 Table). *tko^{25t}* larvae also showed altered levels of some amino acids (Panel C in S3 Fig), notably a deficiency of histidine, aspartic acid and asparagine (Fig 3D), and elevated levels of serine, alanine (especially on high-sugar) and threonine (only on zero-sugar). Two other amino acid changes in *tko^{25t}* that differed between diets were of citrulline and ornithine (Fig 3D), amino acids implicated in growth regulation by virtue of their role in polyamine biosynthesis. Polyamines did show alterations in *tko^{25t}* (Panel D in S3 Fig), but the effect was the

same, regardless of diet, whereas wild-type larvae showed clear increases in polyamine levels when grown on high sugar. Note that *Drosophila* has only an incomplete urea cycle, though urea was also greatly decreased in tko^{25t} larvae (S1 Table).

In addition to elevated pyruvate and lactate, we noted substantial alterations in the level of two other glucose metabolites: the glycolytic intermediate fructose 1,6-biphospate, threefold decreased in tko^{25t} larvae regardless of diet (Fig 3E), and the glucose oxidation end-product gluconate, >10-fold elevated on high-sugar diet irrespective of genotype (Fig 3F).

Finally, tko^{25t} larvae also showed a substantial triglyceride (TAG) accumulation not seen in control larvae (Fig 3G).

Lactate and pyruvate accumulation contribute to growth retardation and NADPH depletion in larvae with mitochondrial dysfunction

We reasoned that the high levels of lactate and pyruvate seen in tko^{25t} larvae may limit flux through glycolysis, potentially accounting for a relative deficiency of ATP in animals largely dependent on glycolysis for ATP production. We therefore tested the effects of adding pyruvate or lactate to the culture medium. Lactate or pyruvate at 25 mg/ml, when added to zero-sugar food, increased the developmental delay of tko^{25t} flies by 1–2 days, partially phenocopying the effect of high-sugar diet (Fig 4A and Panel A in S4 Fig). The supplements also retarded the development of control flies. However, when added to high-sugar diet, they had only a minimal effect.

Next we considered whether the large changes in NADPH, which also correlated with the severity of the mutant phenotype on different diets, might also be influenced by excessive lactate and pyruvate. NADPH is required to drive biosynthetic reactions, notably fatty acid synthesis, but is also needed to maintain redox homeostasis. It is mainly produced by five 'workhorse' enzymes of catabolism (Panel B of S4 Fig), also linked to the provision of carbon skeletons for biosynthesis. We therefore measured the activity of these enzymes in extracts from tko^{25t} and control larvae, and the effects on their activities of the high levels of lactate and pyruvate, as well as gluconate. The maximal activities of the NADPH-producing enzymes were broadly similar in extracts from tko^{25t} and control larvae (Panel C in S4 Fig). However, when we added lactate or pyruvate at the high concentrations observed in tko^{25t} larvae grown in high sugar, we saw inhibition of three of the enzymes that contribute substantially to NADPH production (Fig 4B). The degree of inhibition of malic enzyme by pyruvate may be an under-estimate, since the *in vitro* assay is conducted in substrate excess, whereas *in vivo* the high levels of pyruvate should decrease throughput to very low levels, via product inhibition. Gluconate also had a minor effect on NADP-linked IDH activity. Taking account of the likely inhibition of malic enzyme *in vivo*, and assuming that the effects of the tested metabolites on the other enzymes are additive, this could partially explain NADPH depletion in tko^{25t} larvae.

Further down-regulation of malic enzyme by RNAi produced no significant worsening of the developmental delay, and might even have slightly alleviated it (Fig 4C), whilst effects on wild-type (tko^{25t} heterozygous) flies were minimal. A similar experiment to test for toxic effects of gluconate (or the failure to detoxify glucose), by down-regulating glucose dehydrogenase (Gld), could not be meaningfully executed, since global RNAi against Gld was developmentally lethal to both wild-type and tko^{25t} flies, as is the null mutant [18]. However, advanced glycation end-products did not accumulate in larvae grown on high-sugar diet (Panel B in S3 Fig), indicating that they cannot account for the deleterious effects of high-sugar diet on tko^{25t}. However, as discussed below, the accumulation of gluconate in larvae grown on high-sugar medium implies a mechanism for the additional depletion of NADPH resulting from diet.

The disturbed amino acid levels in tko^{25t} larvae (Fig 3D) prompted us to consider whether a dietary deficiency or excess of amino acids might underlie aspects of the phenotype. To test
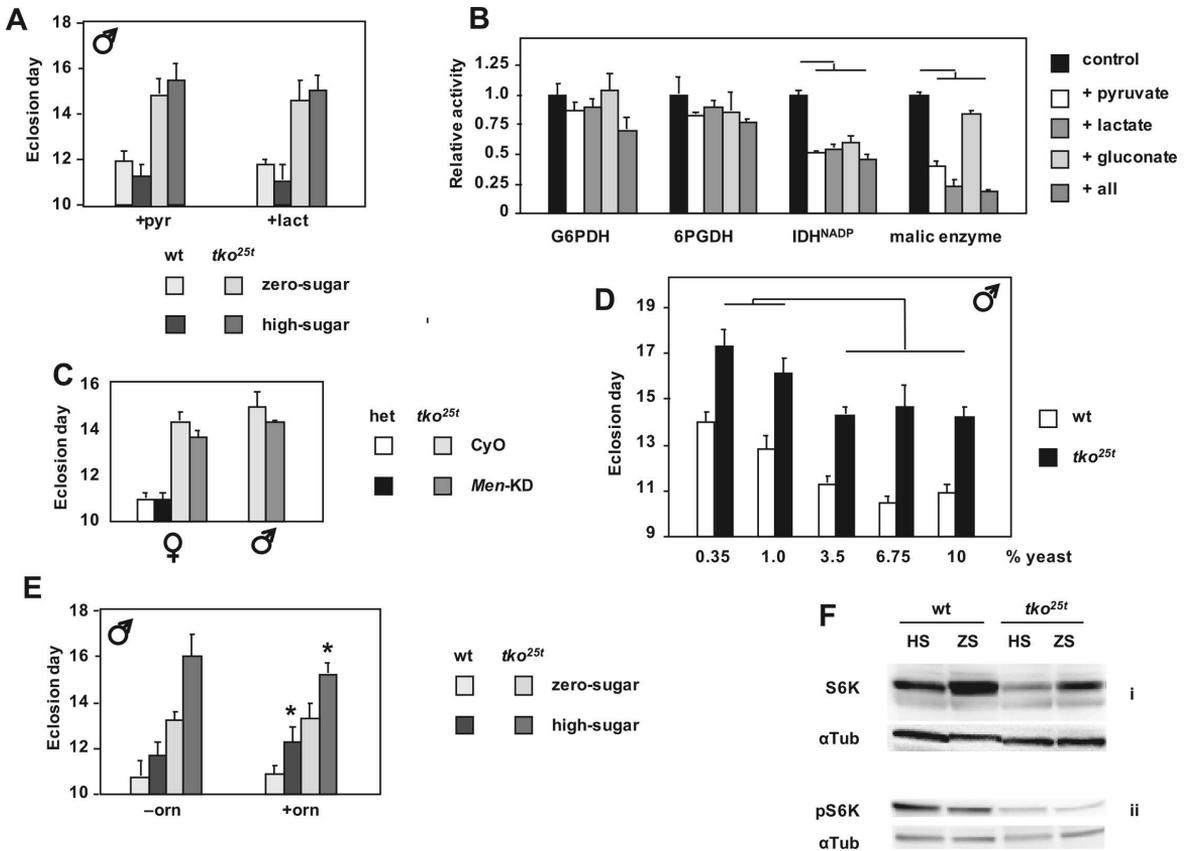
Fig 4. Metabolic phenotype of *tko*[25t] and its modulation. (A) Time to eclosion of male flies of the indicated genotypes and growth conditions, on medium supplemented with pyruvate (pyr) or lactate (lact). In the presence of either supplement there were no significant difference in eclosion timing between *tko*[25t] flies grown in high-sugar versus zero-sugar medium (Student's *t* test, *p* > 0.05). See also Panel A in S4 Fig. (B) Effect on maximal activities of NADPH-producing enzymes from *Drosophila*, of the presence of excess amounts the indicated metabolites (all = pyruvate, lactate and gluconate together). For comparison, all such activities are normalized to those without any additions. Horizontal bars denote values significantly different from control (Student's *t* test, *p* < 0.01). (C) Time to eclosion of flies of the indicated sex, genotype and growth conditions. het–flies heterozygous for *tko*[25t] (which is recessive) and the FM7 balancer chromosome. Progeny carried either the CyO balancer chromosome marker or the RNAi construct for malic enzyme (*Men*-KD). (D) Time to eclosion of *tko*[25t] and wild-type flies grown on media of the indicated composition (see S1 File for details). Horizontal lines indicate significant differences between data classes on different media, for a given genotype (Student's *t* test, *p* < 0.05). On all media tested, eclosion times for *tko*[25t] flies were also significantly different from those of wild-type flies grown on the same medium (Student's *t* test, *p* < 0.01). For corresponding eclosion data of females see Panel B of S1 Fig. (E) Time to eclosion of male flies of the indicated genotypes and dietary conditions, on medium supplemented (or not) with ornithine (orn), as shown. * denotes value significantly different than for flies of the corresponding genotype and dietary condition, with ornithine *versus* to without the supplement (Student's *t* test, *p* < 0.05). (F) Western blots of extracts from L3 larvae of the indicated genotypes and dietary conditions, probed for S6K or pS6K (phosphorylated at Thr-398) and the α-tubulin loading control (αTub). See also Panel F in S4 Fig.

doi:10.1371/journal.pone.0145836.g004

this, we cultured flies on media containing a variable amount of yeast, the major source of dietary protein, but a fixed sucrose concentration at (7.5%). Varying the amount of yeast produced no change in the developmental delay of *tko*[25t] flies (Fig 4D and Panel B in S1 Fig). Above a threshold level of 3.75%, yeast supplementation had no further effect on either *tko*[25t] or control flies. At lower yeast concentrations, both were retarded further, but to the same extent, with males (Fig 4D) and females (Panel B in S1 Fig) affected similarly. Similarly, high-protein diet

had no detrimental effect on flies grown on low-sugar ([Fig 1C](#) and Panels C-E in [S1 Fig](#)), and might even have had a slightly beneficial effect in the zero-sugar medium. Dietary supplementation with ornithine, found at unusually high levels in tko^{25t} larvae grown on high-sugar diet, had only very minor effects ([Fig 4E](#) and Panels D and E in [S4 Fig](#)).

Growth inhibition in flies with mitochondrial dysfunction is associated with modulation of S6K

Since the developmental outcome in tko^{25t} is still a viable fly, its developmental delay must be the result of a coordinated signaling process with most likely both an intracellular and an endocrine component. In order to determine the molecular mechanism restraining growth in tko^{25t} larvae on different diets, we interrogated the status of major signaling pathways already known to be involved in growth regulation. The best characterized such pathway responding to intracellular energy status is that of AMPK [19]. ATP depletion against a constant level of AMP, as documented in tko^{25t} larvae, should lead to activation of AMPK by phosphorylation at Thr-172 (human numbering), which then down-regulates many downstream growth-related functions. Western blotting using AMPK-specific antibodies, revealed increased levels of phosphorylated AMPK in tko^{25t} compared to wild-type larvae (Panel F, sub-panels i and ii in [S4 Fig](#)) which was further enhanced on high-sugar diet, although none of these changes was dramatic. The best-characterized response pathway to extracellular signals, including diet and insulin/insulin-like growth factor signaling (IIS), involves the kinase Akt, whose activation by phosphorylation at serine-505 has a growth-promoting readout that also facilitates glucose-related metabolism [20]. Accordingly, growth of wild-type larvae on high-sugar diet led to a modest increase in the phosphorylated form of Akt (Panel F, sub-panels iii and iv in [S4 Fig](#),) which, taking account of the loading control, appeared to be partially abrogated in tko^{25t}. The Akt and AMPK pathways converge on mTOR, the key regulator of cytosolic protein synthesis and growth, whose canonical readout is the phosphoryation status of S6K [21]. Consistent with this, we observed a decreased amount of the isoform of S6K phosphorylated at Thr-398 (one of the mTOR target sites) in tko^{25t} compared with wild-type larvae, although in both genotypes the level of this isoform appeared marginally higher on high-sugar than zero-sugar diet ([Fig 4F](#), panels ii). More strikingly, we observed a substantial decrease in total S6K in tko^{25t} larvae, specifically on high-sugar diet ([Fig 4F](#), panels i; biological replicates in Panel F, sub-panels v and vi in [S4 Fig](#)). Analysis, by QRTPCR, of mRNA levels of the major insulin-like peptides expressed in larvae, showed a consistent, but quantitatively minor up-regulation in tko^{25t} (Panel G in [S4 Fig](#); see also [S2 Table](#)).

Cystolic protein synthesis and secretion are key targets of the metabolic crisis caused by mitochondrial dysfunction on high-sugar diet

Analysis of gene expression at the RNA level by global RNA sequencing revealed systematic and diet-dependent changes in tko^{25t} larvae that can be construed as a combined readout from metabolic disturbance and decreased growth-signaling. We analyzed the data in two ways: firstly, according to the largest proportionate changes, and secondly, the largest absolute changes, ([S3 Table](#) and [S4 Table](#), respectively). We also analyzed separately the changes in protein-coding genes (Sheets A and C of [S3 Table](#) and Sheets A and C of [S4 Table](#)) and non-coding RNAs (Sheets B and D of [S3 Table](#) and Sheets B and D of [S4 Table](#)), and executed all comparisons both by genotype (Sheets A and B of [S3 Table](#) and Sheets A and B of [S4 Table](#)) and by diet (Sheets C and D of [S3 Table](#) and Sheets C and D of [S4 Table](#): see also the full, unselected data in [S2 Table](#)). The following summary conclusions emerge.

As regards the non-coding RNAs, despite some striking changes in abundance, very few of them are functionally assigned at this time, and thus cannot be assessed further. The largest absolute changes in protein-coding genes were seen mostly in those which were already highly expressed, and fell into well-defined functional classes. Wild-type larvae on high-sugar diet, compared with those grown on zero-sugar diet (Sheet C in S3 Table), showed strong induction of genes connected with cytosolic translation, glycolysis, the structural proteins of muscle and the larval cuticle, whist the most strikingly down-regulated genes were gut-specific, and connected with digestive functions, including proteases, lipases, lysozymes, components of the peritrophic membrane and other chitin-binding proteins. In contrast, the vast majority of these genes were either less responsive, unaltered or even oppositely regulated by high-sugar diet in tko^{25t} larvae, where digestive functions were amongst the most prominently up-regulated genes. Comparing tko^{25t} with wild-type larvae (Sheet A in S3 Table), mitochondrial transcripts were down-regulated on both diets, whilst the most striking differences on high-sugar diet were those already indicated above. Intriguingly, whilst many cytosolic translational components were down-regulated in tko^{25t} on high sugar, one that was up-regulated was the inhibitory factor Thor (4E-BP). Many of the genes showing the largest proportionate changes remain functionally unassigned, but genotype-specific changes were rather similar on the two diets (Sheet A in S3 Table), whereas diet-specific changes (Sheet C in S3 Table) were largely different between the two genotypes. One of the most highly induced genes in tko^{25t} larvae irrespective of diet was p24-2, whose mRNA was induced over 1000-fold compared with its level in control larvae. p24-2 is one of two fly homologues of yeast p24, a protein required for vesicle trafficking in the secretory pathway. Up-regulation of p24-2 suggests ER stress, but we saw no changes in the level or splicing pattern of Xbp1 RNA (Panels H and I in S4 Fig), considered a marker for the induction of the classic ER stress response. Other prominent changes in tko^{25t} larvae involved genes involved in antimicrobial defense. An unbiased annotation enrichment analysis of all genes showing at least two-fold changes in expression (S5 Table), executed using the DAVID (Database for Annotation, Visualization and Integrated Discovery, http://david.abcc. ncifcrf.gov) gene ontology database tools, reached broadly similar conclusions.

tko^{25t} is immune to the growth-inhibitory effects of cytosolic protein synthesis inhibition

The strikingly opposite sugar-dependent regulation of highly expressed genes for the machinery of cytosolic protein synthesis and secretion in tko^{25t} compared with wild-type larvae could, in principle, be construed as the cause or consequence of the metabolic disturbances and growth impairment: in other words it could be an adaptive response to limit growth under deranged metabolic conditions, or could be a maladaptive consequence of such disturbances. Thus, we reasoned that imposing an additional stress on the protein synthetic apparatus would worsen the phenotype if the above changes are maladaptive, but would be neutral or possibly even beneficial, if down-regulation of protein synthesis and secretion were part of an adaptive response.

To address this, we cultured wild-type and tko^{25t} flies on media containing low doses of cycloheximide, an inhibitor of cytosolic translational elongation. Cycloheximide produced a dose-dependent growth retardation in wild-type flies, but had almost no effect on tko^{25t} mutant flies, if anything tending to accelerate their development very slightly, especially when analyzing the progeny only from eggs laid on the first day of exposure to the drug, thus minimizing any confounding effects on egg-laying behaviour or oogenesis (Fig 5A and 5B and Panels A-C in S5 Fig). We also noted a tendency toward alleviation of bang-sensitivity (Panel D in S5 Fig), although this was not statistically significant due to the large variances in recovery time. In
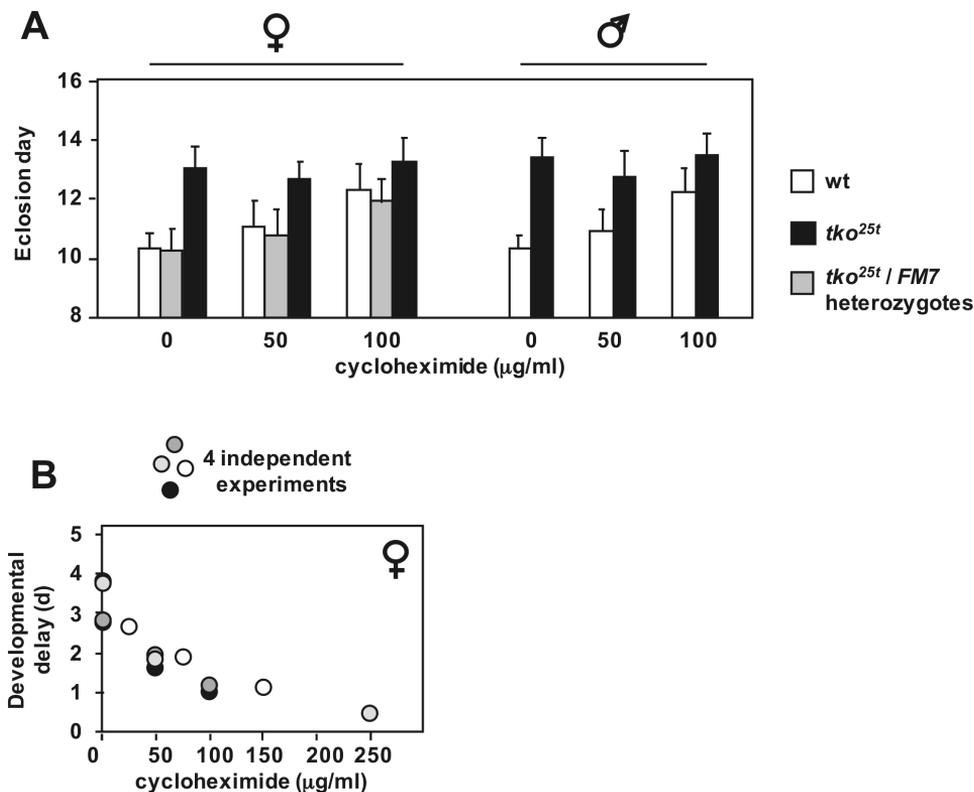
Fig 5. Effect of cycloheximide on development of *tko^25t* and wild-type flies. (A) Means ± SD of times to eclosion of flies of the sex and genotypes indicated, on high-sugar medium, with or without cycloheximide at the indicated concentrations. Based on pairwise *t* tests, and considering all the flies of a given sex and genotype cultured at a specific drug concentration as a single population, mean eclosion times were significantly different ($p < 0.05$) at different cycloheximide concentrations, apart from *tko^25t* flies of either sex at 100 μg/ml, which were not different from *tko^25t* flies cultured in the complete absence of the drug. (B) Pooled eclosion data from four independent experiments conducted with different concentration ranges of cycloheximide. Female developmental delay showed consistent decrease with increasing cycloheximide concentration. Males showed same trend (Panel C in S5 Fig).

doi:10.1371/journal.pone.0145836.g005

addition, *tko^25t* flies were immune to the growth-retarding effects of tunicamycin seen in wild-type flies, when the drug was added to the growth medium at the highest practical dose of 12 μM (Panel E in S5 Fig).

The gut is a crucial tissue for the developmental delay phenotype of *tko^25t* flies

The striking down-regulation of components of the machinery of cytosolic protein synthesis and secretion in *tko^25t* larvae, combined with the observation that the effect of the mutation is epistatic to the developmental delay introduced by low doses of cycloheximide, suggests that one or more tissues responsible for the synthesis of secreted proteins are key targets of the mutation. An obvious candidate is the gut, especially since many secreted gut proteins showed oppositely altered expression in *tko^25t* compared with wild-type larvae. We therefore tested whether gut-specific expression of the wild-type *tko* gene in the *tko^25t* background could
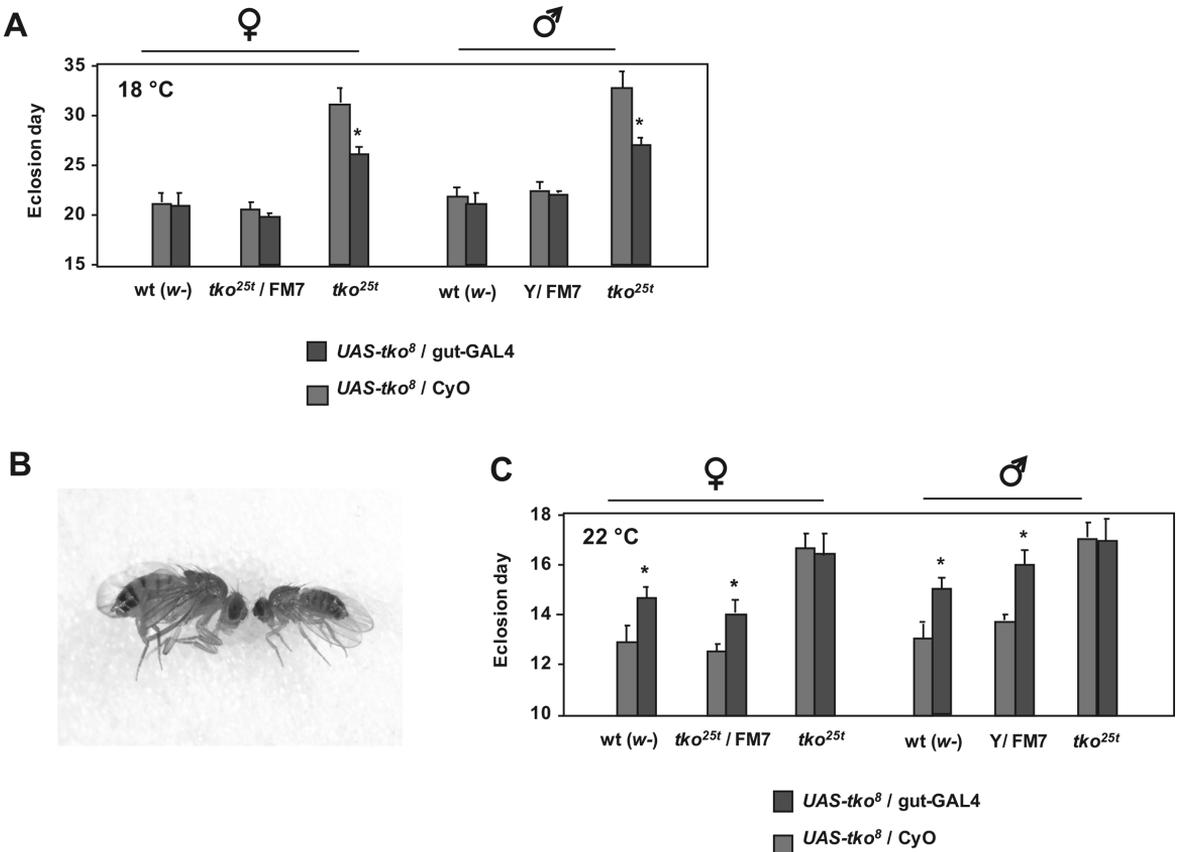
Fig 6. Partial rescue of *tko^25t* by gut-specific expression of *tko*. (A, C) Means ± SD of times to eclosion of flies of the sex and genotypes indicated, on high-sugar medium, at (A) 18°C or (C) 22°C. Asterisks denote significant differences in pairwise *t* tests (*p* < 0.01) between flies of a given sex and genotype carrying the gut-GAL4 driver (Kyoto line 113094) compared with the corresponding flies carrying the CyO balancer chromosome instead. (B) Minute phenotype of the few flies eclosing with the genotype *UAS-tko^8* / gut-GAL4 when cultured at 26°C.

doi:10.1371/journal.pone.0145836.g006

alleviate the mutant phenotype. To do this, we made use of a previously constructed transgenic line containing a GAL4-dependent copy of *tko* (*UAS-tko^8*) [22], which we combined with a gut-specific GAL4 driver line (Kyoto 113094, S6 Fig), in the *tko^25t* and wild-type backgrounds. The effect was extremely temperature-dependent. At 18°C the *UAS-tko^8* and Kyoto 113094 driver combination had no significant effect in the wild-type background, but *tko^25t* flies showed a clear, though partial rescue of their very long developmental delay at this temperature (Fig 6A). At 26°C the combination of *UAS-tko^8* and the Kyoto 113094 driver was lethal or semi-lethal, with just a small number of escaper flies eclosing in the wild-type background, with an ~4 day developmental delay, and exhibiting a minute phenotype (Fig 6B). At 22°C the combination remained deleterious in the wild-type background, with flies showing a 1–2 day developmental delay, but in the *tko^25t* background there was no such effect (Fig 6C).

Discussion

Our starting point in this study was the erroneous assumption that the limited capacity of OXPHOS in tko^{25t} flies would render them highly dependent on glycolysis, and thus addicted to sugar. However, increasing the sugar content of their diet instead led to exacerbation of the mutant phenotype. Comparisons of larvae grown on different diets revealed a set of metabolic disturbances in tko^{25t} larvae (high pyruvate and lactate, low ATP and NADPH) that were generally accentuated by high-sugar diet. Growth in high-sugar produced strikingly opposite changes in gene expression in wild-type and mutant larvae, notably affecting the apparatus of cytosolic protein synthesis and secretion. In addition, we observed altered cell signaling, converging on the cytosolic translation machinery, whilst tko^{25t} was immune to the growth inhibitory effects of low levels of cycloheximide, an inhibitor of cytosolic translation.

Key metabolic consequences of mitochondrial dysfunction

Many of the metabolic disturbances seen in tko^{25t} larvae are consistent with previous studies of OXPHOS deficiency, although their exacerbation by high-sugar diet is novel. Elevated lactate, pyruvate and alanine are common findings in mitochondrial disease patients [23], considered to represent increased dependence on glycolysis under conditions where mitochondrial NADH re-oxidation is impaired [24]. tko^{25t} larvae showed decreased levels of the glycolytic intermediate immediately upstream of the rate-limiting step, i.e. fructose 1,6-biphosphate (Fig 3E), consistent with increased glycolytic flux. Lactate accumulation may reflect the need for lactate dehydrogenase as an alternative pathway to regenerate NAD+ but, since it is accompanied by high pyruvate, may also be a consequence of decreased TCA cycle capacity due to the OXPHOS defect. Pyruvate accumulation may be partially adaptive, by feeding anaplerotic pathways, but addition of dietary pyruvate (or lactate) to tko^{25t} partially phenocopied the effects of high-sugar diet, implying these end-products of glycolysis to be important agents of the metabolic crisis that limits growth, even if only via product inhibition of glycolytic flux, thus compromising the maintenance of ATP levels. The reason for the additional burden of pyruvate and lactate resulting from high-sugar diet is not immediately obvious. It may partly be a consequence of increased substrate availability for glycolysis and other catabolic pathways that converge on pyruvate. Logically, however, it also reflects maladaptive effects of sugar-dependent signaling.

Whilst tko^{25t} larvae are able to maintain normal NAD+/NADH levels, NADP+/NADPH homeostasis is severely disturbed (Fig 3C). As well as its role as an electron donor for biosynthesis, NADPH buffers oxidative stress, most importantly as a cofactor in the regeneration of the reduced form of thioredoxin [25], which in *Drosophila* replaces the functions of glutathione reductase [26]. Mitochondria from tko^{25t} flies produce excess ROS [16], potentially accounting in part for NADPH depletion. High levels of pyruvate and lactate, which we demonstrate to inhibit key NADPH-generating enzymes (Fig 4B), notably IDH and malic enzyme, may also play an influence.

The further depletion of NADPH in tko^{25t} grown in high sugar (Fig 3C) appears to be a compounding of these effects with an independent effect of high-sugar diet. Excess unmodified glucose is toxic because of its ability to react with the lysine side-chains of proteins, bringing about their irreversible inactivation via the Maillard reaction [27, 28]. This toxicity is believed to play a major role in the pathology of diabetes (reviewed in [29]), and organisms use a variety of strategies to minimize exposure of the tissues to excess glucose. *Drosophila* can detoxify glucose via the FAD-linked enzyme glucose dehydrogenase (Gld, CG1152, EC 1.1.99.10), which produces gluconate as an inert end-product, avoiding the generation of peroxide [30, 31]. Thus, as predicted, gluconate accumulates in larvae grown on high-sugar medium (Fig 3F).

Although the exact electron acceptor for Gld is not known [31], its regeneration should depend on the cytochrome P450 system, in which terminal oxidation is coupled to NADPH consumption, in the general reaction $A-H2 + 2NADPH + O2 \rightarrow 2H2O + 2NADP+ A$ (where A is a generic electron acceptor). An effect on NADPH is evident even in wild-type larvae (Fig 3C), although it does not appear to impair development in the absence of the other metabolic disturbances seen in tko^{25t}. However, its compounding with the effects of OXPHOS deficiency in tko^{25t} leads to the highly abnormal situation of a reversal in the NADPH/NADP+ ratio that must have serious consequences for many cellular processes. Notably, the processing of secreted proteins in the ER is highly dependent on NADP+/NADPH homeostasis [32, 33]. Disturbed proteostasis in the secretory pathway [34] would be predicted to affect those tissues most exposed to dietary glucose and most dependent on secretion, i.e. the gut and its associated organs, and the epidermis, which secretes the larval cuticle at each molt. This is concordant with the altered patterns of gene expression that we observed (S4 Table).

The ability of the *Drosophila* larval gut to mount a classic ER stress-response is limited. Xbp1, the key transcription factor required to effect the response, is already reported to be constitutively activated in the larval gut [35], consistent with our own findings (Panerls H and I of S4 Fig). Neither diet nor the tko^{25t} mutation had any further effect on its global expression level or splicing, suggesting that there is only a limited capacity for handling further proteotoxic stress in the ER. The activation of accessory pathways for secretion, such as involving p24-2 (Sheet A in S3 Table), may be a signature of this. P24 proteins are involved in the sorting of glycosylphosphatidylinositol (GPI) anchored proteins into COPII vesicles [36, 37] which then transit to the cell surface via the Golgi. The down-regulation, at the RNA level, of the apparatus of cytosolic protein synthesis and secretion (Sheets A and C in S4 Table), combined with active mechanisms to attenuate both processes (Fig 5 and S5 Fig), such as via S6K modulation (Fig 4F and Panel F in S4 Fig), can be rationalized as a response to proteotoxicity in the ER, due to redox disturbance.

ATP deficiency is a frequently observed or predicted effect of OXPHOS insufficiency, including previous reports on tko^{25t} and other *Drosophila* mutants [10, 12, 16, 38, 39]. However, decreased OXPHOS capacity and limitations on glycolysis due to high pyruvate and/or lactate may not be the only reasons for ATP depletion. Protein folding and refolding are highly ATP-consuming processes, as is the proteolytic degradation of misfolded or aggregated proteins [40]. Disturbed ER proteostasis in the ER may therefore be a drain on already decreased levels of ATP.

The consequences of the amino acid abnormalities detected in tko^{25t} larvae are less clear. Deficiencies in specific amino acids are expected to trigger growth arrest and inhibition of cytosolic protein synthesis through the TOR pathway independently of the effects of ATP depletion. However, dietary supplementation with protein did not rescue tko^{25t}. The amino acid imbalances in mutant larvae (Fig 4D) are therefore best considered as a side-effect of pyruvate overload that, on their own, are insufficient to trigger growth arrest. Excess alanine, also seen in patients with elevated pyruvate [23, 41], probably results from the action of alanine aminotransferase [42]. Similar arguments may apply to serine. The abnormalities in ornithine and citrulline (Fig 3D), combined with the observed changes in mRNAs for enzymes involved in their metabolism (S3 and S4 Tables), are harder to interpret, as are effects on polyamine levels, none of which offer any explanation for growth limitation in tko^{25t} (Panel C in S3 Fig). Moreover, ornithine supplementation in zero-sugar diet did not phenocopy the effects of high sugar, and may even have slightly alleviated it (Fig 4E).

Since it is difficult to manipulate the levels of pyruvate, ATP and NADPH independently, their relative contributions to the developmental phenotype are difficult to apportion. Knockdown of *Men* (malic enzyme), for example, produced no exacerbation and possibly a slight
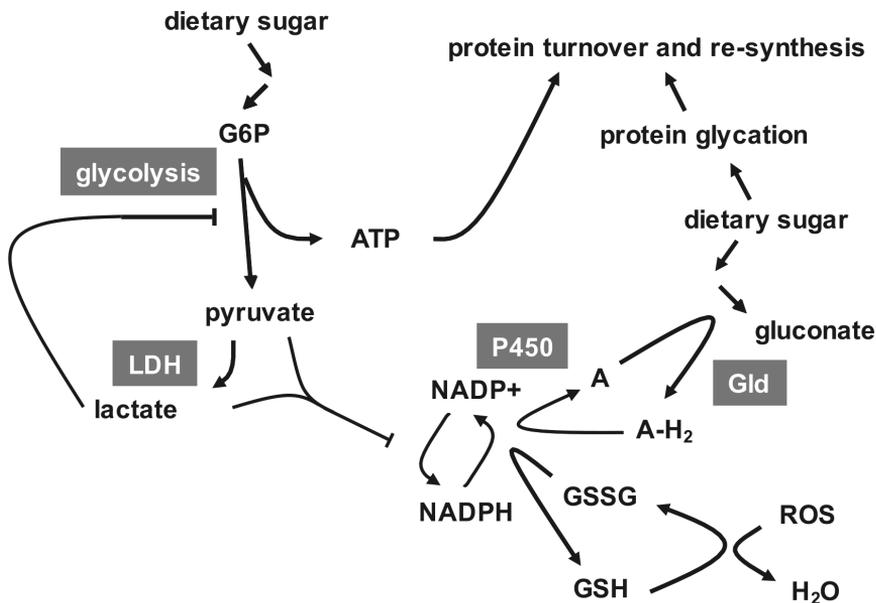
Fig 7. Summary model of the metabolic phenotype of *tko*[25t] in high-sugar medium. High dietary sugar and mitochondrial dysfunction stimulate glycolysis, which is nevertheless limited by the build up of pyruvate and/or lactate, produced by lactate dehydrogenase (LDH, needed to regenerate NAD + when OXPHOS is impaired), restricting ATP production. Pyruvate and lactate accumulation restricts NADPH production, whilst NADPH consumption is increased by the need to maintain glutathione in the reduced state, despite increased mitochondrial ROS production, and by the need to reoxidize the electron acceptor (A) for glucose dehydrogenase (Gld) using the P450 system, preventing further peroxide generation. Glucose dehydrogenase converts excess glucose to gluconate, whilst any glycotoxic damage is compensated by the normal processes of protein refolding, turnover and re-synthesis, which consume ATP.

doi:10.1371/journal.pone.0145836.g007

alleviation of the phenotype (Fig 4C). However, any decrease in flux should directly decrease both NADPH and pyruvate, whilst decreased pyruvate may in turn allow an increased rate of NADPH production and facilitate glycolytic flux. Unknown allosteric effects, undetected metabolites, subcellular compartmentalization of substrates, products and enzymes, and tissue-specificity of metabolic pathways may impact the diet-dependent metabolic crisis of *tko*[25t], summarized in Fig 7.

Growth-related signaling

The metabolic crisis of *tko*[25t] does not lead to lethality or grossly abnormal development, but to a decreased developmental rate, tailoring growth to resources and the ability to mobilize them, and resulting in a viable adult fly. This indicates the operation of a programmed response mechanism. We postulate that, in the wild, this would allow the fly to survive in different nutritional environments, perhaps including those in which it may be exposed to toxins targeted on OXPHOS or mitochondrial translation. The response clearly has both a transcriptional and post-translational dimension, though the underlying signaling machineries may overlap, and may also operate tissue-specifically, accounting for the many changes in expression of genes expressed uniquely in the gut, muscle or epidermis. Furthermore, although transcriptional responses most likely underlie the major changes in mRNA levels, we cannot exclude a contribution from non-coding RNAs regulated in response to the *tko*[25t] mutation or the sugar content of the diet.

We found evidence for the involvement of several well-characterized signaling pathways converging on cytosolic protein synthesis, notably including the ATP-responsive AMPK and nutrient-sensitive (Akt) pathways, as well as the key target of TOR signaling, S6K (Fig 6B). Strikingly, tko^{25t} flies were immune to the growth-inhibitory effect of low doses of cycloheximide, consistent with the translational apparatus being a key downstream target of regulation in the mutant. This is unlikely to be due to drug exclusion. Although induced in tko^{25t} adults [9], the Mdr-related transporter l(2)03659 is expressed at slightly lower levels in tko^{25t} than wild-type larvae (S2 Table) and is not sugar-responsive. Moreover, tko^{25t} flies are more sensitive than wild-type flies to doxycycline [6], an inhibitor of mitochondrial rather than cytosolic protein synthesis.

Cycloheximide inhibits the elongation step of the ribosome cycle [43], which is normally not rate-limiting. Instead, initiation is the target of most translation-regulatory mechanisms, e.g. via the protein kinases targeting initiation factors such as eIF-2A or eIF-4E [44]. However, it would appear that initiation is already working at close to maximal capacity in wild-type *Drosophila* larvae, since cycloheximide inhibits growth in a dose-dependent manner even at low concentrations. In contrast, at doses up to 100 μg/ml, tko^{25t} flies were refractory to cycloheximide (Fig 5B and Panel C in S5 Fig), indicating a condition where initiation, rather than elongation, is constrained, and is thus rate-limiting for protein synthesis and growth. The altered levels of phosphorylated isoforms of known signaling molecules is consistent with the implied down-regulation of translational initiation in tko^{25t}, and its exacerbation by high-sugar diet. Thus, while total levels of the AMPK α-subunit are little altered, tko^{25t} flies show increased amounts of the isoform phosphorylated at Thr-172, which attenuates TOR signaling [19], but a corresponding decrease in the isoform of Akt phophorylated at Ser-505, which activates TOR. The increase in AMPK phosphorylation is consistent with the observed ATP depletion [45], but the mechanism by which Akt signaling attenuated remains unknown, and could involve any of the metabolic changes associated with mitochondrial dysfunction.

Consistent with these changes, tko^{25t} shows decreased amounts of the isoform of the key TOR target [46] S6K, phosphorylated at Thr-398, which in turn activates translational initiation [47]. However, all of these changes are rather modest, raising doubts as to whether they, alone, could account for an effective halving of the growth rate during larval development.

The most important new link between S6K and growth regulation is our finding that the level of S6K protein itself (specifically, the homologue of human S6K1) is strongly decreased in tko^{25t} larvae grown on high-sugar medium (Fig 4F and Panel F in S4 Fig). A recent report of the effects on *Drosophila* lifespan of different diets, combined with knockdown of an ATP synthase subunit [48], also showed modulation of the levels of S6K protein. Although less dramatic than the S6K changes observed here, this may indicate a parallel or accessory stress-response pathway, linking diet, mitochondrial function and regulation of cytosolic translation. Neither Sun et al. [48] nor ourselves were able to address the tissue specificity of S6K modulation, and the underlying molecular mechanism remains unknown, but our data raise a number of interesting, non-mutually excusive possibilities. The first is that further activation of AMPK in susceptible tissues (Panel F in S4 Fig), resulting from the more profound depletion of ATP (Fig 3B), triggers S6K turnover, e.g. via the ubiquitin-proteasome system. A second would invoke a regulator akin to AMPK, but activated instead by the abnormal NADPH/NADP + ratio. A third such putative regulator would be sensitive to elevated gluconate (Fig 3F), which may be considered a specific indicator of the stress of high dietary sugar in the fly. A further possibility is that S6K levels are regulated by the downstream consequences of these metabolic changes, for example in response to proteotoxic stress or translational imbalances (see summary model, Fig 8).
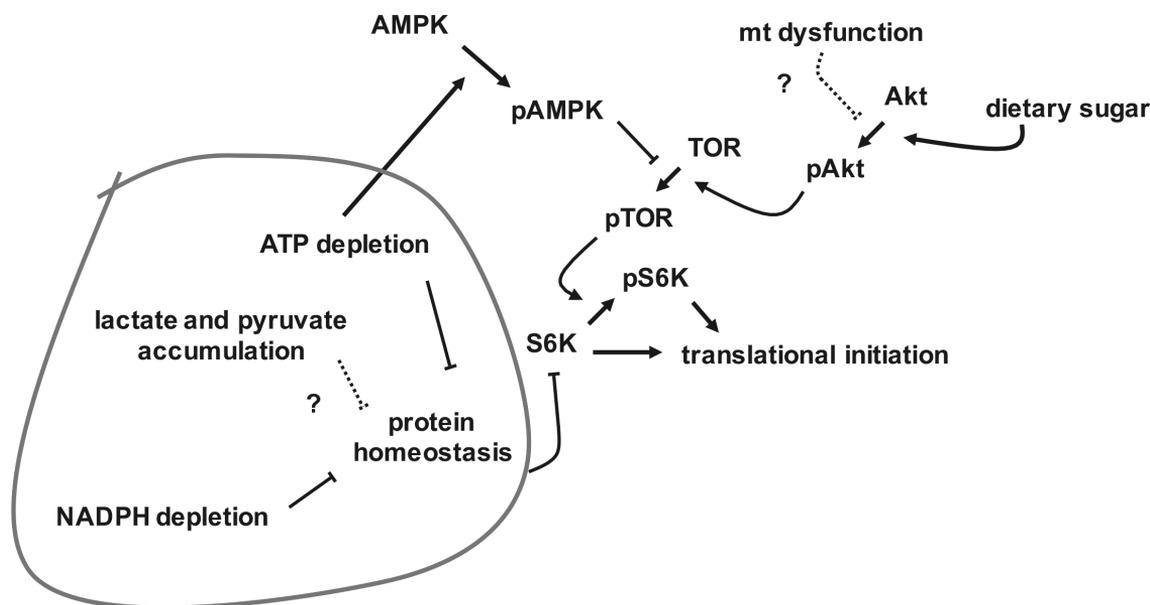
Fig 8. Summary model of the growth phenotype of *tko*²⁵ᵗ in high-sugar medium. NADPH depletion disturbs protein homeostasis in the ER (and may also be exacerbated by it, in a vicious cycle) consuming further ATP. ATP depletion activates AMPK, inhibiting TOR complex activation by phosphorylation (denoted as pTOR), and consequently limiting the activation of S6K and other growth-stimulatory effectors by phosphorylation. Mitochondrial dysfunction is proposed to inhibit Akt activation by an unknown process (dotted line), limiting its activation by dietary sugar. One or more of lactate/pyruvate accumulation, ATP and NADPH depletion, or their combined effects on protein homeostasis (red line), are proposed to stimulate S6K turnover, thus contributing further to the down-regulation of protein synthesis.

doi:10.1371/journal.pone.0145836.g008

The functional differences between modified and unmodified isoforms of S6K are poorly understood, but are likely to extend beyond global regulation of translation [49]. Many of the large quantitative differences in gene expression at the RNA level seen in *tko*²⁵ᵗ grown in high sugar were opposite to those induced by high-sugar diet in wild-type flies, notably those affecting the machineries of cytosolic protein synthesis and secretion as well as glycolysis. This suggests a regulatory event targeting the system responsible for glucose induction of gene expression which includes transcription factors such as sugarbabe [50] and Mondo/Mlx [51], but may also have a post/transcriptional component. These factors, as well as any proteins that interact with them directly or indirectly, should thus be considered as candidates for regulation by S6K.

We did not identify a specific systemic response mechanism to mitochondrial dysfunction in *tko*²⁵ᵗ that would correspond with the endocrine biomarkers GDF15 [52] or FGF21 in mammals [53]. Neither GDF15 nor FGF21 have orthologues in *Drosophila*, although both are members of well-characterized growth factor families that are well represented in the fly. No members of these families showed significantly altered expression at the RNA level in *tko*²⁵ᵗ, although this does not preclude regulation at other levels. Expression of insulin-like peptides was also slightly increased, not depressed in *tko*²⁵ᵗ (Panel G in S4 Fig). Whilst the down-regulation of growth in *tko*²⁵ᵗ might be at least partially cell-autonomous, the fact that it appears to emanate from a deficiency of mitochondrial protein synthesis in a specific tissue (i.e. the gut, Fig 6), and that one readout is altered feeding behaviour (Fig 2D), is likely to involve either a known [54] or still unknown endocrine circuit centered on the gut.

Tissue-specificity of the effects of mitochondrial dysfunction in development

Five pieces of evidence implicate the gut as a crucial tissue mediating the growth retardation of tko^{25t} larvae, particularly its enhancement in high-sugar diet. First, based on dye ingestion, we observed a decreased food intake (Fig 2F). Second, specific gut alpha-glucosidases were down-regulated (Fig 2A), and further down-regulated in high sugar (Fig 2D), suggestive of decreased sugar absorption and accounting, at least partially, for decreased serum sugar (Fig 2E). Third, mRNAs coding for gut-specific enzymes were amongst those most responsive to diet and geno-type, many showing clearly opposite behaviour in tko^{25t} compared with wild-type (Sheets A and C in S4 Table). The transcriptional readout of mitochondrial dysfunction in relation to diet is therefore largely gut-specific. Of note also is the fact that, in high sugar, tko^{25t} larvae showed down-regulation of many mRNAs coding for components of the machineries of cyto-solic translation and secretion (Sheet A in S4 Table) and, at the protein level, of S6K (Fig 4F and Panel F in S4 Fig), considered a key regulator of translation, whilst the gut is one of the most important secretory organs. Fourth, the additional metabolic stress arising from NADPH depletion (Fig 3C) as a by-product of glucose oxidation must logically occur in a tissue exposed to high sugar levels. Given the fact that serum sugar is not elevated in tko^{25t} (Fig 2E) the only major tissues exposed to high sugar should be the epidermis and the gut. Finally, when directly tested using a gut-specific driver at 18°C, expression of the wild-type tko gene was able partially to rescue the developmental delay of tko^{25t} (Fig 6A), implicating the gut as a major tissue where insufficiency of mitochondrial protein synthesis impairs growth. The effect of GAL4 drivers is known to be temperature-dependent [55], with increased activity at 25°C compared with 18°C. Intriguingly, gut-specific over-expression of wild-type tko in the wild-type but not the tko^{25t} background at 22°C also produced a developmental delay (Fig 6C), suggesting that the expression level of the tko gene product (mitoribosomal protein S12), which in bacteria is a key component of the small subunit assembly pathway [56], may need to be tightly regulated in order to ensure the appropriate ratio of mitochondrial and cytosolic translational capacity. Over-expression of tko at even higher temperatures resulted in a phenotype of semi-lethality, with escapers having a classic minute phenotype (Fig 6B), seen previously in mutants with cytoribosome deficiency [57] or defective insulin signaling [58], but not in tko^{25t}. The finding further highlights the importance of coordinated protein synthesis in cytosolic and mitochondrial compartments.

Relevance to pathophysiology of metabolic and mitochondrial disease

Despite its sensitivity to high-sugar diet, tko^{25t} cannot be considered an exact model for diabe-tes in humans, since serum sugar levels are lower in the mutant than in wild-type flies (Fig 2E). The expression of several of the insulin-like peptides is slightly increased at the RNA level (Panel G in S4 Fig), but their exact functions in metabolic or growth regulation remain unclear, and mRNA levels may not reflect those of the peptides themselves [59]. Moreover, pAkt, con-sidered a primary mediator of insulin signaling [20, 60], although down-regulated in tko^{25t} compared with wild-type (Panel F in S4 Fig), was still modestly increased in response to high-sugar diet (Panel F in S4 Fig).

Changes in insulin-signaling may contribute to lowered serum sugar (Fig 2E), enhanced expression of excretory sugar transporters (Fig 2A and 2C), decreased muscle biosynthesis (Sheets A and C in S4 Table) and increased triglycerides (Fig 3G), but these may be considered as adaptive responses to mitochondrial dysfunction rather than a pathological signature and, at least to some degree, are seen also in tko^{25t} larvae grown on zero-sugar medium.

Because it is also manifest on zero-sugar medium, the elevated level of triglycerides seen in tko^{25t} is not simply a classic 'sugar-into-fat' response to sugar overload. More likely, fat

deposition represents an alternate system for storing energy needed to fuel metamorphosis, partially replacing the accumulation of muscle. Larval body wall muscle is largely turned over during metamorphosis [61], but tko^{25t} larvae exhibit down-regulation of mRNAs coding for structural proteins of muscle (Sheet A in S4 Table). The response of wild-type larvae to high-sugar diet involves up-regulation of muscle and cuticular components, as well as glycolysis and the cytosolic translation system (Sheet A in S4 Table). Unlike yeast or cancer cells, where high-glucose media promote more rapid growth [62], wild-type *Drosophila* larvae do not grow more rapidly on a high-sugar diet, possibly even slightly slower (Fig 1 and Panel A in S1 Fig). Increased biosynthesis of cuticle and muscle might be a signature of an avoidance response to a high-sugar environment. As already noted, sugar overload should be toxic to the epidermis and to the gut, due to protein glycation and/or NADPH depletion resulting from glucose oxidation. Increased production of cuticle proteins may protect the epidermis, whilst the accumulation of body wall muscle will facilitate the movement of the larva to a less stressful environment. The metabolic consequences of mitochondrial dysfunction may limit this response in tko^{25t} larvae. Muscle is also one of the most energy-consuming tissues, and developmental reprogramming that limits muscle biosynthesis, storing biomass for later catabolism during metamorphosis instead as fat, may be considered an energy-sparing response to ATP depletion that is signaled via AMPK or its downstream targets.

The metabolic crisis experienced by tko^{25t} larvae in high sugar diet may have a more general relevance in mitochondrial disease. Other data supports the idea that ketogenic or low carbohydrate diet is beneficial for mitochondrial disease patients or animal models thereof [63, 64]. The combination of ATP deletion and glycotoxic stress is likely to occur in many contexts relevant to human pathology. Although glucose homeostasis operates differently in mammals, some secretory tissues are naturally susceptible to glucose overload, notably the gut, and perhaps most importantly, the islet cells of the pancreas, which must respond to physiological fluctuations in glucose. *Drosophila* Gld does not have a strict orthologue in mammals: however, it is member of a multigene family of choline-glucose dehydrogenases that ultimately consume NADPH, whose many mammalian members remain functionally unidentified.

Our findings implicate pyruvate overload, ATP depletion and disturbed NADP/NADPH homeostasis as key elements of the metabolic crisis resulting from OXPHOS deficiency, especially in the presence of high dietary sugar, with deranged protein homeostasis in the secretory pathway as an unexpected outcome. As well as suggesting possible new drug targets in mitochondrial disease, they may also be relevant to cancer. To facilitate rapid growth, many tumors switch to aerobic glycolysis for ATP production (the Warburg effect), at the same time frequently down-regulating OXPHOS, commonly by accumulating mtDNA mutations. However, if what is true of *Drosophila* larvae is also true of such tumors, high glucose levels should provoke a metabolic crisis that curtails growth or may even lead to apoptosis, if NADPH/NADP + homeostasis is pushed beyond a certain limit. Since many of the commonly used drugs in cancer chemotherapy are metabolized via the NADPH-consuming cytochrome P450 system, NADPH depletion should be considered a possible mechanism by which they are really provoking tumor destruction. In this case, tumors that become chemo-resistant via activation of multi-drug resistance pathway might still be vulnerable to glucose overload.

In humans, pyruvate treatment has been suggested to be effective in some cases of mitochondrial disease [65], whereas other studies found no convincing benefits from treatments such as with dichloroacetate, designed to increase mitochondrial pyruvate utilization and thus decrease cytosolic pyruvate load (for review see [66]). In tko^{25t} larvae, pyruvate supplementation is clearly deleterious, but dichloroacetate treatment also provided no benefit and tended to exacerbate rather than relieve developmental delay on both high and zero-sugar diets (Panel J in S4 Fig). Thus, the issue is not pyruvate levels *per se*, but the inability of OXPHOS-defective

mitochondria to metabolize pyruvate. Therapies targeted on pyruvate might therefore cause more harm than good, by increasing pyruvate overload in the mitochondria.

Experimental Procedures

Drosophila stocks and maintenance

tko^{25t} [3] in the Oregon R background was as described previously [6]. w^{1118}, standard balancers, gut-specific Kyoto GAL4 line 113094, and VDRC RNAi lines targeted on *Men* and *Gld* (#104016 and #108361, respectively) were obtained from stock centers. Except for use in specific experiments, flies were maintained at room temperature in plugged plastic vials containing standard high-sugar medium (see SI for full details), supplemented with 0.5% propionic acid (Sigma-Aldrich) and 0.1% (w/v) methyl 4-hydroxybenzoate (Nipagin, Sigma-Aldrich), then transferred to vials containing appropriate media for mating and larval culture in a 12 h light-dark cycle at 25°C, except where stated. To avoid selection of suppressors, tko^{25t} flies were maintained using FM7 balancer and homo/hemizygotes generated as needed for experiments. In general, to avoid any confounding effects from the balancer, wild-type flies in the same background were used as controls in parallel in all experiments. UAS-tko^8 flies, described previously [22] were maintained in the tko^{25t} background, and their phenotype rechecked prior to experiments.

Culture media

Fly food was created according to different recipes as detailed in SI. Most experiments used standard high-sugar medium [67], denoted HS, and 'zero-sugar' medium, denoted ZS, containing only agar, dried yeast extract, soya and maize flours, but no added sugars. Isocaloric media with lowered sugar content but other components in varying proportions were as indicated in S1 File. Various supplements, as indicated in figures and legends, were generally added from stock solutions after medium was cooled to 50°C, including sodium pyruvate or lactate (25 mg/ml), ornithine (5 or 20 μg/ml) and cycloheximide (up to 250 μg/ml). For tunicamycin (12 μM), low-melting point agarose was used instead of agar, wth cooling to 37°C before addition of drug.

Developmental time and behavioral assays

Crosses were conducted in a minimum of 3, usually 4 or 5 replicates, and mean developmental time to eclosion (at 25°C, except where indicated), as well as bang-sensitivity were measured as described previously [15]. Standard deviations were calculated based on the distributions of mean eclosion day from replicate vials (except where indicated) or, for bang-sensitivity, from the distribution of recovery times from mechanical shock of all individual flies of a given sex and genotype tested (in batches of 30–50 flies). Larval feeding behaviour was assayed by dye ingestion. Briefly, individual larvae grown on HS or ZS medium were placed on petri dishes of the same medium containing 0.16% erioglaucine for 20 min, washed with PBS, dried, and then homogenized in 100 μl PBS. Homogenates were centrifuged at 12,000 g_{max} and dye uptake was measured spectrophotometrically (absorbance at 630 nm) using the supernatant fractions.

Metabolite analysis

Steady-state levels of ATP, lactate and pyruvate were measured by enzyme-linked luminometry (ATP) or fluorometry in extracts from batches of 20 larvae or adult flies, using commercially available kits according to manufacturer's protocols (Molecular Probes, Life Technologies for ATP, Abcam for pyruvate and lactate). Hemolymph extracts from batches of 30–50 larvae

were treated overnight with trehalase (Sigma-Aldrich), following which total serum sugars were assayed using glucose (HK) reagent (Thermo Scientific). Triglyceride levels were measured essentially according to Tennesen et al. [68], using triglyceride reagent (Thermo Scientific), with subtraction of the background signal due to free glycerol. For global metabolite analysis, batches of 15 larvae were snap-frozen in liquid nitrogen, deproteinized by chloroform extraction, centrifugation and micro-filtration, then analyzed separately for anions and cations by CE-TOFMS in the presence of suitable standards. For full details see S1 File.

Enzymatic analyses

Malic enzyme, glucose-6-phosphate dehydrogenase, 6-phosphogluconate dehydrogenase and isocitrate dehydrogenase were assayed essentially as described previously [69, 70, 71]. Isocitrate dehydrogenase and glutamate dehydrogenase activities were also analyzed separately using a commercially available IDH activity kit (Abcam), in order to evaluate the contribution of NAD^+/NADH- and $NADP^+$/NADPH-dependent isoforms to the total enzyme activity. See S1 File for full details.

RNA analysis

For QRTPCR, RNA extraction from *Drosophila* adults and larvae, cDNA synthesis, PCR and data analysis were performed as described previously [67], using primer sets shown in S6 Table. For RNA-sequencing, RNA was extracted from flash-frozen batches of 30 larvae using miRNA Easy Mini Kit (Qiagen) and manufacturer's instructions. Three biological replicate samples were produced by pooling 4 independent preparations to produce each replicate. RNA sequencing was performed on Hiseq 2500 sequencers (Illumina) using paired-end library and 100 bp read-legnth and otherwise standard protocols. Expression analysis was performed using Chipster. Sequencing reads were mapped to the *Drosophila* reference genome (BDGP release 5.72) using TopHat version 2.0.9, and differential expression analysis was performed using CuffDiff. The splicing pattern of Xbp1 was analysed by RT-PCR, PstI digestion and agarose gel electrophoresis [72].

Protein analysis

Total protein was extracted from batches of 20 frozen larvae in phosphate buffer containing 150 mM NaCl, 1 mM EDTA, 2 M urea, 1.3% (w/v) SDS, 10 mg/ml each Complete protease inhibitor mix (Roche) and PhosSTOP phosphatase inhibitor mix (Roche), diluted into 4 x Laemmli loading buffer and (see S1 File for details) and electrophorsesed on Criterion TGX AnyKD precast SDS-PAGE gels (Bio-Rad). Protein was transferred to 0.45 μm Hybond ECL nitrocellulose membrane (Amersham, GE Heathcare Life Sciences). Blots were processed and visualized by standard methods (see S1 File for full details). Primary antibodies, used at 1:1,000 dilution, were against: Akt #4691 (Cell Signaling), phospho-Akt #4054 (Cell Signaling), AMPK #80039 (Abcam), phospho-AMPK #4188 (Cell Signaling), S6K #64804 (Abcam), phospho-S6K #9029 (Cell Signaling) and alpha-tubulin #52866 (Abcam, 1:10,000) with appropriate HRP-conjugated secondary antibodies (Vector Laboratories, 1:10,000): Horse Anti-Mouse IgG #PI-2000 or Goat Anti-Rabbit IgG #PI-1000. For further details see S1 File.

Supporting Information

S1 Fig. Supplementary data on modulation of *tko*[25t] phenotype by diet. Time to eclosion of *tko*[25t] and wild-type flies of sex as shown, grown on media of the indicated composition (see SI for details). In (A) asterisks denote significant differences from flies of the same genotype

grown on 0% sucrose medium (Student's t test, * showing $p < 0.05$, ** showing $p < 0.01$). For corresponding eclosion data of males see Fig 1A. In (B) and (E), horizontal lines indicate significant differences between flies of a given genotype, grown on different media (Student's t test, * showing $p < 0.05$, ** showing $p < 0.01$). For corresponding eclosion data of males grown on high-sugar media, see Fig 4D. In (C) asterisks (**) denote significant difference from flies of the same genotype grown on all other media tested (Student's t test, $p < 0.01$), which were not significantly different from each other. For corresponding eclosion data of males see Fig 1B. In (D) there were no significant differences from flies of the same genotype, grown on other media (Student's t test, $p > 0.05$). In all experiments eclosion times for tko^{25t} flies were also significantly different from those of wild-type flies grown on the same medium (Student's t test, $p < 0.01$). For corresponding eclosion data of males see Figs 1 and 4D.
(PDF)

S2 Fig. Supplementary data on the 'anti-sugar' response of tko^{25t} flies. Expression levels of various genes, based on QRTPCR, in adult females of the indicated genotypes, grown on high-sugar medium. (A) Malpighian tubule-specific sugar transporters, (B) gut-specific α-glucosidases. All signals normalized to the levels in wild-type females. Horizontal bars denote values significantly different between genotypes (Student's t test, * indicating $p < 0.05$, ** indicating $p < 0.01$).
(PDF)

S3 Fig. Supplementary data on metabolite levels in tko^{25t} and wild-type flies. Relative levels of different metabolites in adult females or L3 larvae (as shown) of the indicated genotypes and growth conditions, based on (A) findings from enzyme-liked assays, (B) fluorescence spectrometry or (C, D) mass spectrometry. Absolute values are shown for (C) amino acids. Values in (A, B) are normalized to those for wild-type larvae grown on ZS medium, enabling them to be plotted alongside for comparison. A similar plot for those amino acids exhibiting substantial changes (here boxed in red) is shown in Fig 3D. Values in (D) for polyamines are normalized to the level of putrescine in wild-type larvae grown on ZS medium, enabling them to be plotted alongside for comparison. Absolute values from mass spectrometry are given in S1 Table. Horizontal bars denote significantly different data classes (Student's t test, $p < 0.05$), except in (C), where significant differences in amino acid levels between wild-type and tko^{25t} are shown in Fig 3D, and presented in full in S7 Table.
(PDF)

S4 Fig. Supplementary indicative data on dietary modulation of tko^{25t} phenotype. (A) Time to eclosion of female flies of the indicated genotypes and dietary conditions, on medium supplemented with pyruvate (pyr) or lactate (lact). In the presence of either supplement there were no significant difference in eclosion timing between tko^{25t} flies grown on high-sugar versus zero-sugar medium (Student's t test, $p > 0.05$). See also Fig 4A. (B) Summary diagram of the major NADPH-producing enzymes. (C) Activities of the major NADPH-producing enzymes in extracts from *Drosophila* L3 larvae of the indicated genotypes and dietary conditions. (D, E) Time to eclosion of female flies of the indicated genotypes and dietary conditions, on medium supplemented (or not) with ornithine (orn), at the concentrations shown. * denotes value significantly different than for flies of the corresponding genotype and dietary condition, with ornithine *versus* without the supplement (Student's t test, $p < 0.05$). (F) Western blots of extracts from L3 larvae of the indicated genotypes and dietary conditions, probed for AMPK, pAMPK (phosphorylated at Thr-172), Akt, pAkt (phosphorylated at Ser-505) or S6K, plus the α-tubulin loading control (αTub). See also Fig 4F. (G) QRTPCR of mRNAs for four of the *Drosophila* insulin-like peptide (dILP) genes, in larvae of the indicated genotype and dietary

condition. Despite the trend, differences between genotypes were not significant for the dILP genes considered individually (Student's t test, $p > 0.05$). (H, I) Analysis of Xbp1 splicing by RTPCR. (H) Agarose gel showing the product fragments diagnostic for the spliced (216S) and unspliced (239U) forms of Xbp1 mRNA (fragment sizes in bp). (I) Analysis by QRTPCR, in larvae of the indicated genotype and dietary condition, revealing only modest differences (all values normalized to those for wild-type larvae grown on high-sugar medium). (J) Time to eclosion of female flies of the indicated genotypes and dietary conditions, on medium supplemented with 12.5 mg/ml dichloroacetate (DCA). Males showed the same trends.
(PDF)

S5 Fig. Supplementary data on effect of cycloheximide and tunicamycin on developmental timing of tko^{25t} and wild-type flies. (A, B) Repeats of experiment shown in Fig 5A, but using various ranges of cycloheximide concentrations. (A) Means ± SD of times to eclosion of flies of the sex and genotypes indicated, on media containing increasing amounts of cycloheximide. Based on pairwise t tests, and considering all the flies of a given sex and genotype cultured at a specific drug concentration as a single population, mean eclosion times were significantly different ($p < 0.01$) at different cycloheximide concentrations for tko^{25t} males or females at all doses tested, compared with flies grown on medium without drug, but the values for the different doses of drug tested were not different from each other. For control flies, values at all concentrations were significantly different from those without drug and from each other, except for 25 *versus* 75 μg/ml. (B) Means ± SD of times to eclosion of flies of the sex and genotypes indicated, on high-sugar medium, with or without cycloheximide (50 μg/ml). Based on pairwise t tests, and considering all the flies of a given sex and genotype cultured at a specific drug concentration as a single population, eclosion timed for flies cultured without drug were significantly different from those cultured with drug in each case ($p < 0.01$). (C) Pooled eclosion data from four independent experiments conducted with different concentration ranges of cycloheximide. Male developmental delay showed consistent decrease with increasing cycloheximide concentration. Females showed the same trend (Fig 5B). (D) Bang-sensitivity (recovery times) of tko^{25t} flies of the sexes indicated, grown on high-sugar medium with or without cycloheximide (150 μg/ml). Wild-type flies were not bang-sensitive. (E) Means ± SD of times to eclosion of flies of the sex and genotypes indicated, on high-sugar medium, with or without tunicamycin (12 μM). Asterisks denote significant differences between flies of a given sex and genotype cultured with or without drug ($p < 0.01$). A repeat experiment gave the same result.
(PDF)

S6 Fig. Verification that Kyoto GAL4 driver line 113094 directs expression specifically in the gut. Micrographs of dissected L3 larvae expressing GFP driven by Kyoto GAL4 line 113094 ('gut-GAL4'), full genotypes as indicated, left-hand panels in visible light, right-hand panels showing green fluorescence. (A) nuclear-localized Stinger-GFP, (B) membrane-localized mCD8-GFP, (C) portion of top image from (B) at higher magnification, to show more detail of structures. As arrowed, GFP is expressed in the salivary glands (sg), gastric caecae (gc), foregut and mid-gut (mg), most strongly in its distal portion, but not in the imaginal discs (id), brain (b), hind-gut (hg), Malpighian tubule (mt), fat body (fb), proventriculus (p), or carcass (c). [Faint signal in carcass is background auto-fluorescence].
(PDF)

S1 File. Supplemental information. Supplemental Materials and Methods, Supplemental References, legends to Supplemental Figures.
(PDF)

S1 Table. Metabolome analysis; Sheet A: Results of Anion-Nucleotide; Sheet B: Results of Cation; Sheet C: Graphs of data from Sheet A; Sheet D: Graphs of data from Sheet B.
(XLS)

S2 Table. Output of RNAseq analysis: four pairwise comparisons at larval L3 stage, rank-ordered with no filtering.
(XLS)

S3 Table. Sheet A: Transcripts most reponsive to genotype (proportionate change in expression in c tko^{25t} ompared with wild-type)–Protein coding; Sheet B: Transcripts most reponsive to genotype (proportionate change in expression in tko^{25t} compared with wild-type)–Non-coding RNAs; Sheet C: Transcripts most reponsive to diet (proportionate change in expression in HS compared with ZS)–Protein coding; Sheet D: Transcripts most reponsive to diet (proportionate change in expression in HS compared with ZS)—Non-coding RNAs.
(XLS)

S4 Table. Sheet A: Genes regulated by genotype, absolute changes–Protein-coding genes; Sheet B: Genes regulated by genotype, absolute changes–Non-coding RNAs; Sheet C: Genes regulated by diet, absolute changes–Protein-coding genes; Sheet D: Genes regulated by diet, absolute changes–Non-coding RNAs.
(XLS)

S5 Table. Gene ontology analysis of transcriptomic data.
(DOC)

S6 Table. Oligonuceotide primers used for QRTPCR.
(XLS)

S7 Table. Statistical analysis of metabolome data.
(XLS)

Acknowledgments

Author Contributions

Conceived and designed the experiments: E. Kemppainen JG GG HTJ CDD. Performed the experiments: E. Kemppainen JG GG TT E. Kiviranta TS. Analyzed the data: E. Kemppainen JG GG TT E. Kiviranta TS HTJ CDD. Contributed reagents/materials/analysis tools: KS. Wrote the paper: HTJ E. Kiviranta JG.

References

1. Smits P, Smeitink J. and van den Heuvel L. Mitochondrial translation and beyond: processes implicated in combined oxidative phosphorylation deficiencies. J Biomed Biotechnology. 2010;e737385.

2. Boczonadi V, Horvath R. Mitochondria: impaired mitochondrial translation in human disease. Int. J. Biochem. Cell Biol. 2014; 48:77–84. doi: 10.1016/j.biocel.2013.12.011 PMID: 24412566

3. Royden CS, Pirrotta V, Jan LY. The tko locus, site of a behavioral mutation in D. melanogaster, codes for a protein homologous to prokaryotic ribosomal protein S12. Cell. 1987; 2:165–173.

4. Shah ZH, O'Dell KM, Miller SC, An X, Jacobs HT. Metazoan nuclear genes for mitoribosomal protein S12. Gene. 1997; 204:55–62. PMID: 9434165

5. Toivonen JM, Boocock MR, Jacobs HT. Modelling in Escherchia coli of mutations in mitoribosomal protein S12: novel mutant phenotypes of rpsL. Mol Microbiol. 1999; 31:1735–1746. PMID: 10209746

6. Toivonen JM, O'Dell KM, Petit N, Irvine SC, Knight GK, Lehtonen M, et al. Technical knockout, a Drosophila model of mitochondrial deafness. Genetics. 2001; 159:241–254. PMID: 11560901

7. Miller C, Saada A, Shaul N, Shabtai N, Ben-Shalom E, Shaag A, et al. Defective mitochondrial translation caused by a ribosomal protein (MRPS16) mutation. Ann. Neurol. 2004; 56:734–738. PMID: 15505824

8. Saada A, Shaag A, Arnon S, Dolfin T, Miller C, Fuchs-Telem D, et al. Antenatal mitochondrial disease caused by mitochondrial ribosomal protein (MRPS22) mutation. J. Med. Genet. 2007; 44:784–786. PMID: 17873122

9. Fernández-Ayala DJ, Chen S, Kemppainen E, O'Dell KM, Jacobs HT. Gene expression in a Drosophila model of mitochondrial disease. PLoS One. 2010; 5:e8549. doi: 10.1371/journal.pone.0008549 PMID: 20066047

10. Vartiainen S, Chen S, George J, Tuomela T, Luoto KR. O'Dell KM, Jacobs HT. Phenotypic rescue of a Drosophila model of mitochondrial ANT1 disease. Dis. Model. Mech. 2014; 7:635–48. doi: 10.1242/dmm.016527 PMID: 24812436

11. Zhang YQ, Roote J, Brogna S, Davis AW, Barbash DA, Nash D, Ashburner M. Stress sensitive B encodes an adenine nucleotide translocase in Drosophila melanogaster. Genetics. 1999; 153: 891–903. PMID: 10511565

12. Kemppainen KK, Kemppainen E, Jacobs HT. The alternative oxidase AOX does not rescue the phenotype of tko25t mutant flies. G3 (Bethesda). 2014; 4:2013–2021.

13. Sanz A, Fernández-Ayala DJ, Stefanatos R, Jacobs HT. Mitochondrial ROS production correlates with, but does not directly regulate lifespan in Drosophila. Aging. 2010; 2:200–223. PMID: 20453260

14. Kemppainen KK, Rinne J, Sriram A, Lakanmaa M, Zeb A, Tuomela T, et al. Expression of alternative oxidase in Drosophila ameliorates diverse phenotypes due to cytochrome oxidase deficiency. Hum. Mol. Genet. 2014; 23:2078–2093. doi: 10.1093/hmg/ddt601 PMID: 24293544

15. Kemppainen E, Fernández-Ayala DJ, Galbraith LC, O'Dell KM, Jacobs HT. Phenotypic suppression of the Drosophila mitochondrial disease-like mutant tko(25t) by duplication of the mutant gene in its natural chromosomal context. Mitochondrion. 2009; 9:353–363. doi: 10.1016/j.mito.2009.07.002 PMID: 19616644

16. Chen S, Oliveira MT, Sanz A, Kemppainen E, Fukuoh A, Schlicht B, et al. A cytoplasmic suppressor of a nuclear mutation affecting mitochondrial functions in Drosophila. Genetics. 2012; 192:483–493. doi: 10.1534/genetics.112.143719 PMID: 22851652

17. Dow JA, Davies SA. The Malpighian tubule: rapid insights from post-genomic biology. J. Insect Physiol. 2006; 52:365–378. PMID: 16310213

18. Cavener DR, Otteson DC, Kaufman TC. A rehabilitation of the genetic map of the 84B-D region in Drosophila melanogaster. Genetics. 1986; 114:111–123. PMID: 3095179

19. Hardie DG. AMPK: positive and negative regulation, and its role in whole-body energy homeostasis. Curr. Opin. Cell. Biol. 2014; 33:1–7. doi: 10.1016/j.ceb.2014.09.004 PMID: 25259783

20. Hietakangas V, Cohen SM. Regulation of tissue growth through nutrient sensing. Annu. Rev. Genet. 2009; 43:389–410. doi: 10.1146/annurev-genet-102108-134815 PMID: 19694515

21. Magnuson B, Ekim B, Fingar DC. Regulation and function of ribosomal protein S6 kinase (S6K) within mTOR signalling networks. Biochem. J. 2012; 441:1–21. doi: 10.1042/BJ20110892 PMID: 22168436

22. Jacobs HT, Fernández-Ayala DJ, Manjiry S, Kemppainen E, Toivonen JM, O'Dell KM. Mitochondrial disease in flies. Biochim. Biophys. Acta. 2004; 1659:190–196. PMID: 15576051

23. Clarke C, Xiao R, Place E, Zhang Z, Sondheimer N, Bennett M, et al. Mitochondrial respiratory chain disease discrimination by retrospective cohort analysis of blood metabolites. Mol. Genet. Metab. 2013; 110:145–152. doi: 10.1016/j.ymgme.2013.07.011 PMID: 23920046

24. Danhauser K, Smeitink JA, Freisinger P, Sperl W, Sabir H, Hadzik B, et al. Treatment options for lactic acidosis and metabolic crisis in children with mitochondrial disease. J. Inherit. Metab. Dis. 2015; 38:467–475. doi: 10.1007/s10545-014-9796-2 PMID: 25687154

25. Mustacich D, Powis G. Thioredoxin reductase. Biochem. J. 2000; 346:1–8. PMID: 10657232

26. Kanzok SM, Fechner A, Bauer H, Ulschmid JK, Müller HM, Botella-Munoz J, et al. Substitution of the thioredoxin system for glutathione reductase in Drosophila melanogaster. Science. 2001; 291:643–646. PMID: 11158675

27. Hodge JE. Chemistry of browning reactions in model systems. J. Agric. Food Chem. 1953; 1:928–943.

28. Grandhee SK, Monnier VM. Mechanism of formation of the Maillard protein cross-link pentosidine. Glucose, fructose, and ascorbate as pentosidine precursors. J. Biol. Chem. 1991; 266:11649–11653. PMID: 1904866

29. Ahmed N. Advanced glycation endproducts—role in pathology of diabetic complications. Diabetes Res. Clin. Pract. 2005; 67:3–21. PMID: 15620429

30. Cavener DR, MacIntyre RJ. Biphasic expression and function of glucose dehydrogenase in Drosophila melanogaster. Proc. Natl. Acad. Sci. USA. 1983; 80:6286–6288. PMID: 6413974

31. Ferri S, Kojima K, Sode K. Review of glucose oxidases and glucose dehydrogenases: a bird's eye view of glucose sensing enzymes. J. Diabetes Sci. Technol. 2011; 5:1068–1076. PMID: 22027299

32. Santos CX, Tanaka LY, Wosniak J, Laurindo FR. Mechanisms and implications of reactive oxygen species generation during the unfolded protein response: roles of endoplasmic reticulum oxidoreductases, mitochondrial electron transport, and NADPH oxidase. Antioxid. Redox Signal. 2009; 11:2409–2427. doi: 10.1089/ARS.2009.2625 PMID: 19388824

33. Kojer K, Riemer J. Balancing oxidative protein folding: the influences of reducing pathways on disulfide bond formation. Biochim. Biophys. Acta. 2014; 1844:1383–1390. doi: 10.1016/j.bbapap.2014.02.004 PMID: 24534645

34. Tan SX. Teo M, Lam YT, Dawes IW, Perrone GG. Cu, Zn superoxide dismutase and NADP(H) homeostasis are required for tolerance of endoplasmic reticulum stress in Saccharomyces cerevisiae. Mol. Biol. Cell. 2009; 20:1493–1508. doi: 10.1091/mbc.E08-07-0697 PMID: 19129474

35. Ryoo HD, Li J, Kang MJ. Drosophila XBP1 expression reporter marks cells under endoplasmic reticulum stress and with high protein secretory load. PLoS One. 2013; 8:e75774. doi: 10.1371/journal.pone.0075774 PMID: 24098723

36. Fujita M, Watanabe R, Jaensch N, Romanova-Michaelides M, Satoh T, Kato M, et al. Sorting of GPI-anchored proteins into ER exit sites by p24 proteins is dependent on remodeled GPI. J. Cell. Biol. V 2011; 194:61–75.

37. Castillon GA, Aguilera-Romero A, Manzano-Lopez J, Epstein S, Kajiwara K, Funato K, et al. The yeast p24 complex regulates GPI-anchored protein transport and quality control by monitoring anchor remodeling. Mol. Biol. Cell. 2011; 22:2924–2936. doi: 10.1091/mbc.E11-04-0294 PMID: 21680708

38. Fergestad T, Bostwick B, Ganetzky B. Metabolic disruption in Drosophila bang-sensitive seizure mutants. Genetics. 2006; 173:1357–1364. PMID: 16648587

39. Terhzaz S, Cabrero P, Chintapalli VR, Davies SA, Dow JA. Mislocalization of mitochondria and compromised renal function and oxidative stress resistance in Drosophila SesB mutants. Physiol. Genomics. 2010; 579:633–637.

40. Newsholme E, Leech A. Functional Biochemistry in Health and Disease (Wiley-Blackwell, Chichester, UK, 2010)

41. Haas RH, Parikh S, Falk MJ, Saneto RP, Wolf NI, Darin N, et al. The in-depth evaluation of suspected mitochondrial disease. Mol. Genet. Metab. 2008; 94:16–37. doi: 10.1016/j.ymgme.2007.11.018 PMID: 18243024

42. Adeva M, González-Lucán M, Seco M, Donapetry C. Enzymes involved in l-lactate metabolism in humans. Mitochondrion. 2013; 13:615–629. doi: 10.1016/j.mito.2013.08.011 PMID: 24029012

43. Schneider-Poetsch T, Ju J, Eyler DE, Dang Y, Bhat S, Merrick WC, et al. Inhibition of eukaryotic translation elongation by cycloheximide and lactimidomycin. Nat. Chem. Biol. 2010; 6:209–217. PMID: 20118940

44. Jackson RJ, Hellen CU, Pestova TV. The mechanism of eukaryotic translation initiation and principles of its regulation. Nat. Rev. Mol. Cell. Biol. 2010; 11:113–127. doi: 10.1038/nrm2838 PMID: 20094052

45. Pan DA, Hardie DG. A homologue of AMP-activated protein kinase in Drosophila melanogaster is sensitive to AMP and is activated by ATP depletion. Biochem. J. 2002; 367:179–186. PMID: 12093363

46. Albert V, Hall MN. mTOR signaling in cellular and organismal energetics. Curr. Opin. Cell. Biol. 2014; 33:55–66. doi: 10.1016/j.ceb.2014.12.001 PMID: 25554914

47. Holz MK, Ballif BA, Gygi SP, Blenis J. mTOR and S6K1 mediate assembly of the translation preinitiation complex through dynamic protein interchange and ordered phosphorylation events. Cell. 2005; 123:569–580. PMID: 16286006

48. Sun X, Wheeler C, Yolitz J, Laslo M, Alberico T, Sun Y, et al. Cell Reports. 2014; 8:1–12.

49. Sunami T, Byrne N, Diehl RE, Funabashi K, Hall DL, Ikuta M, et al. Structural basis of human p70 ribosomal S6 kinase-1 regulation by activation loop phosphorylation. J. Biol. Chem. 2010; 285:4587–4594. doi: 10.1074/jbc.M109.040667 PMID: 19864428

50.   Zinke I, Schütz CS, Katzenberger JD, Bauer M, Pankratz MJ. Nutrient control of gene expression in Drosophila: microarray analysis of starvation and sugar-dependent response. EMBO J. 2002; 21:6162–6173. PMID: 12426388

51.   Havula E, Teesalu M, Hyötyläinen T, Seppälä H, Hasygar K, Auvinen P, et al. Mondo/ChREBP-Mlx-regulated transcriptional network is essential for dietary sugar tolerance in Drosophila. PLoS Genet. 2013; 9:e1003438. doi: 10.1371/journal.pgen.1003438 PMID: 23593032

52.   Fujita Y, Ito M, Kojima T, Yatsuga S, Koga Y, Tanaka M. GDF15 is a novel biomarker to evaluate efficacy of pyruvate therapy for mitochondrial diseases. Mitochondrion. 2015; 20:34–42. doi: 10.1016/j.mito.2014.10.006 PMID: 25446397

53.   Suomalainen A, Elo JM, Pietiläinen KH, Hakonen AH, Sevastianova K, Korpela M, et al. FGF-21 as a biomarker for muscle-manifesting mitochondrial respiratory chain deficiencies: a diagnostic study. Lancet. Neurol. 2011; 10:806–818. doi: 10.1016/S1474-4422(11)70155-7 PMID: 21820356

54.   Lemaitre B, Miguel-Aliaga I. The digestive tract of Drosophila melanogaster. Annu. Rev. Genet. 2013; 47:377–404. doi: 10.1146/annurev-genet-111212-133343 PMID: 24016187

55.   Brand AH, Manoukian AS, Perrimon N. Ectopic expression in Drosophila. Methods Cell Biol. 1994; 44:635–654. PMID: 7707973

56.   Calidas D, Lyon H, Culver GM. The N-terminal extension of S12 influences small ribosomal subunit assembly in Escherichia coli. RNA. 2014; 20:321–330. doi: 10.1261/rna.042432.113 PMID: 24442609

57.   Lambertsson A. The minute genes in Drosophila and their molecular functions. Adv. Genet. 1998; 8:69–134.

58.   Böhni R, Riesgo-Escovar J, Oldham S, Brogiolo W, Stocker H, Andruss BF, et al. Autonomous control of cell and organ size by CHICO, a Drosophila homolog of vertebrate IRS1-4. Cell. 1999; 97:865–875. PMID: 10399915

59.   Nässel DR, Liu Y, Luo J. Insulin/IGF signaling and its regulation in Drosophila. Gen. Comp. Endocrinol. 2015 (in press); doi: 10.1016/j.ygcen.2014.11.021

60.   Park S, Alfa RW, Topper SM, Kim GE, Kockel L, Kim SK. A genetic strategy to measure circulating Drosophila insulin reveals genes regulating insulin production and secretion. PLoS Genet. 2014; 10: e1004555. doi: 10.1371/journal.pgen.1004555 PMID: 25101872

61.   Roy S, VijayRaghavan K. Muscle pattern diversification in Drosophila: the story of imaginal myogenesis. Bioessays. 1999; 21:486–498. PMID: 10402955

62.   Birsoy K, Possemato R, Lorbeer FK, Bayraktar EC, Thiru P, Yucel B, et al. Metabolic determinants of cancer cell sensitivity to glucose limitation and biguanides. Nature. 2014; 508:108–112. doi: 10.1038/nature13110 PMID: 24670634

63.   Kang HC, Lee YM, Kim HD, Lee JS, Slama A. Safe and effective use of the ketogenic diet in children with epilepsy and mitochondrial respiratory chain complex defects. Epilepsia. 2007; 48:82–88.

64.   Ahola-Erkkilä S, Carroll CJ, Peltola-Mjösund K, Tulkki V, Mattila I, Seppänen-Laakso T, et al. Ketogenic diet slows down mitochondrial myopathy progression in mice. Hum. Mol. Genet. 2010; 19:1974–1984. doi: 10.1093/hmg/ddq076 PMID: 20167576

65.   Fujii T, Nozaki F, Saito K, Hayashi A, Nishigaki Y, Murayama K, et al. Efficacy of pyruvate therapy in patients with mitochondrial disease: a semi-quantitative clinical evaluation study. Mol. Genet. Metab. 2014; 112:133–138. doi: 10.1016/j.ymgme.2014.04.008 PMID: 24830361

66.   Kerr DS. Review of clinical trials for mitochondrial disorders: 1997–2012. Neurotherapeutics. 2013; 10:307–319. doi: 10.1007/s13311-013-0176-7 PMID: 23361264

67.   Fernández-Ayala DJ, Sanz A, Vartiainen S, Kemppainen KK, Babusiak M, Mustalahti E, et al. Expression of the Ciona intestinalis alternative oxidase (AOX) in Drosophila complements defects in mitochondrial oxidative phosphorylation. Cell Metab. 2009; 5:449–60.

68.   Tennessen JM, Barry WE, Cox J, Thummel CS. Methods for studying metabolism in Drosophila. Methods. 2014; 68:105–115. doi: 10.1016/j.ymeth.2014.02.034 PMID: 24631891

69.   Hinman LM, Blass JP. An NADH-linked spectrophotometric assay for pyruvate dehydrogenase complex in crude tissue homogenates. J. Biol. Chem. 1981; 256:6583–6586. PMID: 7240230

70.   Merritt TJ, Duvernell D, Eanes WF. Natural and synthetic alleles provide complementary insights into the nature of selection acting on the Men polymorphism of Drosophila melanogaster. Genetics. 2005; 171:1707–1718. PMID: 16143603

71.   Merritt TJ, Kuczynski C, Sezgin E, Zhu CT, Kumagai S, Eanes WF. Quantifying interactions within the NADP(H) enzyme network in Drosophila melanogaster. Genetics. 2009; 182:565–574. doi: 10.1534/genetics.109.100677 PMID: 19307608

72. Park SY, Ludwig MZ, Tamarina NA, He BZ, Carl SH, Dickerson DA, et al. Genetic complexity in a Dro-sophila model of diabetes-associated misfolded human proinsulin. Genetics. 2014; 196:539–555. doi: 10.1534/genetics.113.157602 PMID: 24281154

PUBLICATION
II

Mitochondrial dysfunction generates a growth-restraining signal linked to pyruvate in *Drosophila* larvae

Jack George, Tea Tuomela, Esko Kemppainen, Antti Nurminen, Samuel Braun, Cagri Yalgin & Howard T. Jacobs

Mitochondrial dysfunction generates a growth-restraining signal linked to pyruvate in *Drosophila* larvae

Jack George, Tea Tuomela, Esko Kemppainen, Antti Nurminen, Samuel Braun, Cagri Yalgin & Howard T. Jacobs

Taylor & Francis
Taylor & Francis Group

OPEN ACCESS

Check for updates

Mitochondrial dysfunction generates a growth-restraining signal linked to pyruvate in *Drosophila* larvae

Jack George [a], Tea Tuomela [a], Esko Kemppainen [a], Antti Nurminen[a], Samuel Braun[a], Cagri Yalgin[a,b], and Howard T. Jacobs[a,b]

[a]Faculty of Medicine and Health Technology, Tampere University, Tampere, Finland; [b]Institute of Biotechnology, University of Helsinki, Helsinki, Finland

ABSTRACT

The *Drosophila* bang-sensitive mutant tko^{25t}, manifesting a global deficiency in oxidative phosphorylation due to a mitochondrial protein synthesis defect, exhibits a pronounced delay in larval development. We previously identified a number of metabolic abnormalities in tko^{25t} larvae, including elevated pyruvate and lactate, and found the larval gut to be a crucial tissue for the regulation of larval growth in the mutant. Here we established that expression of wild-type tko in any of several other tissues of tko^{25t} also partially alleviates developmental delay. The effects appeared to be additive, whilst knockdown of tko in a variety of specific tissues phenocopied tko^{25t}, producing developmental delay and bang-sensitivity. These findings imply the existence of a systemic signal regulating growth in response to mitochondrial dysfunction. Drugs and RNAi-targeted on pyruvate metabolism interacted with tko^{25t} in ways that implicated pyruvate or one of its metabolic derivatives in playing a central role in generating such a signal. RNA-seq revealed that dietary pyruvate-induced changes in transcript representation were mostly non-coherent with those produced by tko^{25t} or high-sugar, consistent with the idea that growth regulation operates primarily at the translational and/or metabolic level.

Introduction

Mitochondrial dysfunction is a common underlying cause or manifestation of human disease [1–3]. Whilst mammalian models such as the mouse have provided insights into the underlying processes, the use of *Drosophila* to understand mitochondrial pathophysiology has been relatively neglected, despite its versatility and the availability of a wide variety of easily applied genetic tools.

Deficient mitochondrial protein synthesis is frequently associated with mitochondrial diseases [4], and *Drosophila* provides a valuable model to study the physiological effects of limitations on mitochondrial translation in the context of animal development. The *Drosophila tko* gene, encoding mitoribosomal protein S12, a core component of the mitoribosomal decoding centre, has been a particular object of study in this regard. The canonical mutant tko^{25t} displays a range of phenotypic features that resemble mitochondrial disease in humans, including developmental delay, impaired sound-responsiveness, bang-

sensitivity (paralytic seizures induced by mechanical shock) and antibiotic sensitivity [5]. Other tko^{25t} phenotypes are unique to *Drosophila*, such as male courtship defect [5]. These phenotypic features reflect an underlying deficiency of mitoribosomes [5] and consequent global deficiency of the enzymatic functions of oxidative phosphorylation (OXPHOS) that depend upon mitochondrial translation products, manifesting in both adults [5] and larvae [6]. All of these phenotypes are reversed by ubiquitous expression of a transgenic copy of the wild-type *tko* gene, using the UAS/GAL4 system [6]. Since developmental delay occurs during the larval stages [5], this prompts the question as to which of the larval tissues mediates the crucial signalling that regulates growth in response to limitations on mitochondrial protein synthesis, and by what mechanism.

In a follow-up study [7], we obtained some relevant clues as to the underlying mechanism(s) whereby the growth rate of tko^{25t} larvae is adjusted, so as to take account of the decreased capacity for processing

---

nutritional resources caused by mitochondrial dysfunction. In particular, we observed that components of the apparatus of cytosolic protein synthesis and secretion were down-regulated in tko^{25t} larvae, both at the transcript level and via a key regulatory step of cytosolic protein synthesis, the ribosomal protein S6 kinase (S6K). tko^{25t} larvae were also found to be unaffected by low levels of the cytosolic protein synthesis inhibitor cycloheximide, which retarded the development of wild-type larvae, also implicating the cytoribosome as a crucial target in larval growth regulation. Many other genes that were downregulated in tko^{25t} at the RNA level encoded secreted proteins of the gut and cuticle, suggesting that growth rate in tko^{25t} could be adjusted to compensate for stress in the protein secretory system caused by disruption of redox homeostasis.

In the same study [7] we determined that the strength of the tko^{25t} phenotype depends upon the culture conditions, specifically the sugar content of the growth medium. When tko^{25t} flies were cultured on high-sugar medium, their growth was further impaired compared with those grown on low-sugar medium, and many of the observed changes in gene expression were more pronounced. The effect of high sugar was accompanied by increases in the level of pyruvate and lactate in the larvae, whilst supplementation of the medium with pyruvate or lactate exacerbated developmental delay. tko^{25t} larvae also manifested low levels of ATP and a greatly decreased NADPH/NADP ratio, both of which were enhanced by high-sugar medium [7].

A key result from the previous study was the observation that expression of wild-type tko specifically in portions of the larval gut, a major secretory tissue, partially alleviated the developmental delay of tko^{25t} [7]. Since the driver used in this experiment did not express at a high level in all regions of the gut, we reasoned that other gut-specific drivers used in combination might provide a more complete rescue of the phenotype. To embark on such a study, we initially implemented what we assumed would be negative controls, directing wild-type tko expression in other regions of the larva with high specificity. However, this produced the unexpected result that partial rescue of developmental delay was conferred by expression in each of the tissues tested (muscle, fat-body, neurons, as well as gut), with some evidence of additive effects. Conversely, tko knockdown in each specific tissue produced a partial developmental delay, accompanied by bang sensitivity, the canonical adult phenotype of tko^{25t}.

These new findings indicate the existence of a systemic and possibly metabolic signal integrating growth across the entire larva, in response to limitations on mitochondrial translational or OXPHOS capacity. Given the previous findings implicating pyruvate and/or lactate as key regulatory metabolites, we studied the effects of drugs and RNAi targeted on pyruvate and its metabolic transactions. The findings are consistent with pyruvate metabolism playing a central role in generating the signal that links growth and mitochondrial function in *Drosophila* larvae.

Materials and methods

Drosophila strains and culture

Drosophila strains were procured from stock centres, supplied by colleagues or maintained long term in our laboratory. A full list of GAL4 drivers, RNAi lines and other strains used in the study are provided in Tables 1, 2 and 3, respectively. Markers carried on standard balancers were used to distinguish experimental from control progeny. Except where stated, flies were cultured on standard high-sugar medium (HS), as detailed in [7]. A variant, 'zero-sugar' medium (ZS), containing standard dietary supplements but no added sugars [7], was used where indicated. Note that HS and ZS media are not isocaloric: in an earlier study [7] the extent of developmental delay in tko^{25t} flies was shown to depend only on the sugar content of the medium, not its calorific value. Sodium pyruvate, dichloroacetate or UK5099 (Sigma-Aldrich), were added to these media from aqueous stock solutions after the medium had been cooled to below 65°C, giving the final concentrations indicated in the figures.

Developmental and bang-sensitivity assays

Mean developmental time to eclosion and bang-sensitivity were measured as previously [5,7], in temperature-controlled incubators, with temperature verified daily throughout the experiment. In all crosses where developmental time to eclosion was measured, at least 3 (usually 4) replicate vials were studied, and the entire experiment was repeated to validate the findings.

Table 1. GAL4 drivers used in the study.

Name[a]	Stock centre ID[b] or source	Alias, if any	Chromosome	Expression pattern[c]	References[d]
da-GAL4	BL 8641		3	ubiquitous	[8]
gut-GAL4	KY 113094	NP3084	2	midgut, proventriculus, gastric ceca, salivary glands	[7,9], Fig. S1
elav-GAL4	BL 458	c155	X	neurons, embryonic neuroblasts and glioblasts	[10,11]
nrv2-GAL4	BL 6800		2	glial cells, weak expression in some neurons	[12–16], Fig. S1
G14	kind gift of John Sparrow	G14-Gal4	2	muscle, salivary glands	[17–19]
Mef2-GAL4	BL 27390	GAL4-Mef2, DMef2-GAL4	3	muscle	[20]
Kr-GAL4	kind gift of John Sparrow		2	early embryo, larval midgut	[21,22], Fig. S1
Lsp2-GAL4	BL 6357		3	Fat body (third larval instar and adult)	[23,24], Fig. S1

[a]as used here.
[b]BL = Bloomington, KY = Kyoto.
[c]consensus or most recent revision from published literature, or based on figures of this paper.
[d]literature citation(s) or figure of this paper.

Table 2. RNAi lines used in the study.

Symbol of targeted gene	Stock centre ID[a]	Library	Chromosome (insertion)	Reference[b]
tko	BL 38251	TRiP	2	[25,26]
Mpc1	BL 67817	TRiP	2	[25,27]
Pdk	BL 28635	TRiP	3	[25,26]
Men	BL 38256	TRiP	2	[25,26]
Men	VDRC 330428	shRNA	2	[28]
Men	VDRC 104016	KK	2	[28,29]
Men-b	BL 57489	TRiP	2	[25,27]
Men-b	VDRC 100812	KK	2	[28,29]
Ldh	VDRC 110190	KK	2	[29]

[a]BL = Bloomington, VDRC = Vienna Drosophila Research Centre.
[b]literature citation(s).

RNA analysis

Quantitative reverse-transcription PCR (qRTPCR) to confirm the effectiveness of RNAi was conducted as previously [7,37], using RpL32 as an internal standard and verified primer pairs (all shown 5′ to 3′) as follows: for *Pdk* – GGATTCG GAACAGATGCAAT and CGCGATAGAACTTT GAGCTTG, for *Mpc1* – GCCGACACACAAA AGAGTCC and GCTGGACCTTGTAGGCAAAT, for *Men* – ACTCGATCCTACGACGCTGT and TGAGGAAGGACTCTGCGAAT. RNA sequencing and data analysis were carried out as previously [7], using RNA from Oregon R or *tko*^{25t} L3-stage larvae cultured on different media. Note that initial statistical filtering by Cuffdiff (chipster. csc.fi) excludes genes in any pairwise comparison where the differences fail significance testing, regardless of their magnitude. For further analysis (see Results), arbitrary thresholds were then applied to restrict the analysis to genes showing substantial differences in expression, as measured by either of two parameters: >8 fold change

Table 3. Other *Drosophila* strains used in the study.

Name[a]	Stock centre ID[b]	Alias, if any	Chromosome (insertion, mutation or balancer)	Other features[c]	References[d]
tko^{25t}	n/a	tko(25t)	X	Bang-sensitive; coding-region mis-sense mutant	[30–32]
UAS-tko$^+$(1)	n/a		3	transgenic for wild-type copy of *tko* cDNA; without driver does not alleviate bang sensitivity of *tko*^{25t}	[6]
UAS-tko$^+$(8)	n/a		2	transgenic for wild-type copy of *tko* cDNA; without driver does not alleviate developmental delay of *tko*^{25t}	[6]
FM7	BL 995		X	balancer chromosome	[33]
CyO	BL 4959		2	balancer chromosome	[34]
TM3Sb	n/a	TM3-Sb	3	balancer chromosome, currently available from stock centre combined with CyO	[34]
UAS-Stinger	BL 65402	UAS-GFP, UAS-Stinger	2	transgenic expressor of nuclear-targeted GFP	[35]
UAS-mCD8-GFP	KY 108068	mCD8-GFP, + many variants	2	transgenic expressor of membrane-targeted GFP	[36]

[a]as used here.
[b]BL = Bloomington, KY = Kyoto, n/a not currently available from stock centres.
[c]consensus or most recent revision from published literature, or based on figures of this paper.
[d]literature citation(s) or figure of this paper (Figure 1).

or >100 units of FPKM (mass fraction). Raw sequence data have been deposited at ArrayExpress (www.ebi.ac.uk/ArrayExpress/).

Metabolite analysis

Batches of 20 larvae were homogenized in 100 μl of 6M guanidine hydrochloride on ice. The homogenate was incubated at 95°C for 5 min and centrifuged at $12000g_{max}$ for 5 min at 4°C. The supernatants were stored at −80°C, and later diluted 1:10 and with PBS (pH 7.4) for analysis. Pyruvate and lactate were measured with commercially available fluorescence-based determination kits (Abcam) according to manufacturer's instructions. 10 μl of sample was combined with 50 μl of either lactate or pyruvate reaction mix, incubated at room temperature for 30 min after which fluorescence was measured (excitation at 535 nm, emission at 590 nm) using a plate reader. Lactate and pyruvate standards were used to generate standard curves and concentrations were normalized to soluble protein as measured using the Bradford method.

Statistics

For pairwise comparisons between groups, the two-tailed (unpaired) Student's t test (Microsoft Excel) was applied. For multiple comparisons, we used one-way ANOVA with Tukey *post hoc* HSD test online (astatsa. com). For comparisons where multiple factors were being assessed, two-way ANOVA (GraphPad Prism or online tool at vassarstats.net/anova2u.html, as indicated) was used, together with Dunnett's or Tukey's *post hoc* multiple comparisons tests as indicated, where interactions were detected, or where more than two levels were compared.

Results

Wild-type tko *expression in diverse tissues alleviates developmental delay in* tko[25t]

Using the line UAS-tko[+](8) [6], in which a wild-type *tko* transgene is expressed under the control of GAL4, we tested the tissue-specificity of developmental delay in the *tko*[25t] background, by combining it with different GAL4 drivers directing distinct tissue patterns of expression. In addition to almost complete rescue

using *da*-GAL4 and the partial rescue with gut-GAL4 documented previously, we found that drivers specific for the fat body (*Lsp2*-GAL4), muscle (G14 and *Mef2*-GAL4) and CNS (neurons, *elav*-GAL4) all gave a partial rescue (Figure 1), although this was most pronounced or significant in each case at different characteristic temperatures (Table S1).

We confirmed the specificity of patterns of expression of these drivers using GAL4-dependent constructs for GFP (Fig. S1). The alleviation of the phenotype was due to a positive effect of the transgene/driver combination, and not due to a negative effect of the CyO balancer chromosome in the *tko*[25t] background (Fig. S2). Note, however, that this was not true of the TM3Sb balancer (Fig. S2), the use of which was therefore avoided in all experiments described.

The partial rescue produced by several drivers appeared to be additive, based on two lines of evidence. First, we attempted to combine pairs of drivers and the UAS-tko[+](8) transgene. This experiment was technically challenging for several reasons: the problematic nature of the TM3Sb balancer precluded its use; some transgenic combinations had poor viability, especially as homozygotes, and the drivers did not all perform optimally at the same temperature. However, the combination of the fat-body and muscle drivers *Lsp2*-GAL4 and G14 appeared to give an additive enhancement at 22°C (Fig. S3), although this should be interpreted cautiously, due to the imperfect experimental design. The second piece of evidence for a combinatorial effect was that a second transgenic line, UAS-tko[+](1), which already showed a one-day alleviation of developmental delay compared with *tko*[25t] flies bearing no transgene [6], showed a further alleviation of developmental delay when combined with different GAL4 drivers (Figure 2). These findings suggest the operation of a systemic signal that integrates the degree of mitochondrial dysfunction across tissues, calibrating growth to the ability of the organism to process nutritional resources.

RNAi-mediated tko *knockdown in diverse tissues phenocopies* tko[25t]

To further test this hypothesis, we used RNA-mediated knockdown of *tko* to profile the tissues in which the resulting mitochondrial translational deficit leads to a *tko*[25t]-like phenotype. Ubiquitous *tko* knockdown using the *da*-GAL4 driver and the
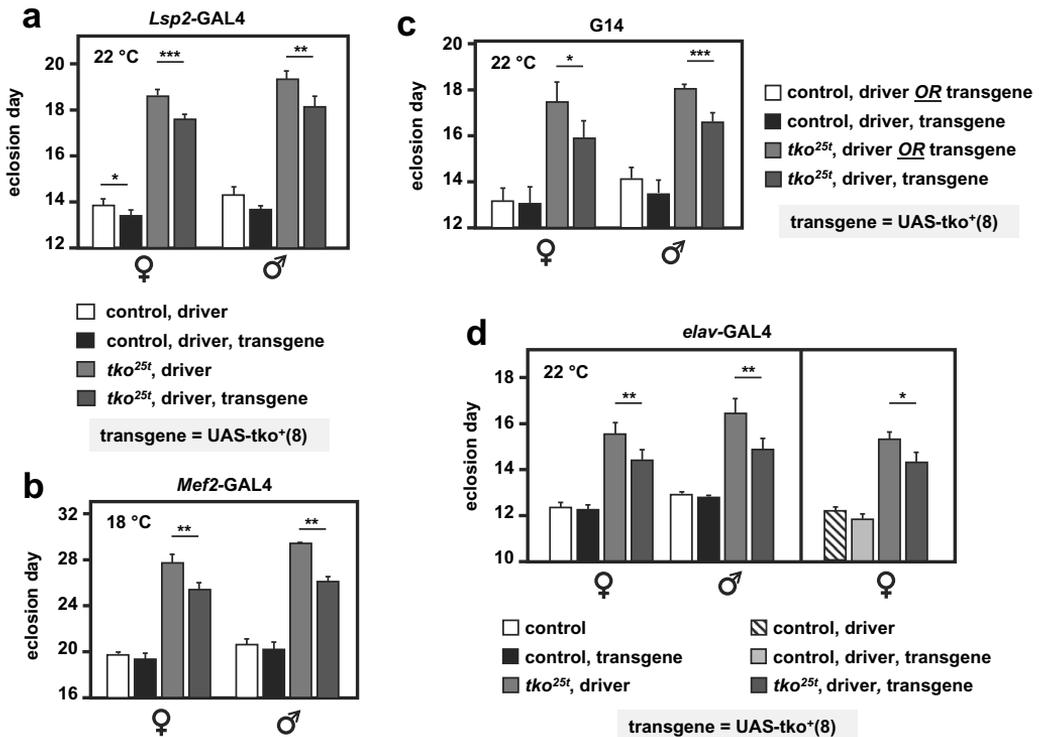
Figure 1. tko^{25t} developmental delay is partially alleviated by tko^+ expression directed by different drivers. Time to eclosion (means ± SD, n ≥ 3 replicate vials for each cross), of flies of the indicated genotypes, using UAS-tko^+(8) with the indicated drivers. Controls were FM7 balancer flies with (a, b and d – right-hand panel) driver but no transgene, (c), driver *or* transgene (these classes could not be distinguished due to the nature of the cross, since the G14 driver is not viable as a homozygote), and (d – left-hand panel) neither transgene nor driver, as dictated by the chromosomal location of the drivers. Because the *elav*-GAL4 driver is located on the X chromosome, one of the two reciprocal crosses used in (d) generates only informative females and not males. Horizontal lines denoted by asterisks (*, **, ***) indicate significant differences in pairwise comparisons of flies of a given sex and *tko* genotype, with and without actively driven tko^+ (Student's *t* test, $p < 0.05, 0.01, 0.001$, respectively. The specificity of each driver was confirmed by parallel crosses in which it was used to direct the synthesis of nuclear- or membrane-localized GFP (see Fig. S1). Note that we avoided the use of the TM3 balancer because we established that it conferred a developmental delay in conjunction with tko^{25t}, whereas the chromosome 2 balancer CyO did not (Fig. S2). The partial rescue of developmental delay was also observed at other temperatures with some drivers (see Table S1) and using the alternate transgene UAS-tko^+(1) – see Figure 2. Note that most GAL4 drivers exhibit the classic pattern of temperature dependence [38], i.e. increased activity at higher temperature. However, for the strongest drivers, this may also lead to deleterious effects of over-expression at high temperature, such that a lower temperature produces optimal effects.

Bloomington TRiP line 38251 targeted on *tko* resulted in a phenotype resembling an exaggerated version of tko^{25t}. At 25°C *tko* knockdown was lethal, whilst at 22°C, it was lethal to males and semilethal to females, which eclosed with a long delay (5–9 d) and were too weak to permit a meaningful test of their bang-sensitivity. At 18°C females eclosed with a 7 to 8-d delay (Figure 3(a)) and were highly bang-sensitive (Figure 4(a)), whilst the few males that eclosed were even more delayed (Figure 3(a)) and extremely weak. Knockdown

using tissue-specific drivers produced a milder version of the same phenotype, whether knockdown was targeted specifically to neurons (using *elav*-GAL4, Figures 3(b), 4(b)) or muscle (*Mef2*-GAL4 at 18°C, Figures 3(c), 4(c)). Even more limited knockdown targeted on the early embryo, and portions of the midgut (*Kr*-GAL4, Figure 3(d), Fig. S1) also produced a significant, though very modest developmental delay, but without bang-sensitivity (Figure 4(e)). *Mef2*-GAL4-driven *tko* knockdown at higher temperatures (22, 25°C) again gave
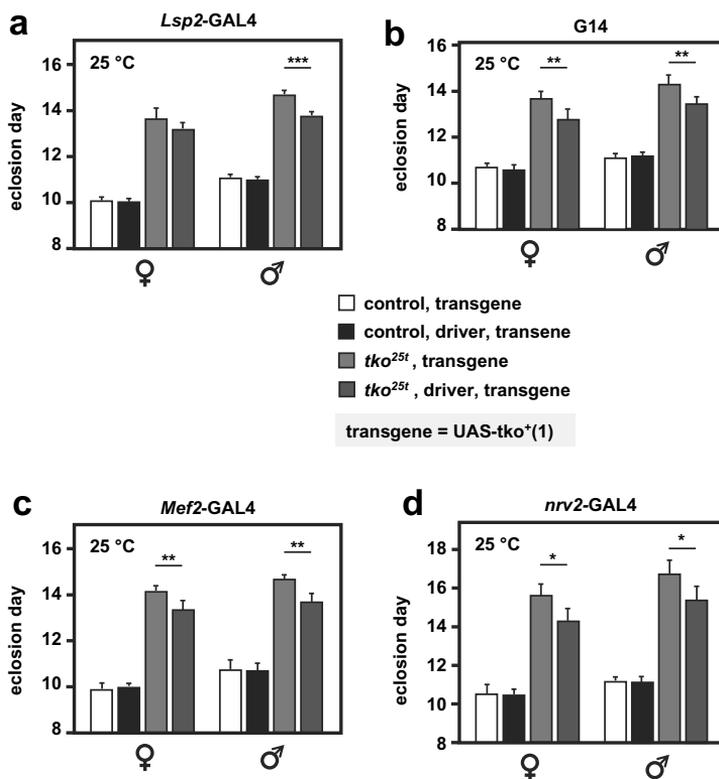
Figure 2. Alleviation of *tko*[25t] developmental delay in a second UAS-*tko*[+] line. Time to eclosion at 25°C (means ± SD, n ≥ 3 replicate vials for each cross), of flies of the indicated genotypes, using various drivers plus the UAS-*tko*[+](1) transgene, shown previously to confer a modest rescue of developmental delay without any driver [6]. Controls were FM7 balancer flies with transgene but without driver, as shown. Horizontal lines denoted by asterisks (*, **, ***) indicated significant differences in pairwise comparisons of flies of a given sex and *tko* genotype, with and without actively driven *tko*[+](Student's *t* test, $p < 0.05$, 0.01, 0.001, respectively. The specificity of each driver was confirmed by parallel crosses in which it was used to direct the synthesis of nuclear- or membrane-localized GFP (see Figure S1). Note that we avoided the use of the TM3 balancer because we established that it conferred a developmental delay in conjunction with *tko*[25t], whereas the chromosome 2 balancer CyO did not (Fig. S2).

semilethality and severe weakness, which was more severe in males. *elav*-GAL4-driven knockdown also gave sex- and temperature-dependent bang-sensitivity: at 25°C flies were extremely weak, whilst developmental delay was seen at all temperatures but was generally significant only in males (Figure 4(b)). Driving *tko* knockdown with the glial driver *nrv2*-GAL4 gave no bang sensitivity (Figure 4(d)).

Drugs that affect pyruvate metabolism impact larval growth

In principle, a systemic signal regulating growth according to mitochondrial function could be endocrine or metabolic in nature. Candidate metabolites

for such a role that were previously shown to be markedly abnormal in *tko*[25t] larvae, include pyruvate and lactate, which were approximately threefold elevated, and NADPH and ATP, which were highly depleted [7]. Since ATP and NADPH may be considered too labile to perform an intercellular role, we focused our attention on pyruvate and lactate, which are interconvertible through lactate dehydrogenase, and which were previously found to exacerbate and phenocopy the developmental delay of *tko*[25t], when added to the medium ([7], Figure 5(a)). We investigated the developmental effect of two drugs known to affect pyruvate metabolism, dichloroacetate (DCA), an inhibitor of pyruvate dehydrogenase kinase (Pdk) and UK5099, an inhibitor of the mitochondrial pyruvate carrier, which could be predicted to have
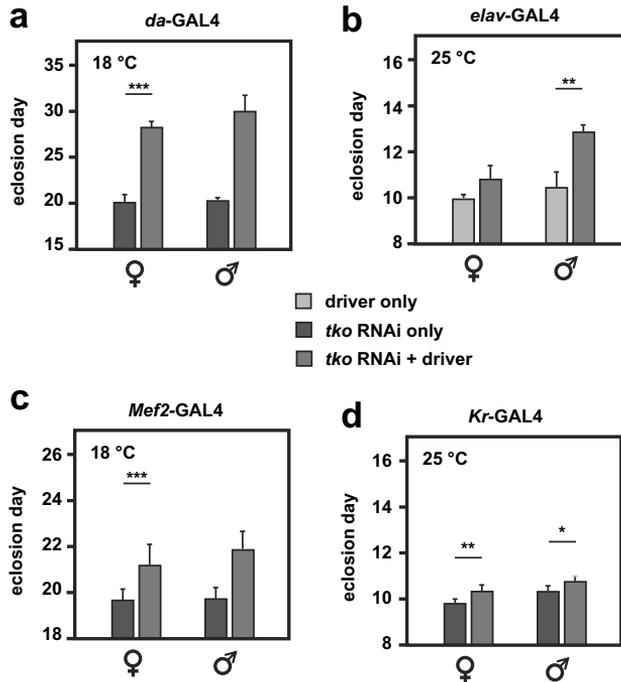
Figure 3. RNAi knockdown of *tko* by different drivers results in developmental delay. Times to eclosion (means ± SD, n ≥ 3 replicate vials for each cross) for flies of the indicated sex and genotype, using the various drivers at the temperatures shown. Horizontal lines denoted by asterisks (*, **, ***) indicate significant differences in pairwise comparisons between knockdown and control flies of a given sex, using a given driver (Student's *t* test, $p < 0.05, 0.01, 0.001$, respectively). Note that males were in general more severely affected and in some cases (e.g. *da*-GAL4) too few males eclosed to permit a statistically meaningful analysis. Note that most GAL4 drivers exhibit the classic pattern of temperature dependence [38], i.e. increased activity at higher temperature. However, for the strongest drivers this may also lead to highly deleterious effects at high temperature, such that, at a lower temperature, results are more informative.

opposite effects on mitochondrial pyruvate utilization. We tested different concentrations of pyruvate and DCA for their effects on the development of wild-type and *tko²⁵ᵗ* females in ZS medium (Figure 5(b)), and performed a more extensive study at single, effective concentrations on different media and both sexes, including heterozygous *tko²⁵ᵗ* females (Figure 5(a)). Like pyruvate, DCA produced an additional, dose-dependent developmental delay in both *tko²⁵ᵗ* as well as in wild-type flies (Figure 5(a, b, S5)).

UK5099 (25 µg/ml) also exacerbated the developmental delay of *tko²⁵ᵗ*, but had no significant effect on the eclosion timing of wild-type flies (Figure 5(a, S5)).

Genetic manipulations that affect pyruvate metabolism impact larval growth and survival

Next, we analyzed the effects of knocking down the genes coding for the key proteins of pyruvate

metabolism targeted by these drugs. The mitochondrial pyruvate carrier is a heterodimer of the ubiquitous subunit Mpc1 (CG14290) and a differentially expressed second subunit, Mpc2, encoded in *Drosophila* by a small gene family (CG9396, CG9399 and CG32832, the latter being testis specific). Pdk is encoded by a single-copy gene (*Pdk*, CG8808). Using the available RNAi lines for *Mpc1* and *Pdk* from the Harvard Medical School TRiP library, we first confirmed that knockdown for each of the two genes using the ubiquitously acting *da*GAL4 driver gave viable flies, and used qRTPCR to verify that knockdown was effective at the RNA level (Figure 6(a)). We then evaluated the effects of knockdown on wild-type and *tko²⁵ᵗ* flies gown in standard high-sugar medium, or on medium supplemented with 25 mg/ml pyruvate (Figure 6(b)). *Mpc1* or *Pdk* knockdown produced no effect on eclosion timing in wild-type flies cultured on standard medium. However, when pyruvate was
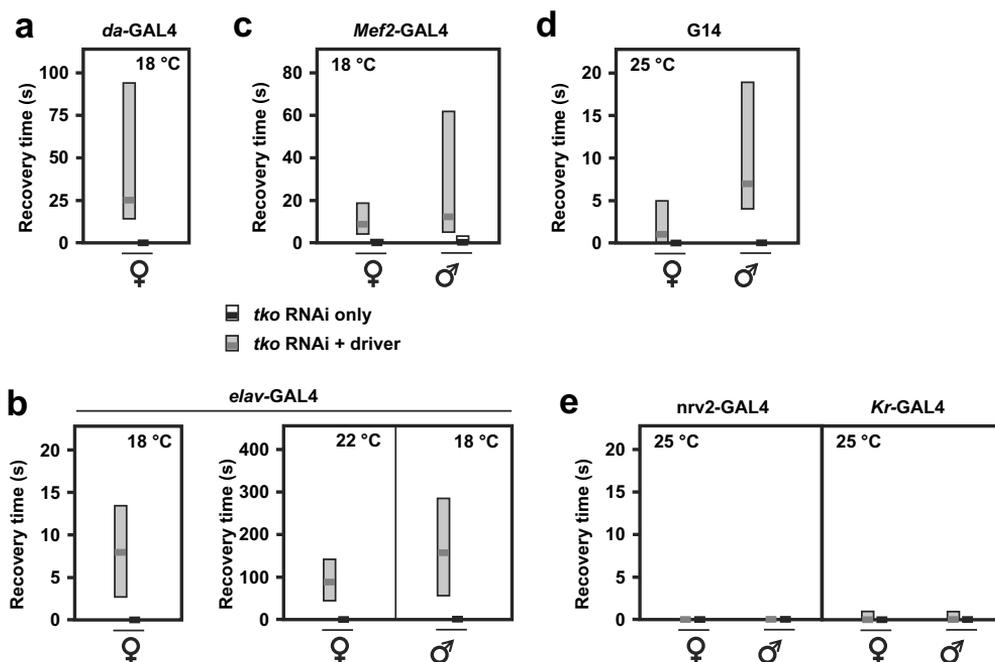
Figure 4. RNAi knockdown of *tko* by different drivers results in bang-sensitivity. Box-plots of recovery times from mechanical shock (bold black or red lines – medians, respectively, for controls and *tko* knockdown flies, with filled boxes representing first to third quartiles) of flies of the indicated genotype, sex and culture temperature. Note the different scales required to plot these data. White bars for control flies were in most cases not plottable, since median and both quartiles were at or very close to zero.

added to the medium, *Mpc1* knockdown exacerbated the developmental delay produced in wild-type flies, but not that of *tko*[25t] (Figure 6(b), panel i), whilst *Pdk* knockdown had no effect on eclosion timing of wild-type flies on either medium, but mildly alleviated the developmental delay of *tko*[25t] (Figure 6(b), panel ii) on pyruvate-supplemented medium (see Fig. S6 for summary of the relevant statistical analyses by two-way ANOVA).

Knockdown of two other genes of pyruvate metabolism, coding, respectively, for the cytosolic and mitochondrial isoforms of malic enzyme, produced more dramatic results in combination with *tko*[25t]. In our previous study, we observed that knockdown of *Men*, the gene encoding the cytosolic isoenzyme, produced no significant effects on *tko*[25t] (Figure 4(c) of [7]). In the present study we were able to make use of more potent and specific TRiP lines for *Men*, as well as one further dsRNA line from the VDRC collection, all of which gave a strong knockdown of the gene at the RNA level under the control of *da*-GAL4 (Figure 7(a)), but had no significant effect

on the development of otherwise wild-type flies (Figure 7(b)). However, in combination with *tko*[25t] they were all developmentally lethal or semilethal at both 29°C and 25°C (Figure 7(c)). Both of the *Men-b* knockdown lines produced a developmental delay in wild-type flies, and were again synthetically lethal with *tko*[25t] (Fig. S4), but this result should be interpreted cautiously, since we were not able to demonstrate convincing and consistent knockdown of *Men-b* at the RNA level by qRTPCR, using several different primer sets. Knockdown of lactate dehydrogenase (*Ldh*) was lethal to both wild-type and *tko*[25t] larvae, making comparable experiments uninformative.

Despite their similar effects on eclosion timing (Figure 5), the addition of pyruvate and DCA to the low-sugar culture medium had opposite effects on the tissue levels of pyruvate and lactate in L3 larvae (Figure 8), although the changes were only significant for pyruvate levels (Tables S3). Pyruvate addition increased both lactate and pyruvate to levels comparable with those seen in high-sugar medium, whilst DCA lowered them, in accord with the expectation
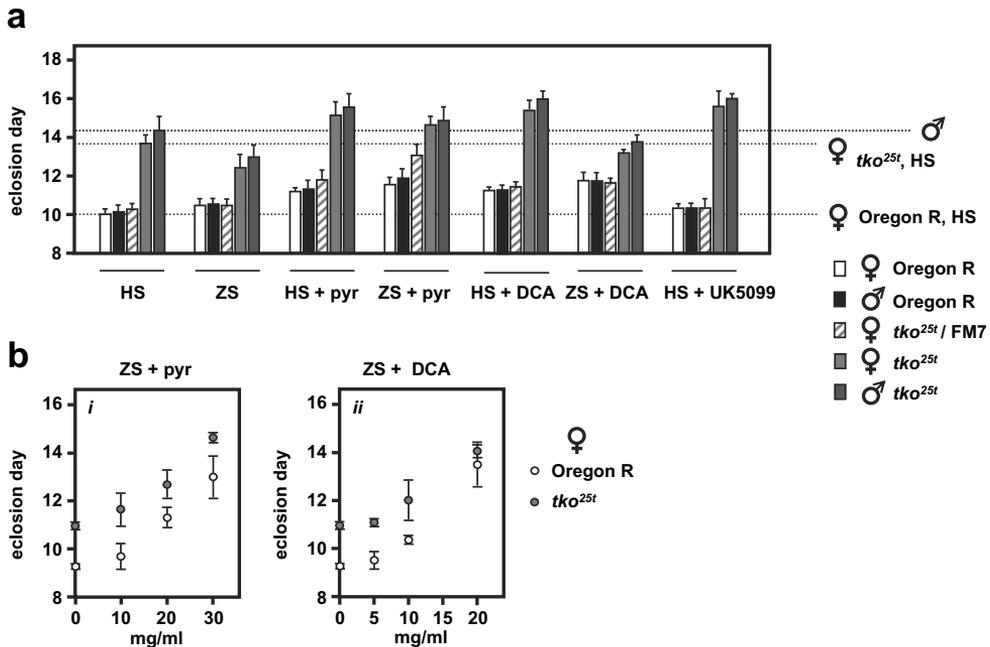
Figure 5. Drugs affecting pyruvate metabolism modify the *tko*[25t] phenotype. Means ± SD of times to eclosion of flies of the indicated genotypes and sex, at 25°C, on different media: HS – standard high-sugar medium, ZS – zero sugar medium, with addition of the indicated drugs that were present throughout the experiment: pyr – pyruvate, 25 mg/ml in (a) and concentrations as indicated in (b), DCA – dichloroacetate, 12.5 mg/ml in (a) and concentrations as indicated in (b), UK5099 – 25 μg/ml. For statistical analysis of data from (a) by two-way ANOVA, see Figure S5. In summary, this revealed a significant effect of both genotype and drug addition ($p < 0.001$) for both diets and sexes, as well as an interaction between genotype and drug addition for both sexes on HS diet ($p < 0.01$) and for females only, on ZS diet ($p < 0.001$). Tukey *post hoc* HSD test ($p < 0.05$) was used, where appropriate, to determine the source of variation (see Figure S5 and comments in main text). Note that some of the data from (a) was previously published in [7], but without this statistical analysis, but is included here for full comparison. For a summary diagram of the reactions targeted by these drugs and by RNAi (see Figure 10).

that it would augment pyruvate metabolism by removing inhibition from (i.e. activating) PDH. The different effects of pyruvate and DCA imply that growth rate cannot be determined directly or solely by pyruvate concentration averaged across the tissues. Instead, a metabolite of pyruvate, or pyruvate in a specific intracellular or tissue-compartment, is likely to be instrumental.

Gene expression changes induced by pyruvate are non-coherent with those induced by tko[25t]

Growth of *tko*[25t] in high sugar was previously observed to downregulate some components of the protein synthetic and secretory machinery, as well as a number of key genes involved in developmental progression. These effects were seen also

seen in zero-sugar medium but were less pronounced. We used RNA-seq to test whether pyruvate addition produced the same changes in gene expression, applying similar criteria as in the previous study [7]. Using each of two parameters (i) absolute magnitude of changes measured by mass fraction (FPKM), and (ii) fold-change, we created lists of the genes showing the most pronounced alterations in expression due to pyruvate supplementation (Table S4). We considered both protein-coding and non-coding RNAs, as well as increases and decreases. From these 'base-comparison' lists of pyruvate-regulated genes (198 in the mass-fraction list and 248 in the fold-change list, applying arbitrary thresholds of >100 FPKM units or >eightfold change, Tables S4) we asked how many are regulated similarly in each of
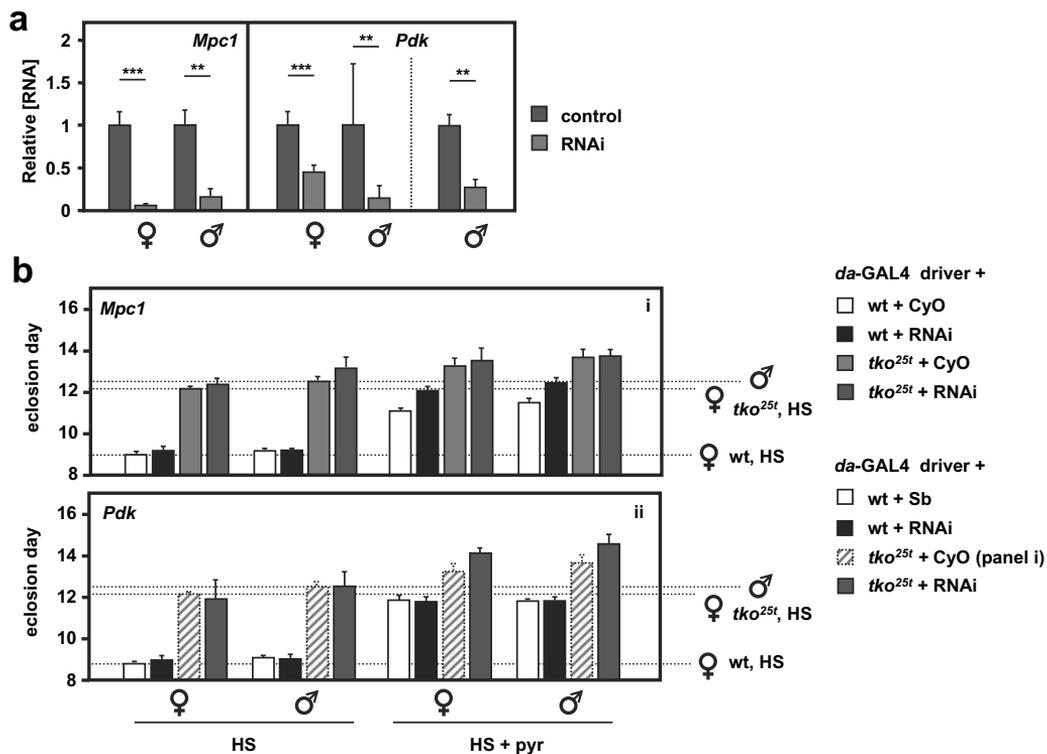
Figure 6. RNAi-mediated knockdown of *Mpc1* or *Pdk* modifies the *tko²⁵ᵗ* phenotype. (A) *Mpc1* or *Pdk* RNA levels measured by qRTPCR and (B) time to eclosion of flies of the indicated genotypes (i.e. with relevant RNAi construct or balancer as shown), at 25℃, means ± SD, n ≥ 3 vials from each cross on the indicated medium: HS – high-sugar medium, with or without the addition of 25 mg/ml pyruvate. Horizontal dotted lines represent the mean eclosion times of Oregon R females and *tko²⁵ᵗ* females and males on HS medium, to facilitate comparisons. Statistical analysis by two-way ANOVA (Fig. S6) revealed a significant effect of genotype under all conditions, but both *Mpc1* and *Pdk* knockdown produced significant effects and showed significant interaction with genotype only in HS medium supplemented with pyruvate; *Mpc1* knockdown retarding the development only of wild-type and *Pdk* knockdown retarding only that of *tko²⁵ᵗ* flies of both sexes. Note that, in panel ii of (B), the CyO balancer flies from panel i, generated in the same experiment, are presented as the best indicative control. The TM3 balancer chromosome, whether marked with *Sb* or *Ser*, confers a developmental delay of >1 d that precludes its use as a control in such experiments, other than to allow identification of the non-balancer RNAi-bearing flies. Apart from this, all comparisons between control and knockdown flies of a given sex and genotype were from the same experiment, although Oregon R and *tko²⁵ᵗ* flies were analyzed from separate crosses, as were flies cultured on different media. For a summary diagram of the reactions targeted by RNAi and by various drugs see Figure 10.

six additional comparisons (Figure 9). In each output we considered the genes from the base-comparison list in five categories: those regulated in the same direction, either (i) above or (ii) below the arbitrary thresholds, those regulated in the opposite direction, again (iii) above or (iv) below threshold, and (v) those missing from the compared list, due to the initial statistical filtering. This analysis enabled us to draw the following conclusions, illustrated in Figure 9. First, most of the genes up- or down-regulated by pyruvate in wild-type larvae were regulated similarly by pyruvate in *tko²⁵ᵗ* (comparison 1 in Figure 9). Second, only a minor subset of genes (≤15%) were regulated in the same direction by high-sugar (comparisons 2 and 3). Many genes were oppositely regulated by the presence of *tko²⁵ᵗ* (comparisons 4 and 5), and many pyruvate-regulated genes in wild-type showed either no effect or a change in the opposite direction in *tko²⁵ᵗ* larvae (comparison 6). The two approaches (mass-fraction and fold-change) gave similar outcomes. The functionally identified genes regulated similarly by pyruvate and by sugar were mostly linked to development
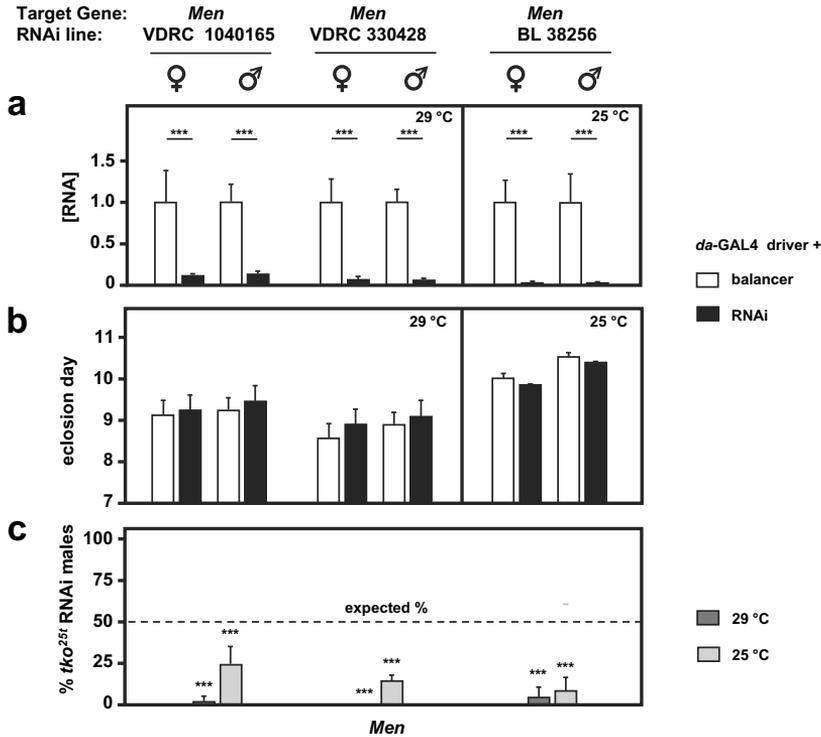
Figure 7. RNAi-mediated knockdown of *Men* (malic enzyme is synthetically (semi)lethal with *tko*[25t]. (a) *Men* RNA levels measured by qRTPCR and (b) time to eclosion of flies of the indicated genotypes (i.e. with relevant *Men* RNAi construct or balancer as shown), means ± SD, n ≥ 3 vials from each cross. Eclosion timing is shown for the temperature at which flies were also cultured for qRTPCR (25°C or 29°C as shown). Eclosion timing at the other temperature was qualitatively similar, as shown in Fig. S4A. Horizontal bars denoted by asterisks (**) indicate significant differences, in pairwise comparisons of RNAi and balancer control flies of each given genotype and sex analyzed (Student's *t* test, *p* < 0.001). (c) Proportion (%) of eclosing RNAi male progeny that also carried *tko*[25t], as opposed to the FM7 balancer, from crosses of the general type: *tko*[25t]/FM7; daGAL4 x FM7/Y; RNAi. Means ± SD, n ≥ 3 vials from each cross. Asterisks (***) above the bars denotes significant deviation from expected frequency of 50% (chi-squared test with Yates' continuity correction, *p* < 0.001). See also Fig. S4. For a summary diagram of the reactions targeted by RNAi and by various drugs see Figure 10.

(cuticular, muscle and a few gut proteins: Tables S5, sheet 1). Many of them, or others in the same functional categories, were oppositely altered in *tko*[25t] (Tables S5, sheet 2). Many of the remaining genes regulated by dietary pyruvate, that were not affected by sugar or by *tko*[25t], code for components of the gene expression machinery or for OXPHOS and other mitochondrial functions (Table S4).

Discussion

Developmental delay in *tko*[25t] depends on a systemic signal

Three lines of evidence presented in this paper support the idea that a systemic signal links mitochondrial function to growth rate in *Drosophila* development. First, the developmental delay of *tko*[25t] mutant larvae could be partially corrected (Figure 1) by expression of the wild-type allele via any of several different tissue-specific drivers, showing little or no overlap in the specificity of their expression (Fig. S1). Second, as far as could be demonstrated, these effects were additive (Figure 2, S4). Third, RNAi-mediated knockdown of *tko* using similarly specific drivers regenerated the mutant phenotype of *tko*[25t], including both developmental delay as well as (at least in some cases) bang-sensitivity. These observations imply that diminished mitochondrial function in a specific tissue is somehow integrated across the entire larva, presumably by
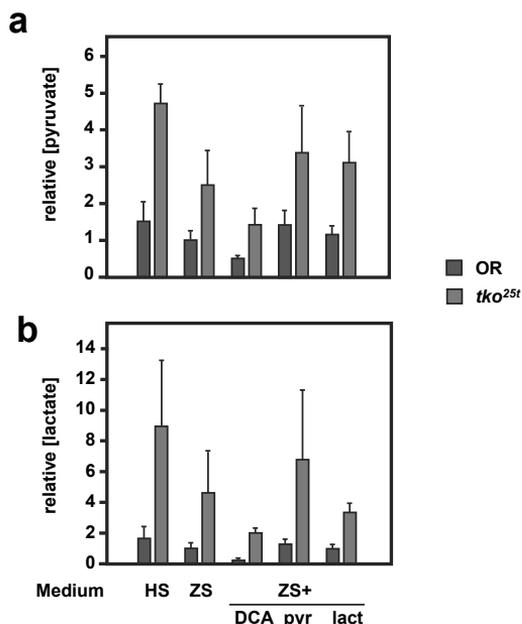
Figure 8. DCA modifies pyruvate and lactate levels oppositely from the effect of pyruvate addition. (a) Pyruvate and (b) lactate levels (means ± SD, n ≥ 3, generally four batches for each group) in L3 larvae of the indicated genotypes (OR = Oregon R wild-type). HS – high-sugar medium, ZS – zero-sugar medium, DCA – with addition of 12.5 mg/ml DCA, pyr, lac – with addition of 25 mg/ml pyruvate or lactate, respectively. Data are normalized to the values for wild-type on ZS medium. For statistical analysis, see Tables S3. For a summary diagram of the reactions targeted by drugs and RNAi see Figure 10.

the sharing of metabolites and their processing. Furthermore, this is not an all-or-none phenomenon, where growth is switched between two alternate programs whenever mitochondrial function crosses some threshold: the amount of developmental delay is variable, implying that the overall metabolic capacity of the larva is somehow being measured physiologically, and growth rate adjusted accordingly. These findings could be further strengthened by the use of additional drivers, especially in combination, although the problematic nature of the TM3 balancer means that we would need first to identify those carried on chromosome 3 that were viable as homozygotes (also with no maternal effects) and which had no unreported off-target expression patterns.

As indicated above, we hypothesized that such a signal could be either endocrine or metabolic in nature, or a combination of both. Endocrine signals

of metabolic – specifically mitochondrial stress are well established in other organisms, such as FGF21 or GDF15 in mammals [39]. Although both of these growth-factor superfamilies have representatives in insects, neither has a clear orthologue in *Drosophila*. The closest match to human GDF15, Glass bottom boat, is much more similar to other members of the BMP/TGFβ superfamily, whilst none of the three *Drosophila* FGFs (Pyramus, Thisbe and Branchless) is a convincing match to human FGF21, and each of them plays a well-studied role in specific developmental programs (see [40] for review).

Two other well-known endocrine systems in *Drosophila* do provide a more direct connection between growth regulation and mitochondrial metabolism, namely the insulin-like peptides and the steroid hormone ecdysone. The insulin/IGF signalling system in the fly [41,42] is responsive to metabolic and nutritional signals to co-ordinate growth and behaviour, whilst ecdysteroids, partly synthesized in mitochondria [43,44], regulate progression between the different developmental stages, especially the onset of metamorphosis [45]. It will be worthwhile to study whether either interacts with *tko*[25t].

Tissue-specificity of the bang-sensitive phenotype

Bang-sensitivity is reported as a feature of mutants in two other genes for core functions of mitochondria, namely *sesB* (adenine nucleotide translocase) [46] and *kdn* (citrate synthase) [47]. These mutants, as well as *tko*[25t], show ATP depletion [47–49]. Global *tko* knockdown was here shown to phenocopy both the developmental delay (Figure 3) and bang-sensitivity (Figure 4) of the original *tko*[25t] mutant, supporting the view that *tko*[25t] is a simple hypomorph. However, the two phenotypes are clearly separable, based on the fact that the transgenic line UAS-tko[+](8) shows no rescue of developmental delay in the absence of a GAL4 driver, but does exhibit effective rescue of bang-sensitivity [6], due, presumably, to an insertional effect [50]. The use of tissue-specific drivers to knock down *tko* sheds further light on this, since exclusively neuronal or muscle drivers both gave a bang-sensitive phenotype (Figure 4(a–c)), whereas a glial driver or one active in embryogenesis and in parts of the larval midgut (Fig. S1A) did not (Figure 4(d,e)). These findings imply
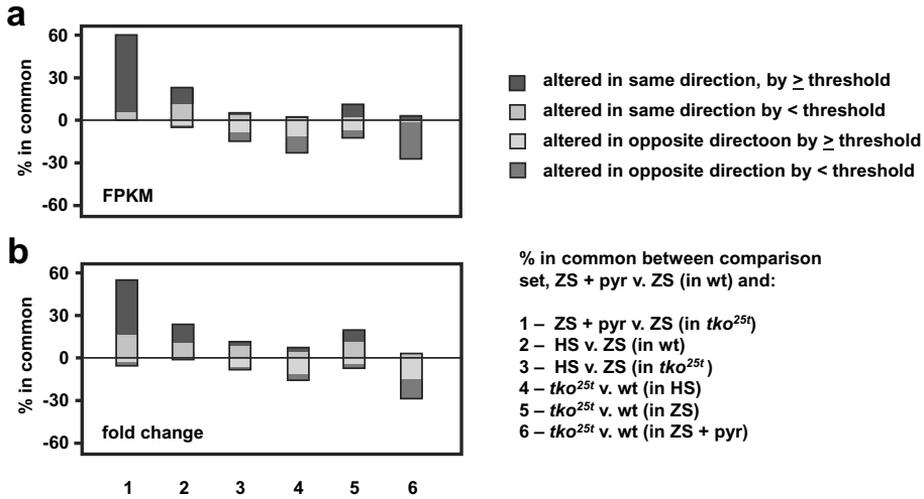
Figure 9. Gene expression changes induced by pyruvate are mostly different from those induced by high-sugar or tko^{25t}. Plotted comparisons are based on analysis by (a) FPKM (mass-fraction) and (b) fold-change, with arbitrary threshold of 100 FPKM units or eightfold change, respectively. The plot ignores the actual direction of change and the nature of the regulated transcripts (protein-coding or non-coding RNA) but instead shows whether the direction of change is the same or different between the base-comparison (genes regulated by pyruvate addition to zero-sugar medium) and the comparisons as enumerated. In each case, the changes to the remaining genes from the base-comparison set did not pass statistical filtering in the other comparisons.
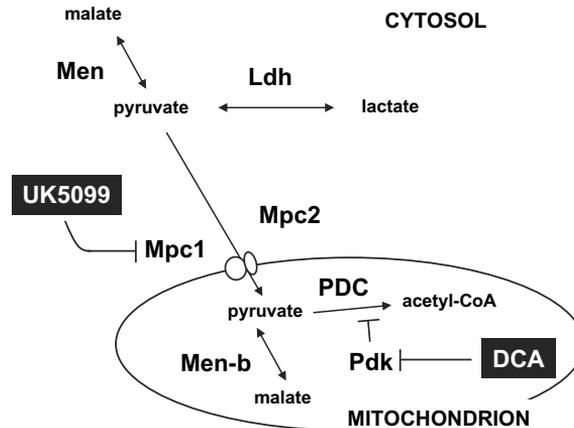
Figure 10. Summary diagram of steps in the pyruvate metabolic network targeted by drugs and RNAi. Metabolites are shown in black text, proteins in red, and drugs in white on black. Mpc1, Mpc2, Pdk, Men, Men-b and Ldh are shown by the systematic names from flybase. PDC – pyruvate dehydrogenase complex. For clarity, enzymes not targeted in the present experiments (such as pyruvate kinase and pyruvate carboxylase) are omitted.

that adequate mitochondrial OXPHOS capacity in muscle and in neurons, but not in other tissues, is required to avoid the prolonged paralytic seizures characteristic of tko^{25t}. The severity of the bang-sensitive phenotype produced by knockdown of tko using different GAL4 drivers is comparable with, or in some cases stronger, than that produced by tko^{25t}. However, since the relative strength of the various tissue-specific drivers is not easily measured, the significance of this cannot be assessed.

Lactate and pyruvate metabolism is linked to growth regulation in tko^{25t}

Candidates for a metabolic signal of mitochondrial dysfunction were already suggested by the previous

observation of elevated pyruvate and lactate levels in tko^{25t} larvae [7], and the fact that their addition to the culture medium phenocopied the effects of high-sugar on tko^{25t}. Serum lactate is already considered a key biomarker for diagnosing OXPHOS disorders in humans [39], whilst pyruvate has been identified as a crucial regulator of stemness and growth in mammalian cells [51]. In flies, the enzyme that inter-converts lactate and pyruvate, lactate dehydrogenase (Ldh, or ImpL3) has previously been implicated as a target of growth signalling by the estrogen-related receptor [52]. This offered an attractive starting point for the present study.

Drugs and genetic manipulations that affect pyr-uvate metabolism (summarized in Figure 10) impacted the development of tko^{25t} (and, in some cases, wild-type flies), broadly supporting the view that pyruvate accumulation is a marker for a metabolic process that limits growth. The growth-inhibiting effects of pyruvate and of DCA were also dose-dependent. However, measurements of lactate and pyruvate levels in flies grown on different media (Figure 8) implied that neither was a direct predictor of developmental phenotype, which may instead depend on a downstream product of pyruvate meta-bolism. Thus, pyruvate or lactate supplementation resulted in only a modest increase in the steady-state level of pyruvate, whereas DCA, which substantially decreased pyruvate and lactate levels (Figure 8), pro-duced paradoxical effects on developmental timing, accelerating the growth of tko^{25t} on zero-sugar med-ium, but retarding that of wild-type flies, whilst in high-sugar medium it compounded rather than alle-viated tko^{25t} developmental delay (Figure 5(b)). Pdk knockdown exacerbated the developmental delay of tko^{25t} (Figure 6(b), ii), but only under conditions of pyruvate overload. Although DCA is a potent inhi-bitor of Pdk [53], it may also have other targets [54–56] and is accumulated in cells via the plasma-membrane monocarboxylate transporters, MCTs [57]. Moreover, in cancer cells, it has been reported to inhibit the pentose phosphate pathway [58] and thereby decrease the level of NADPH, which is already depleted in tko^{25t}, especially when grown on high-sugar medium [7]. Such off-target effects may account for the different outcomes of DCA treatment and Pdk knockdown.

UK5099, predicted to limit mitochondrial pyru-vate utilization by inhibiting the mitochondrial pyruvate carrier, produced a clear exacerbation of the tko^{25t} developmental phenotype (Figure 5(b)), whilst $Mpc1$ knockdown produced different effects, slowing the growth of wild-type flies under pyruvate overload, but exhibiting only minor effects on tko^{25t} development that were essentially epistatic to the effect of added pyruvate (Figure 6(b), i). Although originally identified as an inhibitor of the mitochon-drial pyruvate carrier [59], UK5099 was subsequently shown to block MCTs as well [60–63]. If it blocks lactate efflux in $vivo$, its net effect may be to increase cytosolic lactate and/or pyruvate independently of its effects on mitochondria, potentially accounting for the different outcome of $Mpc1$ knockdown. Other, more specific inhibitors, such as PS10 for Pdk [64], or GW604714X and GW450863X for the mitochon-drial pyruvate carrier [65], may prove useful in dis-entangling these effects, although their efficacy and specificity would need to be verified for $Drosophila$.

The findings with Men are also consistent with pyruvate being a critical metabolite, although the effect on tko^{25t} was lethality rather than extended develop-ment. One possibility is that a high level of pyruvate facilitates NADPH depletion via the NADPH-dependent conversion of pyruvate to malate catalyzed by Men. If, as hypothesized earlier, NADPH depletion is a critical element of growth signalling in tko^{25t} [7], a decreased capacity of pyruvate to malate conversion could undermine this signalling, with catastrophic consequences for a larva with severe limitations on TCA-cycle and biosynthetic flux, and ATP depletion.

Overall, whilst we can infer that manipulations affecting pyruvate and lactate metabolism affect growth-regulation in tko^{25t}, possible off-target or sec-ondary effects of the drugs and knockdowns preclude a definitive mechanistic conclusion at this time. Unravelling the many possibilities will require the development of methods for assaying fluxes of the key metabolites at the subcellular level in $vivo$, con-sidering separately the mitochondrial and cytosolic pools of pyruvate, malate, NADPH, ATP and their derivatives.

Pyruvate modulates growth rate translationally and/or post-translationally

Growth of tko^{25t} in high-sugar medium was pre-viously observed to affect gene expression in two

ways: first, via a post-translational mechanism affecting S6K, second, via changes in transcript representation [7]. In the present study, we found that only a minor fraction of the genes regulated at the RNA level by pyruvate were regulated in the same way by high sugar, whilst those responding to tko^{25t} were mostly altered in the opposite direction. This was unexpected, given the fact that tko^{25t} responded similarly to pyruvate and high sugar, and suggests that global growth regulation in response to mitochondrial dysfunction and metabolic disturbance occurs mainly at the (post-)translational level. Regulation at the protein level is also suggested by the fact that the list of similarly or oppositely regulated genes at the RNA level includes very few that are connected either to metabolism or to transcription. It remains possible that relevant changes remain buried in the list of transcriptional targets because they change only by rather modest amounts that are below the thresholds set here but are nevertheless critical to the regulation of growth. More plausibly, a global regulator like the cyclin-dependent kinases or AMPK, which would not have to compete with cell-specific transcriptional programs, can respond to a systemic signal in broadly similar ways in all cells.

In conclusion, this study provides evidence that mitochondrial dysfunction triggers a systemic response that curtails the rate of growth of *Drosophila* larvae, and confirms a key role for pyruvate or its metabolic products in eliciting this signal.

Acknowledgments

Disclosure statement

No potential conflict of interest was reported by the authors. During the review process of the manuscript, corresponding author HTJ was appointed as Editor-in-Chief of the journal. However, he remaineduninvolved in, and blinded to, the review and editorial process.

Funding

ORCID

Jack George http://orcid.org/0000-0002-0053-4171
Tea Tuomela http://orcid.org/0000-0002-1010-0561
Esko Kemppainen http://orcid.org/0000-0002-5491-5391

References

[1] Thompson K, Collier JJ, Glasgow RIC, et al. Recent advances in understanding the molecular genetic basis of mitochondrial disease. J Inherit Metab Dis. 2019. [Epub before print]. DOI:10.1002/jimd.12104.

[2] Kanungo S, Morton J, Neelakantan M, et al. Mitochondrial disorders. Ann Transl Med. 2018;6:475.

[3] Murphy MP, Hartley RC. Mitochondria as a therapeutic target for common pathologies. Nat Rev Drug Discov. 2018;17:865–886.

[4] Boczonadi V, Horvath R. Mitochondria: impaired mitochondrial translation in human disease. Int J Biochem Cell Biol. 2014;48:77–84.

[5] Toivonen JM, O'Dell KM, Petit N, et al. *Technical knockout*, a *Drosophila* model of mitochondrial deafness. Genetics. 2001;159:241–254.

[6] Toivonen JM, Manjiry S, Touraille S, et al. Gene dosage and selective expression modify phenotype in a Drosophila model of human mitochondrial disease. Mitochondrion. 2003;3:83–96.

[7] Kemppainen E, George J, Garipler G, et al. Mitochondrial dysfunction plus high-sugar diet provokes a metabolic crisis that inhibits growth. PLoS One. 2016;11:e0145836.

[8] Wodarz A, Hinz U, Engelbert M, et al. Expression of *crumbs* confers apical character on plasma membrane domains of ectodermal epithelia of *Drosophila*. Cell. 1995;82:67–76.

[9] Yin S, Qun Q, Zhou B. Functional studies of *Drosophila* zinc transporters reveal the mechanism for zinc excretion in Malpighian tubules. BMC Biol. 2017;15:12.

[10] Osterwalder T, Yoon KS, White BH, et al. A conditional tissue-specific transgene expression system using inducible GAL4. Proc National Acad Sci USA. 2001;98:12596–12601.

[11] Berger C, Renner S, Lüer K, et al. The commonly used marker ELAV is transiently expressed in neuroblasts and glial cells in the *Drosophila* embryonic CNS. Dev Dyn. 2007;236:3562–3568.

[12] Sun B, Xu P, Wang W, et al. *In vivo* modification of Na$^+$,K$^+$-ATPase activity in *Drosophila*. Comp Biochem Physiol B Biochem Mol Biol. 2001;130:521–536.

[13] Oland LA, Biebelhausen JP, Tolbert LP. The glial investment of the adult and developing antennal lobe of *Drosophila*. J Comp Neurol. 2008;509:526–550.

[14] Górska-Andrzejak J, Salvaterra PM, Meinertzhagen IA, et al. Cyclical expression of Na$^+$/K$^+$-ATPase in the visual system of *Drosophila melanogaster*. J Insect Physiol. 2009;55:459–468.

[15] Edwards TN, Meinertzhagen IA. The functional organisation of glia in the adult brain of Drosophila and other insects. Prog Neurobiol. 2010;90:471–490.

[16] Stork T, Bernardos R, Freeman MR. Analysis of glial cell development and function in *Drosophila*. Cold Spring Harb Protoc. 2012;2012:1–17.

[17] Wang J-W, Beck ES, McCabe BD. A modular toolset for recombination transgenesis and neurogenetic analysis of *Drosophila*. PLoS One. 2012;7:e42102.

[18] Aberle H, Haghighi AP, Fetter RD, et al. *wishful thinking* encodes a BMP type II receptor that regulates synaptic growth in *Drosophila*. Neuron. 2002;33:545–558.

[19] Kemppainen KK, Rinne J, Sriram A, et al. Expression of alternative oxidase in Drosophila ameliorates diverse phenotypes due to cytochrome oxidase deficiency. Hum Mol Genet. 2014;23:2078–2093.

[20] Ranganayakulu G, Elliott DA, Harvey RP, et al. Divergent roles for NK-2 class homeobox genes in cardiogenesis in flies and mice. Development. 1998;125:3037–3048.

[21] Casso D, Ramírez-Weber FA, Kornberg TB. GFP-tagged balancer chromosomes for *Drosophila melanogaster*. Mech Dev. 1999;88:229–232.

[22] Castelli-Gair JE, Greig S, Micklem G, et al. Dissecting the temporal requirements for homeotic gene function. Development. 1994;120:1983–1995.

[23] Reiling JH, Hafen E. The hypoxia-induced paralogs Scylla and Charybdis inhibit growth by down-regulating S6K activity upstream of TSC in Drosophila. Genes Dev. 2004;18:2879–2892.

[24] Takeuchi T, Suzuki M, Fujikake N, et al. Intercellular chaperone transmission via exosomes contributes to maintenance of protein homeostasis at the organismal level. Proc National Acad Sci USA. 2015;112:E2497–E2506.

[25] Perkins LA, Holderbaum L, Tao R, et al. The transgenic RNAi project at harvard medical school: resources and validation. Genetics. 2015;201:843–852.

[26] Yan D, Neumüller RA, Buckner M, et al. A regulatory network of *Drosophila* germline stem cell self-renewal. Dev Cell. 2014;28:459–473.

[27] Pletcher RC, Hardman SL, Intagliata SF, et al. A genetic screen using the *Drosophila melanogaster* TRiP RNAi collection to identify metabolic enzymes required for eye development. G3. 2019;9:2061–2070.

[28] Ni JQ, Zhou R, Czech B, et al. A genome-scale shRNA resource for transgenic RNAi in *Drosophila*. Nat Methods. 2011;8:405–407.

[29] Dietzl G, Chen D, Schnorrer F, et al. A genome-wide transgenic RNAi library for conditional gene inactivation in *Drosophila*. Nature. 2007;448:151–156.

[30] Judd BH, Shen MW, Kaufman TC. The anatomy and function of a segment of the X chromosome of *Drosophila melanogaster*. Genetics. 1972;71:139–156.

[31] Royden CS, Pirrotta V, Jan LY. The *tko* locus, site of a behavioral mutation in *Drosophila melanogaster*, codes for a protein homologous to prokaryotic ribosomal protein S12. Cell. 1987;51:165–173.

[32] Shah ZH, O'Dell KMC, Miller SCM, et al. Metazoan nuclear genes for mitoribosomal protein S12. Gene. 1997;204:55–62.

[33] Merriam JR. FM7: a 'new' first chromosome balancer. Drosophila Inf Serv. 1969;44:101.

[34] Lindsley DL, Zimm GG. The genome of *Drosophila melanogaster*. NY: Academic Press; 1992.

[35] Barolo S, Carver LA, Posakony JW. GFP and beta-galactosidase transformation vectors for promoter/enhancer analysis in *Drosophila*. BioTechniques. 2000;29:726–732.

[36] Lee T, Luo L. Mosaic analysis with a repressible neurotechnique cell marker for studies of gene function in neuronal morphogenesis. Neuron. 1999;22:451–461.

[37] Fernandez-Ayala DJ, Sanz A, Vartiainen S, et al. Expression of the *Ciona intestinalis* alternative oxidase (AOX) in *Drosophila* complements defects in mitochondrial oxidative phosphorylation. Cell Metab. 2009;9:449–460.

[38] Brand AH, Perrimon N. Targeted gene expression as a means of altering cell fates and generating dominant phenotypes. Development. 1993;118:401–415.

[39] Finsterer J, Zarrouk-Mahjoub S. Biomarkers for detecting mitochondrial disorders. J Clin Med. 2018;7:16.

[40] Muha V, Müller HA. Functions and mechanisms of fibroblast growth factor (FGF) signalling in *Drosophila melanogaster*. Int J Mol Sci. 2013;14:5920–5937.

[41] Nässel DR, Liu Y, Luo J. Insulin/IGF signaling and its regulation in *Drosophila*. Gen Comp Endocrinol. 2015;221:255–266.

[42] Grönke S, Clarke DF, Broughton S, et al. Molecular evolution and functional characterization of Drosophila insulin-like peptides. PLoS Genet. 2010;6:e1000857.

[43] Gilbert LI. Halloween genes encode P450 enzymes that mediate steroid hormone biosynthesis in *Drosophila melanogaster*. Mol Cell Endocrinol. 2004;215:1–10.

[44] Niwa R, Niwa YS. Enzymes for ecdysteroid biosynthesis: their biological functions in insects and beyond. Biosci Biotechnol Biochem. 2014;78:1283–1292.

[45] Yamanaka N, Rewitz KF, O'Connor MB. Ecdysone control of developmental transitions: lessons from *Drosophila* research. Annu Rev Entomol. 2012;58:497–516.

[46] Zhang YQ, Roote J, Brogna S, et al. *stress sensitive B* encodes an adenine nucleotide translocase in *Drosophila melanogaster*. Genetics. 1999;153:891–903.

[47] Fergestad T, Bostwick B. Ganetzky B metabolic disruption in *Drosophila* bang-sensitive seizure mutants. Genetics. 2006;173:1357–1364.

[48] Chen S, Oliveira MT, Sanz A, et al. A cytoplasmic suppressor of a nuclear mutation affecting mitochondrial functions in *Drosophila*. Genetics. 2012; 192:483–493.

[49] Vartiainen S, Chen S, George J, et al. Phenotypic rescue of a *Drosophila* model of mitochondrial ANT1 disease. Dis Models Mech. 2014;7:635–648.

[50] Jacobs HT, Fernández-Ayala DJ, Manjiry S, et al. Mitochondrial disease in flies. Biochim Biophys Acta. 2004;1659:190–196.

[51] Schell JC, Wisidagama DR, Bensard C, et al. Control of intestinal stem cell function and proliferation by mitochondrial pyruvate metabolism. Nat Cell Biol. 2017;19:1027–1036.

[52] Tennessen JM, Baker KD, Lam G, et al. The Drosophila estrogen-related receptor directs a metabolic switch that supports developmental growth. Cell Metab. 2011;13:139–148.

[53] Whitehouse S, Cooper RH, Randle PJ. Mechanism of activation of pyruvate dehydrogenase by dichloroacetate and other halogenated carboxylic acids. Biochem J. 1974;141:761–774.

[54] Gong F, Peng X, Sang Y, et al. Dichloroacetate induces protective autophagy in LoVo cells: involvement of cathepsin D/thioredoxin-like protein 1 and Akt-mTOR-mediated signaling. Cell Death Dis. 2013;4:e913.

[55] Woo SH, Seo SK, Park Y, et al. Dichloroacetate potentiates tamoxifen-induced cell death in breast cancer cells via downregulation of the epidermal growth factor receptor. Oncotarget. 2016;7:59809–59819.

[56] Yang Y, Sun Y, Chen J, et al. AKT-independent activation of p38 MAP kinase promotes vascular calcification. Redox Biol. 2018;16:97–103.

[57] Carpenter L, Halestrap AP. The kinetics, substrate and inhibitor specificity of the lactate transporter of Ehrlich-Lettre tumour cells studied with the intracellular pH indicator BCECF. Biochem J. 1994;304:751–760.

[58] De Preter G, Neveu MA, Danhier P, et al. Inhibition of the pentose phosphate pathway by dichloroacetate unravels a missing link between aerobic glycolysis and cancer cell proliferation. Oncotarget. 2015;7:2910–2920.

[59] Halestrap AP. The mitochondrial pyruvate carrier: kinetics and specificity for substrates and inhibitors. Biochem J. 1975;148:85–96.

[60] Wiemer EA, Michels PA, Opperdoes FR. The inhibition of pyruvate transport across the plasma membrane of the bloodstream form of *Trypanosoma brucei* and its metabolic implications. Biochem J. 1995;312:479–484.

[61] Halestrap AP, Price NT. The proton-linked monocarboxylate transporter (MCT) family: structure, function and regulation. Biochem J. 1999;343:281–299.

[62] Yang J, Ruchti E, Petit JM, et al. Lactate promotes plasticity gene expression by potentiating NMDA signaling in neurons. Proc National Acad Sci USA. 2014;111:12228–12233.

[63] Baufeld A, Vanselow J. Lactate promotes specific differentiation in bovine granulosa cells depending on lactate uptake thus mimicking an early post-LH stage. Reprod Biol Endocrinol. 2018;16:15.

[64] Wu CY, Satapati S, Gui W, et al. A novel inhibitor of pyruvate dehydrogenase kinase stimulates myocardial carbohydrate oxidation in diet-induced obesity. J Biol Chem. 2018;293:9604–9613.

[65] Hildyard JC, Ammälä C, Dukes ID, et al. Identification and characterisation of a new class of highly specific and potent inhibitors of the mitochondrial pyruvate carrier. Biochim Biophys Acta. 2005;1707:221–230.

PUBLICATION
III

Minimal effects of *spargel* (PGC-1) overexpression in a *Drosophila* mitochondrial disease model

Jack George & Howard T. Jacobs

The Company of
Biologists

RESEARCH ARTICLE

Minimal effects of *spargel* (PGC-1) overexpression in a *Drosophila* mitochondrial disease model

Jack George and Howard T. Jacobs*

ABSTRACT

PGC-1α and its homologues have been proposed to act as master regulators of mitochondrial biogenesis in animals. Most relevant studies have been conducted in mammals, where interpretation is complicated by the fact that there are three partially redundant members of the gene family. In *Drosophila*, only a single PGC-1 homologue, *spargel* (*srl*), is present in the genome. Here, we analyzed the effects of *srl* overexpression on phenotype and on gene expression in *tko*[25t], a recessive bang-sensitive mutant with a global defect in oxidative phosphorylation, resulting from a deficiency of mitochondrial protein synthesis. In contrast to previous reports, we found that substantial overexpression of *srl* throughout development had only minimal effects on the *tko*[25t] mutant phenotype. Copy number of mtDNA was unaltered and *srl* overexpression produced no systematic effects on a representative set of transcripts related to mitochondrial OXPHOS and other metabolic enzymes, although these were influenced by sex and genetic background. This study provides no support to the concept of Spargel as a global regulator of mitochondrial biogenesis, at least in the context of the *tko*[25t] model.

KEY WORDS: Mitochondria, Mitochondrial biogenesis, Mitochondrial disease, Transcriptional co-activator

INTRODUCTION

The PGC-1 coactivators are widely considered to be global regulators of bioenergy metabolism, specifically acting to promote mitochondrial biogenesis in many different contexts (Spiegelman, 2007). However, the fact that there are three such factors encoded in mammalian genomes (PGC-1α, PGC-1β and PPRC1, also denoted as PRC) complicates their analysis, due to the combination of tissue or physiological specialization and genetic redundancy (Finck and Kelly, 2006).

In the *Drosophila* genome, a single member of the PGC-1 coactivator family, *spargel* (*srl*), is present. A *srl* hypomorph, carrying a P-element promoter insertion, was found to have decreased weight, decreased accumulation of storage nutrients in males and female sterility (Tiefenböck et al., 2010). In the mutant larval fat body there was decreased respiratory capacity and diminished expression of genes required for mitochondrial biogenesis and activity, with evidence of co-operation with the *Drosophila* NRF-2α homologue Delg, and with insulin signaling.

Faculty of Medicine and Health Technology, FI-33014 Tampere University, Finland.

*Author for correspondence (howard.jacobs@tuni.fi)

 J.G., 0000-0002-0053-4171; H.T.J., 0000-0003-1895-6003

These findings are consistent with Spargel acting as a general regulator of mitochondrial biogenesis in the fly. Many subsequent studies have been construed similarly (Mukherjee et al., 2014).

As part of a previous study of phenotypes connected with the *Drosophila* mutant *tko*[25t], we found evidence consistent with such a role for Spargel in regard to mitochondrial functions (Chen et al., 2012). *tko*[25t] carries a point mutation in the gene encoding mitoribosomal protein S12 (Royden et al., 1987; Shah et al., 1997), which confers larval developmental delay, bang sensitivity, defective male courtship and impaired sound responsiveness (Toivonen et al., 2001). The mutant has an under-representation of mitoribosomal small subunit rRNA and is deficient in all four enzymes of the oxidative phosphorylation (OXPHOS) system that depend on mitochondrial DNA (mtDNA)-encoded subunits (Toivonen et al., 2001, 2003). The *tko*[25t] phenotype can be rescued by an additional genomic copy of the mutant *tko* locus (Kemppainen et al., 2009) and partially compensated by altered mtDNA background (Chen et al., 2012) or low-sugar diet (Kemppainen et al., 2016).

In our earlier study, flies overexpressing *srl* showed a modest but statistically significant alleviation of the mutant phenotype (Chen et al., 2012). When we later catalogued our strain collection, we concluded that this experiment may have used a strain carrying a genomic duplication of *srl* (designated *srl*[GR], Tiefenböck et al., 2010), rather than the GAL4-dependent *srl* cDNA construct. In order to clarify the effects on *tko*[25t] phenotype of *srl* overexpression at different levels, we proceeded to combine the mutant with different *srl* constructs, having first profiled their effects on expression. In an initial experiment using *srl*[GR], we were able to substantiate the earlier finding of a modest alleviation of developmental delay. However, this was not upheld in subsequent repeats of the experiment, nor by other strain combinations that overexpress *srl* at a higher level; nor did *srl* overexpression systematically modulate mtDNA copy number or the expression of genes for OXPHOS subunits, the mitochondrial nucleoid protein TFAM or other metabolic pathways. We thus find no consistent evidence to support a role for *srl* in boosting mitochondrial biogenesis in *tko*[25t] flies.

RESULTS

srl expression in wild-type and *tko*[25t] mutant flies

To assess the effects of *srl* overexpression in *tko*[25t] mutant flies and heterozygous controls, we first measured the extent of overexpression using qRT-PCR, after combining the relevant chromosomes carrying *srl*[GR], UAS-*srl*, the ubiquitously acting *da*GAL4 driver, the *tko*[25t] mutation and appropriate balancer chromosomes (Fig. 1). To reproduce as closely as possible the previously studied conditions, we created *tko*[25t] flies that were hemizygous for both *srl*[GR] and *da*GAL4, even though there should be no UAS construct present (Fig. 1A). We also analyzed the sexes separately since, in initial trials, we observed a consistently higher endogenous *srl* expression in females than males. Hemizygosity for the *srl*[GR] construct conferred an increase in *srl* RNA in both sexes,

Biology Open

1

Fig. 1. *srl* can be overexpressed by genomic duplication or using the GAL4 system. qRT-PCR measurements of *srl* RNA in adult flies (*n*=4 batches of 10 flies) of the indicated genotypes and sex, normalized to values for control females: (A) *tko*^{25t}/FM7 heterozygotes, which have a wild-type phenotype; (B–D) Oregon R (OR) wild-type. (A) Effect of genomic duplication of *srl* (hemizygosity for *srl*^{GR}) with or without the additional presence of the *da*GAL4 driver in the *tko*^{25t} background. (B) Effect of UAS-*srl*, with or without the *da*GAL4 driver, in the *tko*^{25t} background, alongside OR. Asterisks denote significant differences between flies expressing UAS-*srl* driven by *da*GAL4 and non-expressing controls of the same sex and *tko* genotype (Student's *t*-test, *P*<0.001). (C) Effect of the *tko*^{25t} background (two separate experiments separated by vertical line; repeat experiments shown to emphasize the reproducibility of the main finding, i.e. decreased *srl* expression in *tko*^{25t} females compared with controls). Asterisk denotes significant difference from OR flies of the same sex (Student's *t*-test, *P*<0.05). (D) Combined effect of the *tko*^{25t} background and hemizygosity for *srl*^{GR}. Note that, in this experiment, we substituted the *tub*GS driver background for *da*GAL4, so as to check that the increased expression from *srl*^{GR} is not due to the *da*GAL4 driver background. Asterisks denote significant differences based on Student's *t*-test with Bonferroni correction, comparing flies of a given sex between genotypes: *P*<0.05, **P*<0.01, ***P*<0.001. Note that all statistical analyses are based on ΔC$_T$ values from the qRT-PCR data, not the fold differences as plotted (see Materials and Methods).

proportionate to gene dosage (Fig. 1A). In contrast, UAS-*srl* driven by *da*GAL4 resulted in a more substantial increase in *srl* RNA: ~4-fold in females and >100-fold in males (Fig. 1B). *srl* RNA was at lower abundance in *tko*^{25t} females (though not males: Fig. 1C), and was restored to the wild-type level by *srl*^{GR} (Fig. 1D). To test whether increased *srl* RNA due to UAS-*srl* expression was reflected at the protein level, we generated two antibodies against peptides of Spargel, which each detected a major band of approximate molecular weight ~105 kDa and a minor band of ~125 kDa (Fig. 2A), close to the predicted molecular weight of the protein (118 kDa). These bands were detected in both males and females (Fig. 2B: note that the ~125 kDa band appears more faintly in females, but is always present at long exposure). The same two bands were detected in S2 cells induced to express V5 epitope-tagged Spargel after transient transfection (Fig. 2C,D). At higher magnification (Fig. 2C*i,ii*), immunocytochemistry revealed a 'speckled' nuclear localization similar to that observed by Mukherjee and Duttaroy (2013) using *srl*-GFP, providing further

validation of the (AA214) antibody. UAS-*srl* driven by *da*GAL4 led to a modest increase in detected Spargel protein, based on western blot signal compared with the GAPDH loading control (Fig. 2E,F). Note, however, that this increase (~20–50% depending on background), was proportionately far smaller than that seen at the RNA level. The large disparity in *srl* RNA between males and females (Fig. 1) was not evident in the detected protein, which was actually at a higher level in males (by ~40%).

srl overexpression has no systematic effects on *tko*^{25t} phenotype

To clarify the effects of *srl* overexpression on the phenotype of *tko*^{25t} we conducted a number of tests in which we varied the overexpression construct used and the genetic background. Using the *srl*^{GR} construct to produce modest overexpression we recorded a small decrease in the developmental delay of *tko*^{25t} flies (Fig. 3A). However, this was influenced by the presence of the *da*GAL4 driver, since the eclosion day of *tko*^{25t} flies lacking both *da*GAL4 and the

2
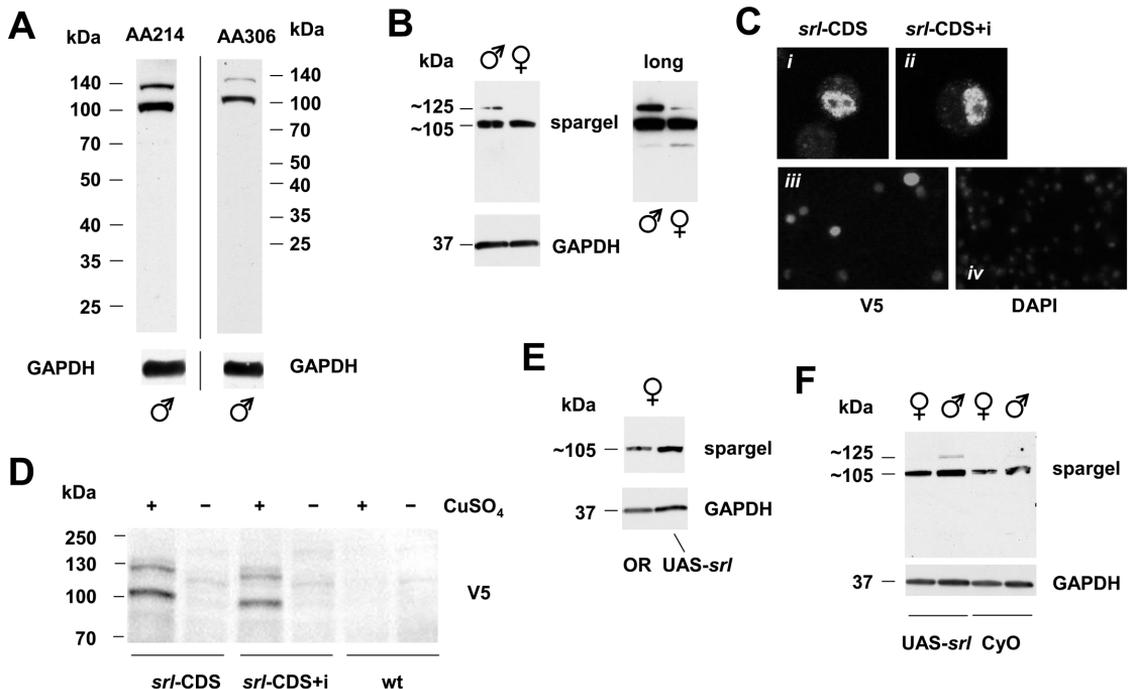
Fig. 2. *srl* overexpression at the protein level is modest. (A,B,E,F) Western blots of protein extracts from *Drosophila* adults of the sex and genotype indicated, probed with customized *srl*-directed antibodies AA214 (A, left-hand panel, B, E, F) or AA306 (A, right-hand panel), and with antibody against GAPDH as loading control. Sizes of molecular weight markers in kDa shown in A and D, or used to extrapolate sizes of major bands detected in B, E and F. Note longer exposure of same blot in right-hand panel of B. (C) Immunocytochemistry and (D) western blot, using V5 antibody, on cells transfected with Cu-inducible *srl*-expressing constructs (*srl*-CDS with coding sequence only, *srl*-CDS+i with intron); in C, *i* and *ii* show single cells at high magnification; *iii* and *iv* show cells probed with V5 antibody or DAPI to confirm successful transient transfection. Densitometry on Spargel ~105 kDa band in replicate blots (*n*=3) normalized against GAPDH (mean fold-differences±s.d.) showed, for B, Spargel in males was at 1.39±0.11 times its level in females, for E, Spargel in *srl* overexpressing (UAS-*srl*/*da*GAL4) females was at 1.18±0.10 times its level in Oregon R wild-type females and for F, Spargel in *srl* overexpressing (UAS-*srl*/*da*GAL4) flies was at 1.53±0.01 times its level in CyO balancer/*da*GAL4 controls.

srl^{GR} construct was not significantly different from that of flies endowed with both. Furthermore, although the alleviation of developmental delay was significant in this first experiment, as inferred previously (Chen et al., 2012), it was not seen in any of the three repeats of the experiment (e.g. the one shown in Fig. 3B). There was also no significant difference in eclosion time between *tko^{25t}* flies homozygous for the *srl^{GR}* construct and *tko^{25t}* controls in either sex (Fig. 3C). Furthermore, hemizygosity for the extra copy of *srl* produced no rescue of bang-sensitivity (Fig. 3D). More substantial overexpression of *srl* driven by *da*GAL4 using the UAS-*srl* construct did not alleviate developmental delay: rather there was a trend towards a slight deterioration, although this was significant only in one repeat of the experiment and in males only, as shown (Fig. 3E).

srl expression is not altered by diet during development

Previously, Spargel was shown to mediate insulin signaling (Mukherjee and Duttaroy, 2013), which is considered the primary system linking growth to nutritional resources. In contrast, *tko^{25t}* exhibits an apparently paradoxical growth retardation when cultured on high-sugar diet (Kemppainen et al., 2016), suggesting that insulin signaling has been abrogated or even reversed, for example, as a result of a counteracting signal arising from mitochondrial dysfunction. We therefore considered the hypothesis that *srl* was downregulated in *tko^{25t}* by a diet-dependent mechanism and that its

expression and growth-promoting function might be restored in *tko^{25t}* larvae or adults cultured on minimal medium.

For this, we compared flies grown on standard high-sugar medium, containing complex dietary additives, with those grown on a minimal medium containing only agar and (10%) yeast. As previously, the low-sugar minimal medium partially accelerated the development of *tko^{25t}* flies (Fig. 4A), whilst at the same time retarding that of controls (Fig. 4A,B). However, diet-induced effects on the expression of *srl* were minimal. *srl* expression in control (wild-type Oregon R) L3 larvae of both sexes was slightly decreased in minimal medium compared with high-sugar medium (Fig. 4C,D), although this was not statistically significant in all experiments (e.g. Fig. 4C, right-hand panel). *srl* expression in *tko^{25t}* larvae (Fig. 4C, right-hand panel) was lower than in controls by approximately the same factor as in adults, but was unaffected by the different culture media, as was *srl* expression in *tko^{25t}* adults (Fig. 4D).

Overexpression of *srl* has no systematic effects on genes related to core mitochondrial functions

Despite the fact that *srl* overexpression had no impact on the *tko^{25t}* phenotype, we explored whether such overexpression nevertheless influenced the level of mtDNA or that of transcripts related to core functions of mitochondria, specifically OXPHOS subunits and the major nucleoid protein TFAM (Fig. 5). With the exception of TFAM,

3
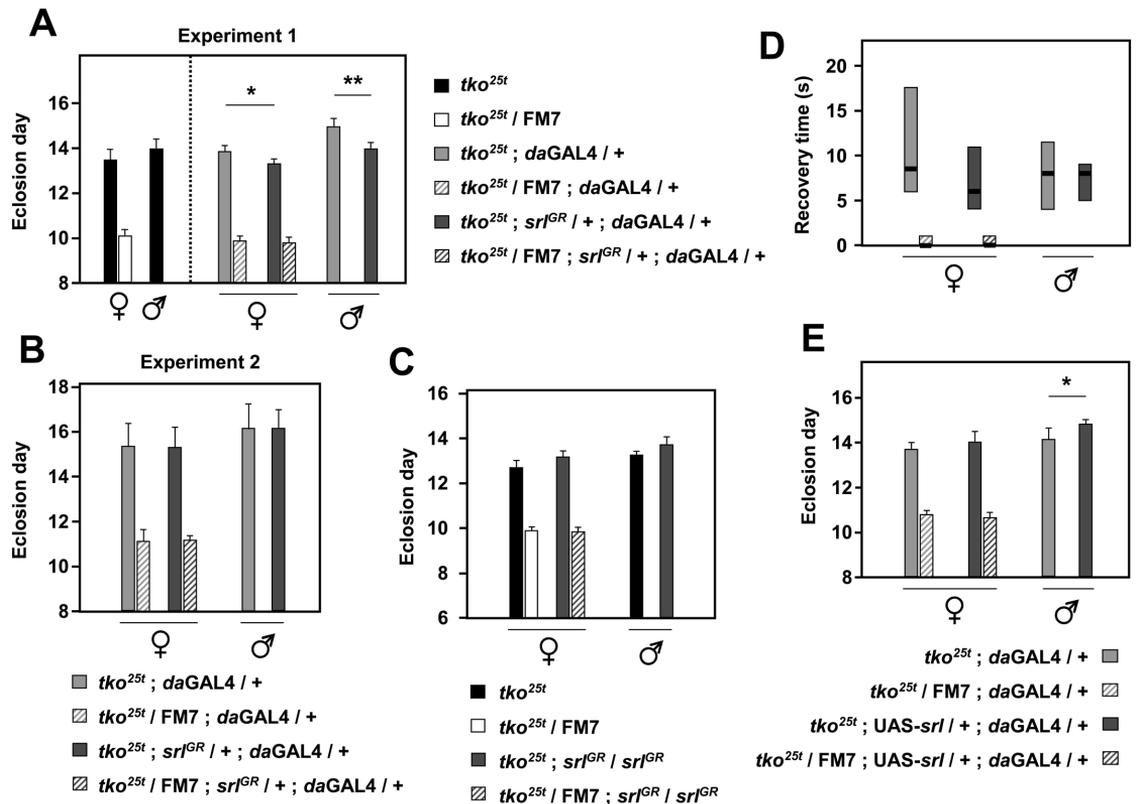
Fig. 3. *srl* overexpression does not modify *tko*²⁵ᵗ phenotype. (A–C,E) Days to eclosion (means±s.d.) and (D) bang sensitivity (box plot, 1st to 3rd quartiles, medians as thick black bars) of flies of the indicated genotypes and sex (*n*=5 replicate vials of 10–50 flies each). Dashed vertical line in A separates the experimental and '*tko*²⁵ᵗ only' control (i.e. lacking both *da*GAL4 and *srl*ᴳᴿ) crosses conducted in parallel (similar controls were implemented routinely but are omitted from the other panels for clarity). A and B show two repeat experiments (denoted experiment 1 and experiment 2: a third repeat is not shown) in which *tko*²⁵ᵗ ; *da*GAL4 males were crossed to *tko*²⁵ᵗ/FM7 females either with or without *srl*ᴳᴿ as shown. The same cross was used to generate the data in D. In C, crosses for *tko*²⁵ᵗ alone or in combination with homozygous *srl*ᴳᴿ were conducted in parallel, without the presence of *da*GAL4. In E, progeny carried *da*GAL4 and either UAS-*srl* or CyO from a single cross. Asterisks denote statistically significant differences between progeny flies of a given sex and *tko* genotype, either with or without the presence of an *srl* overexpression construct (Student's *t*-test; *P<0.05, **P<0.01). Two other repeats of this experiment gave similar findings.

all genes studied showed a similar profile of expression in the different strains tested, with higher relative expression in males, higher expression in the *tko*²⁵ᵗ background, including *tko*²⁵ᵗ heterozygotes over the FM7 balancer, attenuation of this increase by the *da*GAL4 driver and further slight attenuation by UAS-*srl*. These observations are consistent with expression levels being determined by sex and by genetic background, possibly involving effects on the *RpL32* reference transcript, rather than by *srl* expression, which followed a different pattern (Fig. 1B). They provide no support for any enhancing effect of *srl*. In the case of TFAM, expression was slightly lower in males than in females, and was little affected by *da*GAL4 or UAS-*srl* (Fig. 5, top right). Note that *srl* overexpression was verified (Fig. 1B) in the same RNA samples.

In previous studies, the expression of genes for some of the enzymes participating in other metabolic pathways known to be influenced by PGC-1 homologues in various contexts, such as lipid catabolism, including beta-oxidation of fatty acids (Huang et al., 2017), or gluconeogenesis (Rhee et al., 2003), were found to be upregulated in *tko*²⁵ᵗ, both in larvae (Kemppainen et al., 2016) and adults (Fernández-Ayala et al., 2010). We therefore tested whether

srl over-expression driven by *da*GAL4 was able to influence the expression of genes for such enzymes in *tko*²⁵ᵗ, despite the absence of any effect on growth rate. Once again, using the same materials as in the experiment shown in Fig. 5, we found no significant effect of *srl* overexpression on the transcripts of two genes for enzymes of fatty acid oxidation (*yip2* and *Thiolase*) and two for gluconeogenesis (*PCB* and *Pepck1*), although all of them were affected by sex, by genetic background and by the interaction of these factors (two-way ANOVA, Fig. 6A).

Next, we measured relative mtDNA copy number in *tko*²⁵ᵗ and control flies, with and without *srl* overexpression. ANOVA revealed no significant differences between groups (Fig. 6B). Thus, *srl* overexpression does not appear to influence mitochondrial or metabolic functions in *tko*²⁵ᵗ in any systematic way.

DISCUSSION

Previous studies, where the expression of *srl* was downregulated either in the whole fly or in a specific tissue, suggested a global role for *srl* in growth regulation. Here we tested whether overexpression of *srl* was able to compensate the phenotype of *tko*²⁵ᵗ, a mutant with decreased

4
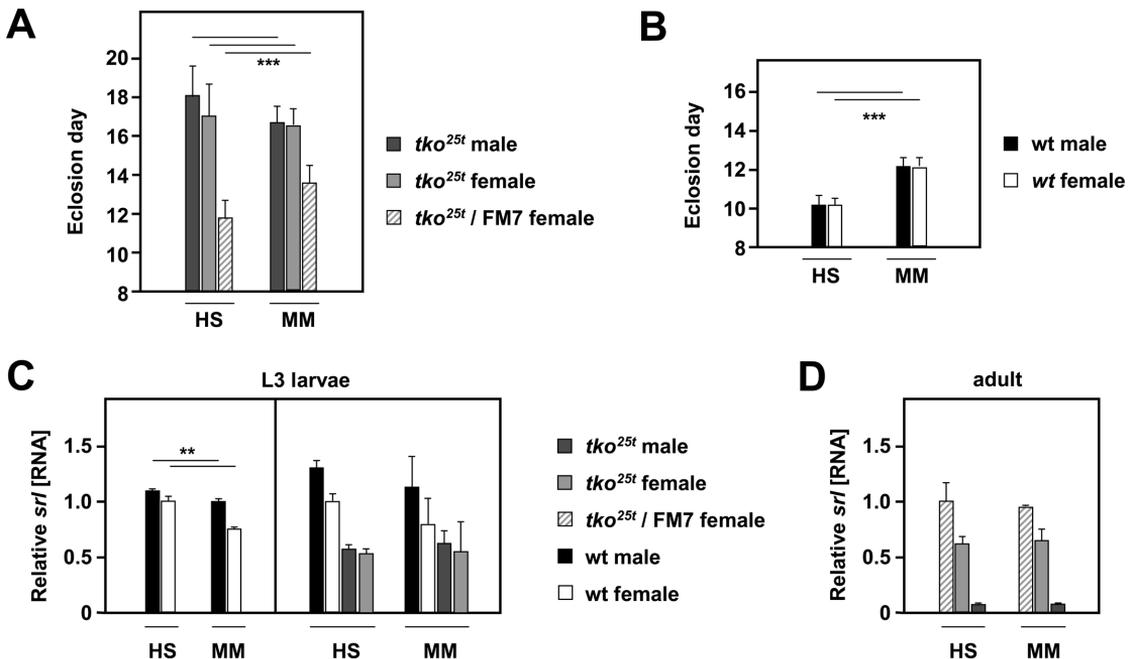
Fig. 4. *srl* expression does not correlate with growth rate on different media. (A,B) Means±s.d. of times to eclosion of flies of the indicated genotypes and sex on different media. HS, standard high-sugar medium; MM, minimal medium; wt, wild-type Oregon R. Flies grown in (A) bottles, *n*=739 individuals, (B) replicate vials, *n*=310 flies. (C,D) qRT-PCR measurements (*n*=4 batches of 10 flies) of *srl* RNA in L3 larvae and adult flies of the indicated genotypes and sex on the different media, normalized to values for (C) Oregon R wild-type females or (D) *tko²⁵ᵗ*/FM7 heterozygous females. Vertical bar in C divides datasets for two separate experiments. Asterisks denote statistically significant differences between indicated classes of flies of a given sex and genotype on the different media: Student's *t*-test, **P<0.01, ***P<0.001. Note, however, that comparison of values for the equivalent classes in the experiment shown in the right-hand part of C gave no significant differences.

mitochondrial biosynthesis and which grows slowly. We found that *srl* RNA was at decreased levels in *tko²⁵ᵗ* flies (Figs 1 and 4) even when cultured in minimal medium where the growth defect is partially alleviated. As suggested in a previous study, we initially detected a small compensatory effect of *srl* overexpression in *tko²⁵ᵗ* flies endowed with an additional copy of *srl* (Fig. 3A). However, further repeats (e.g. Fig. 3B) and trials with *srl^GR* in two copies (Fig. 3C) failed to substantiate any rescue of developmental delay or bang-sensitivity (Fig. 3D). Even the much more substantial *srl* overexpression produced by UAS-*srl* (Fig. 1B) was ineffective (Fig. 3E). Overexpression of *srl* had no effect on mtDNA copy number, nor on transcripts of genes connected with mitochondrial OXPHOS or other metabolic pathways. There are several potential explanations for these essentially negative results that we now consider, noting that that *srl* overexpression was also previously found not to compensate for decreased OXPHOS capacity resulting from a mutation in the adenine nucleotide translocase (Vartiainen et al., 2014).

Translational and post-translational regulation
The first possibility is that, as suggested by the lack of congruence between RNA and protein levels, *srl* is translationally regulated, negating any effect of overexpression. Translational regulation is well established (see recent reviews by Zhao et al., 2019; Shi and Barna, 2015), applies to mitochondrial biogenesis (Zhang and Xu, 2016), and is prominent in early development (Winata and Korzh, 2018; Barckmann and Simonelig, 2013), playing roles in axial

specification and other processes in *Drosophila* (Wilhelm and Smibert, 2005; Kugler and Lasko, 2009). It is also a cardinal feature of the integrated stress response (Ryoo and Vasudevan, 2017), which can be activated by mitochondrial dysfunction.

A second idea is that *srl* might be post-translationally regulated, which could also override effects of overexpression. Post-translational regulation is brought about by many different mechanisms (Gill, 2004; Lee et al., 2005; Johnson, 2009; Bauer et al., 2015; Narita et al., 2019; Klein et al., 2018). Many of them have been documented as affecting the PGC-1 family in mammals (reviewed by Austin and St-Pierre, 2012), which is also subject to differential splicing (Meirhaeghe et al., 2003; Martínez-Redondo et al., 2015). The two antibodies that we generated against Spargel detect the same bands on western blots, validated by epitope tagging in S2 cells. The higher molecular weight band (~125 kDa) probably represents the predicted full-length protein of 119 kDa. The nature of the processing that generates the major (~105 kDa) band is unknown, but can be considered a suggestive indicator of post-translational regulation of Spargel.

***tko²⁵ᵗ* signaling**
A third possible explanation for the finding that *srl* overexpression fails to modify the *tko²⁵ᵗ* growth phenotype could be that the mutation might elicit a growth-inhibitory signal, overriding any effect of *srl*. Therefore, we should not just dismiss the conventional view that the PGC-1 coactivators are global regulators of mitochondrial biogenesis. Such a function may apply in many other physiological

1 = Oregon R   2 = *tko²⁵ᵗ*   3 = *tko²⁵ᵗ* ; + / CyO ; *da*GAL4 / +   4 = *tko²⁵ᵗ* ; + / UAS-*srl* ; *da*GAL4 / +

■ male   ■ female   □ heterozygous *tko²⁵ᵗ* / FM7 female
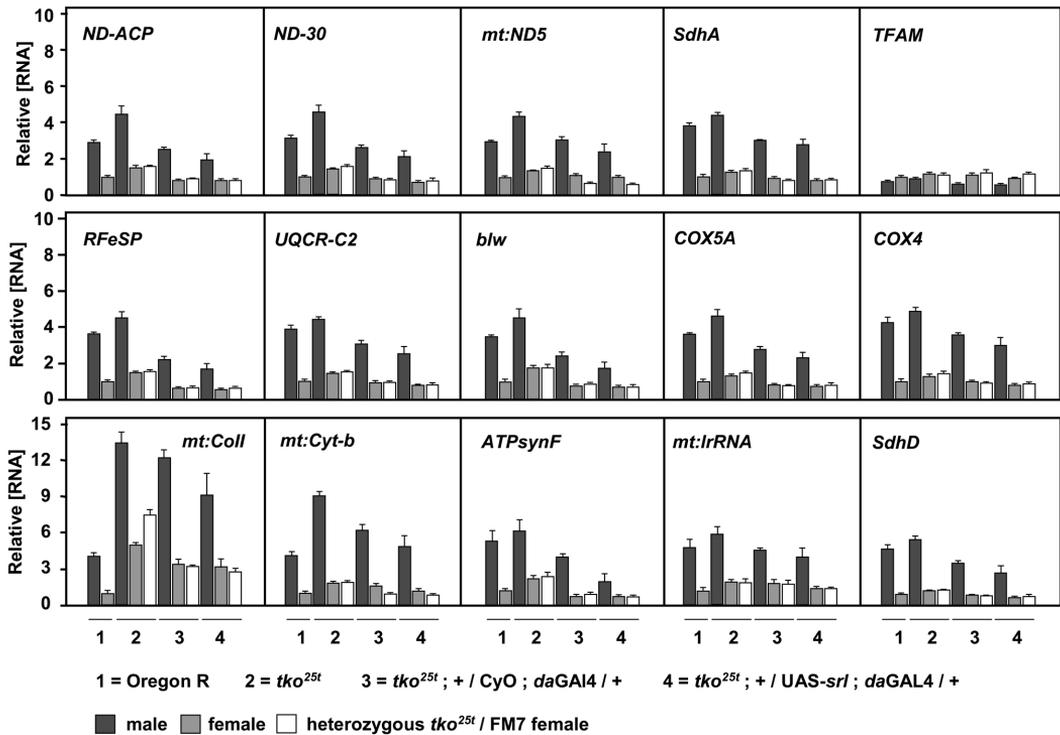
Fig. 5. *srl* overexpression in *tko²⁵ᵗ* does not increase levels of transcripts for core mitochondrial functions. qRT-PCR measurements (*n*=4 batches of 10 flies) of RNA levels of the indicated genes (symbols as in flybase.org) in adult flies of the indicated genotypes and sex, normalized to corresponding values for Oregon R (wild-type) females. For clarity, and because expression profiles were qualitatively so similar for all genes studied (except *TFAM*), statistical estimates are omitted.

contexts. Indeed, if Spargel acts in this way as a 'master switch', its effects may still be masked by metabolic signaling at a lower level in the hierarchy of gene regulation. Based on previous data (Kemppainen et al., 2016), a strong candidate for growth regulation in *tko²⁵ᵗ* is ribosomal protein S6 kinase (S6K), which is influenced by multiple signaling pathways including mTOR (Magnuson et al., 2012), insulin/Akt (Manning, 2004) and AMPK (Mihaylova and Shaw, 2011). Contradicting this idea, Mukherjee and Duttaroy (2013) found that *srl* can partially override defects in cell growth mediated by defective insulin/mTOR signaling and that mutants in S6K can be rescued by *srl* overexpression. However, since S6K regulation in *tko²⁵ᵗ* seems to be at the level of the protein itself, not its phosphorylation, *srl* over-expression may be insufficient to negate it.

A different role for *spargel*
Spargel may also play a broader role than just promoting mitochondrial biogenesis. Although mitochondrial biogenesis is reciprocally affected by PGC-1α knockout (Lin et al., 2004; Leone et al., 2005) and overexpression (Lehman et al., 2000; Lin et al., 2002), the PGC-1 family also impacts thermogenesis in brown fat (Uldry et al., 2006), neuromuscular differentiation (Lin et al., 2002; Handschin et al., 2007), hepatic gluconeogenesis (Yoon et al., 2001) and oxygen radical detoxification (St-Pierre et al., 2006). As a coactivator, PGC-1 interacts with sequence-specific transcription factors which specify the genes to be regulated, but the known transcriptional targets of *srl* are not limited to those involved in mitochondrial biogenesis (Tiefenböck et al.,

2010), and it has elsewhere been implicated in various cell differentiation and cell survival programs, or in functional maintenance during aging (Tinkerhess et al., 2012; Wagner et al., 2015; Merzetti and Staveley, 2015; Diop et al., 2015; Ng et al., 2017; Staats et al., 2018). Rera et al. (2011) reported an increase in mitochondrial markers in flies globally overexpressing *srl*. However, this is also consistent with a general enhancement of muscle differentiation. Finally, we should not exclude the possibility that *srl* could promote mitochondrial biogenesis by an effect other than on transcription, even if this would not affect the levels of mtDNA/ TFAM, mitoribosomes or mitochondrial mRNAs in *tko²⁵ᵗ* flies, nor modify the *tko²⁵ᵗ* phenotype. However, since there is no precedent for a transcriptional coactivator influencing the levels of target proteins but not their mRNAs, this must be considered highly unlikely.

Issues in fly genetics
Our initial results using *srl^GR* (Fig. 3A) were consistent with previous studies, but partial rescue of *tko²⁵ᵗ* could not subsequently be reproduced. The reasons for the discrepancy are not clear, but we posit that both the original, apparent rescue and its non-reproducibility are most probably attributable to genetic background effects, and subject to genetic drift during stock maintenance. Unknown and therefore uncontrolled environmental variables may also have played a role. Note, in addition, that our initial finding (Fig. 3A) indicates a small negative effect of the *da*GAL4 driver. Transgenes, drivers and deleterious mutations are routinely maintained over balancer
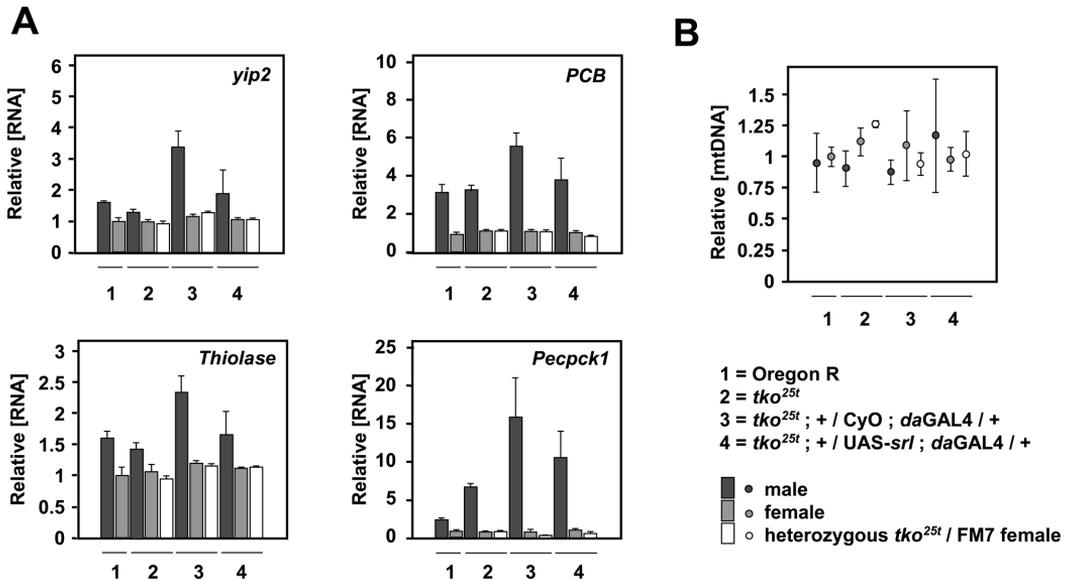
Fig. 6. *srl* overexpression in *tko²⁵ᵗ* does not increase mtDNA copy number or transcript levels for other metabolic enzymes. (A) qRT-PCR measurements of RNA levels (*n*=4 batches of 10 flies) of the indicated genes (symbols as in flybase.org) in adult flies of the indicated genotypes and sex normalized to corresponding values for Oregon R (wild-type) females. Statistical analysis confirmed a significant effect of both sex and genotype and of interaction between these factors for all four genes (two-way ANOVA, *P*<0.001). However, as for the genes studied in Fig. 5, narrowly comparing expression of flies of a given sex in the presence of *da*GAL4, with or without UAS-*srl*, showed no significant differences (Student's *t*-test with Bonferroni correction), despite the general trend of slight decrease in males. (B) qPCR measurements of mtDNA copy number (*n*=4 batches of five flies), means±s.d. normalized to Oregon R females. There were no significant differences between groups (one-way ANOVA).

chromosomes. Balancers are preferable to homozygosity, so as to prevent the inadvertent selection of suppressors, and are unavoidable in cases where homozygosity is lethal. However, balancers also allow new mutations to accumulate, protected from negative selection. These too potentially compromise the reproducibility of effects on mild phenotypes, such as developmental delay in *tko²⁵ᵗ*. Although genetic drift can be minimized by alternating rounds of homozygosity and rebalancing, in practice it cannot be completely prevented. Whilst burdensome, our study highlights the value of multiple repeat experiments to confirm quantitatively minor phenotypic variations, preferably with retesting in different backgrounds. Such measures are nevertheless much easier to implement and interpret in *Drosophila*, compared with mammalian models where inconsistent or strain-dependent findings abound.

Although we found no effects on phenotype, mtDNA copy number or gene expression from *srl* overexpression in *tko²⁵ᵗ*, it should be noted that all our assays were conducted on whole adult flies. Therefore, our findings largely reflect the situation in the muscle-rich thorax, where mtDNA and its transcription and translation products are at their most abundant (Calleja et al., 1993). Although we cannot exclude an *srl*-dependent effect in some tissue other than muscle, to detect it would require extensive dissection procedures or the use of highly tissue-specific drivers. The present results provide no basis upon which to embark on such a study.

MATERIALS AND METHODS
Drosophila strains and culture
The *srl^{GR}* and UAS-*srl* strains (Tiefenböck et al., 2010), both supplied over a CyO balancer, were a kind gift from Christian Frei (ETH Zürich, Switzerland). The *tko²⁵ᵗ* strain, originally sourced through Kevin O'Dell

(University of Glasgow, UK), was backcrossed into Oregon R background (Toivonen et al., 2001) and maintained long-term in our laboratory over the FM7 balancer. The Oregon R wild-type and *da*GAL4 driver strains were originally obtained from Bloomington Stock Center and the *tub*GS driver was the kind gift of Scott Pletcher (University of Michigan, USA). All stocks were maintained at room temperature and grown experimentally in plugged plastic vials at 25°C on a 12 h light/dark cycle in standard high-sugar medium (HS, Kemppainen et al., 2016) or, where specified in figures, in a minimal medium (MM) consisting of agar, 10% yeast and standard antimicrobial agents (0.1% nipagin and 0.5% propionic acid, Sigma-Aldrich).

Molecular cloning
Genomic DNA was extracted from adult *Drosophila* and used as a PCR template with chimeric gene-specific primers to amplify *srl* from the start codon up until, but not including, the stop codon. The chimeric primers contained EcoRI and NotI restriction sites for restriction digestion and insertion into the copper-inducible plasmid pMT-V5/HisB (Thermo Fisher Scientific), resulting in the introduction of an in-frame C-terminal V5 epitope tag. A primer deletion strategy was used on this plasmid to create an intronless version of *srl* tagged with V5. Both resulting plasmids were sequence-verified before use in transfections.

Developmental time and bang-sensitivity assays
Three replicate crosses were set up and tipped five times to fresh vials for egg laying, as previously described (Kemppainen et al., 2009). The mean developmental time to eclosion (at 25°C), as well as bang-sensitivity, were measured as described previously (Kemppainen et al., 2009). Unweighted means and standard deviations of eclosion day for each sex and inferred genotype were then computed for each cross, and used in statistical analyses, generally applying Student's *t*-test (unpaired, two-tailed) to compare the mean eclosion day of flies of a given sex and genotype with and without the expression of a given *srl* overexpression construct. For bang-sensitivity,

7

medians and quartiles of recovery time for flies of a given sex and genotype were plotted in a box-plot format.

RNA analysis

Total RNA was extracted from batches of ten 2 day-old flies and from L3 (wandering stage) larvae using a homogenizing pestle and trizol reagent as previously described (Kemppainen et al., 2016). cDNA was synthesized using the High-capacity cDNA Reverse Transcription Kit (Thermo Fisher Scientific) according to manufacturer's instructions. Expression levels were determined by qRT-PCR using Applied Biosystems StepOnePlus™ Real-Time PCR System with Fast SYBR™ Green Master Mix kit (Applied Biosystems) with, as template, 2 µl of cDNA product diluted 10-fold, in a 20 µl reaction, together with 500 nM of each gene-specific primer pair as follows (all given 5′ to 3′, gene symbols in the following list following current practice in flybase.org): *RpL32* (CG7939), TGTGTCACCAGGAACTTCTT-GAA and AGGCCCAAGATCGTGAAGAA; *ND-ACP* (CG9160), ACAA-GATCGATCCCAGCAAG and ATGTCGGCAGGTTTAAGCAG; *ND-30* (CG12079), AAGGCGGATAAGCCCACT and GCAATAAGCACCTCC-AGCTC; *mt:ND5* (CG34083), GGGTGAGATGGTTTAGGACTTG and AAGCTACATCCCCAATTCGAT; *SdhA* (CG17246), CATGTACGACAC-GGTCAAGG and CCTTGCCGAACTTCAGACTC; *TFAM* (CG4217), AA-CCGCTGACTCCCTACTTTC and CGACGGTGGTAATCTGGTG; *RFeSp* (CG7361), GGGCAAGTCGGTTACTTTCA and GCAGTAGTAGCCAC-CCCAGT; *UQCR-C2* (CG4169), GAGGAACGCGCCATTGAG and AC-GTAGTGCAGCAGGCTCTC; *Blw* (CG3612), GACTGGTAAGACCGCT-CTGG and GGCCAAGTACTGCAGAGGAG; *COX5A* (CG14724), AGG-AGTTCGACAAGCGCTAC and ATAGAGGGTGGCCTTTTGGT; *COX4* (CG10664), TCTTCGTGTACGATGAGCTG and GGTTGATTTCCAGG-TCGATG; *mt:CoII* (CG34069), AAAGTTGACGGTACACCTGGA and TGATTAGCTCCACAGATTTC; *mt:Cyt-b* (CG34090), GAAAATTCCGA-GGGATTCAA and AACTGGTCGAGCTCCAATTC; *ATPsynF* (CG4692), CTACGGCAAAGCCGATGT and CGCTTTGGGAACACGTACT; *mt:lrRNA* (CR34094), ACCTGGCTTACACCGGTTTG and GGGTGTAGCCGTTCA-AATTT; *SdhD* (CG10219), GTTGCAATGCCGCAAATCT and GCCACC-AGGGTGGAGTAG; *srl* (CG9809), GGAGGAAGACGTGCCTTCTG and TACATTCGGTGCTGGTGCTT; *yip2* (CG4600), GTCCTCCTCCACCGAT-GGTAT and CAAAGCCGGTTGATTCCAAGG; *Thiolase* (CG4581), GGA-GTCCGCACACCCTTTC and TGCAGCAATGACAAAAGCGAG; *PCB* (CG1516), AATCGGTGGCGGTCTACTC and TTGCCCACTATGTACGA-CTCG; *Pepck1* (CG17725), TGATCCCGAACGCAC-CATC and CTCAGG-GCGAAGCACTTCTT. Mean values were normalized first against *RpL32* and then against an arbitrary standard, namely wild-type (Oregon R) adult females, except where stated. Primer pairs were routinely validated based on uniform melting profiles, and standard curves showing efficiencies of at least 90%. For further details of qRT-PCR methods in our laboratory see Fernandez-Ayala et al. (2009) and Saari et al. (2019).

mtDNA copy number measurement

Batches of five adult flies of a given sex were crushed in 500 µl DNA lysis buffer (75 mM NaCl, 50 mM EDTA, 20 mM HEPES/NaOH, pH 7.8). 5 µl of 20% SDS and 20 µl of Proteinase K (10 mg/ml, Thermo Fisher Scientific) were added to each sample and vortexed to mix. Samples were briefly centrifuged, left on a heat block at 50°C for 4 h, then vortexed and centrifuged at 16,000 g_{max} for 1 min to pellet debris. Supernatants were decanted and nucleic acid was precipitated with 420 µl of isopropanol with repeated inversion and overnight incubation at −20°C. Samples were centrifuged at 16,000 g_{max} for 30 min at 4°C to pellet the DNA, which was washed with 500 µl of ice-cold 70% ethanol. Final pellets were left to air dry for 10 min, then resuspended in 100 µl of TE buffer (10 mM Tris/HCl, 1 mM EDTA, pH 7.8) overnight at 50°C. DNA concentration was measured by nano-drop spectrophotometry and samples were diluted to 2.5 ng/µl. Relative DNA levels of *RpL32* (single-copy nDNA) and *mt:lrRNA* (16S, mtDNA) were determined by qPCR using Applied Biosystems StepOnePlus™ Real-Time PCR System with Fast SYBR™ Green Master Mix kit (Applied Biosystems), using as template 2 µl of DNA in a 20 µl reaction, together with gene-specific primer pairs each at 500 nM, as follows (all shown 5′ to 3′): *RpL32*–TGTGTCACCAGGAACTTCTTGAA and AGG CCCAAGATCGTGAAGAA; *mt:lrRNA*–ACCTGGCTTACACCGGTTTG

and GGGTGTAGCCGTTCAAATTT. mtDNA copy number was inferred from the cycle-time difference (ΔC_T) of the two test genes, i.e. 2expΔC_T. Standard deviation (s.d.) was calculated from the mtDNA copy number values in a genotype group, and means (and s.d. values) were finally normalized to those of Oregon R females.

Protein analysis

Batches of ten 2-day-old adult flies were crushed in 100 µl of lysis buffer (0.3% SDS in PBS plus one EDTA-free cOmplete™ Protease Inhibitor Cocktail Tablet, Roche), incubated for 15 min and centrifuged at 15,000 g_{max} for 10 min (all manipulations at room temperature). Supernatants were decanted and protein concentrations determined by the Bradford assay. Aliquots of 50 µg protein in SDS-PAGE sample buffer containing 0.2 M dithiothreitol were heat-denatured for 5 min at 95°C then electrophoresed on AnyKD midi criterion™ gels (Bio-Rad) in ProSieve™ EX running buffer (Lonza). Transfer to Nitrocellulose membrane (Perkin-Elmer) was performed using ProSieve™ EX transfer buffer (Lonza). Membranes were blocked in 5% non-fat milk in PBS-0.05% Tween (Medicago) for 30 min at room temperature, with gentle agitation. Primary antibody diluted in the same buffer was added and reacted at 4°C overnight. After three 10 min washes, secondary antibody was added in the same buffer containing 5% non-fat milk for a further 2 h. Membranes were washed twice for 10 min in PBS-0.05% Tween and then for a final 10 min in PBS. Primary antibodies and dilutions were as follows: Srl214AA (against peptide CFDLADFITKDDFAENL) and Srl306AA (against peptide CPAKMGQTPDELRYVDNVKA), custom rabbit polyclonal antibodies (21st Century Biochemicals, both 1:5000), GAPDH (Everest Biotech EB06377, goat polyclonal, 1:5000), anti-V5 (Thermo Fisher Scientific, mouse monoclonal #R96025, 1:10,000). Appropriate HRP-conjugated secondary antibodies (Vector Laboratories, 1:5000). 5 ml of Luminata™ Crescendo Western HRP substrate solution (Merck) was added for 5 min before imaging with a Bio-Rad imager.

Transfections and immunocytochemistry

Transfection and induction of S2 cells with V5-tagged *srl* constructs and subsequent staining for imaging was performed as previously (González de Cózar et al., 2019). The primary antibody used was mouse anti-V5 (Life Technologies) along with the corresponding Alexa Fluor® 488 or Alexa Fluor® 647 secondary antibodies (Abcam), with image acquisition by confocal microscopy.

Image processing

Images have been cropped and/or rotated for clarity and optimized for contrast and brightness, but without other manipulations.

Statistical analysis

Data were analyzed using Student's *t*-test (two-tailed, with Bonferroni multiple-test comparison where indicated), one-way or two-way ANOVA, as appropriate (Microsoft Excel and GraphPad Prism). *n* numbers (batches of flies, representing at least 20 individual flies in total in each case, or replicate vials, representing 50–250 individual flies in total in each case) as indicated in figure legends. No exclusion criteria were applied. Note that, for statistical analysis of quantitative PCR data, ΔC_T values were used, because they are normally distributed, whereas the extrapolated fold-changes are not, having been subjected to an exponential transformation. Thus, to apply standard statistical tests such as ANOVA or Student's *t*-test, the ΔC_T values must be used.

Competing interests
The authors declare no competing or financial interests.

Author contributions
Conceptualization: J.G., H.T.J.; Methodology: J.G., H.T.J.; Formal analysis: J.G., H.T.J.; Investigation: J.G.; Resources: H.T.J.; Data curation: H.T.J.; Writing - original

Biology Open

draft: H.T.J.; Writing - review & editing: J.G., H.T.J.; Supervision: H.T.J.; Project administration: H.T.J.; Funding acquisition: H.T.J.

References

Austin, S. and St-Pierre, J. (2012). PGC1α and mitochondrial metabolism–emerging concepts and relevance in ageing and neurodegenerative disorders. *J. Cell. Sci.* **125**, 4963-4971. doi:10.1242/jcs.113662

Barckmann, B. and Simonelig, M. (2013). Control of maternal mRNA stability in germ cells and early embryos. *Biochim. Biophys. Acta* **1829**, 714-724. doi:10.1016/j.bbagrm.2012.12.011

Bauer, N. C., Doetsch, P. W. and Corbett, A. H. (2015). Mechanisms regulating protein localization. *Traffic* **16**, 1039-1061. doi:10.1111/tra.12310

Calleja, M., Peña, P., Ugalde, C., Ferreiro, C., Marco, R. and Garesse, R. (1993). Mitochondrial DNA remains intact during *Drosophila* aging, but the levels of mitochondrial transcripts are significantly reduced. *J. Biol. Chem.* **268**, 18891-18897.

Chen, S., Oliveira, M. T., Sanz, A., Kemppainen, E., Fukuoh, A., Schlicht, B., Kaguni, L. S. and Jacobs, H. T. (2012). A cytoplasmic suppressor of a nuclear mutation affecting mitochondrial functions in *Drosophila*. *Genetics* **192**, 483-493. doi:10.1534/genetics.112.143719

Diop, S. B., Bisharat-Kernizan, J., Birse, R. T., Oldham, S., Ocorr, K. and Bodmer, R. (2015). PGC-1/Spargel counteracts high-fat-diet-induced obesity and cardiac lipotoxicity downstream of TOR and Brummer ATGL lipase. *Cell Rep.* **10**, 1572-1584. doi:10.1016/j.celrep.2015.02.022

Fernandez-Ayala, D. J., Sanz, A., Vartiainen, S., Kemppainen, K. K., Babusiak, M., Mustalahti, E., Costa, R., Tuomela, T., Zeviani, M., Chung, J. et al. (2009). Expression of the *Ciona intestinalis* alternative oxidase (AOX) in *Drosophila* complements defects in mitochondrial oxidative phosphorylation. *Cell Metab.* **9**, 449-460. doi:10.1016/j.cmet.2009.03.004

Fernández-Ayala, D. J., Chen, S., Kemppainen, E., O'Dell, K. M. and Jacobs, H. T. (2010). Gene expression in a *Drosophila* model of mitochondrial disease. *PLoS ONE* **5**, e8549. doi:10.1371/journal.pone.0008549

Finck, B. N. and Kelly, D. P. (2006). PGC-1 coactivators: inducible regulators of energy metabolism in health and disease. *J. Clin. Invest.* **116**, 615-622. doi:10.1172/JCI27794

Gill, G. (2004). SUMO and ubiquitin in the nucleus: different functions, similar mechanisms? *Genes Dev.* **18**, 2046-2059. doi:10.1101/gad.1214604

González de Cózar, J. M., Gerards, M., Teeri, E., George, J., Dufour, E., Jacobs, H. T. and Jöers, P. (2019). RNase H1 promotes replication fork progression through oppositely transcribed regions of *Drosophila* mitochondrial DNA. *J. Biol. Chem.* **294**, 4331-4344. doi:10.1074/jbc.RA118.007015

Handschin, C., Kobayashi, Y. M., Chin, S., Seale, P., Campbell, K. P. and Spiegelman, B. M. (2007). PGC-1alpha regulates the neuromuscular junction program and ameliorates Duchenne muscular dystrophy. *Genes Dev.* **21**, 770-783. doi:10.1101/gad.1525107

Huang, T.-Y., Zheng, D., Houmard, J. A., Brault, J. J., Hickner, R. C. and Cortright, R. N. (2017). Overexpression of PGC-1α increases peroxisomal activity and mitochondrial fatty acid oxidation in human primary myotubes. *Am. J. Physiol. Endocrinol. Metab.* **312**, E253-E263. doi:10.1152/ajpendo.00331.2016

Johnson, L. N. (2009). The regulation of protein phosphorylation. *Biochem. Soc. Trans* **37**, 627-641. doi:10.1042/BST0370627

Kemppainen, E., Fernández-Ayala, D. J. M., Galbraith, L. C. A., O'Dell, K. M. and Jacobs, H. T. (2009). Phenotypic suppression of the *Drosophila* mitochondrial disease-like mutant tko(25t) by duplication of the mutant gene in its natural chromosomal context. *Mitochondrion* **9**, 353-363. doi:10.1016/j.mito.2009.07.002

Kemppainen, E., George, J., Garipler, G., Tuomela, T., Kiviranta, E., Soga, T., Dunn, C. D. and Jacobs, H. T. (2016). Mitochondrial dysfunction plus high-sugar diet provokes a metabolic crisis that inhibits growth. *PLoS ONE* **11**, e0145836. doi:10.1371/journal.pone.0145836

Klein, T., Eckhard, U., Dufour, A., Solis, N. and Overall, C. M. (2018). Proteolytic cleavage-mechanisms, function, and "omic" approaches for a near-ubiquitous posttranslational modification. *Chem. Rev.* **118**, 1137-1168. doi:10.1021/acs.chemrev.7b00120

Kugler, J.-M. and Lasko, P. (2009). Localization, anchoring and translational control of *oskar, gurken, bicoid* and *nanos* mRNA during *Drosophila* oogenesis. *Fly* **3**, 15-28. doi:10.4161/fly.3.1.7751

Lee, D. Y., Teyssier, C., Strahl, B. D. and Stallcup, M. R. (2005). Role of protein methylation in regulation of transcription. *Endocr. Rev.* **26**, 147-170. doi:10.1210/er.2004-0008

Lehman, J. J., Barger, P. M., Kovacs, A., Saffitz, J. E., Medeiros, D. M. and Kelly, D. P. (2000). Peroxisome proliferator-activated receptor gamma coactivator-1 promotes cardiac mitochondrial biogenesis. *J. Clin. Invest.* **106**, 847-856. doi:10.1172/JCI10268

Leone, T. C., Lehman, J. J., Finck, B. N., Schaeffer, P. J., Wende, A. R., Boudina, S., Courtois, M., Wozniak, D. F., Sambandam, N., Bernal-Mizrachi, C. et al. (2005). PGC-1alpha deficiency causes multi-system energy metabolic derangements: muscle dysfunction, abnormal weight control and hepatic steatosis. *PLoS Biol.* **3**, e101. doi:10.1371/journal.pbio.0030101

Lin, J., Wu, H., Tarr, P. T., Zhang, C.-Y., Wu, Z., Boss, O., Michael, L. F., Puigserver, P., Isotani, E., Olson, E. N. et al. (2002). Transcriptional co-activator PGC-1 alpha drives the formation of slow-twitch muscle fibres. *Nature* **418**, 797-801. doi:10.1038/nature00904

Lin, J., Wu, P.-H., Tarr, P. T., Lindenberg, K. S.,, St-Pierre, J., Zhang, C.-Y., Mootha, V. K., Jäger, S., Vianna, C. R., Reznick, R. M. et al. (2004). Defects in adaptive energy metabolism with CNS-linked hyperactivity in PGC-1alpha null mice. *Cell* **119**, 121-135. doi:10.1016/j.cell.2004.09.013

Magnuson, B., Ekim, B. and Fingar, D. C. (2012). Regulation and function of ribosomal protein S6 kinase (S6K) within mTOR signalling networks. *Biochem. J.* **441**, 1-2. doi:10.1042/BJ20110892

Manning, B. D. (2004). Balancing Akt with S6K: implications for both metabolic diseases and tumorigenesis. *J. Cell. Biol.* **167**, 399-403. doi:10.1083/jcb.200408161

Martínez-Redondo, V., Pettersson, A. T. and Ruas, J. L. (2015). The hitchhiker's guide to PGC-1α isoform structure and biological functions. *Diabetologia* **58**, 1969-1977. doi:10.1007/s00125-015-3671-z

Meirhaeghe, A., Crowley, V., Lenaghan, C., Lelliott, C., Green, K., Stewart, A., Hart, K., Schinner, S., Sethi, J. K., Yeo, G. et al. (2003). Characterization of the human, mouse and rat PGC1 beta (peroxisome-proliferator-activated receptor-gamma co-activator 1 beta) gene *in vitro* and *in vivo*. *Biochem. J.* **373**, 155-165. doi:10.1042/bj20030200

Merzetti, E. M. and Staveley, B. E. (2015). spargel, the PGC-1α homologue, in models of Parkinson disease in *Drosophila melanogaster*. *BMC Neurosci.* **16**, 70. doi:10.1186/s12868-015-0210-2

Mihaylova, M. M. and Shaw, R. J. (2011). The AMPK signalling pathway coordinates cell growth, autophagy and metabolism. *Nat. Cell Biol.* **13**, 1016-1023. doi:10.1038/ncb2329

Mukherjee, S. and Duttaroy, A. (2013). Spargel/dPGC-1 is a new downstream effector in the insulin-TOR signaling pathway in *Drosophila*. *Genetics* **195**, 433-441. doi:10.1534/genetics.113.154583

Mukherjee, S., Basar, M. A., Davis, C. and Duttaroy, A. (2014). Emerging functional similarities and divergences between *Drosophila* Spargel/dPGC-1 and mammalian PGC-1 protein. *Front. Genet.* **5**, 216. doi:10.3389/fgene.2014.00216

Narita, T., Weinert, B. T. and Choudhary, C. (2019). Functions and mechanisms of non-histone protein acetylation. *Nat. Rev. Mol. Cell. Biol.* **20**, 156-174. doi:10.1038/s41580-018-0081-3

Ng, C.-H., Basil, A. H., Hang, L., Tan, R., Goh, K.-L., O'Neill, S., Zhang, X., Yu, F. and Lim, K.-L. (2017). Genetic or pharmacological activation of the *Drosophila* PGC-1α ortholog spargel rescues the disease phenotypes of genetic models of Parkinson's disease. *Neurobiol. Aging* **55**, 33-37. doi:10.1016/j.neurobiolaging.2017.03.017

Rera, M., Bahadorani, S., Cho, J., Koehler, C. L., Ulgherait, M., Hur, J. H., Ansari, W. S., Lo, T., Jones, D. and Walker, D. W. (2011). Modulation of longevity and tissue homeostasis by the *Drosophila* PGC-1 homolog. *Cell Metab.* **14**, 623-634. doi:10.1016/j.cmet.2011.09.013

Rhee, J., Inoue, Y., Yoon, J. C., Puigserver, P., Fan, M., Gonzalez, F. J. and Spiegelman, B. M. (2003). Regulation of hepatic fasting response by PPARgamma coactivator-1alpha (PGC-1): requirement for hepatocyte nuclear factor 4alpha in gluconeogenesis. *Proc. Natl. Acad. Sci. USA* **100**, 4012-4107. doi:10.1073/pnas.0730870100

Royden, C. S., Pirrotta, V. and Jan, L. Y. (1987). The *tko* locus, site of a behavioral mutation in *D. melanogaster*, codes for a protein homologous to prokaryotic ribosomal protein S12. *Cell* **51**, 165-173. doi:10.1016/0092-8674(87)90144-9

Ryoo, H. D. and Vasudevan, D. (2017). Two distinct nodes of translational inhibition in the Integrated Stress Response. *BMB Rep.* **50**, 539-545. doi:10.5483/BMBRep.2017.50.11.157

Saari, S., Garcia, G. S., Bremer, K., Chioda, M. M., Andjelković, A., Debes, P. V., Nikinmaa, M., Szibor, M., Dufour, E., Rustin, P. et al. (2019). Alternative respiratory chain enzymes: Therapeutic potential and possible pitfalls. *Biochim. Biophys. Acta Mol. Basis Dis.* **1865**, 854-866. doi:10.1016/j.bbadis.2018.10.012

Shah, Z. H., O'Dell, K. M. C., Miller, S. C. M., An, X. and Jacobs, H. T. (1997). Metazoan nuclear genes for mitoribosomal protein S12. *Gene* **204**, 55-62. doi:10.1016/S0378-1119(97)00521-0

Shi, Z. and Barna, M. (2015). Translating the genome in time and space: specialized ribosomes, RNA regulons, and RNA-binding proteins. *Annu. Rev. Cell Dev. Biol.* **31**, 31-54. doi:10.1146/annurev-cellbio-100814-125346

Spiegelman, B. M. (2007). Transcriptional control of energy homeostasis through the PGC1 coactivators. *Novartis Found. Symp.* **286**, 3-6. doi:10.1002/9780470985571.ch2

Staats, S., Wagner, A. E., Lüersen, K., Künstner, A., Meyer, T., Kahns, A. K., Derer, S., Graspeuntner, S., Rupp, J., Busch, H. et al. (2018). Dietary ursolic acid improves health span and life span in male *Drosophila melanogaster*. *Biofactors* **45**, 169-186. doi:10.1002/biof.1467

St-Pierre, J., Drori, S., Uldry, M., Silvaggi, J. M., Rhee, J., Jäger, S., Handschin, C., Zheng, K., Lin, J., Yang, W. et al. (2006). Suppression of reactive oxygen

9

Biology Open

species and neurodegeneration by the PGC-1 transcriptional coactivators. *Cell* **127**, 397-408. doi:10.1016/j.cell.2006.09.024

Tiefenböck, S. K., Baltzer, C., Egli, N. A. and Frei, C. (2010). The *Drosophila* PGC-1 homologue Spargel coordinates mitochondrial activity to insulin signalling. *EMBO J.* **29**, 171-183. doi:10.1038/emboj.2009.330

Tinkerhess, M. J., Healy, L., Morgan, M., Sujkowski, A., Matthys, E., Zheng, L. and Wessells, R. J. (2012). The *Drosophila* PGC-1α homolog spargel modulates the physiological effects of endurance exercise. *PLoS ONE* **7**, e31633. doi:10. 1371/journal.pone.0031633

Toivonen, J. M., O'Dell, K. M., Petit, N., Irvine, S. C., Knight, G. K., Lehtonen, M., Longmuir, M., Luoto, K., Touraille, S., Wang, Z. et al. (2001). *Technical knockout*, a *Drosophila* model of mitochondrial deafness. *Genetics* **159**, 241-254.

Toivonen, J. M., Manjiry, S., Touraille, S., Alziari, S., O'Dell, K. M. C. and Jacobs, H. T. (2003). Gene dosage and selective expression modify phenotype in a *Drosophila* model of human mitochondrial disease. *Mitochondrion* **3**, 83-96. doi:10.1016/S1567-7249(03)00077-1

Uldry, M., Yang, W., St-Pierre, J., Lin, J., Seale, P. and Spiegelman, B. M. (2006). Complementary action of the PGC-1 coactivators in mitochondrial biogenesis and brown fat differentiation. *Cell Metab.* **3**, 333-341. doi:10.1016/j.cmet.2006.04.002

Vartiainen, S., Chen, S., George, J., Tuomela, T., Luoto, K. R., O'Dell, K. M. C. and Jacobs, H. T. (2014). Phenotypic rescue of a *Drosophila* model of

mitochondrial ANT1 disease. *Dis. Model. Mech.* **7**, 635-648. doi:10.1242/dmm. 016527

Wagner, A. E., Piegholdt, S., Rabe, D., Baenas, N., Schloesser, A., Eggersdorfer, M., Stocker, A. and Rimbach, G. (2015). Epigallocatechin gallate affects glucose metabolism and increases fitness and lifespan in *Drosophila melanogaster*. *Oncotarget* **6**, 30568-30578. doi:10.18632/ oncotarget.5215

Wilhelm, J. E. and Smibert, C. A. (2005). Mechanisms of translational regulation in *Drosophila*. *Biol. Cell* **97**, 235-252. doi:10.1042/BC20040097

Winata, C. L. and Korzh, V. (2018). The translational regulation of maternal mRNAs in time and space. *FEBS Lett.* **592**, 3007-3023. doi:10.1002/1873-3468. 13183

Yoon, J. C., Puigserver, P., Chen, G., Donovan, J., Wu, Z., Rhee, J., Adelmant, G., Stafford, J., Kahn, C. R., Granner, D. K. et al. (2001). Control of hepatic gluconeogenesis through the transcriptional coactivator PGC-1. *Nature* **413**, 131-138. doi:10.1038/35093050

Zhang, Y. and Xu, H. (2016). Translational regulation of mitochondrial biogenesis. *Biochem. Soc. Trans.* **44**, 1717-1724. doi:10.1042/BST20160071C

Zhao, J., Qin, B., Nikolay, R., Spahn, C. M. T. and Zhang, G. (2019). Translatomics: the global view of translation. *Int. J. Mol. Sci.* **20**, 212. doi:10. 3390/ijms20010212

Biology Open

10

PUBLICATION
IV

Germline knockdown of *spargel* (PGC-1) produces embryonic lethality in *Drosophila*

Jack George & Howard T. Jacobs

Mitochondrion, 49: 189-199

https://doi.org/10.1016/j.mito.2019.08.006

Publication reprinted with the permission of the copyright holders.

Germline knockdown of *spargel* (PGC-1) produces embryonic lethality in *Drosophila*

Jack George, Howard T. Jacobs*

Faculty of Medicine and Health Technology, Tampere University, Finland

ABSTRACT

The PGC-1 transcriptional coactivators have been proposed as master regulators of mitochondrial biogenesis and energy metabolism. Here we show that the single member of the family in *Drosophila*, *spargel* (*srl*) has an essential role in early development. Female germline-specific RNAi knockdown resulted in embryonic semilethality. Embryos were small, with most suffering a catastrophic derangement of cellularization and gastrulation, although genes dependent on localized determinants were expressed normally. The abundance of mtDNA, representative mitochondrial proteins and mRNAs were not decreased in knockdown ovaries or embryos, indicating that *srl* has a more general role in early development than specifically promoting mitochondrial biogenesis.

1. Introduction

The transcriptional coactivators of the PGC-1 family have been proposed as global regulators of mitochondrial biogenesis and metabolism (Spiegelman, 2007). Three members of the family, PGC-1α, PGC-1β and PPRC1 (or PRC) are encoded in mammalian genomes and are differentially expressed in tissue-specific or physiologically responsive patterns (Finck and Kelly, 2006). For example, PGC-1α is strongly induced in brown fat when hormonally stimulated (Puigserver and Spiegelman, 2003), whilst PPRC1 is instead induced by the addition of serum to quiescent cells, and has been shown to activate genes connected with the metabolic needs of growing cells (Andersson and Scarpulla, 2001).

In contrast, only a single member of the gene family, *spargel* (*srl*), is found in *Drosophila*, facilitating its study without the confounding factors of gene diversification and redundancy. In principle, given the molecular genetic toolkit available in *Drosophila*, this should allow the metabolic and developmental context of its expression to be elucidated, and its downstream effects on gene expression to be profiled, potentially revealing its ancestral function(s). In one such study, a spontaneously isolated hypomorph of *srl* was found to have a metabolic deficiency (in males), comprising decreased weight, and decreased accumulation of storage nutrients (Tiefenböck et al., 2010). Females of the line were sterile, and the mutant phenotypes seen in both sexes were compensated by the transgenic introduction of an additional genomic copy of the wild-type *srl* gene. Furthermore, alterations to the global pattern of gene expression in the fat body of the mutant males was consistent with a requirement for a sufficient expression of *srl* to maintain mitochondrial functions, although many other targets were identified, suggesting that *srl* may have a wider function. Although the question of its specificity remains unresolved, subsequent authors have also reported positive effects of *srl* on mitochondria and metabolism (Mukherjee et al., 2014), reinforcing the mammalian paradigm of PGC-1 function.

The female sterility of the *srl[1]* hypomorph, which is associated with an apparent delay in oogenesis (Mukherjee et al., 2014), could be interpreted in accordance with this paradigm, given that mitochondria and mitochondrial DNA are important components of the oocyte cytoplasm in *Drosophila*, as in other metazoans. Following their proliferation during oogenesis and delivery into the oocyte (Tourmente et al., 1990), mitochondria are partitioned to the cells of the embryo during cellularization and contribute vital metabolic functions that are tightly regulated during embryogenesis (Akiyama and Okada, 1992) and are essential for the growth of the resulting larva (Galloni, 2003; Adán et al., 2008). As such, a failure of transcription of genes for mitochondrial products during oogenesis would be a logical consequence of *srl* downregulation, leading to their catastrophic under-representation in the embryo and larva. Without functional mitochondria, a viable oocyte might fail to form.

In order to test these ideas, and gain insight into the role of *srl* in early development, we employed an RNAi approach. Initially we set out to test whether the female sterility caused by *srl* downregulation was a

somatic or germline effect, and whether it affected egg production and/or viability. To this end, we took advantage of the germline-specific MTD-GAL4 driver (Rørth, 1998; Hudson and Cooley, 2014). By combining this with an RNAi targeted on *srl*, using the VALIUM20 system (Ni et al., 2011), we confirmed that that the effect was germline-specific. Whilst ovaries appeared normal in germline *srl* knockdown females, most embryos did not develop properly, with failure to form a uniform blastoderm and gross morphological abnormalities observed from around the time of cellularization onwards. We proceeded to investigate various parameters in an attempt to establish whether *srl* knockdown led to a specific defect in the expression of mitochondrial genes or functions, as predicted by the widely held assumption that the PGC-1 coactivators act as master regulators of mitochondrial biogenesis in different contexts. However, the findings suggest an alternative or more global role of *srl* in development. Given the reasons for adopting *Drosophila* as the model organism for this study, our findings suggest that a global role of this kind, lined to growth and transcriptional switching in early development, may be the ancestral function of the PGC-1 coactivators. More specific roles in regard to metabolic reprogramming, energy homeostasis and mitochondrial biogenesis may have evolved subsequently or in parallel.

2. Materials and methods

2.1. Drosophila strains and maintenance

Oregon R (wild-type) and balancer lines were originally sourced from stock centres. Germline-specific drivers MTD-GAL4 (Bloomington 31777), *nos*-GAL4 drivers *NGT40* (Bloomington 4442) and *NGTA* (Bloomington 32563) (Tracey Jr et al., 2000; Wheeler et al., 2002), as well as TRiP RNAi lines targeted on *spargel*: HMS00857 (Bloomington 33914), HMS00858 (Bloomington 33915) and GL01019 (Bloomington 57043), were sourced from Bloomington Stock Center. Flies were maintained at 25 °C in a 12 h light-dark cycle in plugged plastic vials containing standard high-sugar medium (Kemppainen et al., 2016), supplemented with 0.5% propionic acid (Sigma-Aldrich) and 0.1% (w/v) methyl 4-hydroxybenzoate (Nipagin, Sigma-Aldrich). For embryo collection, approximately 200 female virgin flies of either Oregon R or one of the respective *spargel* knockdown lines crossed to MTD- or *nos*-GAL4 drivers were mated with approximately 100 Oregon R males in mating chambers with standard medium plates and left to lay eggs at 25 °C for the times indicated in figure legends.

2.2. Developmental assays

Batches of 10 female virgin flies of a given genotype were pre-mated with five Oregon R males on standard medium for 2 days, then tipped to fresh vials and allowed to lay eggs over a 24 h period. The adult flies were then discarded and the laid eggs were counted. The number of adult flies eventually eclosing from each vial was also counted to generate a percentage based on the number of embryos that completed development, using 5–20 vials for each genotype. To measure fecundity, females of a given genotype were mated as above to Oregon R males that were then discarded. Females were tipped to fresh vials every 5 days, and the number of eggs laid over a 24 h period measured four times, i.e. at days 5, 10, 15 and 20.

2.3. mtDNA copy number measurement

Batches of 10 ovary pairs or 50–200 embryos were crushed in 500 μl DNA lysis buffer (75 mM NaCl, 50 mM EDTA 20 mM HEPES/NaOH, pH 7.8). 5 μl of 20% SDS and 20 μl of Proteinase K (10 mg/ml, ThermoFisher Scientific) were added to each sample and vortexed to mix. Samples were briefly centrifuged, left on a heat block at 50 °C for 4 h, then vortexed and centrifuged at 16,000 g_{max} for 1 min to pellet debris. Supernatants were decanted and nucleic acid was precipitated

with 420 μl of isopropanol with repeated inversion and overnight incubation at −20 °C. Samples were centrifuged at 16,000 g_{max} for 30 min at 4 °C to pellet the DNA, which was washed with 500 μl of ice-cold 70% ethanol. Final pellets were left to air dry for 10 mins, then resuspended in 100 μl of TE buffer (10 mM Tris/HCl, 1 mM EDTA, pH 7.8) overnight at 50 °C. DNA concentration was measured by nano-drop spectrophotometry and samples were diluted to 2.5 ng/μl. Relative DNA levels of RpL32 (single-copy nDNA) and mt:lrRNA (16S, mtDNA) were determined by qPCR using Applied Biosystems StepOnePlus™ Real-Time PCR System with Fast SYBR™ Green Master Mix kit (Applied Biosystems), using as template 2 μl of DNA in a 20 μl reaction, together with gene-specific primer pairs each at 500 nM, as follows (all shown 5′ to 3′): RpL32 – TGTGCACCAGGAACTTCTTGAA and AGGCCCAAGATCGTGAAGAA; mt:lrRNA –ACCTGGCTTACACCGGTTTG and GGGTGTAGCCGTTCAAATTT. mtDNA copy number per haploid copy of nDNA was inferred from the cycle-time difference (ΔC_T) of the two test genes, i.e. $2\exp\Delta C_T$. SD was calculated from the mtDNA copy number values in a genotype group, and means and SD values were normalized to that of Oregon R for the given tissue or stage (Quiros et al., 2017).

2.4. RNA extraction and analysis

Total RNA was extracted from batches of 20 pairs of ovaries (dissected and placed in PBS), or from 100 to 200 embryos (at 80 or 160 min AEL, dechorionated in 50% household bleach (Domestos) for 2 min and rinsed thee times in PBS) or from batches of 2-day old adult flies using a plastic homogenizing pestle and trizol reagent as previously described (Kemppainen et al., 2016). cDNA was synthesized using the High-capacity cDNA Reverse Transcription Kit (ThermoFisher Scientific) according to manufacturer's instructions. Expression levels were determined by qRT-PCR using Applied Biosystems StepOnePlus™ Real-Time PCR System with Fast SYBR™ Green Master Mix kit (Applied Biosystems) using, as template, 2 μl of cDNA product diluted 10-fold, in a 20 μl reaction, together gene-specific primer pairs, each at 50 nM, as follows (all given 5′ to 3′, gene symbols in the following list following current practice in FlyBase (Thurmond et al., 2019; Chintapalli et al., 2007)): *RpL32* (CG7939), TGTGCACCAGGAACTTCTTGAA and AGGCCCAAGATCGTGAAGAA; *srl* (CG9809), GGAGGAAGACGTGCCTTCTG and TACATTCGGTGCTGGTGCTT; *ND-ACP* (CG9160), ACAAGATCGATCCCAGCAAG and ATGTCGGCAGGTTTAAGCAG: *ND-30* (CG12079), AAGGCGGATAAGCCCACT and GCAATAAGCACCTCCAGCTC; *mt:ND5* (CG34083), GGGTGAGATGGTTTAGGACTTG and AAGCTACATCCCCAATTCGAT; *SdhA* (CG17246), CATGTACGACACGGTCAAGG and CCTTGCCGAACTTCAGACTC; *SdhD* (CG10219) GTTGCAATGCCGCAAATCT and GCCACCAGGGTGGAGTAG; *RFeSP* (CG7361), GGGCAAGTCGGTTACTTTCA and GCAGTAGTAGCCACCCCAGT; *UQCR-C2* (CG4169), GAGGAACGCGCCATTGAG and ACGTAGTGCAGCAGGCTCTC; *blw* (CG3612), GACTGGTAAGACCGCTCTGG and GGCCAAGTACGCAGAGGAG; *COX5A* (CG14724), AGGAGTTCGACAAGCGCTAC and ATAGAGGGTGGCCTTTTGGT; *COX4* (CG10664), TCTTCGTGTACGATGAGCTG and GGTTGATTTCCAGGTCGATG; *mt:Cyt-b* (CG34090), GAAAATTCCGAGGGATTCAA and AACTGGTCGAGCTCCAATTC; *ATPsynF* (CG4692), CTACGGCAAAGCCGATGT and CGCTTTGGGAACACGTACT; *mt:lrRNA* (CR34094), ACCTGGCTTACACCGGTTTG and GGGTGTAGCCGTTCAAATTT; *TFAM* (CG4217), AACCGCTGACTCCCTACTTTC and CGACGGTGGTAATCTGGGG; *Gapdh1* (CG12055) GACGAAATCAAGGCTAAGGTCG and AATGGGTGTCGCTGAAGAAGTC. Mean values were normalized first against that for *RpL32* and then against an arbitrary standard, usually Oregon R from the same stage or material, as indicated in figure legends. Statistical analysis used the primary dC_T data, whilst plotted data shows the normalized fold-changes.

2.5. Protein analysis

Batches of 20 pairs of ovaries (dissected and placed in PBS) or of 100–200 embryos at 80 or 160 mins AEL, dechorionated in 50%

household bleach (Domestos) for 2 min and rinsed three times in PBS) were crushed in 50 μl lysis buffer (0.3% SDS in PBS, plus one EDTA-free cOmplete™ Protease Inhibitor Cocktail tablet (Roche) per 10 ml). After 15 min incubation at room temperature, samples were centrifuged at 15,000 g_{max} for 10 min at room temperature. Supernatants were decanted and protein concentrations determined using the Bradford assay. Samples were ran on AnyKD™ Criterion™ TGX™ Midi gels (Bio-Rad) in ProSieve™ EX running buffer (Lonza) with either Prestained Pageruler™ (or Pageruler™ Plus) Ladder (ThermoFisher Scientific), or Spectra™ Multicolor Broad Range Protein Ladder (ThermoFisher Scientific) as molecular weight markers. Transfer was performed using the Trans-Blot® Turbo™ Transfer System (Bio-Rad) with the midi nitrocellulose-specific transfer pack. Membranes were blocked in 5% non-fat milk in PBS-0.05% Tween (Medicago) for 30 min at room temperature with gentle shaking, then incubated similarly with primary antibodies, as listed below, at 4 °C overnight. After three 10 min washes in PBS-0.05% Tween, membranes were incubated with secondary antibody in the same buffer for 2 h at room temperature, and washed twice in PBS-0.05% Tween and then for a final 10 min in PBS. 5 ml of Luminata™ Crescendo Western HRP substrate solution (Merck) was added for 5 min before imaging (Bio-Rad ChemiDoc MP). Densitometry was implemented using ImageJ software. Primary antibodies and dilutions were as follows: ATP5A 1:50,000 Abcam#14748, COXIV 1:1000 Abcam#16056, NDUFS3 1:2500, Abcam#14711, β-actin – DSHB JLA20-s 1:2500 (all mouse monoclonals), GAPDH 1:5000 Everest Biotech EB06377 (goat polyclonal), Histone H4 (Abcam, #10158, rabbit polyclonal,1:5000) and Srl214AA (against peptide CFDLADFIT-KDDFAENL), customized rabbit polyclonal (21st Century Biochemicals, 1:5000). Appropriate HRP-conjugated secondary antibodies (Vector Laboratories) were used at 1:5000). Note that the Srl214AA antibody was verified previously by over-expression, co-migration with epitope-tagged Spargel, and use of a second antibody raised against a different Spargel peptide (George & Jacobs, 2019).

2.6. Brightfield imaging

Embryos laid over 24 h at 25 °C were collected from mating-chamber plates (as above), placed in PBS, rinsed twice in PBS and mounted in PBS onto a slide, for viewing with an Olympus DP73 microscope.

2.7. Time-lapse imaging of embryonic development

Embryos laid over 30 min at 25 °C were collected from mating-chamber plates (as above) and placed in a droplet of halocarbon oil 700 (Sigma-Aldrich) in a 6-well plate. Humidity was maintained by placing a water-soaked cotton-wool plug in adjacent wells. Images were taken every 2 min for 24 h or until hatching, using the Cell-IQ live-cell imaging platform (Imagen) at 10× magnification and a constant 25 °C.

2.8. Immunohistochemistry and fluorescent imaging

Batches of approximately 20 ovaries were dissected in PBS, fixed in 4% paraformaldehyde (pH 7.2) on ice for 20 min, rinsed twice with PBT (PBS-0.05% Tween), washed twice for 15 min in PBT-BSA (0.5% BSA) and incubated with primary antibody in PBT-BSA overnight at 4 °C. After two rinses with PBT, samples were washed twice for 15 min in PBT-BSA then incubated with secondary antibody in PBT-BSA for 2 h at room temperature. After two further rinses with PBT and two further washes for 15 min in PBT-BSA samples were mounted using ProLong Gold Antifade Mountant with DAPI (ThermoFisher Scientific). Embryos laid over 4 h at 25 °C were collected from mating-chamber plates (as above), dechorionated using 50% household bleach (Domestos) and rinsed three times in PBS. 500 μl of heptane and 500 μl of 4% paraformaldehyde (pH 7.2) were added and the embryos left to fix over 10–60 min. The aqueous bottom layer was removed, leaving the

Table 1
Densitometric analysis[a] of Western blots.

Stage	Protein	Oregon R	33914[b]	33915[b]	Statistical analysis[c]
Ovary[d]	Spargel	1.00 ± 0.24	1.29 ± 0.33	0.82 ± 0.24	ns
	ATP5A	1.00 ± 0.01	0.87 ± 0.06	0.96 ± 0.05	ns
	GAPDH	1.00 ± 0.21	0.40 ± 0.02	0.81 ± 0.10	Oregon R/ 33914* 33914/ 33915**
Embryo[e]	COXIV	1.00 ± 0.01	1.46 ± 0.18	nd	ns
	ATP5A	1.00 ± 0.03	0.78 ± 0.15	nd	ns
	NDUFS3	1.00 ± 0.29	0.81 ± 0.06	nd	ns
	GAPDH	1.00 ± 0.05	1.22 ± 0.17	nd	ns

[a] Using Inage J, with normalization to values for Oregon R for each protein and stage.
[b] From females/mothers of the indicated RNAi lines crossed to MTD-GAL4.
[c] Using Student's t-test, with Bonferroni correction where appropriate, * – $p < 0.05$, ** – $p < 0.01$, ns – not significant.
[d] Based on Western blots shown in Fig. 5C.
[e] 160 min AEL, based on Western blots shown in Fig. 6B.

embryos in 500 μl of heptane, to which was added 500 μl of methanol. Embryos were vortexed for 2 min to remove the vitelline membrane. Heptane, methanol and all material at the interphase was removed, leaving only the devitellinised embryos, which were rinsed three times with methanol, washed three times for 15 min in PBT-BSA (0.5% BSA), and processed thereafter as for ovaries. For ovaries the primary antibody used was against ATP5A – Abcam#14748, 1:5000 and for embryos: Even skipped – DSHB-2B8, Hunchback – Abcam#197787, Dorsal – DSHB-7A4, all at a dilution of 1:500. Appropriate Alexa Fluor® 488 secondary antibodies (Abcam) were used at 1:1000. Images were acquired using a Zeiss LSM800 confocal microscope or, for large-scale embryo size and staining-pattern analysis, with a Hamamatsu S60 nanozoomer WSI digital slide scanner C13210-01 microscope at 5× magnification. ImageJ software (Regions of Interest tool) was used to calculate the areas of DAPI-stained embryos for estimating their overall size estimation. Embryos stained for localized markers were also examined manually and judged to be positive or negative for the relevant characteristic staining pattern (see Fig. 4).

2.9. Image processing

Images have been cropped, rotated and framed for clarity, with addition of scale bars where appropriate, as well as optimized for contrast and brightness, but without other manipulations.

3. Results

3.1. srl expression is developmentally regulated

Database information on the expression level of *srl*, based on in situ hybridization and RNA-seq (Berkeley Drosophila Genome Project, Flyatlas) indicates sharp changes in early development and a generally modest expression in adult, which is highest in the ovaries. To compare this expression quantitatively between tissues and stages, we conducted qRT-PCR on RNA extracted from staged early embryos, from each of the larval instars, and from separate sexes from L3 up to adult stage (Fig. 1A, B), using RpL32 RNA as an internal standard. Expression was highest in early embryos (stages 1–3), dropped sharply (at least 10-fold) at stages 4–6 (Fig. 1A), around the time of the mid-blastula transition, rose slightly at L1, then remained low throughout development in both sexes (Fig. 1B). In adults it remained low in males, but was approximately 8-fold higher in females (Fig. 1A), as noted previously (George & Jacobs, 2019). Dissection of adult females revealed that this sex difference was accounted for by much higher expression in ovaries than in
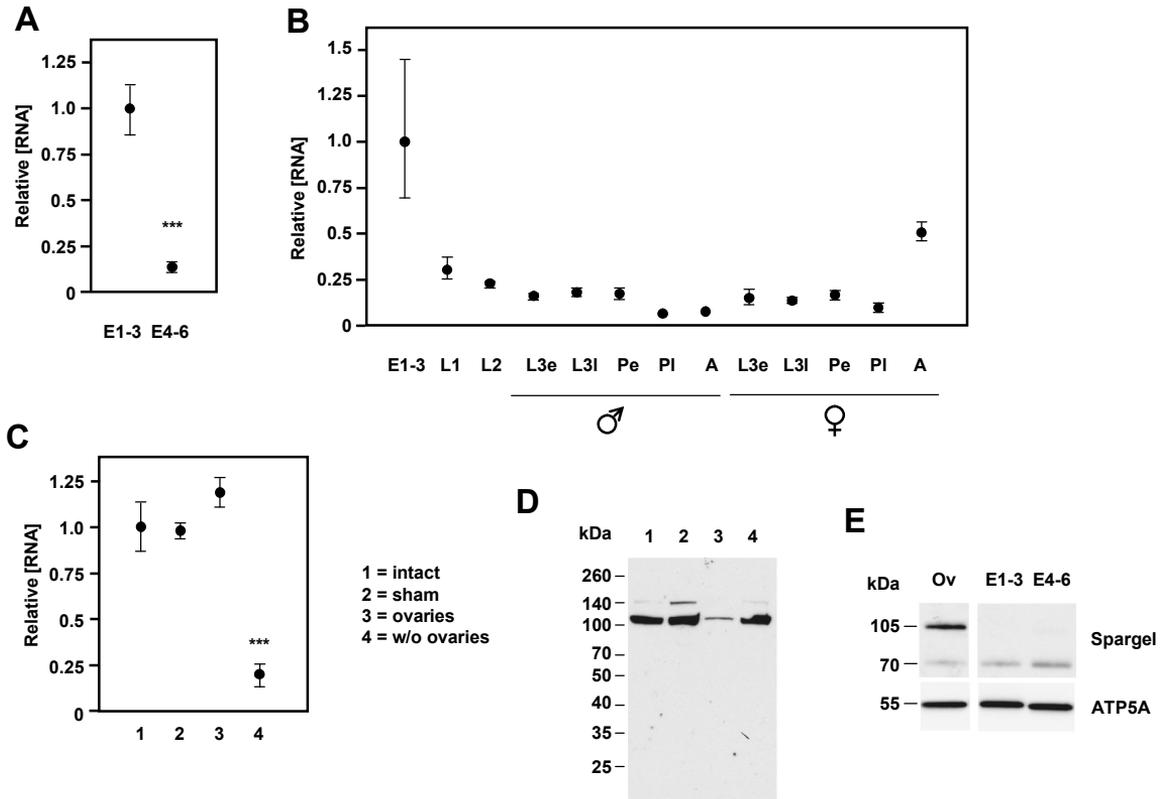
Fig. 1. *srl* expression is developmentally regulated.

(A, B) Relative level of *srl* RNA (by qRT-PCR) in flies at different developmental stages, means ± SD, values normalized to that in stage 1–3 embryos (E1–3, 80 min AEL). E4–6 – stage 4–6 embryos (160 min AEL); L1, L2 – first and second larval instars; L3e – early wandering-stage third-instar larvae; L3 l – late wandering-stage third-instar larvae (one day later); Pe – early pupae (first day); Pl – late pupae (adult structures clearly visible through pupal case); A – 2-day old adult; males and females shown separately from L3e on, when gonads become visibly distinguishable. In (A) *** denotes significant difference from E1–3, Student's *t*-test with Bonferroni correction, based on dC_T values, $n = 4$ batches of embryos for all groups. In (B) $n = 3$ batches of flies for all groups except adult females, where one sample was lost. Statistical analysis by one-way ANOVA with Tukey post hoc HSD test (Table S1) indicated overlaps between most data groups, with only E1–3 being significantly different from all others. (C) Relative *srl* RNA levels (qRT-PCR) and (D, E) Spargel protein level (Western blot probed with the antibody against the peptide indicated in Fig. S4) in (D) intact 2-day old adult females, sham-ovariectomized females, isolated ovaries and ovariectomized females and (E) isolated ovaries and embryonic stages 1–3 (E1–3) and 4–6 (E4–6), as indicated. In (C), means ± SD nornalized to values for intact, adult females, *** denotes significant difference from intact females, Student's *t*-test with Bonferroni correction, based on dC_T values, $p < 0.001$. $n = 4$ batches of females (or ovaries) for all groups. Equal loading in (D) was confirmed by Ponceau S staining (Fig. S1C). As no other normalization control was used in the experiment shown in (D), an equivalent blot from a separate experiment is shown in Fig. S1B, reprobed for GAPDH. ATP5A was used as a loading control in (E), as shown. Molecular weights extrapolated from the migration of molecular-weight markers. Separated images are non-adjacent tracks from the same gel. Note that, the virtually undetectable signal from the major (~105 kDa) band in embryos in (E), indicates a > 20-fold difference in the protein level compared with whole adults, given the wide dynamic range of the Bio-Rad imager system.

the rest of the adult female (Fig. 1C). We then examined the levels of Spargel protein using a previously verified (George & Jacobs, 2019), customized antibody (Fig. 1D, S1A, S1B). As noted previously (George & Jacobs, 2019), the protein was equally represented in males and females (Fig. S1B), despite the disparity in RNA levels. Moreover, in females, the protein was found only at low levels in ovaries, where the RNA is paradoxically most abundant (Fig. 1D, Fig. S1B). Note that samples from ovaries include both germline and somatic (follicle) cells. The ~105 kDa 'main band' was almost undetectable in laid embryos (Fig. 1E), suggesting that, in the ovary, it is mainly of somatic origin.

3.2. Maternal srl knockdown in the female germline results in embryonic lethality

To test the effects of downregulating *srl* expression specifically in

the female germline, we made use of the MTD-GAL4 driver, which directs transgene expression in germ cells throughout oogenesis. We combined it with shRNA lines from the Harvard Medical School TriP collection, targeted on *srl*. We initally tested three such lines. Two of them gave only a weak knockdown of *srl* in whole females (Fig. S1D). The third (Bloomington stock center ID 33914, HMS00857, hereafter referred to more simply as line 33914) produced substantial (> 80%) knockdown (Fig. S1D), and also showed this result when RNA from isolated ovaries was tested (Fig. 2A). One of the lines that showed only a weak knockdown in whole females (Bloomington stock center ID 33915, HMS00858, hereafter referred to as line 33915) did not give knockdown in isolated ovaries either (Fig. 2A), and was used in all subsequent experiments as an additional strain-background negative control, along with wild-type Oregon R. The other negative line (Bloomington stock center ID 57043, GL01019) was not studied further.
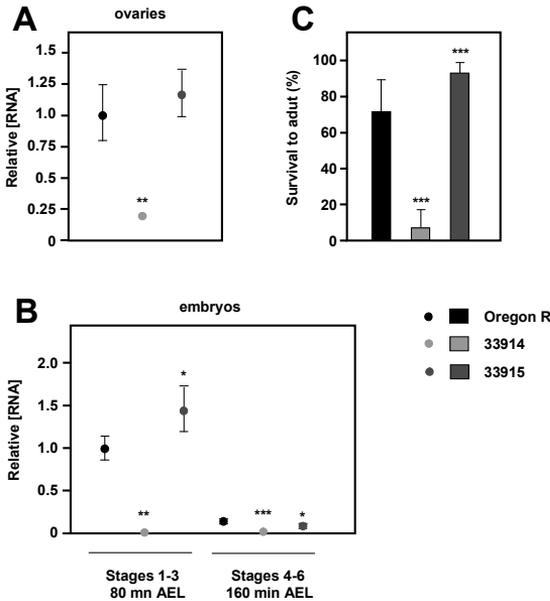
Fig. 2. Germline *srl* knockdown using the MTD-GAL4 driver.
(A, B) Relative level of *srl* RNA (by qRT-PCR) in (A) ovaries of 2-day old females and (B) embryos (stages 1–3 or 4–6, i.e. 80 or 160 min AEL, as indicated) from Oregon R (wild-type) females and females of shRNA lines 33914 and 33915, combined with MTD-GAL4 driver; means ± SD normalized to values for Oregon R females, n = 4 batches of ovaries or embryos for all groups. (C) Survival (egg to adult) for progeny of Oregon R females and females of shRNA lines 33914 and 33915, combined with MTD-GAL4 driver. *, **, *** – significant differences from Oregon R, Student's *t*-test with Bonferroni correction (based on dC$_T$ values for qRT-PCR), $p < 0.05$, 0.01, 0.001, respectively, n = 4 batches of embryos for all groups.

Even when using line 33,914, two *nos*-GAL4 drivers, *NGT40* and *NGTA* (Tracey Jr et al., 2000; Wheeler et al., 2002*)* gave no knockdown (Fig. S1D) and were not used further.

The rate of egg-laying by females with germline *srl* knockdown (line 33914 combined with the MTD-GAL4 driver) was comparable with wild-type or with line 33915 (Fig. S2A). The embryos that developed manifested a drastically lower (> 2 orders of magnitude) level of *srl* RNA than controls (Fig. 2B) 80 min after egg-laying (AEL), and the level remained low at 160 min AEL, the time when control embryos at stage 4–6 showed a substantial drop in *srl* RNA abundance (Fig. 2B). Over 90% of the knockdown embryos failed to complete development (Fig. 2C). However, of the small minority that hatched, almost all developed normally through the larval and pupal stages thereafter, indicating that the developmental defect conferred by maternal *srl* knockdown in the germline occurred specifically during embryogenesis. Examination of knockdown embryos laid over a 24 h period (Fig. 3A) revealed that they varied in their progress through embryogenesis, but most of them failed to reach the later stages in which trachea were visible. Some did not appear to develop at all, and many did not resemble any normal stages, manifesting diverse and typically severe morphological defects. Using time-lapse photography we tracked knockdown embryos through a full 24-hour period. A common pattern (Movie S1) was of grossly abnormal cellularization and gastrulation movements, whilst control embryos cultured in parallel developed as normal (Movie S2).

3.3. Maternal srl knockdown embryos have an abnormal size distribution

The embryos laid over a 4 h period by germline *srl* knockdown mothers were analyzed for size and for the expression of genes involved in patterning of the embryo. Whereas control embryos were normally distributed in size (Fig. 3B), those from knockdown mothers showed a broader size distribution, but with a substantial proportion smaller than the size range of controls and a significantly decreased mean size. Automated Gaussian curve fitting failed (Fig. 3B, middle panel), indicating a left-skewed size distribution. The expression of genes in specific embryonic territories in response to localized determinants was, nevertheless, similar to wild-type controls and to published literature, even in small embryos, for the three test gene products studied (Even skipped – Fig. 4A, Hunchback – Fig. 4B and Dorsal – Fig. 4C).

3.4. Germline srl knockdown does not downregulate transcripts related to mitochondrial function

Given the widely credited view that the main role of the PGC-1 coactivator family is to boost the transcription of genes related to mitochondrial and metabolic function under specific physiological or developmental conditions, the observed embryonic semilethality and morphological abnormalities could be consistent with such a role for *srl* in early development (oogenesis and/or embryogenesis). To investigate this possibility, we studied the steady-state levels (normalized to that of cytosolic ribosomal protein RpL32) of transcripts for a range of genes encoding components of the mitochondrial OXPHOS complexes, as well as the major mitochondrial transcription factor and nucleoid protein TFAM, the mitochondrial large-subunit (16S) rRNA, and one reference gene, the Gapdh1 isoform of the glycolytic enzyme GAPDH. In ovaries from germline knockdown females (MTD-GAL4/33914) the levels of these transcripts showed no significant differences from controls (Fig. 5A). In knockdown ovaries we observed ovarian follicles in all stages of development (Fig. 5B), with a normal amount and distribution of DNA and of the mitochondrial OXPHOS protein Bellwether (*Drosophila* ATP synthase α subunit, ATP5A). By Western blot we also found normal levels of typical OXPHOS proteins such as those detected by antibodies against ATP5A (Fig. 5C, S2C), NDUFS3 (ND-30, Fig. S2C) and COXIV (Fig. S2C), as well as housekeeping proteins β-actin and histone H4 (Fig. S2C). Against this trend, and despite the level of *Gapdh1* mRNA not being significantly less than wild-type (Fig. 5A), we found consistently decreased levels of GAPDH (Fig. 5B, S2C). Surprisingly, and despite the large decrease in *srl* RNA (Fig. 2A), there were no systematic effects observed on the levels of Spargel polypeptides in ovaries (Fig. 5B). Relative mtDNA levels measured by qPCR were not significantly different from those of Oregon R wild-type ovaries (Fig. 5C).

In embryos at the 80 min AEL time point (stage 1–3 in control embryos), we observed increased levels of many of the OXPHOS-related transcripts (Fig. S3A), although in many cases this trend was shared with embryos from MTD-GAL4/33915 mothers, so may be a background effect. The steady-state level of ATP5A (Bellwether) protein was unchanged from controls (Fig. S3B), whilst that of Spargel polypeptides was extremely low, as in controls (Fig. S3B). mtDNA copy number, although more varied than in controls at this time-point (Fig. S3D), was of a similar order of magnitude. More pronounced changes were seen at the 160 min AEL time-point (stage 4–6 in controls), following the period when *srl* mRNA is normally at maximal abundance, but then declines (Fig. 1A), and when development in embryos from knockdown mothers becomes clearly aberrant (Supplementary Movie S1). However, here again the trend from *srl* knockdown was towards increased, not decreased levels of OXPHOS-related transcripts (Fig. 6A), which were clearly elevated compared with both Oregon R and MTD-GAL4/33915 controls. Typical OXPHOS proteins were unchanged compared with wild-type control embryos (Fig. 6B), and this now applied also to GAPDH (Fig. 6B). Relative mtDNA copy number (Fig. 6C, S3D) declined
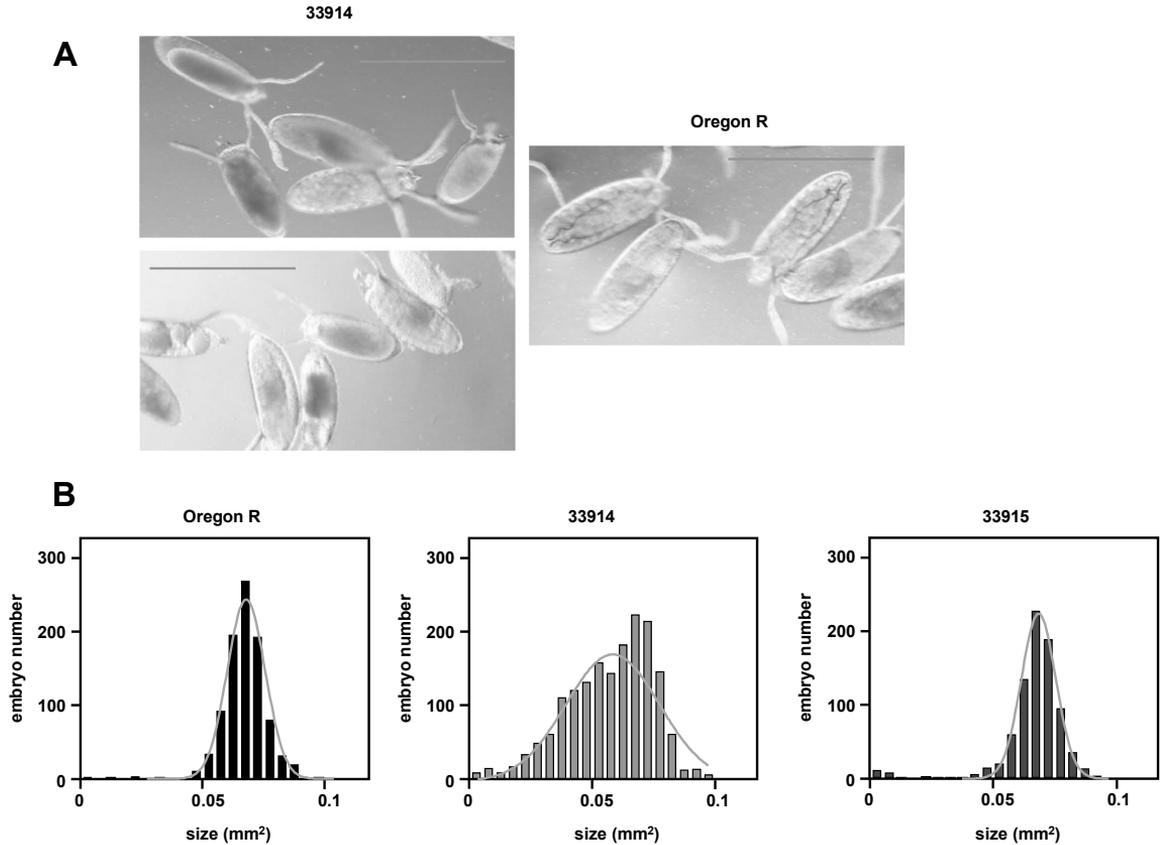
Fig. 3. Germline *srl* knockdown results in abnormal size distribution of embryos.

(A) Images of embryos from mothers of the indicated genotype (Oregon R – wild-type, 33914, 33915 – shRNAi lines combined with MTD-GAL4). Scale bars – 500 μm.
(B) Size histograms of embryos from mothers of the indicated genotypes, (Oregon R – wild-type, 33914, 33915 – shRNAi lines combined with MTD-GAL4), laid over 4 h. Shown in orange are Gaussian curves fitted automatically using GraphPad prism software. Those for Oregon R and 33,915 embryos are consistent with a normal distribution of embryo sizes. The curve for the effective knockdown line 33,914 reveals a left-skewed distribution, with outliers in the range of sizes seen in controls.

substantially between the two embryo time-points, in line with the expected synthesis of nuclear DNA. Although copy number in maternal *srl* knockdown (MTD-GAL4/33914) embryos remained slightly higher than in wild-type (Oregon R), this was shared with the MTD-GAL4/ 33915 control (Fig. 6C, S3D). This indicates that it was most likely a background effect, possibly related to the timing of the final rounds of nuclear DNA synthesis.

4. Discussion

In this study we demonstrated that *srl* function in the germline is required to ensure successful embryogenesis. In summary, gerrmline *srl* knockdown produced embryos with an abnormal size distribution (Fig. 3B) and decreased mean size, which failed to develop normally (Fig. 3A) and exhibited aberrant patterns of cellularization and gastrulation movements that did not resemble any normal developmental stage (Movie S1). However, knockdown produced no detectable abnormalities in the embryonic expression of axial specifiers dependent on localized determinants laid down during oogenesis (Fig. 4) and no significant changes in mtDNA copy number (Figs. 5D, 6C) or OXPHOS proteins (Figs. 5C, 6B). mRNAs for OXPHOS subunits were unchanged in oocytes (Fig. 5A) but generally elevated 160 min AEL (Fig. 6A) Although *srl* was at its highest levels in early embryos and in ovaries,

Spargel protein was paradoxically at very low levels in these developmental stages (Fig. 1), and was not affected by germline knockdown of the RNA. We here discuss the significance and implications of these findings.

4.1. Respective roles of spargel RNA and protein in early development

Two different antibodies raised against non-overlapping peptides from the Spargel protein detect the same bands in Western blots (George & Jacobs, 2019), namely a major isoform migrating at an apparent molecular weight of ~105 kDa and a less abundant isoform migrating at ~120 kDa. The same bands were detected in S2 cells transfected with an epitope-tagged variant of *srl*, probed for the epitope tag (George & Jacobs, 2019). In the present study we also detected a minor band in ovaries (Fig. 5C) and embryos (Fig. S3B), visible only at long exposure, migrating around ~70 kDa. Based on the previous data (George & Jacobs, 2019) we consider that these antibodies are reliable for detecting Spargel polypeptides, although not necessarily all Spargel polypeptides. Any Spargel isoforms in which the two relevant (non-overlapping) peptides used for raising antibodies (see Fig. S4) are both excised or heavily modified would remain undetected. The primary translation products of both of the reported *srl* mRNA splice variants (see FlyBase (Thurmond et al., 2019; Chintapalli et al., 2007)) differ by
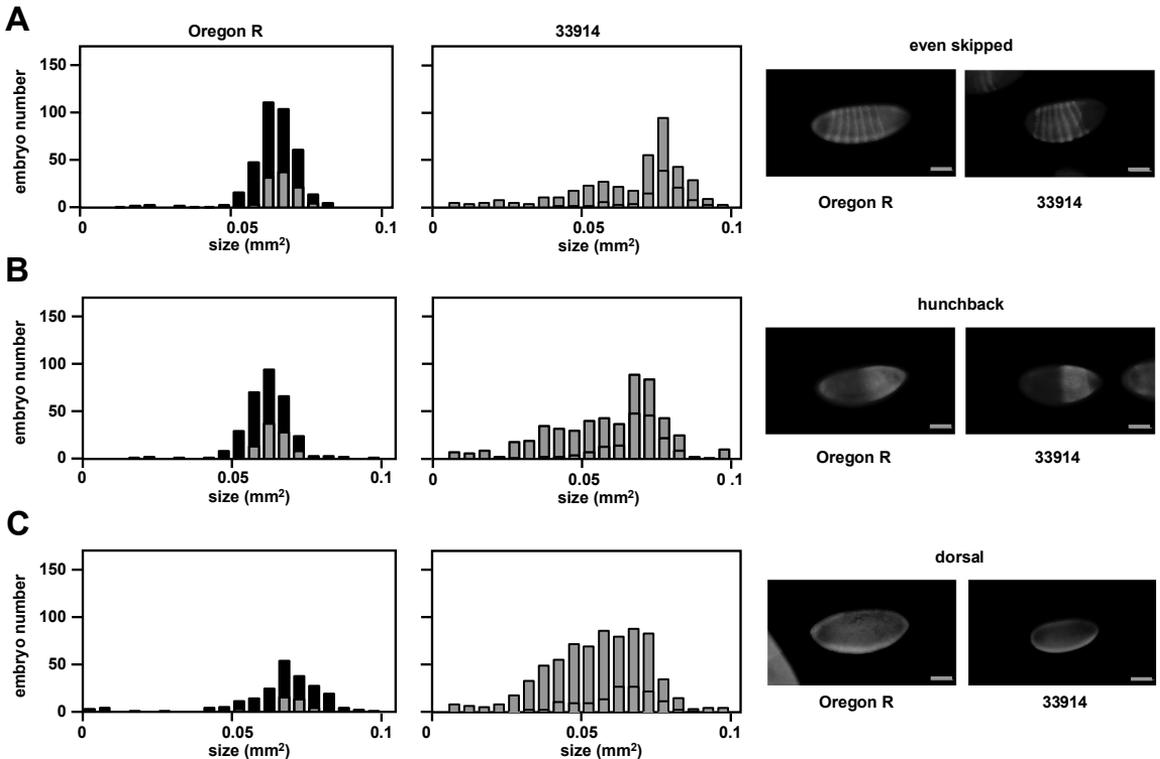
Fig. 4. Germline *srl* expression does not alter embryonic expression of localized determinants.
Size histograms of embryos from mothers of the indicated genotypes, (Oregon R – wild-type, 33914, 33915 – shRNAi lines combined with MTD-GAL4), laid over 4 h, showing the proportion in each size class expressing the indicated markers in the characteristic, localized patterns reported for wild-type embryos, based on immunohistchemistry with counterstaining by DAPI, alongside examples: (A) Even skipped, expressed at stages 4–9 in seven stripes (Frasch et al., 1987), typically displaced slightly towards the posterior pole, (B) Hunchback, present at stages 4–6 (Schroder et al., 1988) in the anterior half of the embryo plus a fainter cap or stripe close to the posterior pole and (C) Dorsal, found at stages 3–9 (Steward, 1989) in a ventral stripe and then in the ventral furrow. Note that each marker is found in a normal pattern in roughly the expected proportion of 33914 (*srl* knockdown) embryos of different size classes. Scale bars – 100 μm.

only a short run of amino acids near the N-terminal region (Fig. S4), are each predicted to be detected by these antibodies. Several observations suggest that we may be missing some vital information, which could relate to one or more isoforms of the protein that are not detected by either of these antibodies, or to a role for *srl* RNA that is distinct from its coding function as the mRNA for Spargel. First and most puzzling is the discordant result regarding the abundance of *srl* RNA and Spargel protein. The RNA was several-fold higher in females than in males, but the difference is accounted for by its much higher representation in the ovaries than in somatic tissues. Ovariectomized females had similar amounts of the RNA as males (Fig. 1B, C). However, the major, ~105 kDa protein isoform follows a distinct, in some ways opposite pattern, being present in similar amounts in adult males and ovariectomized females, but at much lower levels in ovaries. In the early embryo, the RNA was at its highest level of any stage (Fig. 1A), yet the major Spargel protein band of ~105 kDa was virtually undetectable, with only the minor ~70 kDa band clearly visible. Further, despite effective RNAi knockdown of *srl* at the RNA level (Fig. 2), the protein level was essentially unaffected, at least in ovaries (Fig. 5C).

It should be noted that different normalization standards were used for RNA (*RpL32*) and for protein (GAPDH). For RNA normalization *RpL32* is commonly used as reference gene, making our data comparable with that of other studies. For protein normalization, there is no fully agreed universal standard, although GAPDH is widely used, and

shows only minor fluctuations in most contexts. RpL32 has not been widely used as a protein standard in *Drosophila*. We considered the effects of applying the same standard for normalization to both RNA and protein. The abundance of *Gapdh1* mRNA (relative to that for *RpL32*) showed no significant differences between the genotypes in ovary (Fig. 5A), nor in embryos 80 min AEL (Fig. S3A). Moreover, based on the data in Flyatlas (Thurmond et al., 2019; Chintapalli et al., 2007), the abundance of *Gapdh1* and *RpL32* mRNAs in ovary is at a very similar ratio to that in the whole fly (0.76 and 0.86, respectively). Therefore, switching to *Gapdh1* as an alternative normalization standard would make no difference to the overall result for those stages, nor to the major finding of radically different *srl* mRNA and protein abundances. It should also be noted that, at 160 min AEL, there is a sharp drop in *Gapdh1* mRNA abundance in all genotypes (Fig. 6A), making it unsuitable as a reference 'housekeeping' mRNA during the specific context of embryogenesis where, in any case, new protein synthesis contributes little to the steady-state level of abundant housekeeping proteins such as GAPDH.

There is no reported evidence for an antisense *srl* RNA or any truncated RNA lacking the start codon, from the *srl* locus. Therefore, the RNAi target in our experiments must be one or all of the reported *srl* mRNA isoforms. One possible explanation for our findings would be that the Spargel protein detected in ovaries and embryos does not originate in the germline but is imported from follicles cells, whilst the
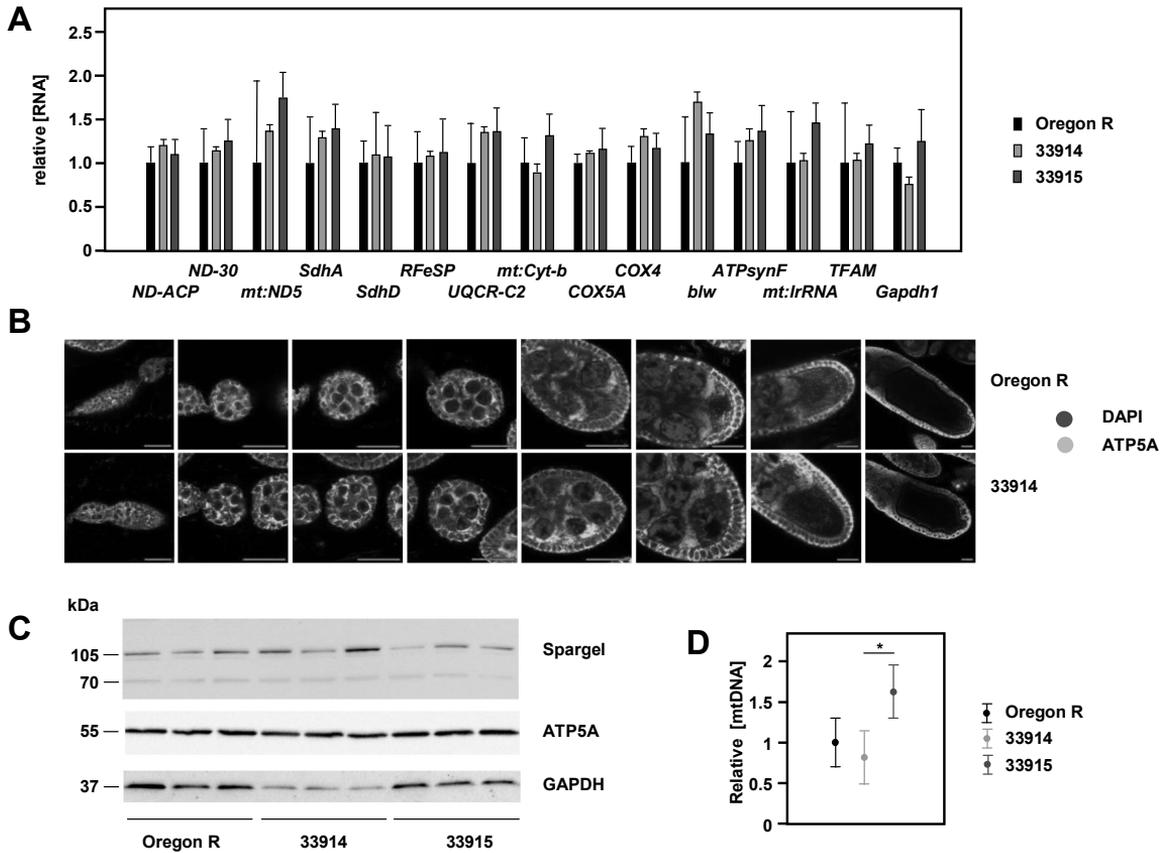
Fig. 5. Effect of germline *srl* knockdown on RNA, protein and mtDNA levels in ovaries.

(A) qRT-PCR measurements of RNA levels of the indicated genes (symbols as in FlyBase (Thurmond et al., 2019; Chintapalli et al., 2007)) in ovaries from females of the indicated genotypes: Oregon R (wild-type), 33914, 33915 – shRNA lines 33914 and 33915 in combination with MTD-GAL4. Means ± SD, n = 4 batches of ovaries for each group. There were no significant differences of the other groups from Oregon R (Student's *t*-test with Bonferroni correction using dC_T values). Note that, because fold-differences rather than dC_T values are plotted, SDs in the two directions are unequal. For clarity, only the larger SD, above the mean, is shown. (B) Images of ovarian follicles at various stages of oogenesis (left to right: germarium, stages 1–6, 10 and 11 or later), from females of the indicated genotypes, stained as shown. Scale bars = 20 μm. (C) Western blots of protein extracts from ovaries of females of the indicated genotypes, probed as indicated. Molecular weights extrapolated from the migration of molecular-weight markers. The images are from different gels of the same protein samples. See Fig. S2B, for a representative Ponceau S-stained membrane confirming equal protein loading. Densitometric signal analysis, normalized to values for Oregon R, is shown in Table 1. (D) Relative mtDNA copy numbers in ovaries of females of the indicated genotypes, normalized to Oregon R, means ± SD, $n \geq 4$ for each group. * indicates significant differences between maternal genotypes (one-way ANOVA with Tukey post hoc HSD test, based on dC_T values, $p < 0.05$). For full statistical analysis on all copy-number measurements, i.e. both in ovaries and embryos, using two-way ANOVA, see Table S2.

abundant *srl* mRNA in the oocyte and early embryo is untranslated, and has a novel but unknown (non-coding) role in early development.

Like PGC-1α in mammals, *srl* is known to be regulated post-translationally by RNF34-mediated ubiquitylation (Wei et al., 2018). In adult muscle, knockdown of *srl* counteracts the metabolic and physiological effects of RNF34 knockdown (Wei et al., 2018), including the promotion of mitochondrial biogenesis. Translational regulation, as hypothesized previously (George & Jacobs, 2019) might account for low levels of the protein despite high levels of the RNA, if *srl* translation is responsive to levels of the encoded protein, as documented for a subset of genes in yeast (Beyer et al., 2004). Although purely speculative at this point, such an idea needs to be thoroughly investigated.

4.2. Maternal spargel is required in the germline for embryo viability

In this study, we showed that the female sterility (Tiefenböck et al.,

2010) or near sterility (Mukherjee et al., 2014) previously seen in *srl[1]* flies is due to an effect specifically in the female germline, affecting the viability of the resulting embryos. Previous studies indicated a delay in oogenesis in the *srl[1]* hypomorph (Mukherjee et al., 2014), although we did not find any difference in fecundity as a result of germline *srl* knockdown (Fig. S2A), nor any obvious difference in ovarian morphology (Fig. 4). The previous findings may therefore have been influenced by somatic insufficiency of *srl* (e.g. in the fat body). Here we showed that *srl* knockdown in the germline affects embryo size (Fig. 3) and produces a dramatic, disruptive effect on embryonic development, commencing around the time of the mid-blastula transition (Movie S1). Nevertheless, we found no specific evidence of an effect on mitochondria.

Gametogenesis clearly does depends upon mitochondrial function in *somatic* cells of the developing gonad (Reeve et al., 2007), although spatial and temporal disruption of mitochondrial movement into the
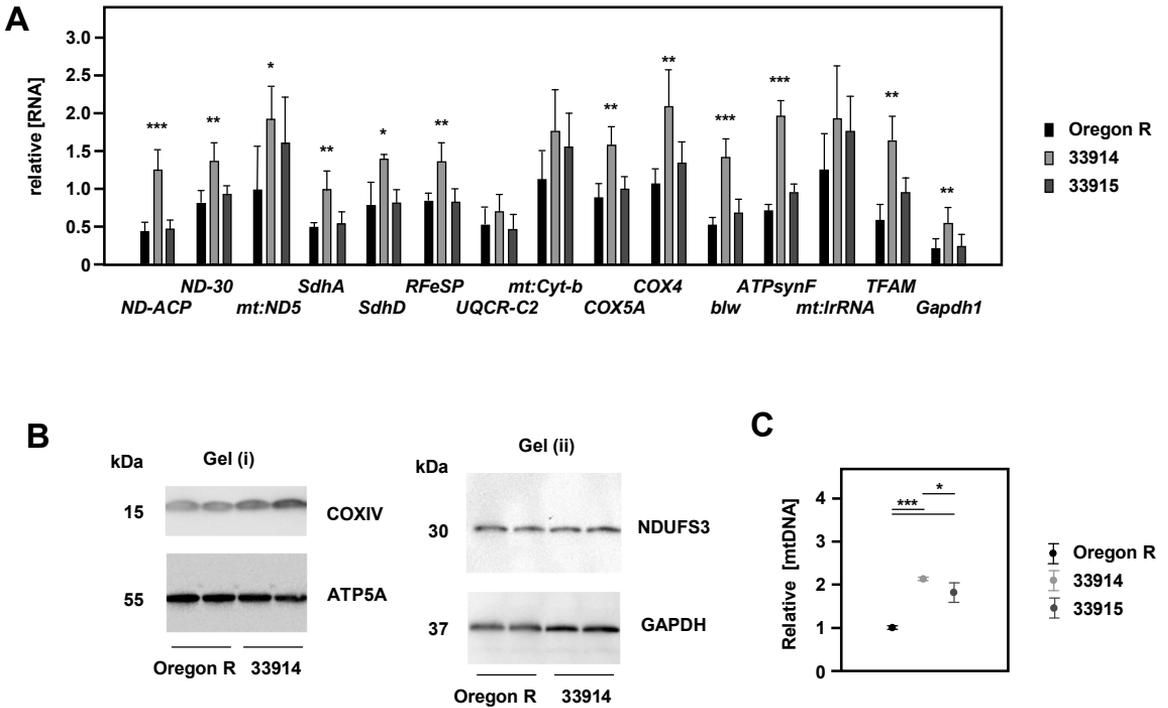
Fig. 6. Effect of germline *srl* knockdown on RNA, protein and mtDNA levels in embryos.
(A) qRT-PCR measurements of RNA levels of the indicated genes (symbols as in FlyBase (Thurmond et al., 2019; Chintapalli et al., 2007)) in embryos from mothers of the indicated genotypes, 160 min AEL: Oregon R (wild-type), 33914, 33915 – shRNA lines 33914 and 33915 in combination with MTD-GAL4. Means + SD, n = 4 batches of embryos for each group. *, **, *** indicate significant differences from Oregon R (Student's *t*-test with Bonferroni correction using dC_T values, $p < 0.05$, 0.01 and 0.001, respectively). Note that, because fold-differences rather than dC_T values are plotted, SDs in the two directions are unequal. For clarity, only the larger SD, above the mean, is shown. (B) Western blots of protein extracts from embryos 160 min AEL, probed as indicated on two separate blots. Molecular weights extrapolated from the migration of molecular-weight markers. Approximately equal loading for each gel was verified by Ponceau S staining (Fig. S3C). (C) Relative mtDNA copy numbers in embryos from mothers of the indicated genotypes, 160 min AEL, normalized to Oregon R, means ± SD, n ≥ 4 for each group. *, *** indicate significant differences between maternal genotypes (one-way ANOVA with Tukey post hoc HSD test, based on dC_T values, $p < 0.05$, 0.001, respectively). For full statistical analysis on all copy-number measurements, i.e. both in ovaries and embryos, using two-way ANOVA, see Table S2.

oocyte from the nurse cells does not prevent the development of viable progeny (Cox & Spradling, 2006).

Mitochondria are a major component of the Balbiani body (Cox & Spradling, 2003), which is involved in the formation of polar granules, the germ plasm (Lehmann, 2016) that specifies the future germline. The widespread and dramatic effects on cellularization are not consistent with any specific effect on future germ cells, although we cannot exclude the possibility that components of the germ plasm may have been incorrectly distributed to other regions of the *srl* knockdown oocyte, where they might interfere with nuclear re-localization or specific aspects of fate specification during blastoderm formation and/or cellularization.

Several lines of argument support the conclusion that the embryonic lethality was due to a genuine RNAi effect, despite the lack of correspondence between *srl* RNA and protein levels, as detected by the antibody. First, knockdown was highly effective at the RNA level, whereas other RNAi lines targeted against *srl* gave no such knockdown and also no observable phenotype. Second, the previously studied hypomorph *srl*[1] also showed female sterility (Tiefenböck et al., 2010), even though it was not possible to establish whether this was a somatic or germline-specific effect. The similar phenotype makes it highly unlikely that our findings are an off-target effect. Although an off-target effect cannot be completely ruled out, the usual way of excluding it, which would be to recode the protein and express it in the RNAi background, would be

uninterpretable, given the non-congruence of the RNA and protein data. Note also that massive overexpression at the RNA level also had only modest effects on the protein (George & Jacobs, 2019). Thus, insufficiency of the *srl* RNA as such, rather than of the encoded protein, may underlie the embryonic phenotype, which would impute an undefined, non-coding function to the RNA.

4.3. Does size matter?

srl knockdown embryos were smaller than their wild-type or control counterparts (Figs. 3, 4), and their sizes spanned a greater range. However, many were in the normal size range, despite the fact that only ~10% of them were able to complete development, implying that size is not the sole determinant of developmental success or failure following *srl* knockdown. Rather, the abnormal size distribution should be considered an indicator of unknown aberrations during oogenesis. Oogenesis was not grossly disturbed (Fig. 5B), and knockdown embryos were ostensibly normal as regards localized determinants (Fig. 4). Compared with controls, the amount of mtDNA relative to nuclear DNA in knockdown ovaries or embryos showed only minor variations that are probably attributable to strain background (Fig. 6D, S3D). Once cellularization was complete (160 min AEL), relative mtDNA copy number was only slightly elevated compared with controls (Fig. 6C, S3D), implying that total nuclear DNA synthesis during embryogenesis

was close to normal. The only consistent differences we could detect in knockdown ovaries was in the representation of GAPDH, which was decreased (Fig. 5C, S2C).

Our tentative interpretation is that a sufficient level of *spargel* gene product is required to ensure the supply of one or more vital components to the oocyte. Noting that the qRT-PCR data at both the 80 min AEL (Fig. S3A) and 160 min AEL (Fig. 6A) time-points has been normalized to the values for each transcript in Oregon R embryos at 80 min AEL, it is evident that there is a general decline in most maternal transcripts (compared with *RpL32*) between these two time-points in control embryos. Yet in knockdown embryos this decline did not occur (Fig. 6A), suggesting a global failure of the transcriptional activation that occurs once the cleavage cycles of nuclear division are complete (Anderson & Lengyel, 1979). This fits the canonical activity of Spargel as a transcriptional coactivator, and would imply that one of its roles in the embryo could be to boost new transcription across the genome, at cellularization. Note, however, that the zygotic activation of *evens-kipped* and *hunchback* transcription during the syncitial phase of embryonic development occurred normally (Fig. 4A, B). These early switches in transcription involve specific mechanisms, such as the dilution of maternally synthesized repressors (Pritchard & Schubiger, 1996), and may be independent of a general requirement for Spargel. The fact that GAPDH protein was decreased in knockdown ovaries (Fig. 5C) also suggests the possibility that Spargel may indeed be acting as a transcriptional coactivator during oogenesis, but with a completely different set of specific targets than those related to mitochondria. A completely different possibility would be that *spargel* has a more specific role in cellularization, which might directly involve the *srl* RNA, which abruptly declines in abundance in control embryos around this time (Fig. 1), rather than the protein.

4.4. Ancestral function(s) of PGC-1 family coactivators

In mammals, only one member of the PGC-1 family, *PPRC1*, is an essential gene, being specifically required for early development in the mouse (He et al., 2012), as well as for the growth program in somatic cells (Andersson & Scarpulla, 2001; Vercauteren et al., 2009). Its functions are less well characterized than those of PGC-1α and PGC-1β. Although PPRC1 is responsive to mitochondrial metabolic stress, which it counteracts (Gleyzer & Scarpulla, 2011), it is less obviously focused on metabolism than PGC-1α and PGC-1β. For this reason, it has been widely assumed that it arose by duplication and diversification, evolving novel functions in the process. The fact that the PGC-1 family is represented in *Drosophila* by a single gene offered a theoretical opportunity to identify the ancestral function of the gene family, and re-assess the meaning of the gene family in mammals.

Previous studies of *srl* have suggested a relationship with metabolism, although the hypomorph *srl¹* was earlier found to have a growth defect and to exhibit female sterility (Tiefenböck et al., 2010), with a few 'escapers' (Mukherjee et al., 2014). Using a highly specific driver/RNAi vector combination, our studies have now shown that this essential function is exercised in the female germline and/or early embryo, but does not involve any specific effect on mitochondria or on gene expression connected to metabolism.

The developmental expression pattern of *PPRC1* shares some similarities with that of *srl*, being abundant during the cleavage stages, or when embryonic stem cells are induced to form embryoid bodies, but then falling away sharply (He et al., 2012). These various features suggest that *srl* has more in common with *PPRC1* than with other members of the PGC-1 family, and that these shared properties may be ancestral. On the other hand, previous data relating *srl* to growth regulation and responsiveness to insulin signalling (Tiefenböck et al., 2010; Mukherjee & Duttaroy, 2013), imply that the ancestral PGC-1 coactivator may have performed functions both in early development and in metabolic regulation of growth, and these only diverged functionally later on in mammals.

4.5. Clinical relevance

In humans, the PGC-1 coactivators have been implicated in key physiological and pathological processes linked to diet and metabolism (Cheng et al., 2018). Moreover, their upregulation has been shown to be beneficial in numerous disease models (Cheng et al., 2018), and they have been proposed as potential drug targets via the use of agents such as bezafibrate, that act as PGC-1 pan-agonists (Komen & Thorburn, 2014). However, such trials have so far met with only limited success (Orngreen et al., 2015). The present study indicates one fundamental reason why this might be the case: namely, that, in addition to their roles in energetic homeostasis, the PGC-1 coactivators are also involved in regulating other processes, including key events in early development performed in *Drosophila* by *srl* and in mammals by PPRC1. Therefore, PGC-1 pan-agonists may simply have too broad an effect, with unintended side effects and self-cancelling modifications of metabolism, unless some way can be found to target PGC-1 regulation of metabolic functions more specifically.

4.6. Conclusions

In conclusion, whilst *spargel* expression in the female germline plays an important function in reproductive viability, there is no evidence supporting mitochondrial biogenesis or metabolic homeostasis as the object of that function. Instead, *spargel* potentially plays a more global role in oogenesis, ensuring adequate resources for the developing embryo after oviposition. We suggest that the PGC-1 coactivator family might better be considered as supplying a boost to transcription in response to several different types of metabolic, developmental or physiological signalling, and that the precise targets of this effect depend more on the tissue and context than on specific properties of the coactivators.

Supplementary data to this article can be found online at https://doi.org/10.1016/j.mito.2019.08.006.

Authors' contributions

HTJ and JG jointly conceived the study. JG performed the experiments and analyses and produced the first draft of the figures. HTJ supervised the work, finalized the figures, and drafted the manuscript, which was finalized by both authors.

Data statement

All data relevant to the work presented here are available from the paper itself or its supplementary files, and may be freely used for academic purposes.

Declaration of Competing Interest

The authors declare that they have no competing interests.

References

Adán, C., Matsushima, Y., Hernández-Sierra, R., Marco-Ferreres, R., Fernández-Moreno, M.A., González-Vioque, E., et al., 2008. Mitochondrial transcription factor B2 is essential for metabolic function in *Drosophila melanogaster* development. J. Biol. Chem. 283, 12333–12342.

Akiyama, T., Okada, M., 1992. Spatial and developmental changes in the respiratory activity of mitochondria in early Drosophila embryos. Development. 115, 1175–1182.

Anderson, K.V., Lengyel, J.A., 1979. 1979. Rates of synthesis of major classes of RNA in *Drosophila* embryos. Dev. Biol. 70, 217–231.

Andersson, U., Scarpulla, R.C., 2001. Pgc-1-related coactivator, a novel, serum-inducible coactivator of nuclear respiratory factor 1-dependent transcription in mammalian cells. Mol. Cell. Biol. 21, 3738–3749.

Beyer, A., Hollunder, J., Nasheuer, H.P., Wilhelm, T., 2004. Post-transcriptional expression regulation in the yeast *Saccharomyces cerevisiae* on a genomic scale. Mol. Cell. Proteomics 3, 1083–1092.

Cheng, C.F., Ku, H.C., Lin, H., 2018. PGC-1α as a pivotal factor in lipid and metabolic regulation. Int. J. Mol. Sci. 19, 3447.

Chintapalli, V.R., Wang, J., Dow, J.A.T., 2007. Using FlyAtlas to identify better *Drosophila* models of human disease. Nat. Genet. 39, 715–720.

Cox, R.T., Spradling, A.C., 2003. A Balbiani body and the fusome mediate mitochondrial inheritance during *Drosophila* oogenesis. Development. 130, 1579–1590.

Cox, R.T., Spradling, A.C., 2006. Milton controls the early acquisition of mitochondria by Drosophila oocytes. Development. 133, 3371–3377.

Finck, B.N., Kelly, D.P., 2006. PGC-1 coactivators: inducible regulators of energy metabolism in health and disease. J. Clin. Invest. 116, 615–622.

Frasch, M., Hoey, T., Rushlow, C., Doyle, H., Levine, M., 1987. Characterization and localization of the even-skipped protein of *Drosophila*. EMBO J. 6, 749–759.

Galloni, M., 2003. Bonsaï, a ribosomal protein S15 homolog, involved in gut mitochondrial activity and systemic growth. Dev. Biol. 264, 482–494.

George, J., Jacobs, H.T., 2019. Minimal effects of *spargel* (PGC-1α) overexpression in a *Drosophila* mitochondrial disease model. Biol. Open. https://doi.org/10.1242/bio.042135. (in press).

Gleyzer, N., Scarpulla, R.C., 2011. PGC-1-related coactivator (PRC), a sensor of metabolic stress, orchestrates a redox-sensitive program of inflammatory gene expression. J. Biol. Chem. 286, 39715–39725.

He, X., Sun, C., Wang, F., Shan, A., Guo, T., Gu, W., Cui, B., Ning, G., 2012. Peri-implantation lethality in mice lacking the PGC-1-related coactivator protein. Dev. Dyn. 241, 975–983.

Thurmond, J., Goodman, J.L., Strelets, V.B., Attrill, H., Gramates, L.S., Marygold, S.J., Matthews, B.B., Millburn, G., Antonazzo, G., Trovisco, V., Kaufman, T.C., Calvi, B.R., the FlyBase Consortium, 2019. FlyBase 2.0: the next generation. Nucleic Acids Res 47 (D1), D759–D765.

Hudson, A.M., Cooley, L., 2014. Methods for studying oogenesis. Methods. 68, 207–217.

Kemppainen, E., George, J., Garipler, G., Tuomela, T., Kiviranta, E., Soga, T., Dunn, C.D., Jacobs, H.T., 2016. Mitochondrial dysfunction plus high-sugar diet provokes a metabolic crisis that inhibits growth. PLoS One 11, e0145836.

Komen, J.C., Thorburn, D.R., 2014. Turn up the power - pharmacological activation of mitochondrial biogenesis in mouse models. Br. J. Pharmacol. 171, 1818–1836.

Lehmann, R., 2016. Germ plasm biogenesis–an Oskar-centric perspective. Curr. Top. Dev. Biol. 116, 679–707.

Mukherjee, S., Duttaroy, A., 2013. Spargel/dPGC-1 is a new downstream effector in the insulin-TOR signaling pathway in *Drosophila*. Genetics. 195, 433–441.

Mukherjee, S., Basar, M.A., Davis, C., 2014. Duttaroy. Emerging functional similarities and divergences between Drosophila Spargel/dPGC-1 and mammalian PGC-1 protein. Front. Genet. 5, 216.

Ni, J.Q., Zhou, R., Czech, B., Liu, L.P., Holderbaum, L., Yang-Zhou, D., et al., 2011. A genome-scale shRNA resource for transgenic RNAi in Drosophila. Nat. Methods 8, 405–407.

Orngreen, M.C., Vissing, J., Laforet, P., 2015. No effect of bezafibrate in patients with CPTII and VLCAD deficiencies. J. Inherit. Metab. Dis. 38, 373–374.

Pritchard, D.K., Schubiger, G., 1996. Activation of transcription in Drosophila embryos is a gradual process mediated by the nucleocytoplasmic ratio. Genes Dev. 10, 1131–1142.

Puigserver, P., Spiegelman, B.M., 2003. Peroxisome proliferator-activated receptor-gamma coactivator 1 alpha (PGC-1 alpha): transcriptional coactivator and metabolic regulator. Endocr. Rev. 24, 78–90.

Quiros, P.M., Goyal, A., Jha, P., Auwerx, J., 2017. Analysis of mtDNA/nDNA ratio in mice. Curr. Protoc. Mouse Biol. 7, 47–54.

Reeve, S., Carhan, A., Dee, C.T., Moffat, K.G., 2007. Slowmo is required for *Drosophila* germline proliferation. Genesis. 45, 66–75.

Rørth, P., 1998. Gal4 in the *Drosophila* female germline. Mech. Dev. 78, 113–118.

Schroder, C., Tautz, D., Seifert, E., Jäckle, H., 1988. Differential regulation of the two transcripts from the *Drosophila* gap segmentation gene *hunchback*. EMBO J. 7, 2881–2887.

Spiegelman, B.M., 2007. Transcriptional control of energy homeostasis through the PGC1 coactivators. Novartis Found. Symp. 286, 3–6.

Steward, R., 1989. Relocalization of the dorsal protein from the cytoplasm to the nucleus correlates with its function. Cell. 59, 1179–1188.

Tiefenböck, S.K., Baltzer, C., Egli, N.A., Frei, C., 2010. The Drosophila PGC-1 homologue Spargel coordinates mitochondrial activity to insulin signalling. EMBO J. 29, 171–183.

Tourmente, S., Lecher, P., Degroote, F., Renaud, M., 1990. Mitochondrial development during *Drosophila* oogenesis: distribution, density and in situ RNA hybridizations. Biol. Cell. 68, 119–127.

Tracey Jr., W.D., Ning, X., Klingler, M., Kramer, S.G., Gergen, J.P., 2000. Quantitative analysis of gene function in the *Drosophila* embryo. Genetics. 154, 273–284.

Vercauteren, K., Gleyzer, N., Scarpulla, R.C., 2009. Short hairpin RNA-mediated silencing of PRC (PGC-1-related coactivator) results in a severe respiratory chain deficiency associated with the proliferation of aberrant mitochondria. J. Biol. Chem. 284, 2307–2319.

Wei, P., Guo, J., Xue, W., Zhao, Y., Yang, J., Wang, J., 2018. RNF34 modulates the mitochondrial biogenesis and exercise capacity in muscle and lipid metabolism through ubiquitination of PGC-1 in *Drosophila*. Acta Biochim. Biophys. Sin 50, 1038–1046.

Wheeler, J.C., VanderZwan, C., Xu, X., Swantek, D., Tracey, W.D., Gergen, J.P., 2002. Distinct in vivo requirements for establishment versus maintenance of transcriptional repression. Nat. Genet. 32, 206–210.